TECHNICAL REPORT STANDARD PAGE

1. Report No.	2. Government Accession No.	3. Recipient's Catalog No.
FHWA/LA-92/264		

4. Title and Subtitle	5. Report Date
Feasibility Evaluation of Utilizing High Strength Concrete in Design and Construction of Highway Bridge Structures	December 1992
	6. Performing Organization Code

7. Author(s)	8. Performing Organization Report No.
R.N. Bruce, H.C. Russell, J.J. Roller, B.T. Martin	264

9. Performing Organization Name and Address	10. Work Unit No.
Department of Civil Engineering 206 Civil Engineering Building, Tulane University New Orleans, LA 70118-5698	11. Contract or Grant No. LTRC Proj. No. 90-4C State Proj. No. 736-15-79

12. Sponsoring Agency Name and Address	13. Type of Report and Period Covered
Louisiana Transportation Research Center 4101 Gourrier Avenue Baton Rouge, LA 70808	Interim Report October 1, 1990 to December 4, 1992
	14. Sponsoring Agency Code

15. Supplementary Notes

Conducted in cooperation with the U.S. Department of Transportation, Federal Highway Administration.

16. Abstract

The objective of this investigation was to evaluate the feasibility of using high-strength concrete in the design and construction of highway bridge structures. A literature search was conducted; a survey of five regional fabrication plants was performed; mix designs were studied in the laboratory and in the field; and three series of tests consisting of a total of nine full-scale specimens were conducted.

The first series included three pile specimens tested in flexure. Each of the pile specimens had a 24-in.(610-mm) square cross section with a 12-in. (305-mm) diameter void running its full length. All the pile specimens were 24 ft (7.31 m) long. the pile specimen concrete, at the time of testing, had an average compressive strength of 8,067 psi (55 MPa).

The second series consisted of three full-size bulb-tee specimens. Flexural tests of two bulb-tee specimens are reported. The third specimen is being used for determination of long term static-load behavior. Results will be given in a separate report. The specimens were standard 54-in. (1,372-mm) bulb-tee sections with a 6 in. (152 mm) thick web. One of the test specimens had a slab 9 ½ in. (241 mm) thick and 10 ft (3,048 mm) wide cast on top of it. The slab had an average concrete comprehensive strength of 7,037 psi (48 MPa). The second specimen was tested without a slab. The concrete of each bulb-tee specimen had an average 28-day compressive strength of 9,800 psi (68 MPa). Each girder specimen contained the same number and configuration of longitudinal prestressing strands and the same amount of web reinforcement.

Three shear tests are also reported. These shear tests were performed using the ends of the two flexural test specimens. Since the shear specimens were taken from the flexural specimens, they had the same cross-sectional configuration and concrete strength as the flexural specimens.

The third series consisted of the fabrication and driving of a single 130-ft (38.6 m) pile specimen. The pile specimen had the same cross-sectional configuration as the pile specimens tested in the laboratory. The concrete of the pile specimens tested in the laboratory. The concrete of the pile specimen had an average 28-day compressive strength of 10,453 psi (72 MPa).

Based on this investigation, the following conclusions are made: (1) High-strength concrete with strengths of 10,000 psi (69 MPa) can be produced using regionally available materials; however, quality control measures presently in use must be upgraded. (2) AASHTO Standard Specifications for Highway Bridges conservatively predicted the behavior of the pile and girder specimens in the area of flexural strength, cracking moment, inclined cracking, shear strength, strand transfer length, effective width of top flange, estimation of prestress losses, modulus of elasticity, and modulus of rupture. (3) Girder chamber/deflection measurements were consistent with values calculated using conventional methods. (4) High-strength concrete can be used effectively in long piles. The higher tensile strength and higher precompression is particularly valuable in soft driving conditions where tensile driving stresses are high. (5) Steam curing of high-strength concrete may reduce strength development at later ages.

A fourth series of tests is scheduled to be completed in the fall of 1993. This series of tests will consist of fatigue testing two full-size bulb-tee specimens. The results of the fatigue tests and the long-term behavior of specimen BT3, will be the subject of a separate report to be completed in January of 1994.

17. Key Words	18. Distribution Statement
High strength concrete, concrete mix design, prestressed member fabrication, full-size bulb-tee testing, pile driving and analysis	No restriction. This document is available to the public through the National Technical Information Service, Springfield, VA 22161.

19. Security Classif. (of this report)	20. Security Classif. (of this page)	21. No. of Pages	22. Price
Unclassified	Unclassified	228	

Form DOT F1700.7 (1-92)

Louisiana Transportation Research

Feasibility Evaluation of Utilizing High Strength Concrete in Design and Construction of Highway Bridge Structures

(Interim Report)

by

R. N. Bruce, Ph.D., P.E.
B. T. Martin, P.E.
TULANE UNIVERSITY

H. G. Russell, Ph.D., P.E.
J. J. Roller
CONSTRUCTION TECHNOLOGY LABORATORIES, INC.

LTRC
Louisiana Transportation Research Center

Sponsored Jointly by Louisiana State University and the Louisiana Department of Transportation and Development

FEASIBILITY EVALUATION OF UTILIZING HIGH-STRENGTH CONCRETE IN DESIGN AND CONSTRUCTION OF HIGHWAY BRIDGE STRUCTURES

INTERIM REPORT

by

R. N. BRUCE, PH.D., P.E.
CATHERINE AND HENRY BOH CHAIR IN CIVIL ENGINEERING,
TULANE UNIVERSITY

H. G. RUSSELL, PH.D., P.E.
VICE-PRESIDENT, CONSTRUCTION TECHNOLOGY LABORATORIES, INC.

J. J. ROLLER
SENIOR ENGINEER, CONSTRUCTION TECHNOLOGY LABORATORIES, INC.

B. T. MARTIN, P.E.
BOH FELLOW, TULANE UNIVERSITY

CONDUCTED FOR

LOUISIANA DEPARTMENT OF TRANSPORTATION AND DEVELOPMENT
Louisiana Transportation Research Center
in cooperation with
U. S. Department of Transportation
FEDERAL HIGHWAY ADMINISTRATION

DECEMBER 1992

ABSTRACT

The objective of this investigation was to evaluate the feasibility of using high-strength concrete in the design and construction of highway bridge structures. A literature search was conducted; a survey of five regional fabrication plants was performed; mix designs were studied in the laboratory and in the field; and three series of tests consisting of a total of nine full-scale specimens were conducted.

The first series included three pile specimens tested in flexure. Each of the pile specimens had a 24-in. (610-mm) square cross section with a 12-in. (305-mm) diameter void running its full length. All the pile specimens were 24 ft (7.31m) long. The pile specimen concrete, at the time of testing, had an average compressive strength of 8,067 psi (55 MPa).

The second series consisted of three full-size bulb-tee specimens. Flexural tests of two bulb-tee specimens are reported. The third specimen is being used for determination of long term static-load behavior. Results will be given in a separate report. The specimens were standard 54-in. (1,372-mm) bulb-tee sections with a 6 in. (152 mm) thick web. One of the test specimens had a slab 9-1/2 in. (241 mm) thick and 10 ft (3,048 mm) wide cast on top of it. The slab had an average concrete compressive strength of 7,037 psi (48 MPa). The second specimen was tested without a slab. The concrete of each bulb-tee specimen had an average 28-day compressive strength of 9,800 psi (68 MPa). Each girder specimen contained the same number and configuration of longitudinal prestressing strands and the same amount of web reinforcement.

Three shear tests are also reported. These shear tests were performed using the ends of the two flexural test specimens. Since the shear specimens were taken

from the flexural specimens, they had the same cross-sectional configuration and concrete strength as the flexural specimens.

The third series consisted of the fabrication and driving of a single 130-ft (39.6 m) pile specimen. The pile specimen had the same cross-sectional configuration as the pile specimens tested in the laboratory. The concrete of the pile specimen had an average 28-day compressive strength of 10,453 psi (72 MPa).

Based on this investigation, the following conclusions are made:

1. High-strength concrete with strengths of 10,000 psi (69 MPa) can be produced using regionally available materials, however, quality control measures presently in use must be upgraded.

2. AASHTO Standard Specifications for Highway Bridges conservatively predicted the behavior of the pile and girder specimens in the area of flexural strength, cracking moment, inclined cracking, shear strength, strand transfer length, effective width of top flange, estimation of prestress losses, modulus of elasticity, and modulus of rupture.

3. Girder camber/deflection measurements were consistent with values calculated using conventional methods.

4. High-strength concrete can be used effectively in long piles. The higher tensile strength and higher precompression is particularly valuable in soft driving conditions where tensile driving stresses are high.

5. Steam curing of high-strength concrete may reduce strength development at later ages.

A fourth series of tests is scheduled to be completed in the fall of 1993. This series of tests will consist of fatigue testing two full-size bulb-tee specimens. The results of the fatigue tests and the long-term behavior of specimen BT3, will be the subject of a separate report to be completed in January of 1994..

IMPLEMENTATION STATEMENT

The implementation statement of this interim report is preliminary in nature; final implementation recommendations await the completion of the investigation. Limited implementation observations and recommendations may be made as a part of this interim report, based on work already done. However, in order to place interim recommendations in perspective with regard to the overall research, an overview of the entire investigation is required.

The investigation is approximately sixty percent complete as of the date of this interim report. The overall research constitutes a comprehensive examination of high-strength concrete, as a material and as a structural element. The scope of the overall project includes the following:

1. A survey of regional fabrication plant capabilities,
2. A determination of the suitability of local materials,
3. A study of mix designs in the laboratory and in the field,
4. The fabrication of full-size structural members in the field,
5. The testing of full-size structural members,
6. The analysis of full-size structural members with respect to production feasibility, strength and behavior, and compliance with design codes.

At the time of this interim report, items 1 through 4 listed above have been completed. Short term static tests in flexure and shear have been completed. The field driving test of a single pile has been completed.

Long term tests are presently being conducted, and are scheduled for completion in late 1993. Fatigue tests are scheduled for completion in the late fall of 1993. Long term tests and fatigue tests are not included in this interim report;

they will be included in the final report of the investigation. It is anticipated that the final report for the project will be submitted in January of 1994.

Thus, the implementation statement for this interim report will address items 1 through 4 listed above, plus those completed parts of item 5.

A survey of regional plant capabilities indicates that there are at least two regional plants, both in Alabama, that are capable of immediate implementation of the fabrication of high-strength concrete structural members having a 28-day compressive strength in the range of 9,000 to 10,000 psi. It is felt that high-strength concrete in this range of compressive strength, can be consistently produced using local materials.

A study of mix designs in the laboratory indicates that 28-day compressive strengths in excess of 10,000 psi can be achieved consistently; and these mix designs can be duplicated in the field while maintaining a 28-day compressive strength in the range of 9,000 psi (62 MPa) to 10,000 psi (69 MPa).

The fabrication of full-size structural members, having a nominal 28-day compressive strength of in the range of 9,000 psi (62 MPa) to 10,000 psi (69 MPa), can be implemented immediately in at least two regional fabrication facilities. In order to achieve this level of compressive strength, a high level of quality control is demanded.

Since the tests of the full-size specimens are complete, including the field driving of a single long pile, the investigators are prepared to make an implementation recommendation in this interim report. The laboratory pile specimens behaved in a manner that would be conservatively predicted using the provisions of the AASHTO Standard Specifications for Highway Bridges.

The field driving test, on a single 130 ft. long pile, indicated that high-strength concrete can be used effectively in long piles. The pile performed well during transportation, handling, and driving. The high-strength concrete and

corresponding high level of precompression were particularly valuable in soft driving conditions where tensile driving stresses are high. Normally, a single test should not form the basis for a blanket recommendation. However, this single test went so well that there are strong indications that consideration should be given to the immediate implementation of the utilization of high-strength concrete in long piles. Such implementation could increase the resistance of the pile to tensile driving stresses, and offer the added advantage of serving to eliminate pile splices in long piles.

The full-size girder tests are still under way; and some important parameters, such as prestress losses and negative camber and fatigue behavior, are yet to be evaluated. Implementation recommendations, at this interim stage, are premature. However, there are strong indications of potential applications and benefits of high-strength concrete in highway bridge structures. Indications are that a wider transverse spacing of the girders may be used effectively, and that the wider spacing can reduce the number of girders. Increased material costs, for high-strength concrete can be compared and balanced against the advantages of longer spans, fewer girders in a typical bridge cross section, decreased weight with corresponding foundation efficiency, and increased durability.

The implications of the work to date are that 28-day concrete compressive strengths up to 10,000 psi should be considered for use by the Louisiana DOTD; and that structural members of 10,000 psi concrete can be designed conservatively using the AASHTO Standard Specifications. It is anticipated that the findings of the complete investigation will result in a recommendation for the utilization of high-strength concrete in highway bridge structures.

TABLE OF CONTENTS

CONTENTS (CONTINUED)

CONTENTS (CONTINUED)

CONTENTS (CONTINUED)

CONTENTS (CONTINUED)

LIST OF TABLES

TABLES (CONTINUED)

TABLES (CONTINUED)

LIST OF FIGURES

FIGURES (CONTINUED)

FIGURES (CONTINUED)

FIGURES (CONTINUED)

1. INTRODUCTION

1.1 OBJECTIVE AND SCOPE

The objective of this investigation is to evaluate the feasibility of using high-strength concrete in the design and construction of highway bridge structures. This investigation includes a literature search, a survey of regional fabrication plant capabilities, a study of mix designs in the laboratory and in the field, the fabrication and testing of full size high-strength concrete test specimens, and the analysis of those specimens with respect to production feasibility, strength, and compliance with design codes. On the basis of the findings of this investigation, recommendations are made regarding the use of high-strength concrete in the design and construction of highway bridge structures. While mechanical properties of high-strength concrete are addressed as part of the investigation, the major emphasis of the research is the determination of the behavior of structural elements made of high-strength concrete.

1.2 OUTLINE OF INVESTIGATION

This investigation began with a literature search concerning high-strength concrete. This selective literature search was conducted focusing primarily on recent research performed in Louisiana, Texas, North Carolina and by Portland Cement Association/Construction Technology Laboratories, Inc. (CTL). A detailed examination of the Standard Specifications of the American Association of State Highway Transportation Officials (1) and the Building Requirements for

Reinforced Concrete of the American Concrete Institute (2) was also performed to determine compliance with design requirements. Concurrent with the literature search, a survey of five regional fabrication plants was conducted to ascertain plant capabilities. Following the completion of a mix design investigation, a mix design was selected and fabrication and laboratory testing of the specimens began. Fabricator input was encouraged at all stages of the project in an effort to familiarize the fabricator with the special requirements of high-strength concrete.

The test program involves four separate series of tests. The first series included flexural tests of three 24 ft (7.3 m) long, concentrically pretensioned pile specimens, having a 24-in. (588-mm) square cross section. A cross section of the pile test specimen can be seen in Figure 1. The pile specimens, tested in the laboratory, were designated P1, P2, and P3. Each of the specimens had the same amount of prestressing reinforcement and was subject to the same initial prestressing force. The concrete in the piles had a design compressive strength of 10,000 psi (69 MPa). As shown in Figure 2, the pile specimens were supported near their ends, creating a test span of 22 ft (6.7 m). The flexural load was applied using two point loads located 9 ft 6 in. (2.9 m) from the supports, with a 3-ft (0.91-m) constant moment region between the load points. Details of fabrication of the laboratory tested pile specimens are shown in Appendix A. The first series included concrete and strand material property tests.

The second series of the test program included three eccentrically pretensioned 54-in. (1,372-mm) bulb-tee specimens that were 70 ft (21.34 m) long. The specimens were designated BT1, BT2, and BT3. Specimens BT1 and BT3 had a 9-1/2 in. (241 mm) thick, and 10 ft (3.05 m) wide deck cast on the top of the girder. The slab was cast on the girders in the laboratory using partially shored construction. Girder BT2 did not have a top slab. Cross sections of girders BT1 and BT2 are shown in Figures 3 and 4 respectively. Each of the bulb-tee girders

had the same area of prestressing reinforcement and was subjected to the same nominal initial prestresssing force. Twenty percent of the prestressing strands were draped to reduce bending stresses near the ends. The concrete in all the girders had a design compressive strength of 10,000 psi (69MPa). Concrete in the slab of specimens BT1 and BT3 had a compressive strength of 7,000 psi (41MPa). Details of fabrication of the bulb-tee girders are shown in Appendix B. This series of tests included concrete and strand material tests.

Girders BT1 and BT2, were designed and tested to study flexural strength and behavior, as well as shear strength and behavior. The bulb-tee specimens were simply supported on a 69-ft (21.03-m) span. As illustrated in Figure 5, the flexural load was applied using two loading points located 28 ft 6 in. (8.69 m) in from the supports creating a 12-ft (3.66-m) constant moment region at mid-span. Following the testing of BT1 and BT2 to failure in flexure, the girders were cut in two near mid span. The two halves of girder BT1, designated BT1-D and BT1-L, and one half of BT2, designated BT2-L, were placed on supports, as shown in Figure 6, and tested to failure in shear. The "D" and "L" in the shear specimen designation indicates the dead and live stressing ends of the strands respectively. The first support bearing was located 6 in. (152 mm) from the formed end of the girder while the second support was located 27 ft (8.23 m) from the first support. Four equal loads were then applied to the girder. The first load point was located 4 ft 6 in. (1.37 m) from the support at the formed end of the specimen, while the second, third, and fourth load points were placed 7 ft 6 in. (2.29 m), 10 ft 6 in. (3.2 m) and 13 ft 6 in. (3.96 m) from the support at the formed end, respectively.

The third series of the test program involved the fabrication and field driving of a 130 ft (39.62 m) long pretensioned pile having the same cross-section as specimens P1, P2, and P3. This pile specimen was designated P4. Details of the fabrication of the field tested specimen are given in Appendix C.

The fourth series of tests involves the long term static testing of specimen BT3 and the fatigue testing of two full-size bulb-tee specimens. Specimen BT3 was designed and loaded as shown in Figure 7, to determine long term behavior. For the fatigue specimens, cyclic loading resulting in an extreme fiber tension of $6\sqrt{f_c'}$ will be applied to the uncracked specimens. This series of tests is expected to be completed in the fall of 1993. The results of the tests will be included in the final report scheduled for completion in January, 1994.

All specimens were designed in accordance with the general design criteria of the AASHTO code.

1.3 ACKNOWLEDGEMENTS

The work on this project was conducted jointly by the Tulane University Department of Civil and Environmental Engineering and Construction Technology Laboratories, Inc., under sponsorship of the Louisiana Transportation Research Center; and in cooperation with the Louisiana Department of Transportation and Development and the Federal Highway Administration.

On the part of the Louisiana Transportation Research Center the work was performed under the administrative direction of Mr. Harold R. Paul, Materials Research Administrator; and Mr. Masood Rasoulian, Materials Research Engineer Supervisor. Mr. Norval P. Knapp, Bridge Design Engineer, and Mr. Paul Fossier, Senior Design Engineer, of the Louisiana Department of Transportation and Development, contributed greatly to the investigation.

Appreciation is expressed to the following individuals who have served on the Project Advisory Committee, established for this project by the Principal

Investigator, and have contributed technical background information and data to this investigation:

Dr. Ned Burns	University of Texas at Austin
Mr. Sherrell Helm	Gulf South Prestressed Concrete Association
Mr. Norval Knapp	Louisiana Dept. of Trans. and Development
Dr. John Kulicki	Modjeski and Masters Consulting Engineers
Mr. Harold Paul	Louisiana Transportation Research Center
Mr. Ken Rear	W. R. Grace & Co.
Dr. Paul Zia	North Carolina State University

On the part of Tulane University, the investigation was directed by Dr. Robert N. Bruce, Jr., Catherine and Henry Boh Chair in Civil Engineering, as Principal Researcher and Mr. Barney T. Martin, Jr., Boh Fellow in Civil Engineering.

On the part of Construction Technology Laboratories, Inc., the investigation was directed by Dr. Henry G. Russell, Vice-President and Mr. J. John Roller, Senior Engineer.

On the part of Sherman Prestressed Concrete, the fabrication was directed by Mr. Jim Glass, Prestressed Concrete Sales Engineer.

1.4 NOTATION

1.4.1 Designation of Test Specimens

The pile specimens and girder specimens were numbered in the order of casting and grouped according to the type of tests conducted.

Specimen Number	Configuration	Test Conducted
P1	24" Square Pile	Flexure
P2	24" Square Pile	Flexure
P3	24" Square Pile	Flexure
P4	24" Square Pile	Field Driving
BT1	Bulb-Tee, Slab	Flexure
BT2	Bulb-Tee	Flexure
BT1-D	Bulb-Tee, Slab	Shear
BT1-L	Bulb-Tee, Slab	Shear
BT2-L	Bulb-Tee	Shear
BT3	Bulb-Tee, Slab	Long Term/Flexure

1.4.2 Symbols

a = length of the shear span, in.

A_{ps} = area of prestressing steel, $in.^2$

b_w = width of the web, in.

d = distance from the extreme compressive fiber of a member to the centroid of the prestressing strand, in.

d_b = nominal diameter of prestressing strand, in.

f_c' = compressive strength of the concrete, psi

f_{cc} = compressive stress at the centroid of the concrete due to the effective prestress force, psi

f_o = flexural stress in the concrete at the bottom face of the beam due to self weight, psi

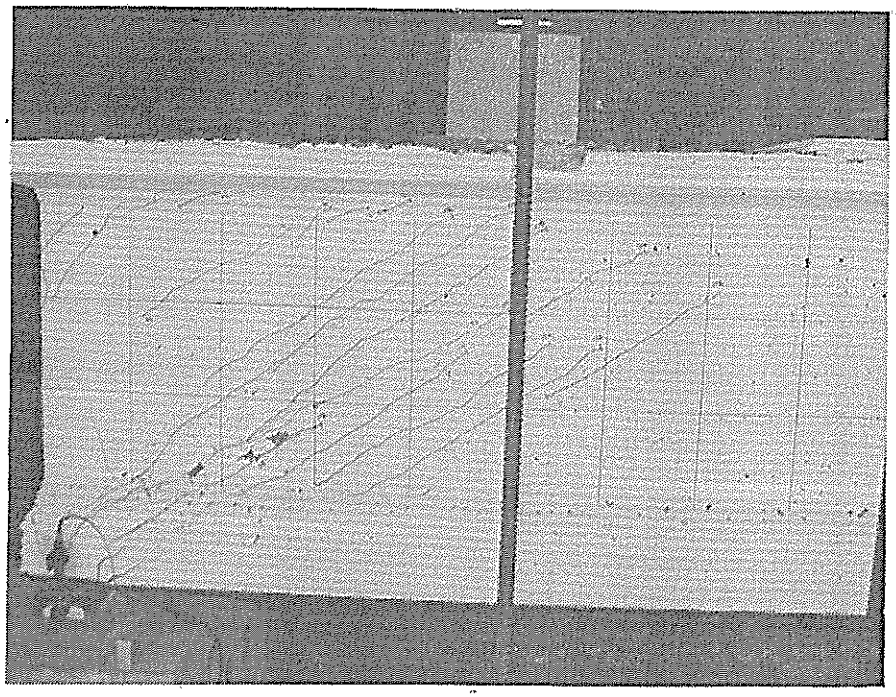

Figure 46. Web cracking of BT2-L.

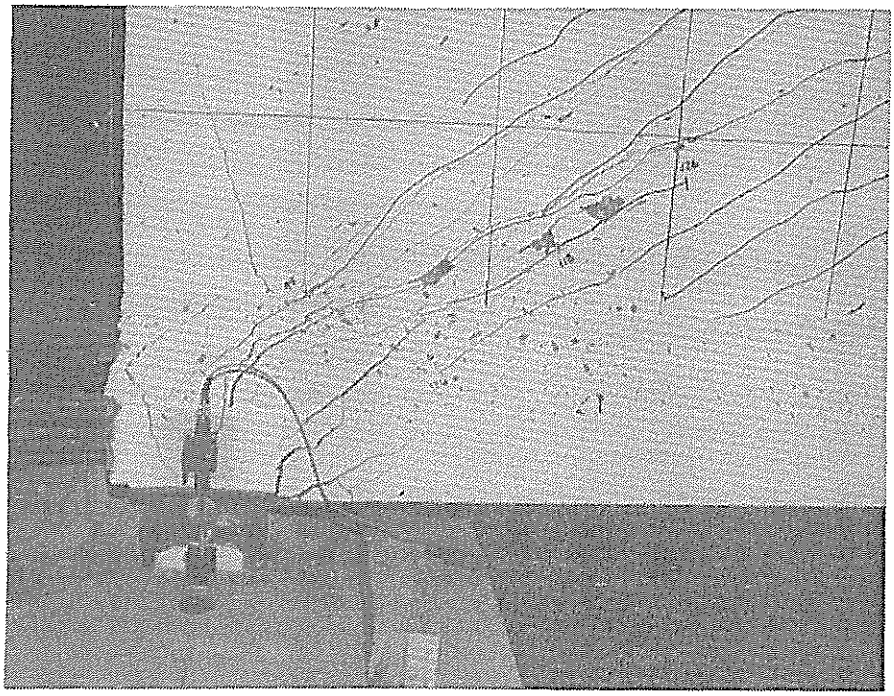

Figure 47. Failure region of specimen BT2-L.

APPENDIX A

MATERIALS, FABRICATION, INSTRUMENTATION, AND LOADING OF THE 24-ft (7.3 m), 24-in. (610-mm) SQUARE PILE SPECIMENS

A.1 MATERIALS

A.1.1 AGGREGATE

The sand for the concrete mix was obtained from the Campbell Pit located off U.S. highway 29, near Flowington, Alabama. The coarse aggregate was obtained from the Calera Quarry located just west of the I-65/U.S. 31 Interchange, north of Calera, Alabama. The coarse aggregate was from the Newala limestone producing formation and was considered high calcium and dolomitic limestone. Both aggregates were tested and found to be in conformance with the Louisiana Department of Transportation and Development (LaDOTD) Standard Specifications (31) for aggregates. Sieve analysis of the aggregates used is reported in Table A.1.

A.1.2 CEMENT

Type I portland cement was used for all pile test specimens. The cement was manufactured by the Citadel Corporation and was certified to conform to ASTM Standard C150-89 , Specifications for Portland Cement (32).

A.1.3 WATER

The water used in the concrete was obtained from the Southern Prestressed, Inc. underground well. The water conformed to LaDOTD Standard Specifications (31) for water used in portland cement concrete.

A.1.4 ADMIXTURES

Four admixtures were used in the concrete mix. These were as follows:

1. MONEX MIGHTY 150 high range water reducer conforming to ASTM C494-90 (33) Type A & F. This item is on the LaDOTD Qualified Products List as #5864.
2. MONEX SEPTAIR air entraining admixture conforming to ASTM C260-86 (34). This item is on the LaDOTD Qualified Products List as #5855.
3. EMSAC DA silica fume - densified 100 percent solids. Since silica fume is still considered experimental by the LaDOTD this product is not on the Qualified Products List
4. DUNDEE Class C flyash conforming to ASTM C 618-91 (35). This item does not have a Louisiana Department of Transportation and Development product source code.

A.1.5 CONCRETE MIX

The mix was designed by the fabricator to yield a nominal 28-day compressive strength of 10,000 psi (69 MPa). The proportions of the four yard batches, by weight, are given in Table A.2.

Six standard 6-in. x 12-in. (152-mm x 305-mm) cylinder specimens and two 6-in. x 6-in. by 22-in. (152-mm x 152-mm x 559-mm) modulus of rupture beams were made from each of the three concrete batches used. Since each pile specimen

was made from its own batch, the control specimens were identified with the pile specimen numbers. For example, control specimen P1 denotes the specimen taken from the batch used to make pile specimen P1.

The compressive strength, modulus of elasticity, splitting tensile strength and modulus of rupture, of the control specimen from each pile are given in Table A.3 for four different test ages. Concrete compressive strength tests were conducted in accordance with ASTM C39-86 (22). Modulus of elasticity tests were conducted in accordance with ASTM C469-87 (23). Splitting tensile strength tests were conducted in accordance with ASTM C496-90 (24). Modulus of rupture tests were conducted in accordance with ASTM C78-84 (25). With the exception of the compressive strength at release (average of two test values), each value in Table A.3 represents a single test result. The average concrete unit weight for piles P1, P2, and P3 was 151.6 lbs/ft^3 (2,427 kg/m^3), 150.0 lbs/ft^3 (2,403 kg/m^3), and 147.1 lbs/ft^3 (2,356 kg/m^3) respectively. A partial stress-strain curve for a typical pile specimen concrete is shown in Figure A.1.

A.1.6 PRESTRESSING STRAND

The low-relaxation prestressing strand used in the pile specimens was domestically fabricated using domestically manufactured steel and was obtained from Florida Wire and Cable Company of Jacksonville, Florida. The nominal diameter of the strand was 1/2 in.(12.7 mm). The strand conformed to ASTM A-416-88, Specifications for Steel Strand, Uncoated Seven Wire Stress Relieved for Prestressed Concrete(36).

A complete stress-strain curve for the production lot from which the project strand was drawn was provided by the manufacturer. This stress-strain curve is reproduced in Figure A.2. Additional tensile tests were performed on eight strand samples, four from the beginning of the coil and four from the end. These tensile

tests were conducted only to determine one percent elongation load, ultimate strength, and modulus of elasticity. The one percent elongation loads and ultimate strengths of the samples ranged from 38,400 lb (171 kN) to 39,000 lb (174 kN) and from 42,200 lb (188 kN) to 42,700 lb (189 kN) respectively. The average modulus of elasticity of the strand was measured as 29,400,000 psi (202,700 MPa). The results of the tensile tests on all eight samples are illustrated in Table A.4. Strand tensile tests were conducted in accordance with ASTM A370, supplement VII (37).

A.1.7 WEB REINFORCEMENT

The spiral reinforcement used in the pile specimens was domestically manufactured by Ivy Steel Products Corporation of Houston, Texas. The W4.5 wire had a nominal diameter of 1/4 in. (6.4 mm). The average tensile strength of four samples tested by the manufacturer was 4,745 lb (21 kN), or 96,664 psi (666 MPa).

A.2 FABRICATION

The pile specimens were fabricated by Southern Prestressed, Inc. at their plant in Pensacola, Florida in accordance with the shop drawings shown in Figure A.3. The three pile specimens were fabricated in a single 120 ft 10 in. (36.8 m) casting bed. All work was performed by the fabricator except for installation of the instrumentation. All phases of the pile specimen fabrication and preparation of the control specimens were observed and supervised by the research personnel to insure all quantities and measurements were known accurately.

A.2.1 PLACING OF THE LONGITUDINAL STRAND

The seven wire prestressing strands were drawn from a single reel located in an outdoor storage area adjacent to the casting bed. Each strand was taken from the reel and threaded through a template at each end of the casting bed. The strands were tensioned using a single strand jack manufactured by G.T. Bynum. The jack had been calibrated within the past six months to have an average gauge reading error of less than one percent. Each strand was initially stressed to 2,000 lb (8.9 kN). The final tension in the strands was determined by elongation and verified by GAUGE readings.

A.2.2 PRESTRESSING OF THE STRAND

In accordance with the present AASHTO code, each of the strands was initially stressed to a value of 0.75 fpu or 30,980 lb (138 kN). In order to accomplish this, the strands were initially tensioned to a proof load of 2,000 lb (8.9 kN) based on gauge readings. After being subjected to the proof load, the strands were marked and stressed to an average elongation of 9.6 in. (244 mm). The load corresponding to this elongation can be obtained from the following expression:

$$e = \frac{P\,L}{A\,E} \tag{28}$$

where e = elongation of strand, in.

P = load per strand, lb

L = nominal length between stressing ends, 120 ft-10 in.

E = modulus of elasticity of the strand 28,600,000 psi

Using the above expression the load in the strand beyond the proof load is calculated to be 28,970 lb (129 kN). When the proof load is added to this value, a total force of 30,970 lb (138 kN) per strand results. The total load applied to each strand was confirmed using the pressure gauge readings of the jack. The jack gauges were calibrated within six months of the date of member fabrication and were found to have an average gauge reading error of less than one percent.

A.2.3 PLACING OF SPIRAL REINFORCING AND FORM ERECTION

The spiral reinforcing was placed after the full prestress force had been applied to the longitudinal strand. The 12-in. (305 mm) diameter void in the center of the pile was formed using a cardboard tube. The cardboard tubes were hung from short lengths of steel angles that were bolted to the top of the forms. These steel angles also served to hold the cardboard tube down during the concrete pour. The exterior sides of piles were formed by a steel pan with an open top. The forms could not be broken apart, hence the piles were removed by lifting them up out of the forms.

A.2.4 INSTALLATION OF INSTRUMENTATION

Carlson strain meters were installed adjacent to the strands in four locations at mid-span after the final tensioning of the strands. The location of the strain gauges are shown in Figures A.4 and A.5. The strain meters on the lower face of the pile were Carlson model A-10 gauges while those on the sides and top face were Carlson model M-8. The model A-10 was used on the lower face because it is a heavier, more rugged strain meter than the M-8 and was better able to withstand fabrication procedures. Each of the strain gauges was taped to the inside face of the strand using duct tape.

The Carlson strain meter has the capacity to measure both longitudinal strains and temperature. The meter contains two coils of steel wire, one of which increases in length and electrical resistance when a deformation occurs, while the other decreases with deformation. The ratio of the two resistances is independent of temperature, except for thermal expansion, and therefore the change in resistance ratio is proportional to strain. The total resistance is independent of strain since one coil increases the same amount as the other decreases due to change in length of the body of the meter. Thus, the total resistance is proportional to temperature.

After installation, each strain gauge was tested to insure it was functioning correctly. Each of the strain meters were read after casting to verify that no damage resulted from the fabrication procedures.

Just before the prestressing strands were cut, a longitudinal line of Whittemore mechanical strain gauge points were glued to the top surface of each pile at both ends, as shown in Figure A.6 and A.7. Sika Dur epoxy manufactured by Sika Corporation was used to glue the gauge points. The gauge points were spaced exactly 5 in. (127 mm) apart, between 5 in. (127 mm) and 60 in. (1.52 m) from the ends of the piles. Using various pairs of Whittemore points, concrete surface strains were measured using a 10-in. (254-mm) Whittemore gauge within the first 60 in. (1.52 m) of each pile end. Concrete surface strain readings were used to determine the strand transfer length required for full development of the prestress strand in the concrete. The longitudinal distance from the ends of the pile at which the concrete surface strains became somewhat uniform provided an indication of the transfer length.

A.2.5 CASTING AND CURING

The concrete was mixed in the fabricator's batch plant located adjacent to the pile casting bed. The batch plant had a single four cubic yard (3.1 m^3) Helzel pan type central mixer.

The fine aggregate was initially weighed to the required amount after adjustments were made for the free moisture content. The coarse aggregate was then cumulatively weighed with the fine aggregate in the scales located above the central mixer. The cement was weighed in another set of scales also located above the central mixer. The fly ash and silica fume were added using weighed bags. Water and admixtures were added and controlled by an automatic dispenser/meter. The scales and automatic dispenser had been calibrated less than three months before the date of fabrication. The weighing dials on the batching equipment were graduated in the following increments: cement, 5 lb (2.27 kg); aggregate, 20 lb (9.07 kg); water, 1 lb (0.45 kg).

The concrete was mixed in four yard batches and then placed into a screw type transporter, taken to the casting bed and placed in the forms. Each pile segment required slightly less than four cubic yards of concrete, hence each member was cast from a separate batch of concrete.

Casting of the pile specimens began at 9:40 a.m. on March 5, 1991 and was completed at 10:45 a.m. on the same day. The daytime temperature on the day of casting ranged from 60 degrees to 75 degrees F. After casting, internal vibration of the concrete using hand held vibrators was performed carefully so as not to damage any of the strain meters on the strands. Short segments of strand were embedded in the pile segment to provide lifting eyes. The pile specimens, along with the control specimens, were cured for approximately 24 hours under a tarpaulin consisting of two layers of waterproof canvas containing a 1/4-in. (6.4 mm) layer of foam insulation sandwiched between. No steam curing was used.

A.2.6 RELEASE OF PRESTRESS

Approximately 21 hours after casting, a control cylinder representing each of the three concrete batches/pile specimens was removed from the casting bed to the plant testing laboratory, and tested to determine compressive strength. A minimum of 5,000 psi (34.5 MPa) was required before release of the prestress. The average compressive strength of the three cylinders tested was 5,515 psi (38 MPa), thus the strength was satisfactory for release of the prestress.

The prestress was released by cutting the strands with an acetylene torch simultaneously at the dead and live end of the casting bed and then in between each of the pile specimens. The strain meters measurements were taken and recorded just before and after release.

A.2.7 TRANSPORTING AND HANDLING OF THE PILE SPECIMENS

Immediately following release of the strands, the pile segments were lifted out of the forms and transported to another location in the casting yard. A wooden frame was built around the strain meter wire leads that extended from the concrete to protect them while in transit. The control specimens remained with the pile segments until the time of shipment. Seven days after release, the pile segments were loaded onto a flatbed truck and transported to Construction Technology Laboratories, Inc. (CTL) in Skokie, Illinois. The control specimens were shipped on the same vehicle packed in a wooden crate containing Styrofoam packing material.

The pile segments and the control specimens were stored indoors at CTL. The pile specimens were handled using the lifting inserts installed at the time of casting.

A.3 LOAD TESTING

A.3.1 TEST SETUP

The pile specimens were simply supported with a total clear span length of 22 ft (6.71 m). Between the pile and the support was a 2-in. (51-mm) diameter, 24-in. (610 mm) long rod between two 24-in. x 6-in. x 1-in. (610-mm x 102-mm x 32- mm) steel plates. The 2-in. (51-mm) rod was free to act as a roller at one end of the span and was welded to act as a knife edge support at the opposite end.

Loads were applied to each pile at two points spaced three feet apart at mid-span. At each of these two locations, a steel tube crosshead was placed across the top of the pile specimen. One end of a threaded rod was connected to the end of each crosshead and the opposite end of the rod was connected to the laboratory floor. Each threaded rod passed through a 100-ton (890-kN) hydraulic jack and a 100-kip (445-kN) load cell located between the crosshead and the upper connection point. The laboratory strong floor was used to react the loads applied to the pile specimens. The loading configuration of the pile specimens is shown in Figures 5 and A.8.

A.3.2 DEFLECTION MEASURING EQUIPMENT

To determine deflections during each load increment, two linear potentiometers were located at mid span. The potentiometers used for these tests are calibrated annually and have an accuracy of plus or minus one percent of the working range. At each increment of load, the digital data acquisition system automatically recorded the pile deflections.

A.3.3 OTHER PREPARATIONS PRIOR TO TESTING

Before each test, the piles were labeled with the test specimen number at each end. The strain meters, load cells, and potentiometers were connected to a Hewlett Packard 3497A digital data acquisition system (DDAS). The DDAS was connected to a Hewlett Packard 9836 computer for all data storage and processing. All data was stored on a floppy disk to provide a permanent record of test specimen behavior.

A.3.4 TEST PROCEDURE

Before the application of any load, readings were recorded for the strain meters and the deflection potentiometers. Loads were applied to the pile specimens in increments of approximately 4,000 lb (17.8 kN). At each load increment, the deflections and strain measurements were automatically recorded. The loads for initial flexural cracking, flexure-shear cracking and ultimate capacity were noted. Cracks were marked with a paint pen and identified with a number corresponding to the increment of loading. Photographs were taken during the test and after failure to provide a permanent record of crack development. A complete test of each specimen required three to four hours. Immediately prior to testing a pile specimen, the pile's control cylinder specimens were tested.

A.3.5 DISMANTLING OF THE TESTED PILE SPECIMENS

After the photographs were taken, the failed pile specimen was removed from the supports and placed on the lab floor for a last photograph showing all three specimens. Once this was completed, the failed specimens were loaded on a truck for proper disposal.

TABLE A.1
GRADATION ANALYSIS OF FINE AND COARSE AGGREGATE

Fine Aggregate - Campbell Sand

Sieve #	Weight Retained	Percent Retained	Percent Passing
3/8"	0	0	100
#4	15	3	97
#8	61	11	89
#16	110	21	79
#30	183	34	66
#50	326	61	39
#100	482	91	9
Pan	532		

Coarse Aggregate - #67 Stone from Calera Quarry

Sieve #	Weight Retained	Percent Retained	Percent Passing
1-1/2"	0	0	100
1"	0	0	100
3/4"	101	4	96
1/2"	783	33	67
3/8"	1363	58	42
#4	2193	93	7
#8	2301	98	2
Pan	2357		

TABLE A.2
CONCRETE MIX PROPORTIONS
(Per Cubic Yard)

Components	Mix Designation (Same as Pile Designation)		
	P1	P2	P3
Cement	755 lb	756 lb	754 lb
Flyash	79 lb	70 lb	70 lb
Silica Fume	50 lb	50 lb	50 lb
Water	175 lb	175 lb	206 lb
Sand	974 lb	976 lb	976 lb
Stone	1,915 lb	1,915 lb	1,913 lb
Water Reducer	0 oz	0 oz	0 oz
Air Entrainment	17.5 oz	17.5 oz	17.5 oz
High Range Water Reducer	157 oz	157 oz	157 oz

*Fabricator recorded a free moisture on the sand of 5percent and 0 percent on the stone.

Metric Equivalent

1 lb = 0.454 kg

1 oz = 29.574 cc

TABLE A.3
CONCRETE MATERIAL PROPERTIES

Pile No.	Concrete Age	Compressive Strength psi	Modulus of Elasticity ksi	Splitting Tensile Strength psi	Modulus of Rupture psi
P1	Release	5,210	4,900	--	--
	28 days	7,400	5,550	575	720*
	56 days	7,660	5,350	494	733
	169 days**	9,790	--	--	--
P2	Release	5,480	5,950	--	--
	28 days	7,900	6,000	670	750*
	56 days	8,290	5,950	694	883*
	169 days**	9,730	--	--	--
P3	Release	5,855	6,200	--	--
	28 days	8,410	5,750	690	665
	56 days	8,250	5,530	592	817*
	169 days**	9,810	--	--	--

Metric Equivalent: 1 ksi = 1000 psi = 6.895 MPa
* Test specimen fractured beneath loading point
** 4-in (102-mm) x 8 in. (203-mm) cores taken from the pile specimens.

TABLE A.4
PRESTRESSING STRAND MATERIAL PROPERTIES

Sample	Area sq. in.	Load @ 1% Extension, lbs.	Breaking Strength, lbs.	Total Elongation, %	Modulus of Elasticity, ksi
Beginning #1	0.151	38,800	42,400	5.9	29,150
Beginning #2	0.151	39,000	42,600	6.5	29,950
Beginning #3	0.151	38,000	42,600	7.2	29,150
Beginning #4	0.151	39,000	42,700	6.1	29,650
End #1	0.151	39,000	42,400	6.1	29,650
End #2	0.151	38,400	42,200	6.0	29,900
End #3	0.151	38,800	42,600	6.6	28,900
End #4	0.151	39,000	42,600	5.9	28,000

Metric Equivalents:

1 sq. in. = 645.2 sq. mm
1 lb = 0.454 kg
1 ksi = 6.895 MPa

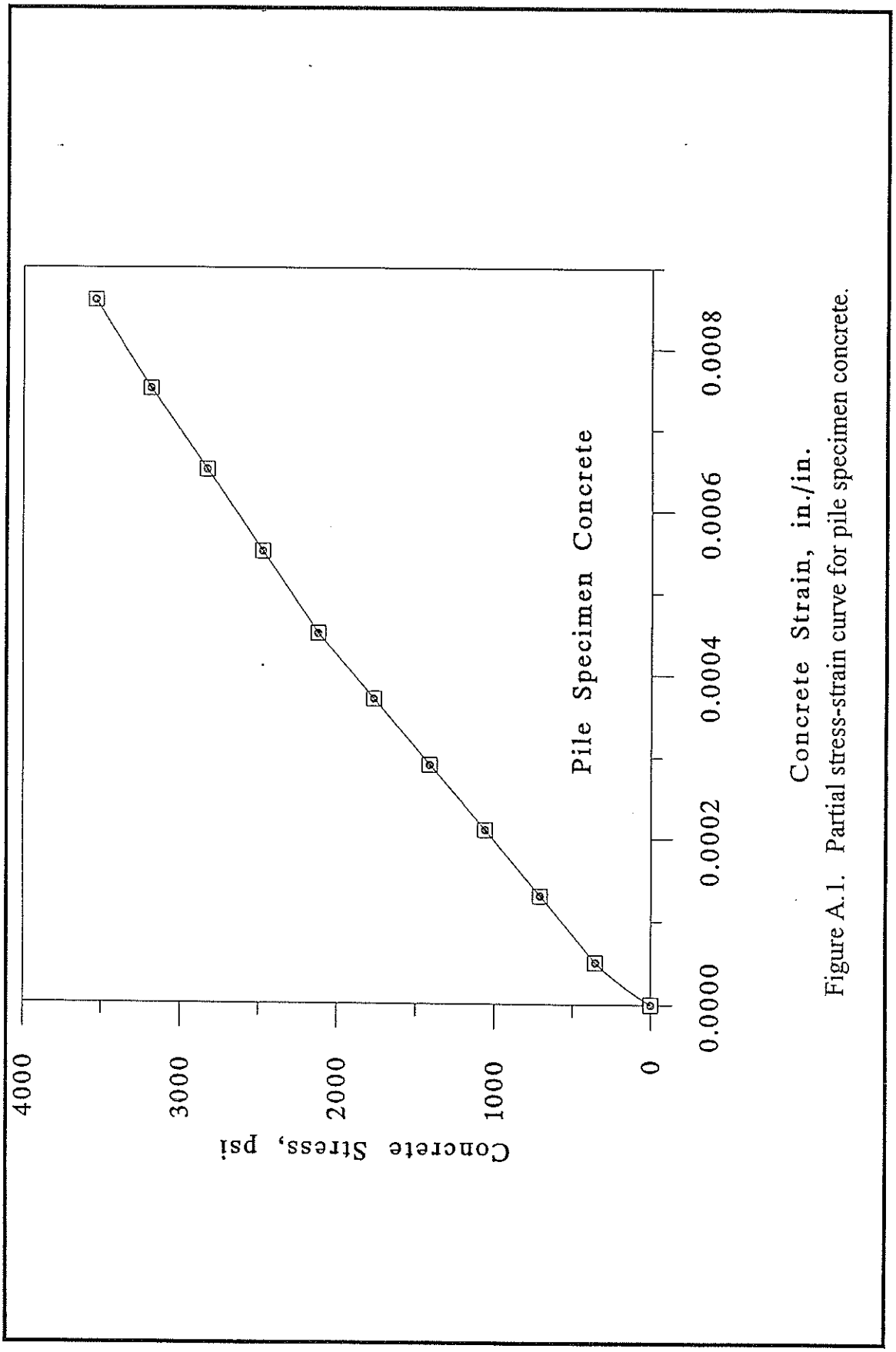

Figure A.1. Partial stress-strain curve for pile specimen concrete.

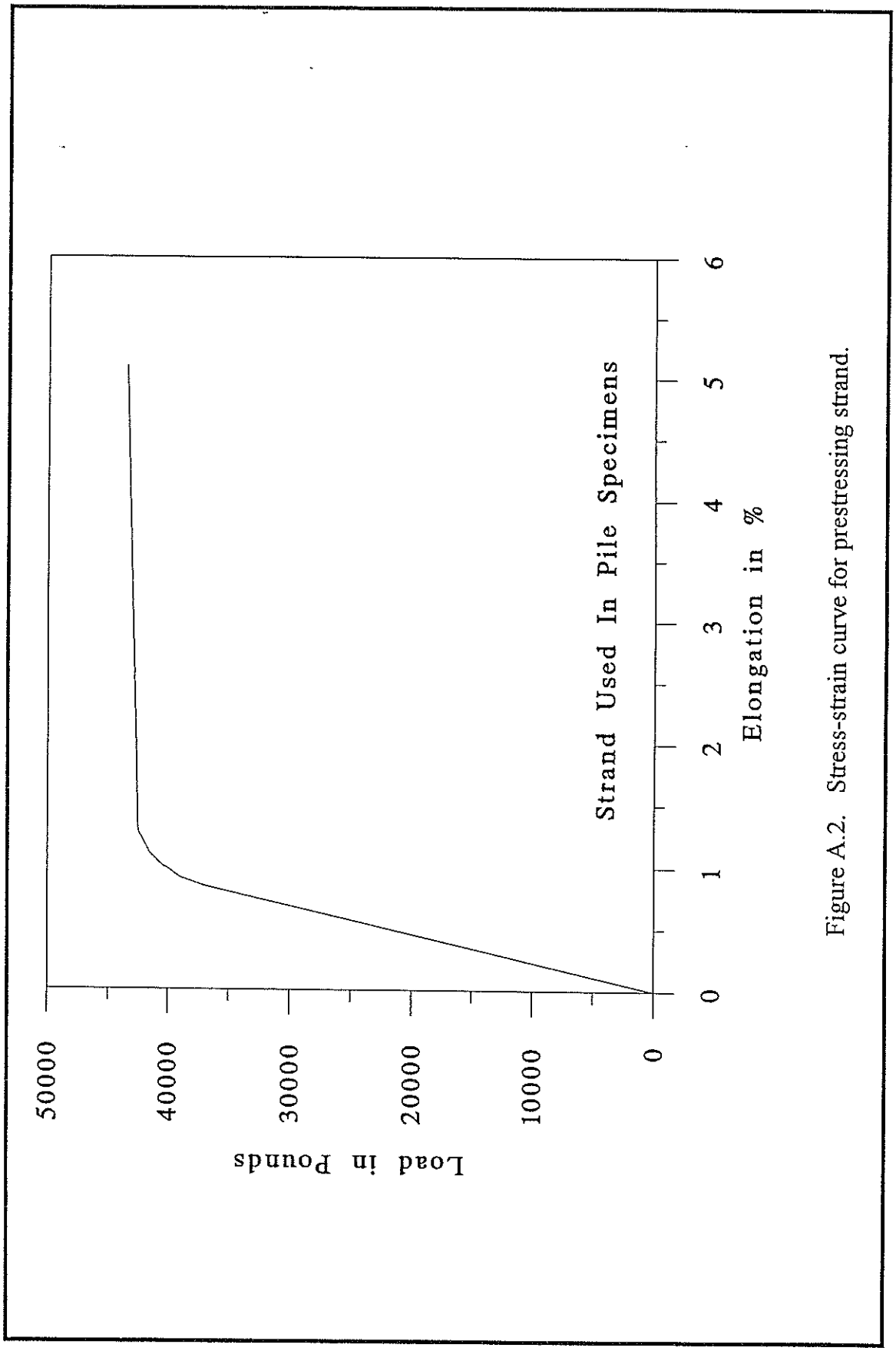

Figure A.2. Stress-strain curve for prestressing strand.

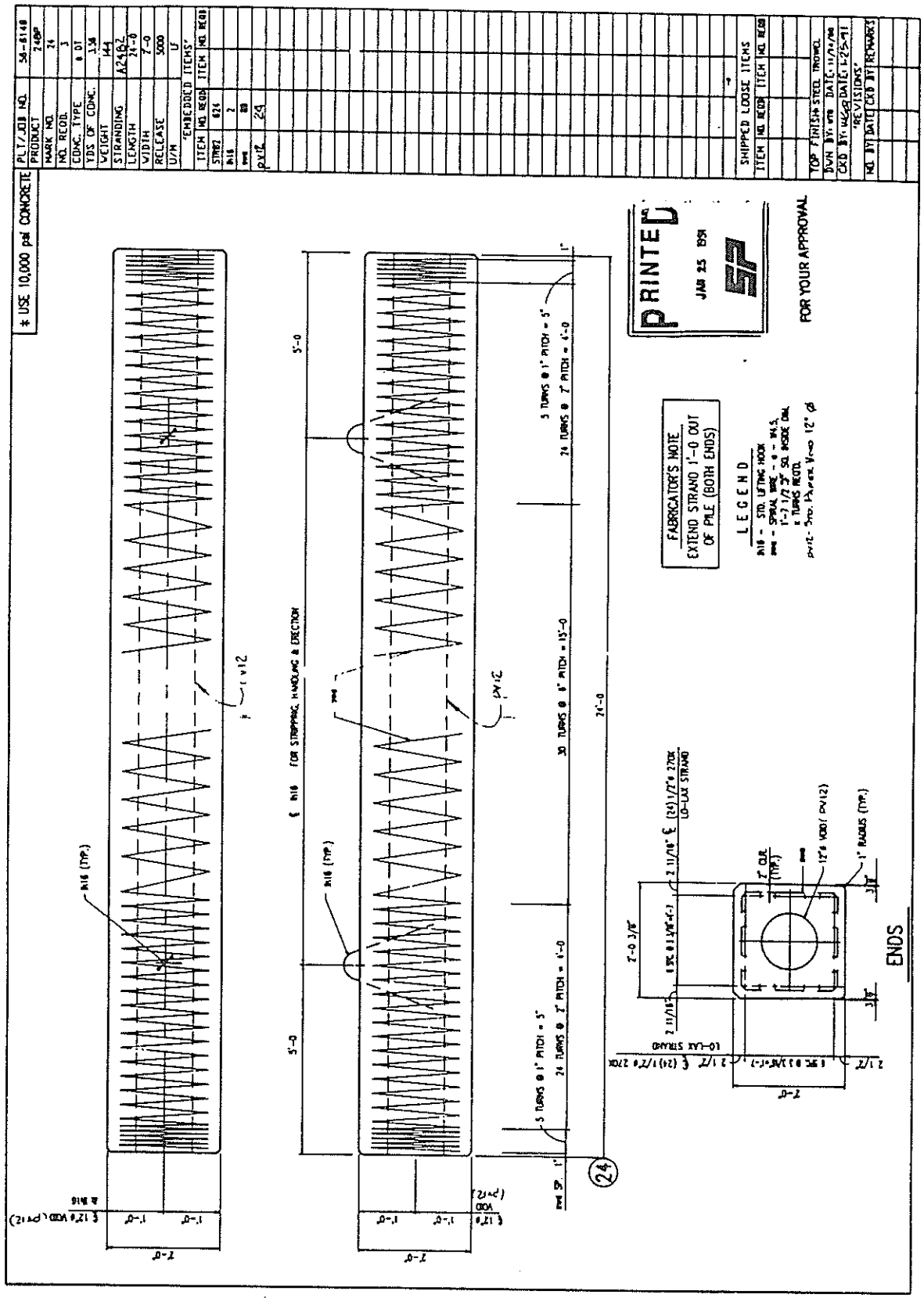

Figure A.3 Shop drawing for laboratory pile specimens P1, P2, and P3.

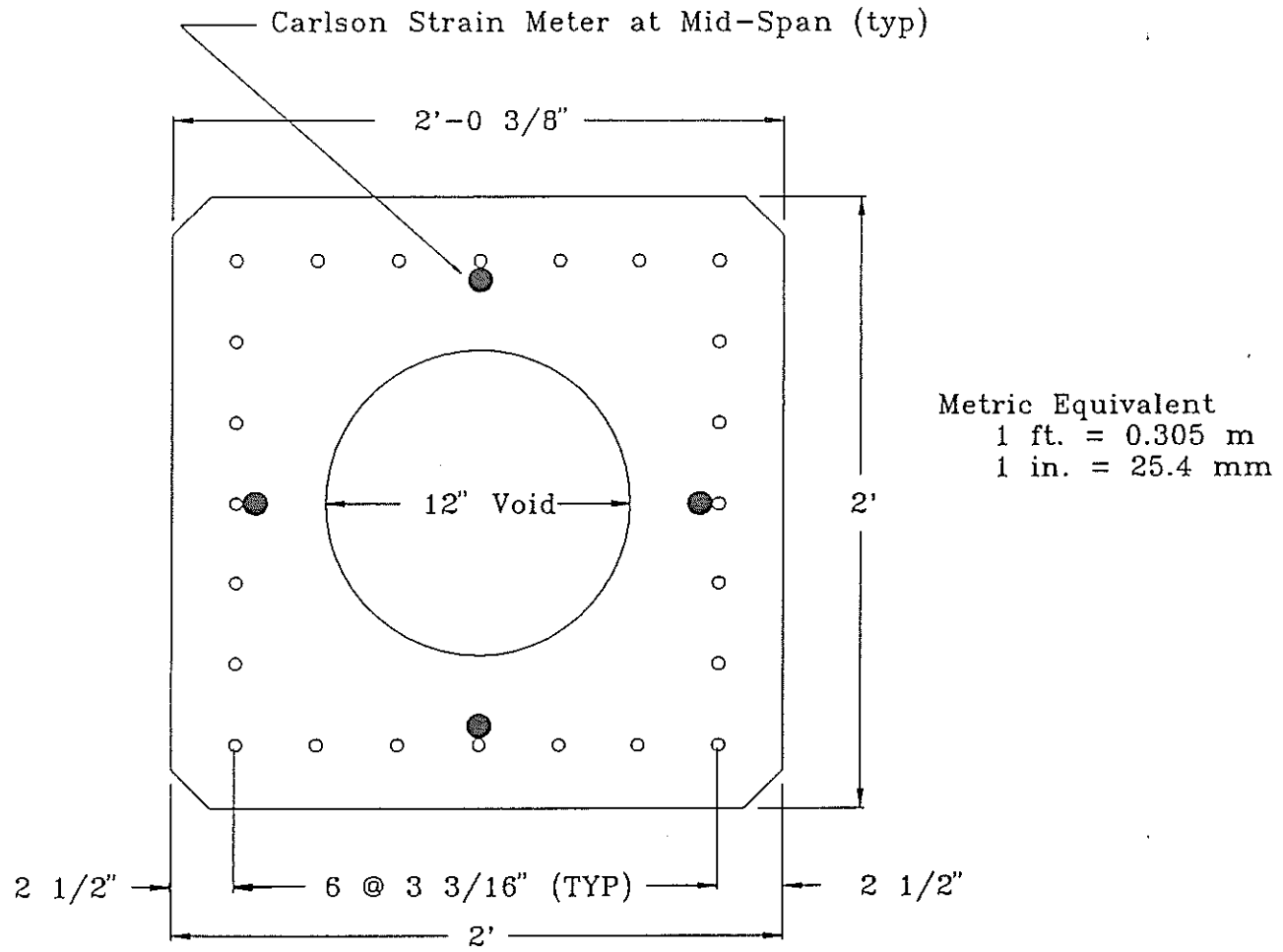

Figure A.4. Location of strain meters.

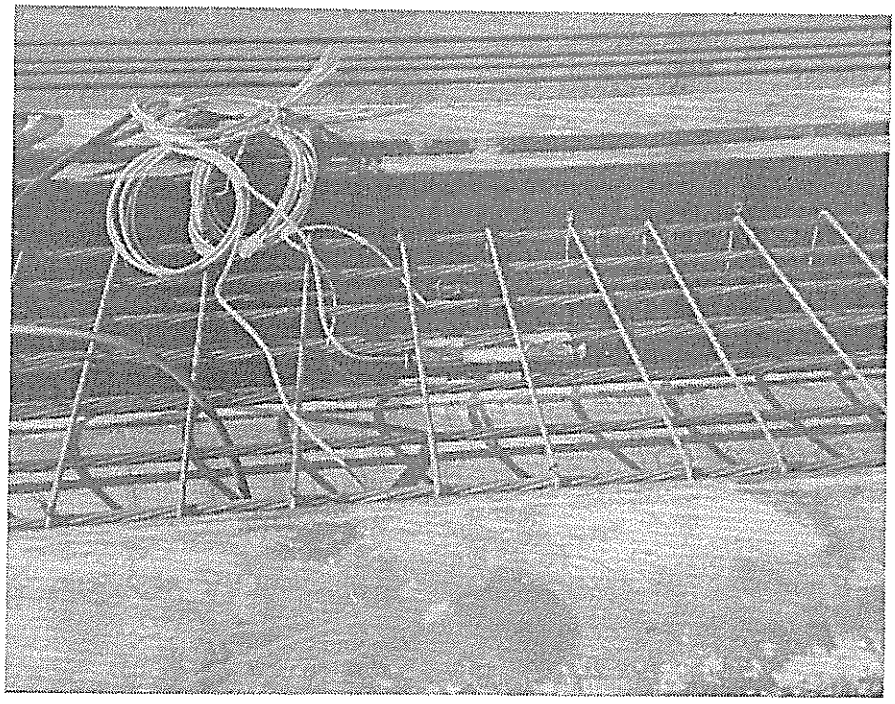

Figure A.5 View of Carlson strain meters.

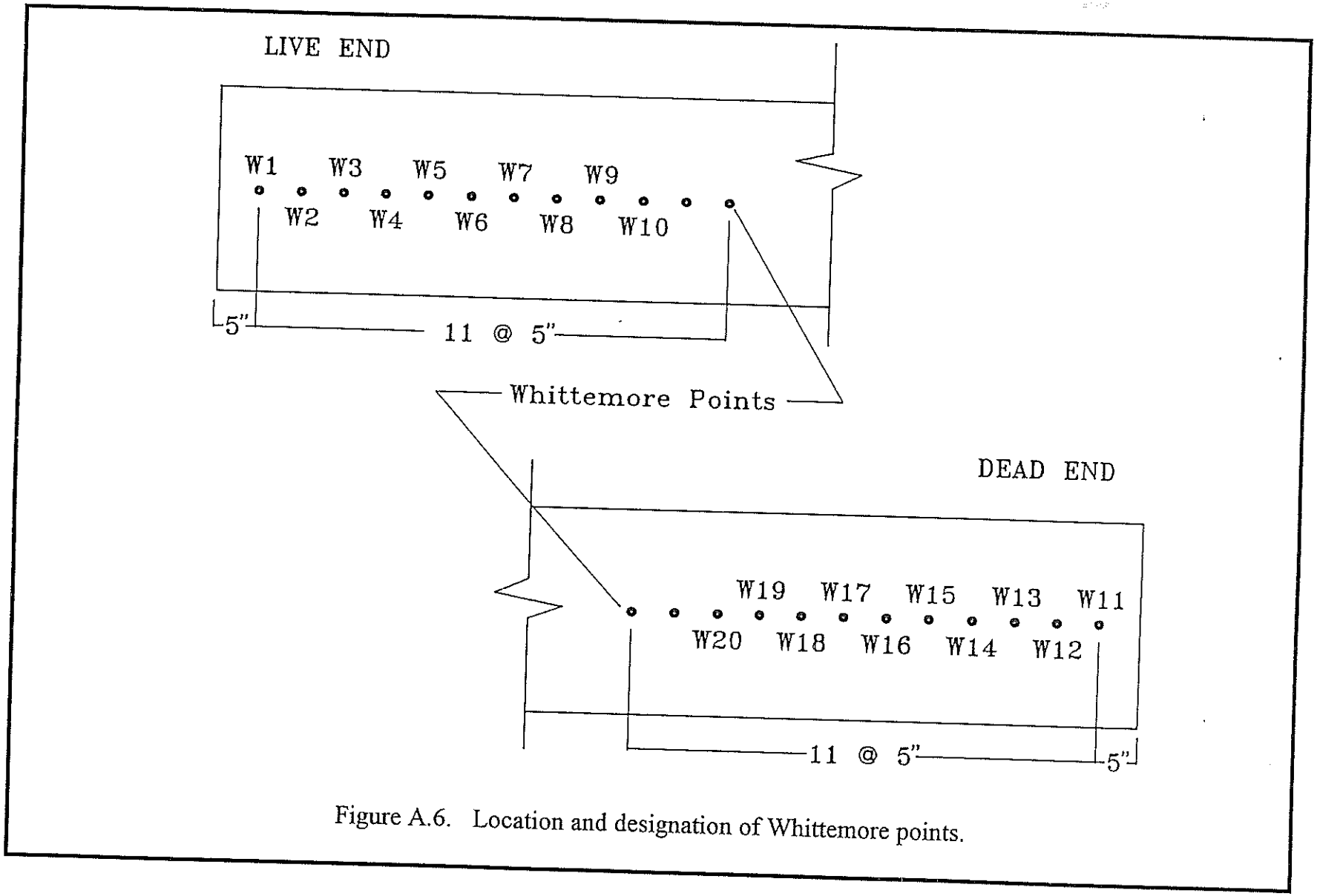

Figure A.6. Location and designation of Whittemore points.

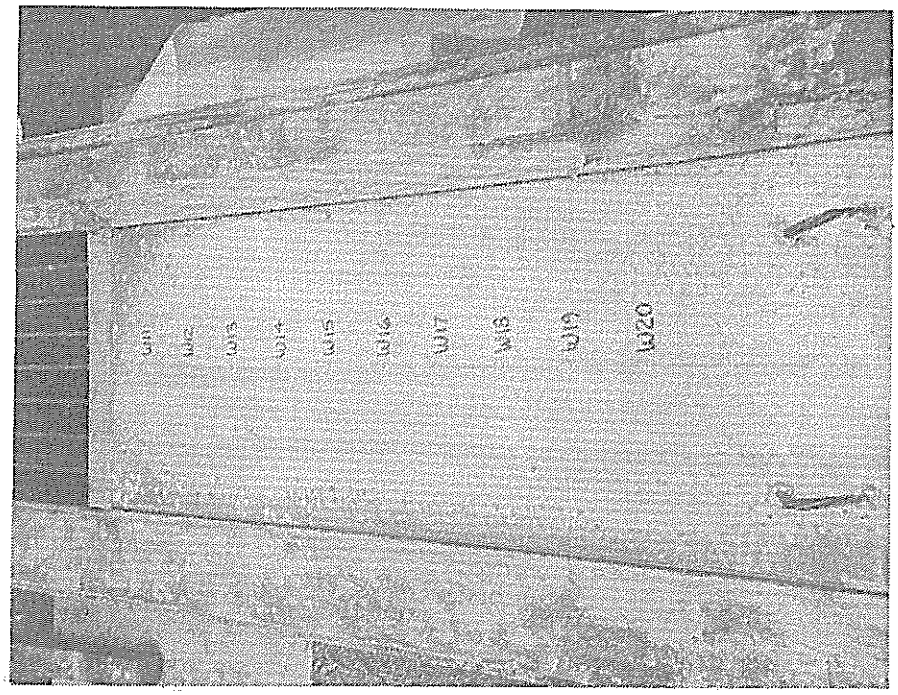

Figure A.7 View of Whittemore points.

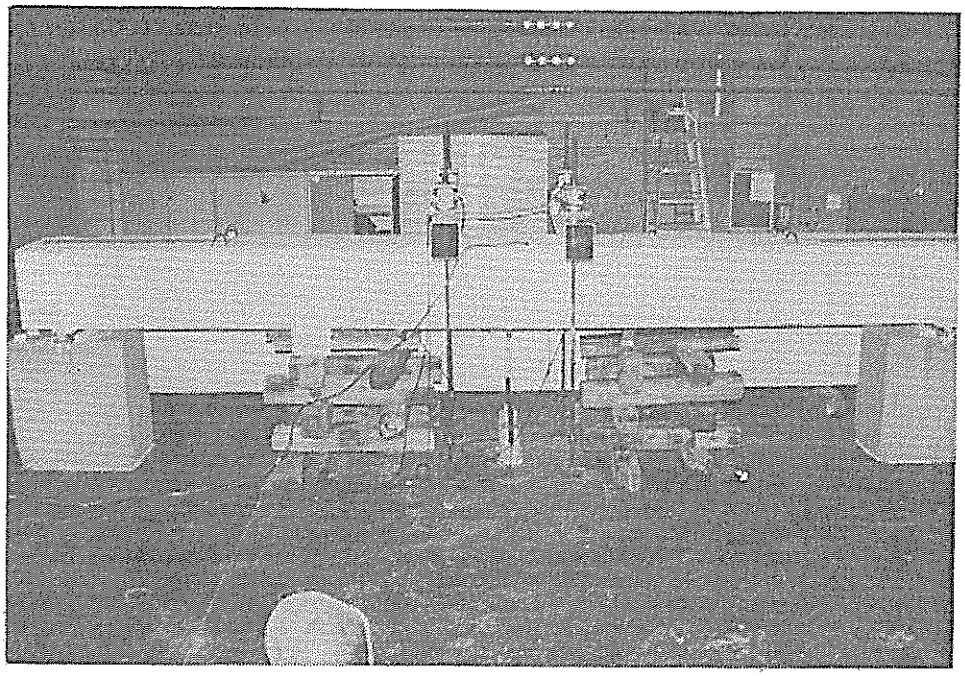

Figure A.8 View of test setup for pile specimens.

APPENDIX B

MATERIALS, FABRICATION AND TESTING PROCEDURES FOR THE BULB-TEE TEST SPECIMENS

B.1 MATERIALS

B.1.1 AGGREGATE

The sand for the concrete mix used in the bulb-tee girders was obtained from Superior Sand in Jemison, Alabama. The coarse aggregate was obtained from Vulcan Stone in Helena, Alabama. Both aggregates were tested and found to be in conformance with the Louisiana Department of Transportation and Development (LaDOTD) Standard Specifications (31) for aggregates. Sieve analyses of the aggregate used is reported in Table B.1.

B.1.2 CEMENT

Type III portland cement was used for all bulb-tee test specimens. The cement was manufactured by the Citadel corporation and was certified to conform to ASTM Standard C150-89 , Specifications for Portland Cement (32).

B.1.3 WATER

The water used in the concrete was obtained from the city water supply of Pelham, Alabama. The water conformed to LaDOTD Standard Specifications for water used in portland cement concrete.

B.1.4 ADMIXTURES

Four admixtures manufactured by W. R. Grace & Co. were used in the concrete mix. These were as follows:

1. W.R.D.A. 79 high range water reducer conforming to ASTM C494-90 (33) Type A & D. This item is on the LaDOTD Qualified Products List as #5832.

2. DARAVAIR air entraining admixture conforming to ASTM C260-86 (34). This item is on the LaDOTD Qualified Products List as #5850.

3. W.R.D.A. 19 Superplasticizer conforming to ASTM C-494-90 as a Type A, or as a Type F admixture. This item is on the LaDOTD Qualified Products List as #5866.

3. FORCE 10,000D silica fume - densified 100 percent solids. Since silica fume is still considered experimental by the LaDOTD this product is not on the Qualified Products List.

B.1.5 CONCRETE MIX

The mix design was developed through a series of laboratory tests performed by the Louisiana Transportation Research Center and field tests performed by the fabricator. The mix was designed to yield a nominal 28-day compressive strength of 10,000 psi (69 MPa). The proportions of the mix developed in the laboratory are shown in Table B.2. This mix design was developed using a 6 ft^3 (0.17 m^3) mixer manufactured by the Gilson Company. The fabricator determined that the laboratory mix designs were not workable using full scale batching. Therefore, the fabricator made some modifications to the mix design which are also shown in Table B.2.

Several concrete control specimens were made from each batch of concrete placed in the bulb-tee specimens. Two 6-in. x 6-in. x 22-in. (152-mm x 152-mm x 559-mm) modulus of rupture beams were made from the concrete batches placed in the middle third of each of the bulb-tee specimens.

The compressive strength and modulus of elasticity at the time of release for each bulb-tee specimen are given in Table B.3. Tests were performed on one cylinder from each batch. The tests were performed at the University of Alabama at Birmingham Department of Civil Engineering. A typical stress/strain curve used to determine modulus of elasticity is shown in Figure B.1.

Compressive strength, modulus of elasticity, poisson's ratio, splitting tensile strength, and thermal coefficient of expansion test conducted at concrete ages of seven days, 28 days, 40 days, and 56 days are reported in Table B.4. Also included in Table B.4 are results from compressive strength, splitting tensile strength, and modulus of rupture tests conducted at an age corresponding to the time of girder testing (approximately 40 days). Tests were performed on one cylinder from each concrete batch. Modulus of rupture tests were conducted on two beam specimens per girder, both taken from the batch placed in the middle third of the girder.

In addition to the tests on the standard cylinder specimens, a 2.7 in. (68.6 mm) diameter core was taken from the girders BT1 and BT2 in the area of each of the three batches of concrete that comprised each girder. The results of these test are also shown in Table B.4. These cores were tested in accordance with ASTM C42-90 (21) at an age of 54 days.

Concrete compressive strength tests were conducted in accordance with ASTM C39-86 (22). Modulus of elasticity and poisson's ratio tests were conducted in accordance with ASTM C469-87 (23). Splitting tensile strength tests were conducted in accordance with ASTM C496-90 (24). Modulus of rupture

tests were conducted in accordance with ASTM C78-84 (25). Thermal coefficient of expansion tests were conducted in accordance with CRD-C39-81. (38).

B.1.6 PRESTRESSING STRAND

The low relaxation prestressing strand used in the bulb-tee specimens was domestically manufactured and was obtained from American Spring Wire Corp. of Bedford Heights, Ohio. The nominal diameter of the strand was 1/2 in. (12.7 mm). The strand conformed to ASTM A-416-88, Specifications for Uncoated Stress Relieved Wire for Prestressed Concrete (36).

A complete stress-strain curve for the production lot from which the project strand was drawn was provided by the manufacturer. This stress-strain curve is reproduced in Figure B.2. Additional tensile tests were performed on sixteen strand samples, four from the beginning of each of the two coils the strand was drawn, and four from the end of each coil. These tensile tests were conducted only to determine one percent elongation load, ultimate strength, and modulus of elasticity. The one percent elongation load and ultimate strengths of the samples ranged from 39,600 lbs lbs (176 kN) to 40,600 lbs (181 kN), and from 43,100 lbs to 44,100 lbs (196 kN), respectively. The results of the tensile tests on all sixteen samples are listed in Table B.5. Strand tensile tests were conducted in accordance with ASTM A370-90a, Supplement IV (37).

B.1.7 WEB REINFORCEMENT

The No. 4, grade 40, web reinforcement used in the bulb-tee specimens was domestically manufactured by Birmingham Steel Corporation of Flowood, Mississippi. The average yield strength and tensile strength, as determined by the manufacturer, were 52,500 psi (362 MPa) and 77,500 psi (534 MPa), respectively.

B.2 FABRICATION

The bulb-tee specimens were fabricated by Sherman Prestressed Concrete at their plant in Pelham, Alabama in accordance with the shop drawings shown in Figure B.3. The three bulb-tee specimens were fabricated in a single 326 ft 8 in. (99.63 m) casting bed. All work was performed by the fabricator except for installation of the instrumentation. All phases of the bulb-tee specimen fabrication and preparation of the control specimens were observed and supervised by the research personnel to insure all quantities and measurements were known accurately.

B.2.1 PLACING OF THE LONGITUDINAL STRAND

The seven wire prestressing strands were drawn from two reels located in an outdoor storage area adjacent to the casting bed. Each strand was taken from the reel and threaded through a template at each end of the casting bed. Intermittent pick-up and hold-down points were positioned to establish the desired strand drape pattern for the six strands coincident with the girder web. The strands were tensioned using a single strand jack manufactured by G. T. Bynum. Calibration tests were not available for the jack, however, the accuracy was verified from load cells placed on selected strands.

B.2.2 PRESTRESSING OF THE STRAND

In accordance with the present AASHTO code, each strand was initially stressed to a value of 0.75 f_{pu} or 30,980 lb (138 kN). In order to accomplish this, the strands were initially tensioned to a proof load of 3,000 lb (13.4 kN). Once this was done, the straight strands were marked and stressed to an average elongation of 25.56 in.(649 mm). Of this elongation, 0.5 in. (12.7 mm) is assumed

to be lost in slippage at the dead end and in seating losses at the live end. In the case of the draped strands, the elongation beyond proof load was calculated to be 20.59 in. (523 mm) with 0.5 in. (12.7 mm) lost in slippage and seating losses, and 4.99 in. (127 mm) gained due to pulling the strand up at the drape-points. The load corresponding to this elongation can be obtained from the following expression:

$$e = \frac{PL}{AE} \tag{29}$$

where

e	=	elongation of strand, in.
P	=	load per strand, lb
L	=	nominal length between stressing ends, in.
E	=	Strand modulus of elasticity - 28,500,000 psi

Using the above expression the load in the straight strand beyond the proof load is calculated to be 27,970 lb. (125 kN). When the proof load is added to this value, a total force of 30,970 lb (138 kN) per strand results. Load cells were placed on selected strands, as shown in Figures B.4 and B.5 to verify jacking loads.

B.2.3 PLACING OF WEB REINFORCEMENT AND FORM ERECTION

The web reinforcing was placed in accordance with the shop drawings after the full prestress force had been applied to the straight and draped strands. The exterior form for the bulb-tee specimens were made of steel and attached to the casting bed at the bottom with adjacent sides tied together across the top.

B.2.4 INSTALLATION OF INSTRUMENTATION

Carlson strain meters were installed adjacent to the strands at the level of the strand pattern centroid in three locations across the bottom flange at mid-span after the final tensioning of the strands. In addition to the Carlson meters, two 1/4-in (6.4-mm) diameter reinforcing bars instrumented with weldable wire strain gauges were installed near the top and bottom surfaces of each girder at mid span. The location of the strain gauges and strain meters can be seen in Figures B.6 through B.8. The strain meters were Carlson model A-10. The welded wire strain gauges were model AWC-8b manufactured by Tokyo Sokki Kenkyujo Company, Ltd. After installation, each strain gauge and strain meter was monitored to insure it was functioning correctly.

Each of the strain gauges and strain meters was also read after casting to determine if any damage had resulted from the casting operation.

Just prior to placing the girder side forms in position, aluminum strips were attached to the forms along one side of the casting bed using 5/32 in. (4 mm) brass bolts. These aluminum channels had attached Whittemore points spaced at five inches (127 mm) on center between zero and 60 in. (1,524 mm) from each girder end. The forms were then placed on the casting bed. Just before the forms were stripped, the nuts holding the channels were removed. The forms were then removed leaving the channel with the Whittemore points embedded in the lower flange of the girder at each end and in the web of Girder BT3 adjacent to the draped strands. The channel was then disconnected and removed leaving only the brass Whittemore points remaining embedded in the concrete. These points were placed at the locations shown in Figure B.9. Using the various pairs of Whittemore points, concrete surface strains were measured using a 10-in. (254-mm) Whittemore gauge within the first 60 in. (1,524 mm) of each girder end. Concrete surface strain readings were used to determine the strand transfer length

required for full development of the prestressing strand in the concrete. The longitudinal distance from the ends of the girder at which the concrete surface strains became somewhat uniform provided an indication of the transfer length.

B.2.5 CASTING AND CURING

The concrete was mixed in the fabricator's batch plant located adjacent to the pile casting bed. The batch plant had a single 8 yd^3 (5.9 m^3) drum type mixer.

The mixer was initially charged with the coarse aggregate, the silica fume, the Daravair, 66 percent of the high range water reducer, and about 90 percent of the water. The drum was then turned for about two minutes. Next, the cement, sand, water reducer and the remainder of the high range water reducer and water were added and mixed for approximately one more minute. Aggregate was initially weighed to the required amount after adjustments were made for the free moisture content. The silica fume was added using weighed bags. Water and admixtures were added and controlled by an automatic dispenser/meter. The scales and automatic dispenser had been calibrated within the year prior to the date of fabrication.

On the day of casting, a total of 11, 4-1/4 yd^3 (3.25 m^3) batches were made. The first two batches were disposed of due to unacceptable slump levels. The last nine batches were cast into the bulb-tee specimens. After mixing each batch was placed into a screw type transporter, taken to the casting bed, and placed into the forms. The location of each batch of concrete was recorded and is shown in Figures B.10 and B.11. Each bulb-tee specimen required slightly less than 12 yd^3 (9.17 m^3) of concrete, hence each member was cast from three separate batches of concrete. The proportions of the 4-1/4 yd^3 (3.25 m^3) batches, by weight, are given in Table B.6.

Casting of the bulb-tee specimens began at 10:30 a.m. on January 22, 1992 and was completed at 1:20 p.m. of the same day. The daytime temperature during the pour ranged from 45 degrees to 55 degrees F. The bulb-tee specimens, along with the control specimens, were steam cured for 24 hours under a tarpaulin consisting of two layers of waterproof canvas containing a 1/4-in. (6.4-mm) layer of foam insulation sandwiched between. The control specimens were also placed under the tarpaulin to undergo the same curing process as the girders. The steam was applied after the concrete had reached initial set. Initial set was defined in accordance with ASTM C 403-90 (39), Time of Setting of Concrete Mixture by Penetration Resistance. Initial set occurred at 8:10 p.m. on January 22, 1992. Steam was turned on immediately after initial set. Temperature probes at two locations along the casting bed indicated a temperature ranging from 120 to 140 degrees F. during the 24 hours of steam application. Steam was cut off at 8:15 p.m. on January 23, 1992 and the specimens were allowed to cool down slowly over the next 12 hours.

During placement, vibration of the concrete was performed carefully so as not to damage any of the internal instrumentation on the strands. Vibration was accomplished using both external form vibrators and hand-held "stinger" vibrators. In order to measure changes in camber, three stainless steel bolts were pressed into the top flange of each specimens prior to the setting of the concrete. One bolt was placed at the center of the longitudinal axis of the specimen while the other two were placed at each end of the specimen directly over the bearing. Short segments of strand were placed at four locations along the specimen to provide lifting eyes.

B.2.6 RELEASE OF PRESTRESS

A control cylinder from each batch used in the fabrication of the bulb-tee specimens was removed from the casting bed and tested to determine compressive

strength. A minimum of 6,000 psi (41.4 MPa) was required before release of the prestress. The average compressive strength of the nine cylinders was 9,250 psi (63.8 MPa), thus the strength was satisfactory for release of the prestress.

Upon removal of the forms, a full-depth vertical crack was discovered near midspan of each of the specimens. The location of the crack was marked. Upon strand release the cracks closed.

The prestress was released by cutting the strands with an acetylene torch. The strain measurements and camber measurements were taken and recorded just before and after release.

B.2.7 TRANSPORTING AND HANDLING OF THE GIRDERS

Immediately following release of the strands, the bulb-tee specimens were lifted from the casting bed and transported to another location in the casting yard. A wooden frame was built around the instrumentation wire leads that protruded from the concrete to protect them while in transit. The control specimens remained with the girder specimens until the time of shipment. Twelve days after release, the bulb-tee specimens were loaded onto tractor-trailer trucks and transported to Construction Technology Laboratories, Inc. (CTL) in Skokie, Illinois. The control specimens were shipped on the same vehicle packed in a wooden crate containing plywood support racks for the cylinders.

The bulb-tee specimens and the control specimens were stored indoors at the CTL facility. The bulb-tee specimens were handled using the lifting inserts installed at the time of casting.

B.2.8 CASTING THE TOP SLAB ON SPECIMENS BT1 AND BT3

Once the bulb-tee specimens had been delivered to the CTL Laboratory preparation was begun to cast the top slab on specimen BT1. The slab was cast on

specimen BT1 at a girder age of 30 days using partially shored construction. Slab reinforcement for BT1 consisted of a single layer of No. 4 bars running longitudinally, spaced at 12 in. (305 mm), and No. 5 bars running transversely, spaced at 12 in. (305 mm). Mild reinforcing bar details for specimen BT1 can be seen in Figure B.12. The top cover on the reinforcing was two inches (51 mm).

The top slab of BT3 was cast at a girder age of 65 days using the same method of forming as used for BT1. The top slab reinforcement consisted of two layers of longitudinal bars in order to more closely represent typical Louisiana Department of Transportation bridge section details. The top layer of longitudinal steel was the same as that of specimen BT1. The second layer of longitudinal steel consisted of No. 5 bars spaced at 6 in. (152 mm). The steel layout of Specimen BT3 is shown in Figure B.13.

The concrete for the top slabs was supplied by a local ready-mix supplier, and was designed to have a minimum strength of 6,000 psi (41.4 MPa) by the time of testing. The concrete was taken from the ready-mix trucks and placed in hoppers that were lifted by the overhead crane in the laboratory. Vibration was used throughout the pouring operation to insure no air pockets in the slab. The slabs were cast in the laboratory and were not steam cured. The slab was covered for three days with a sheet of plastic. The forms were removed three days after casting. Control specimens were made during the casting operation. Three standard 6-in. x 12-in. (152-mm x 305-mm) cylinders were made from the concrete placed at the two ends and middle regions of the slab. A summary of the properties of the concrete in the top slab concrete can be seen in Table B.7. A partial stress-strain curve for the concrete used in the top slab of BT1 can be seen in Figure B.14.

B.3 LOAD TESTING

B.3.1 TEST SETUP

The bulb-tee specimens were simply supported with a total clear span length of 69 ft (21.04 m) for the flexural tests and 27 ft (8.24 m) for the shear tests. Between the girder and the support was a 2-in. (51 mm) diameter, 24-in. (610 mm) long rod between two 24-in. x 6-in. x 1-in. (610-mm x 102-mm x 32- mm) steel plates. The 2-in. (51-mm) rod was free to act as a roller on one end of the span and was welded to act as a knife edge support at the opposite end.

Loads were applied to each flexural specimen at two points spaced twelve feet apart at mid-span. At each of these two locations, a steel tube cross head was placed across the top of the pile specimen. One end of a threaded rod was connected to the end of each cross head and the opposite end of the rod was connected to the laboratory floor. Each threaded rod passed through a 100-ton (890-kN) hydraulic jack and a 100-kip (445-kN) load cell located between the cross head and the upper connection point. The laboratory strong floor was used to react the loads applied to the pile specimens. The loading configuration of the flexural tests on the bulb-tee specimens is shown in Figure 5.

For the shear test the load application equipment was the same. The loads were applied to each of the specimens at four locations as shown in Figure 6.

When the specimens were ready for flexural testing, surface strain gauges were placed on the top flange/slab of each specimen. The surface strain gauge locations used for girder BT1 are shown in Figure B.15, while the strain gauge locations of specimen BT2 are shown in Figure B.16. These polyester strain gauges were model LP-90 manufactured by Tokyo Sokki Kenkyujo Company, Ltd. The areas to receive the strain gauges were ground smooth using a hand held

electric grinder and then coated with a layer of an epoxy/silica fume mixture to fill any existing voids or small pin holes. The hardened epoxy was then ground off leaving a smooth surface. Next the strain gauges were attached to the prepared surface using epoxy and lead wires were attached to the gauges.

B.3.2 DEFLECTION MEASURING EQUIPMENT

To determine deflections during testing, three linear potentiometers were located at mid span. The potentiometers used for these tests are calibrated annually and have an accuracy of plus or minus one percent of the working range. At each increment of load, the digital data acquisition system automatically recorded the bulb-tee deflections.

B.3.3 DIAL GAUGES ON THE PRESTRESSING STRAND

To detect any slippage of the longitudinal prestressing strand during the load application, dial gauges were mounted on selected protruding strands at the ends of the girders. The dial gauges were placed on the same strands in each girder. The location of the dial gauges are shown in Figures B.17 and Figure B.18. The dial gauges could be read to the nearest 0.0001 in. (0.00254 mm)

B.3.4 OTHER PREPARATIONS PRIOR TO TESTING

Before each test, the girders labeled with the test specimen number at each end. The instrumentation wires were then connected to a Hewlett Packard 3497A digital data acquisition system (DDAS). The DDAS was connected to a Macintosh computer for all data storage and processing. All data was stored on a hard drive to provide a permanent record of test specimen behavior.

B.3.5 TEST PROCEDURE

Before the application of any load, initial (zero) readings were recorded for all instrumentation.

Load was applied to the bulb-tee specimens in increments of approximately 5,000 lb (11,000 kg) for the flexural tests and 10,000 lb (22,000 kg) for the shear tests. At each load increment the deflections and strain measurements were automatically recorded. The loads for initial flexural cracking, flexure-shear cracking, and web-shear cracking, and ultimate capacity were noted. Cracks were marked with a paint pen and identified with a number corresponding to the increment of loading. Photographs were taken during the test and after failure to provide a permanent record of crack development. A complete test of each flexural specimen required from eight to ten hours. Shear tests required from two to three hours. Prior to flexural testing a bulb-tee specimen, the control specimens for that member were tested to define test day concrete material properties.

B.3.6 DISMANTLING OF THE TESTED BULB-TEE SPECIMENS

After the completion of all tests, the bulb-tee specimens were removed from the supports. Cores were then taken from the web of each girder specimen. Once this was completed the failed specimens were loaded on a truck for proper disposal.

TABLE B.1
GRADATION ANALYSIS OF FINE AND COARSE AGGREGATE

Fine Aggregate - Superior Sand

Sieve #	Weight Retained	Percent Retained	Percent Passing
3/8"	0	0	100
#4	10	2	98
#8	45	9	91
#16	81	16	84
#30	198	40	60
#50	448	90	10
#100	495	99	1
Pan	500		

Coarse Aggregate - #67 Stone from Helena Quarry

Sieve #	Weight Retained	Percent Retained	Percent Passing
1-1/2"	0	0	100
1"	0	0	100
3/4"	250	5	95
1/2"	--	--	--
3/8"	3751	72	28
#4	5085	98	2
#8	5175	99	1
Pan	5227		

TABLE B.2
CONCRETE MIX PROPORTIONS - LABORATORY AND FIELD TESTS

	Mix Designation	
Components, lbs	Laboratory Tests (per yd^3)	Field Tests (per yd^3)
Cement	752 lb	752 lb
Silica Fume	82 lb	83 lb
Water	188 lb	225 lb
Sand	1104 lb	1185 lb
Stone	1952 lb	2030 lb
Water Reducer	240 oz	35 oz
Air Entrainment	16-20 oz	7 oz
Superplasticizer		210 oz

Metric Equivalents

1 sq. in. = 645.2 sq. mm
1 lb = 0.454 kg
1 ksi = 6.895 MPa

TABLE B.3
MATERIAL PROPERTIES OF CONCRETE USED IN BT SPECIMENS
(At the Time of Strand Release)

Test Age	Batch No.	Compressive Strength		Modulus of Elasticity	
		Individual psi	Average psi	Individual ksi	Average ksi
36 hours	1-1	10,201	9,229	6,542	6,005
	1-2	9,092		6,902	
	1-3	9,075		5,769	
	2-1	9,547		5,864	
	2-2	9,430		5,978	
	2-3	8,955		6,165	
	3-1	8,598		6,096	
	3-2	9,461		5,462	
	3-1	8,703		5,271	

Metric Equivalents
1 ksi = 1000 psi = 6.895 MPa

TABLE B.4
MATERIAL PROPERTIES OF CONCRETE USED IN BT SPECIMENS
(At 7, 28, 40, and 56 Days)

Test Age	Batch No.	Compressive Strength		Modulus of Elasticity		Poisson's Ratio		Splitting Tensile Strength		Thermal Coefficient		Modulus of Rupture
		Individual psi	Average psi	Individual ksi	Average ksi	Individual	Average	Individual psi	Average psi	Individual millionths	Average Millionths	psi
	1-1	10,030		6,500		0.21		720		4.60		
	1-2	–		6,150		0.18		700		4.00		
	1-3	9,220		5,800		0.21		690		6.20		
	2-1	9,320		6,200		0.22		690		6.10		
7 days	2-2	9,130	9,413	5,850	6,078	0.18	0.20	700	678	6.10	5.8889E-06	
	2-3	8,990		5,800		0.21		650		6.10		
	3-1	9,370		6,150		0.23		680		7.90		
	3-2	9,720		6,150		0.17		700		5.80		
	3-3	9,520		6,100		0.17		570		6.20		
	1-1	10,240		6,400		0.19		680		6.00		
	1-2	9,710		6,100		0.22		670		4.30		
	1-3	9,460		5,800		0.21		650		5.70		
	2-1	9,600		5,900		0.22		740		6.10		
28 days	2-2	9,750	9,790	6,150	6,050	0.20	0.20	690	718	5.80	5.78	
	2-3	9,570		5,900		0.16		730		5.80		
	3-1	9,770		6,050		0.18		800		5.90		
	3-2	10,200		6,150		0.23		780		6.00		
	3-3	9,810		6,000		0.22		720		6.40		
	1-1	10,300						650				
	1-2	9,570						670				812
40 days	1-3	9,260	9,742					610	688			
	2-1	9,650						770				
	2-2	9,900						790				837
	2-3	9,770						640				
	1-1	10,300		6,200		0.21		670		3.70		
	1-2	9,630		5,900		0.24		630		6.40		
	1-3	9,890		5,700		0.22		670		5.90		
	2-1	9,850		5,950		0.22		760		5.40		
56 days	2-2	9,430	9,858	6,050	5,983	0.22	0.22	730	694	3.70	4.67	
	2-3	9,700		5,850		0.22		680		5.30		
	3-1	9,730		5,900		0.23		730		6.40		
	3-2	10,110		6,150		0.21		740		1.50		
	3-3	10,080		6,150		0.24		640		3.80		
	1-1	10,000										
CORES	1-2	9,720										
TAKEN AT	1-3	8,560	9,683									
AGE	2-1	9,960										
54 days	2-2	10,230										
	2-3	9,630										

Metric Equivalent: 1 ksi = 1000 psi = 6.895 MPa

TABLE B.5
PRESTRESSING STRAND MATERIAL PROPERTIES

Sample	Area sq. in.	Load @ 1% Extension, lbs.	Breaking Strength, lbs.	Total Elongation, %	Modulus of Elasticity, ksi
COIL 78976					
Beginning #1	0.153	39,600	43,100	6.7	28,700
Beginning #2	0.153	40,500	44,100	6.4	28,900
Beginning #3	0.153	40,200	43,800	7.5	30,950
Beginning #4	0.153	40,500	43,600	6.5	30,800
End #1	0.153	40,400	43,600	6.5	30,400
End #2	0.153	---	43,600	7.4	29,950
End #3	0.153	40,500	44,000	7.1	30,550
End #4	0.153	40,000	43,200	7.2	28,450
COIL 78979					
Beginning #1	0.153	40,400	43,800	7.7	30,200
Beginning #2	0.153	40,600	43,800	6.3	31,950
Beginning #3	0.153	40,200	43,800	6.1	28,850
Beginning #4	0.153	40,400	43,900	7.3	30,550
End #1	0.153	40,500	43,800	7.0	31,150
End #2	0.153	40,200	43,800	6.7	29,600
End #3	0.153	39,600	43,600	6.9	29,350
End #4	0.153	40,100	43,700	6.6	29,800

Metric Equivalents:

1 sq. in. = 645.2 sq. mm
1 lb = 0.454 kg
1 ksi = 6.895 MPa

TABLE B.6
MIX PROPORTIONS USED IN SPECIMEN FABRICATION
(Per Cubic Yard)

	Mix Designation								
	Specimen BT1			Specimen BT2			Specimen BT3		
Item	Batch 1-1	Batch 1-2	Batch 1-3	Batch 2-1	Batch 2-2	Batch 2-3	Batch 3-1	Batch 3-2	Batch 3-3
Cement	753.0 lb	753.0 lb	753.0 lb	753.0 lb	753.0 lb	753.0 lb	753.0 lb	753.0 lb	753.0 lb
Silica Fume	82.3 lb	82.3 lb	82.3 lb	82.3 lb	82.3 lb	82.3 lb	82.3 lb	82.3 lb	82.3 lb
Water*	21.6 gal	21.6 gal	21.6 gal	21.2 gal	20.5 gal	20.0 gal	19.8 gal	19.5 gal	19.5 gal
Sand	1233.0 lb	1232.0 lb	1233.0 lb	1233.0 lb	1233.0 lb	1233.0 lb	1233.0 lb	1233.0 lb	1233.0 lb
Stone	2049.0 lb	2215.0 lb	2049.0 lb	2049.0 lb	2049.0 lb	2049.0 lb	2049.0 lb	2049.0 lb	2049.0 lb
Water Reducer	42.4 oz	56.5 oz	56.5 oz	56.5 oz	56.5 oz	56.5 oz	56.5 oz	56.5 oz	56.5 oz
Air	7.0 oz	7.0 oz	7.0 oz	7.0 oz	7.0 oz	6.1 oz	6.1 oz	6.1 oz	6.1 oz
Super-Plasticizer	209.0 oz	209 oz	209.0 oz	209.0 oz	209.0 oz	209.0 oz	209.0 oz	209.0 oz	209.0 oz

*Tests for "free" moisture on the aggregates revealed 3.9% free moisture on the sand and 1.0% free moisture on the stone.
Metric Equivalents:

1 lb = 0.454 kg
1 gal = 3.785 l
1 oz = 29.574 cc

TABLE B.7
MATERIAL PROPERTIES OF CONCRETE USED IN BT1 TOP SLAB

Test Age	Batch No.	Compressive Strength		Modulus of Elasticity		Poisson's Ratio	
		Individual psi	Average psi	Individual ksi	Average ksi	Individual	Average
10 days	Live-1	6,440	7,037	4,950	4,694	0.20	0.23
	Live-2	5,970		4,700		0.22	
	Live-3	5,920		4,500		0.20	
	Mid-1	7,370		4,700		0.23	
	Mid-2	7,560		4,800		0.24	
	Mid-3	7,640		4,700		0.24	
	Dead-1	7,520		4,650		0.25	
	Dead-2	7,400		4,600		0.21	
	Dead-3	7,510		4,650		0.25	

Metric Equivalents:

1 ksi = 1000 psi = 6.895 MPa

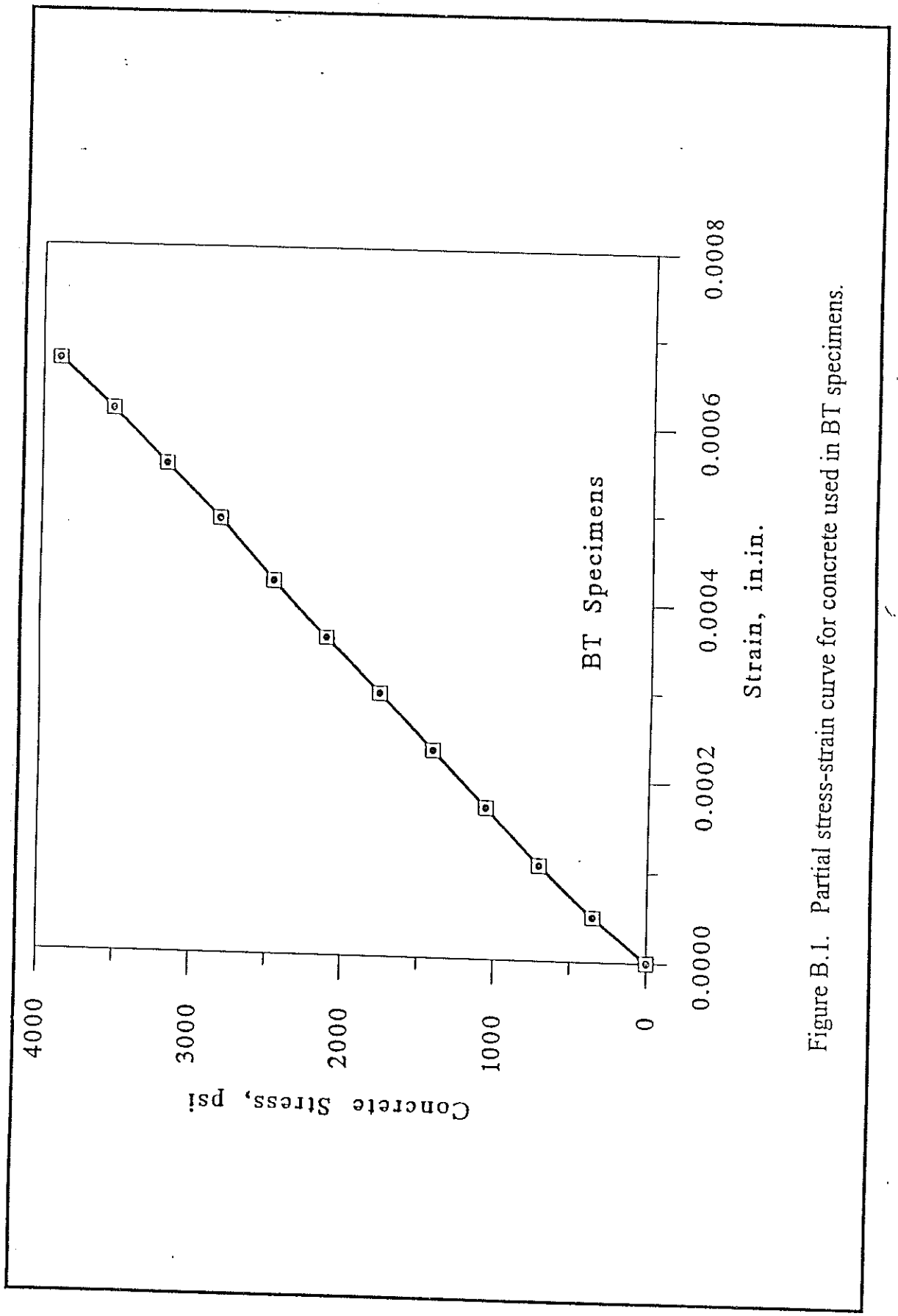

Figure B.1. Partial stress-strain curve for concrete used in BT specimens.

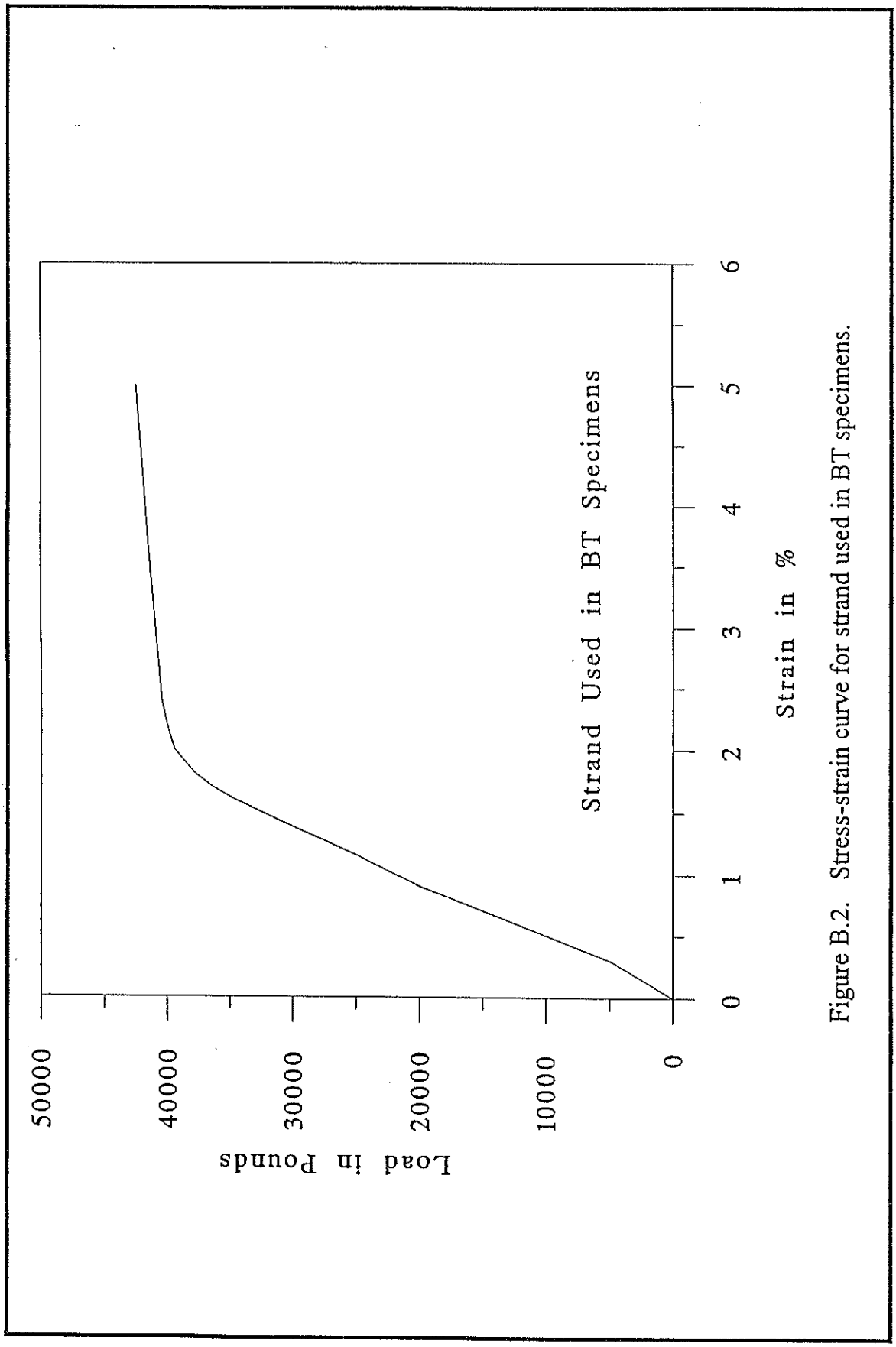

Figure B.2. Stress-strain curve for strand used in BT specimens.

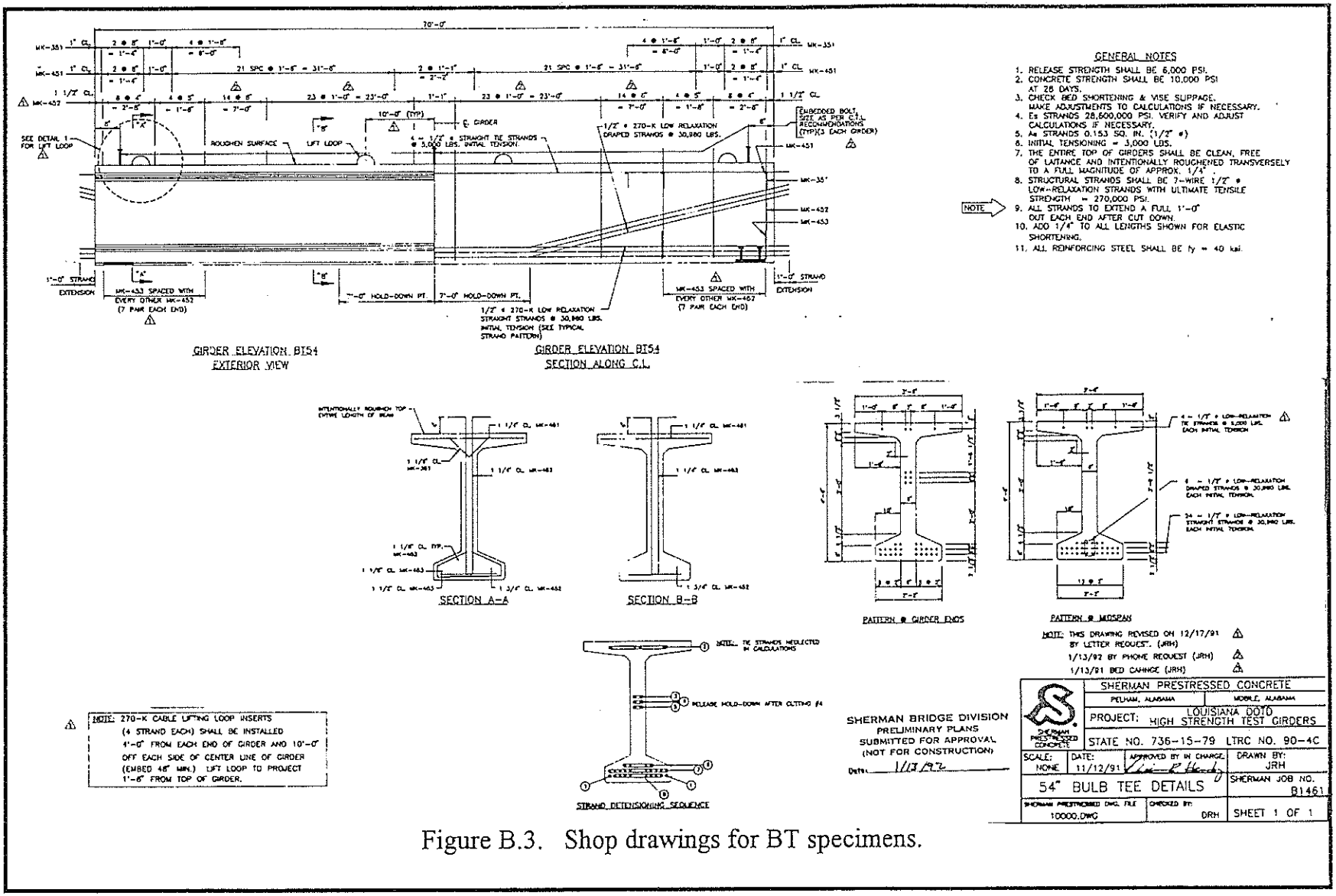

Figure B.3. Shop drawings for BT specimens.

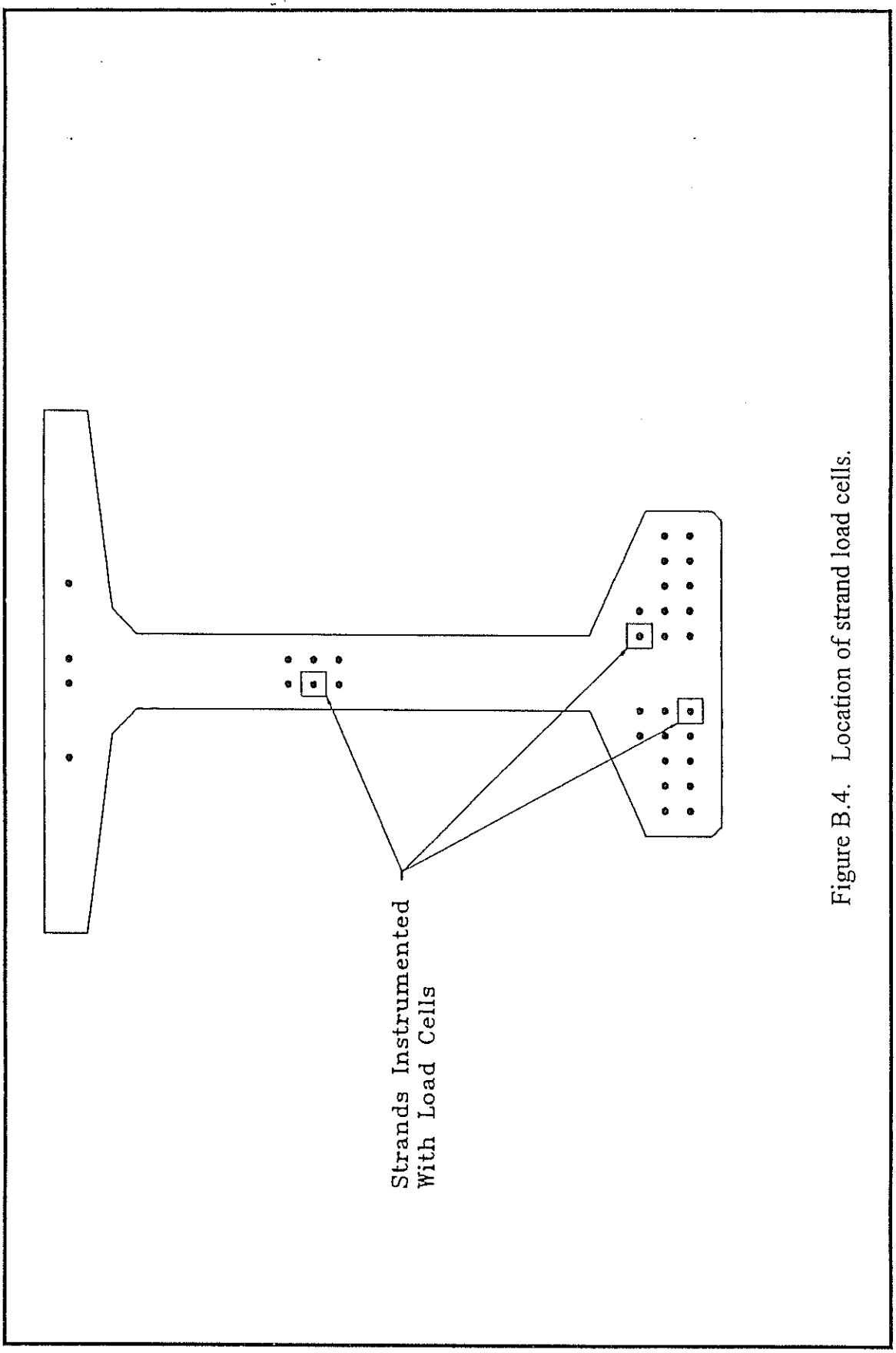

Figure B.4. Location of strand load cells.

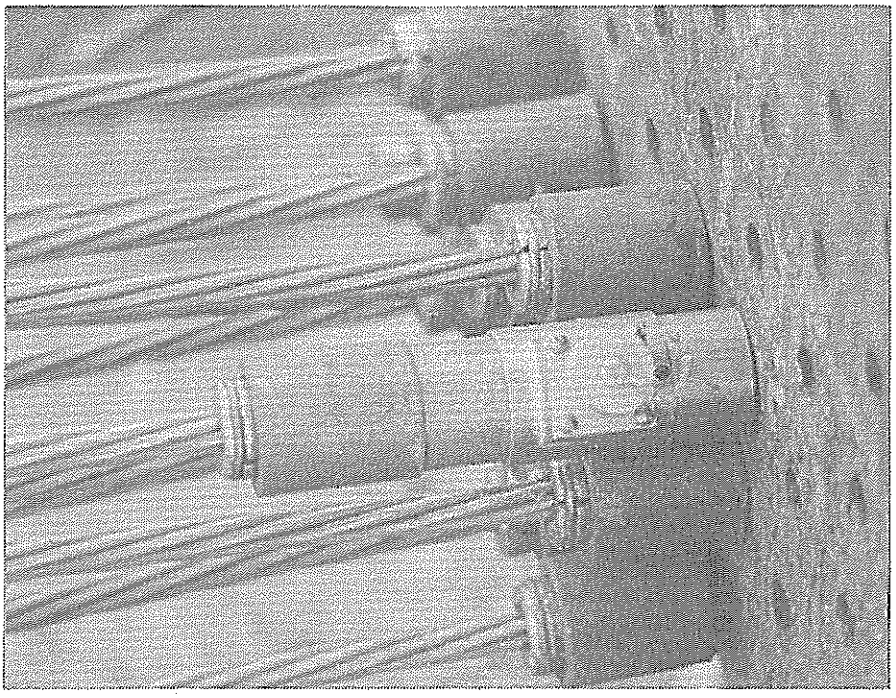

Figure B.5 View of strand load cells.

grew in width and number. As can be seen in Figure 40, just prior to failure, an area of spalling began over the cut-end support bearing of the specimen resulting in the complete failure of the member.

The load-deflection relationship for the mid-span of specimen BT1-L is shown in Figure 41. As in the case of specimen BT1-D, after several increments of load had been applied to the specimen, preexistent cracks that resulted from the flexural test on BT1 began to open at the cut end of member and extend towards the top and bottom flange. These cracks propagated toward the support bearing and continued to grow in length and width. When the cracks extended through the lower flange, the linear relationship between the applied load and deflection was disturbed as shown in Figure 41. The first crack that could be classified as a load induced web-shear crack formed at the cast-end of the member at a shear load of 422.7 kips (1,880 kN). Figures 42 and 43 show that as additional load was applied to the member additional cracks formed at the cut end of the member and the cracks at the opposite end of the member grew in width and number. As can be seen in Figure 44, just prior to failure, spalling began to take place over the cut end support bearing resulting in the failure of the specimen.

The load-deflection relationship for the mid-span of specimen BT2-L is shown in Figure 45. This member did not have the preexisting cracks in the area of the cut end of the member. The first web shear crack formed at the cast end of the member at a shear load of 327.6 kips (1,457 kN). Figures 46 and 47 show that as additional load was applied to the member additional cracks formed at the cast end, and the member eventually failed when cracks ran through the bottom flange at the support bearing. Just prior to failure, spalling occurred over the cast end support bearing. Strand slippage of some of the lower strands occurred at the cast end of the member just prior to member failure.

B. Modes of Failure

Specimens BT1-D and BT1-L failed due to shear-compression failure of the web as a result of the extension and widening of preexistent web cracks. These preexistent cracks resulted from the flexural test on member BT1. The failure did not occur at the end of the member being test for web-shear cracking

Specimen BT2-L failed due to shear compression failure of the web due to web cracking. There was also evidence of bond failure of the strands at the formed end of the member The web in the vicinity of the bearing failed in compression.

8. ANALYSIS OF TESTS OF BULB-TEE SPECIMENS

8.1 INTRODUCTORY REMARKS

The purpose of this chapter is to compare the observed behavior of the bulb-tee test specimens with their expected theoretical behavior. Section 8.2 compares the laboratory measured concrete properties with those predicted using equations contained in the AASHTO and ACI documents. Section 8.3 contains a discussion of flexural cracking. Inclined cracking is discussed in section 8.4. Flexural strength is considered in section 8.5, while shear strength of the specimens is discussed in section 8.6. Section 8.7 contains a discussion of transfer length, camber, and prestress losses. Section 8.8 summarizes the comparisons of the test results with the current procedures of the AASHTO and ACI documents.

8.2 PROPERTIES OF CONCRETE

Sufficient tests were performed to evaluate those mechanical properties of the concrete necessary to predict behavior of structural members. These properties are listed in Tables B.4 and B.5 of Appendix B. In the present AASHTO and ACI documents, standard equations have been developed to predict the modulus of elasticity and modulus of rupture based on the compressive strength of the concrete. These equations are based primarily on investigations performed for concrete with compressive strengths of less than 6000 psi (41 MPa). For this reason ACI published Report no. ACI 363R-84, a State-of-the-Art Report on High-

Strength Concrete (23), listing alternate equations proposed by Carrasquillo (16). These equations are shown in Table 17.

TABLE 17
COMPARISON OF MATERIAL PROPERTY EQUATIONS
ACI 318-89/AASHTO VERSUS ACI 363-84

Property	ACI 318-89/ AASHTO	ACI 363
Modulus of Elasticity	$E_c = w_c^{1.5}\ 33\sqrt{f'_c}$ psi	$E_c = 40,000\sqrt{f'_c} + 1 \times 10^6$ psi
Modulus of Rupture	$f_r = 7.5\sqrt{f'_c}$ psi	$f_r = 11.7\sqrt{f'_c}$ psi

Using the above equations with the measured concrete compressive strength, the 28-day mechanical properties of the concrete used in specimens BT1, BT2 and BT3 were calculated. The mechanical properties developed using these equations and the mechanical properties determined in the laboratory are presented in Table 18. The measured results agree more closely with the ACI/AASHTO values than with ACI 363 values.

TABLE 18
MEASURED VS. CALCULATED MECHANICAL PROPERTIES
(Based on 28-Day Strength)

Specimen	Compressive Strength	Property	Measured	ACI 318/ AASHTO	ACI 363
BT1	9,803 psi	Mod. of Elasticity	6,100 ksi	6,000 ksi	4,960 ksi
		Mod. of Rupture	812 psi	742 psi	1,158 psi
BT2	9,640 psi	Mod. of Elasticity	5,983 ksi	5,950 ksi	4,927 ksi
		Mod. of Rupture	838 psi	736 psi	1,149 psi
BT3	9,927 psi	Mod. of Elasticity	6,066 ksi	6,040 ksi	4,985 ksi
		Mod. of Rupture		747 psi	1,166 psi

8.3 FLEXURAL CRACKING

In a prestressed concrete flexural member, flexural cracking occurs when the tensile stress resulting from the total applied load exceeds the compression due to the prestress and the modulus of rupture of the concrete at the location of the crack. The load at which flexural cracking occurs may be calculated if the following quantities are known: (1) the effective prestressing force of the longitudinal reinforcement, (2) the cross-sectional properties and weight of the member, and (3) the modulus of rupture of the concrete. The effective prestress force can be determined from the initial jacking loads minus the losses as determined by the strain meter readings taken at the time of the test. The cross-sectional properties can be measured and the modulus of rupture of the concrete can be obtained from standard tests.

The above quantities can be expressed in terms of a resisting moment by an equation of the following form:

$$\mathbf{M_{cr}} = \frac{\mathbf{I}}{\mathbf{y_b}}\left(\mathbf{f_r} + \mathbf{f_{pe}} - \mathbf{f_0}\right) \qquad (12)$$

where

M_{cr} = bending moment due to total applied load at flexural cracking, in.-lb

I = moment of inertia of entire uncracked section, in^4

y_b = distance from the centroid of section to bottom fiber, in.

f_r = modulus of rupture of the concrete used in the region of maximum applied moment, psi

f_{pe} = stress at the bottom of the girder resulting from the effective prestressing force, psi

f_o = flexural stress in the concrete at the bottom face of the beam due to self weight and deck weight where applicable, psi

The total applied load corresponding to formation of the initial flexural crack can also be obtained from the load-deflection relationship of the specimens. As discussed previously in Chapters 5 and 7, the load causing the initial flexural crack disrupts the linear relationship between load and deflection.

In this investigation, the observed cracking moments for a given specimen and the extrapolated values from the moment-deflection curves were approximately the same.

For this investigation, the computed cracking loads, from Eq. (12), were calculated from the measured physical dimensions of the specimens, the measured mechanical properties of the concrete and the measured values of prestress losses. The prestress losses were consistent for the specimens tested with an average value of 10 percent used for each specimen. The computed and observed total flexural cracking moments for the girders are shown in Table 19. The observed cracking moment was arrived at by the following relation:

$$\mathbf{M_{cr} = a\frac{P_{fc}}{2}} \qquad (13)$$

where

P_{fc} = total applied load corresponding to initial flexural cracking, lb

a = length of the shear span, in.

TABLE 19
COMPUTED AND OBSERVED FLEXURAL CRACKING MOMENTS
(Based on Measured Mechanical Properties)

Specimen No.	Computed Cracking Moment		Observed Cracking Moment		Observed/ Computed
	(ft-kip)	(kN-m)	(ft-kip)	(kN-m)	
BT1	3,367	4,569	3,092	4,196	0.92
BT2	2,924	3,968	2,750	3,732	1.06

As in the case of the pile specimens, in order to determine the appropriateness of using AASHTO equations, the cracking moments were calculated again based on the measured physical dimensions and prestress losses, and the AASHTO predicted values for material properties based on the compressive strength of the concrete. These values are shown in Table 20.

TABLE 20
COMPUTED AND OBSERVED FLEXURAL CRACKING MOMENTS
(Based on AASHTO Predicted Mechanical Properties)

Specimen No.	Computed Cracking Moment		Observed Cracking Moment		Observed/ Computed
	(ft-kip)	(kN-m)	(ft-kip)	(kN-m)	
BT1	3,095	4,200	3,092	4,196	1.00
BT2	2,724	3,697	2,750	3,732	1.01

8.4 INCLINED CRACKING

As discussed in Chapter 7, the second significant stage of cracking in the bulb-tee specimens was that of inclined cracking in the shear spans. Flexure-shear

cracking and web-shear cracking of the specimens will be discussed in sections 8.4.1 and 8.4.2 respectively.

8.4.1 Flexure-Shear Concrete Cracking

Specimens BT1 and BT2 were designed to fail in a flexural mode. Shear strength was not a primary consideration of this phase of the investigation. However, the loads resulting in the formation of flexure-shear cracks were noted during the testing and the cracks mapped.

A flexure-shear crack originates as a vertical flexural crack in the shear span and becomes inclined toward the load points. As described in Chapter 5, the flexure-shear crack that typically leads to failure of a beam usually originates in the shear span at a distance from the load point corresponding approximately to the effective depth, d, of the member. The effective depth at midspan of specimen BT1 was 60.9 in. (1,547 mm) while the effective depth of specimen BT2 at midspan was 49.9 in. (1,267 mm).

As discussed in Chapter 6, the ACI code and the AASHTO specifications suggest that the applied shear resulting in the formation of flexure-shear cracks in a prestressed concrete member consists of two basic components; the shear that results in the formation of a flexural crack, $\frac{V}{M}(M'_{cr})$, and the shear required to incline the crack, $0.6\sqrt{f'_c}\, b_w d$. Hence, the total shear, V_{ci}, resulting in the formation of flexure-shear cracks is expressed in the AASHTO specifications and the ACI code as follows:

$$V_{ci} = 0.6\sqrt{f'_c} b_w d + V_d + \frac{V}{M}(M'_{cr}) \qquad (14)$$

where

V_{ci} = total shear producing flexure-shear cracking, lb.

f_c' = strength of the concrete at time of test, psi

b_w = width of the web, in.

d = effective shear depth, in.

V_d = dead load shear at the location under consideration, lb.

M_{cr}' = moment required to cause flexural cracking, in./lb

$\frac{V}{M}$ = shear to moment ratio at location under consideration

In the laboratory, the total shear resulting in an inclined crack of approximately 45 degrees first reaching the uncracked neutral axis of the specimen was considered as the concrete cracking shear, V_{ci}. To verify Equation 14, the crack identified as resulting from V_{ci} was traced to its origin on the tensile face of the member. As in previous research (20), this origin occurred at an approximate distance equal to d from the point of applied load. M_{cr}' was then calculated at this location using Equation 12 for both the measured and AASHTO/ACI predicted values of the modulud of rupture. The calculatated values of M_{cr}' compared to the measured values are listed in Table 21 and Table 22.

TABLE 21

COMPUTED AND OBSERVED FLEXURE-SHEAR CRACKING MOMENT, M_{cr}'
(Based on Measured Mechanical Properties)

Specimen No.	Computed Flexure-Shear Cracking Moment		Observed Flexure-Shear Cracking Moment		Observed/ Computed
	(ft-kip)	(kN-m)	(ft-kip)	(kN-m)	
BT1	3,475	4,715	3,230	4,383	0.93
BT2	2,913	3,953	3,232	4,386	1.11

TABLE 22

COMPUTED AND OBSERVED FLEXURE-SHEAR CRACKING MOMENT, M'_{cr}
(Based on AASHTO Predicted Mechanical Properties)

Specimen No.	Computed Flexure-Shear Cracking Moment		Observed Flexure-Shear Cracking Moment		Observed/ Computed
	(ft-kip)	(kN-m)	(ft-kip)	(kN-m)	
BT1	3,203	4,347	3,230	4,383	1.01
BT2	2,712	3,680	3,232	4,386	1.19

Once the location of the flexure-shear crack was known, and M'_{cr} determined, the total shear, V_{ci}, producing flexure-shear concrete cracking was calculated using Equation 14. The computed and observed shear resulting in flexure-shear concrete cracking are shown in Tables 23 and 24.

TABLE 23

COMPUTED AND OBSERVED SHEAR RESULTING IN FLEXURE-SHEAR CRACKING
(Based on Measured Mechanical Properties)

Specimen No.	Computed Cracking Shear		Observed Cracking Shear		Observed/ Computed
	(kips)	(kN)	(kips)	(kN)	
BT1	192	854	176	783	0.92
BT2	144	640	143	636	0.99

TABLE 24
COMPUTED AND OBSERVED SHEAR RESULTING IN
FLEXURE-SHEAR CRACKING
(Based on AASHTO Predicted Properties)

Specimen No.	Computed Cracking Shear		Observed Cracking Shear		Observed/ Computed
	(kips)	(kN)	(kips)	(kN)	
BT1	180	801	176	783	0.98
BT2	136	605	143	636	1.05

8.4.2 Web-Shear Concrete Cracking

The test set-up for specimens BT1-D, BT1-L and BT2-L was designed to result in the formation of web shear cracks. Due to the conditions of the specimens, mentioned in Chapter 7, only one of the specimens, BT2-L, actually failed in a measurable form of web shear. Web shear cracks form when the principal tensile stresses in the concrete, resulting from the combination of shear and flexural stress, exceed the tensile strength of the concrete. Since concete behavior is reasonably elastic up to failure in tension, calculations may be based upon ordinary equations of elasticity.

Principal stress calculations and tests of typical beams indicate that a web-shear crack may be expected to occur at, or below, the centroid of a concrete section (20,28). Consequently, the shear that will produce web shear cracking may be estimated based on the principal tension at the concrete centroid. Web-shear cracking will occur if the principal tension exceeds the direct tensile strength of the concrete, f_t'.

The principal tensile stresses can be found from Mohr's circle which yields the following relationship:

$$f_t' = \sqrt{v_{cw}^2 + \left(\frac{f_{cc}}{2}\right)^2} - \frac{f_{cc}}{2} \qquad (15)$$

where

v_{cw} = nominal shear stress in the concrete, $V_{cw}/b_w d$, resulting from all applied loads, member weight and applied loads.

f_{cc} = compressive stress at the centroid of the concrete due to the effective prestress

The nominal shear stress, v_{cw}, corresponding to diagonal cracking can be solved yielding

$$v_{cw} = f_t' \sqrt{1 + \frac{f_{cc}}{f_t'}} \qquad (16)$$

The direct tensile strength is taken by ACI and AASHTO to be conservatively equal to $3.5\sqrt{f_c'}$, yielding

$$v_{cw} = 3.5\sqrt{f_c'} \sqrt{1 + \frac{f_{cc}}{3.5\sqrt{f_c'}}} \qquad (17)$$

AASHTO and ACI have chosen to closely approximate Equation 17 using the simpler expression

$$v_{cw} = 3.5\sqrt{f_c'} + 0.3 f_{cc} \qquad (18)$$

The external shear V_{cw}, at which web-shear cracking is likely, is increased by the vertical component of the prestressed force V_p that normally acts in the opposite sense to the load-induced shear. Thus, based on AASHTO and ACI documents

$$V_{cw} = b_w d\left(3.5\sqrt{f_c'} + 0.3f_{cc}\right) + V_p \qquad (19)$$

where

V_{cw} = shear force resulting in web shear cracking, lb.
V_p = vertical component of force in the tendon, lb

The cracking strain of concrete has been reported to be approximately 0.0001 (29). Using this value and the average of the measured values of the modulus of elasticity of the concrete, a tensile stress, f_t', of 600 psi is derived. Using Equation 17 and this value of f_t', a theoretically more precise equation for the shear resulting in web-shear cracking can be derived as shown below.

$$V_{cw} = b_w d\left(600\sqrt{1 + \frac{f_{cc}}{600}}\right) \qquad (20)$$

Equation 20 is only appropriate for the concrete used in the bulb-tees and is shown here only to illustrate the conservativeness of Equation 19. Because of concerns regarding the applicability of Equation 19 to beams fabricated of high-strength concrete, the current version of the ACI Code requires that concretes with strengths greater than 10,000 psi be provided with more web reinforcement. Since the concrete used in the bulb-tees is approximately 10,000 psi, the use of Equation 19 is appropriate.

The computed web-shear cracking loads based on equations 19 and 20 are given in Tables 25 and 26, respectively.

TABLE 25
COMPUTED AND OBSERVED WEB-SHEAR CRACKING LOAD
(Based on ACI/AASHTO Equation)

Specimen No.	Computed Web-Shear Cracking Load		Observed Web-Shear Cracking Load		Observed/ Computed
	(kip)	(kN)	(kip)	(kN)	
BT1-D	257.0	1,143	443.0	1,971	1.72
BT1-L	257.0	1,143	430.0	1,913	1.67
BT2-L	209.0	930	327.0	1,455	1.56

TABLE 26
COMPUTED AND OBSERVED WEB-SHEAR CRACKING LOAD
(Based on a Maximum Tensile Strain of 0.0001)

Specimen No.	Computed Web-Shear Cracking Load		Observed Web-Shear Cracking Loadt		Observed/ Computed
	(kip)	(kN)	(kip)	(kN)	
BT1-D	368.0	1,637	443.0	1,971	1.20
BT1-L	368.0	1,637	430.0	1,913	1.17
BT2-L	298.0	1,326	327.0	1,455	1.10

8.5 SHEAR STRENGTH

As discussed in Chapter 7, only specimen BT2-L failed in shear. However, since bond failure was also evident, the shear load at the time of failure must be considered as an indication of minimum shear strength. The laboratory measured

value of applied shear at the time of failure was 445 kips (2,415 kN). The shear strength at the location of failure was calculated using the following equation recommended in both the AASHTO and ACI standards:

$$V = V_c + V_s \tag{21}$$

where

V	=	Shear strength of the member, lbs
V_c	=	Shear strength provided by the concrete, lbs
V_s	=	Shear strength provided by the reinforcement, lbs

Based on Equation 21, the calculated value of shear strength would be 396 kips (2,150 kN). These two values yield a measured to calculated strength ratio of 1.15. This test indicates that even though the member experienced bond failure at the end, the AASHTO/ACI equations yielded a conservative answer.

8.6 FLEXURAL STRENGTH

The calculated ultimate moment for the bulb-tee specimens was computed using two methods. The first method utilizes the equivalent rectangular stress distribution presented in both the AASHTO Standard Specifications for Highway Bridges (1) and the ACI Building Code Requirement for Reinforced Concrete (ACI 318-89) (2). Since the properties of the concrete and strand were carefully determined, and the loading precisely applied, a reduction factor of unity is applied to the expression. The formula from which the ultimate moment capacity was calculated is

$$M_u = \phi A_{ps} f_{ps} d\left(1 - 0.60\frac{\rho f_{ps}}{f_c'}\right) \quad (22)$$

where

M_u = ultimate resisting moment, in.-lb

A_{ps} = area of prestressed reinforcement in tension zone, in^2

ϕ = capacity reduction factor

d = distance from extreme compression fiber to centroid of prestressing steel, in.

ρ = $\frac{A_{ps}}{bd}$

b = width of compression face of member, in.

f_c' = specified compressive strength of concrete, psi

f_{ps} = calculated stress in prestressing steel at beam failure using the equation shown below:

$$f_{ps} = f_{pu}\left[1 - \frac{\gamma_p}{\beta_1}\left(\frac{\rho_p f_{pu}}{f_c'}\right)\right] \quad (23)$$

where

f_{pu} = tensile strength of prestressing strand, psi

γ_p = factor for type of prestressing strand, 0.28 for f_{py}/f_{pu} not less than 0.90

β_1 = 0.65 for all concrete with f'c greater than 8,000 psi

ρ_p = ratio of prestressed reinforcement

The observed ultimate moment is calculated by the following expression:

$$M_u = \left(\frac{L_{tot}}{2}\right)a + M_{DL} \quad (24)$$

where M_u = observed ultimate moment, in.-lb

L_{tot} = observed total applied load, lb

a = length of shear span, in.

M_{DL} = dead load moment at location of failure, in.-lb

The ultimate moment capacity computed using the method prescribed by AASHTO and ACI for flexural members and the observed total ultimate moment capacity for the specimens are shown in Table 27.

TABLE 27
COMPUTED AND OBSERVED ULTIMATE MOMENT
(based on AASHTO/ACI Equations)

Specimen No.	Computed Ultimate Moment Capacity		Observed Ultimate Moment Capacity		Observed/ Computed
	(kip-ft)	(kN-m)	(kip-ft)	(kN-m)	
BT1	6,170	8,374	6,975	9,467	1.13
BT2	4,870	6,610	4,607	6,253	0.95

As is evident from the above table, the equations normally used for flexural members in the AASHTO and ACI specifications reasonably underestimated the ultimate capacity of the bulb-tee specimen BT1. However, BT2 failed prematurely.

The second method used to compute the ultimate moment capacity of the BT specimens was strain compatibility. The properties of the concrete and strand, as measured in the laboratory, were used in the strain compatibility analysis.

The ultimate moment capacity determined through an analysis based on strain compatibility, is compared to measured quantities in Table 28.

TABLE 28
COMPUTED AND OBSERVED ULTIMATE MOMENT
(Based on Strain Compatibility)

Specimen No.	Computed Ultimate Moment Capacity		Observed Ultimate Moment Capacity		Observed/ Computed
	(kip-ft)	(kN-m)	(kip-ft)	(kN-m)	
BT1	6,293	8,541	6,975	9,467	1.11
BT2	4.941	6,706	4,607	6,253	0.93

Table 27 illustrates that the strain compatibility approach does not yield values significantly closer to the observed values for the bulb-tee specimens than the more general AASHTO and ACI equations.

As stated in Chapter 7, specimen BT2 failed under a total applied load less than expected to produce flexural failure. An investigation was performed to determined the cause of this failure. Numerous possibilities were identified as potential reasons for the lower load capacity. These were:

Specimen Defects:
- Vertical fabrication crack due to shrinkage
- Variable top flange thickness

Test Defects:
- Non-plumb loading rods
- Unsymmetrical transverse loads

Design Flaws:
- Compressive failure in the region
- Excessive vertical shear at the web
- Transverse flexure in the top flange
- Lateral instability of the girder

The explanation for the premature failure of the member involves a combination of several of the above factors. First of all, using influence surfaces (30) it was calculated that at the time of failure the load transferred from the crosshead beam to the cantilever flange of the girder was sufficient to cause cracking in the flange at the flange-web juncture. This was borne-out during the test when such a crack was detected in the constant moment region of the girder near one of the crossheads. As long as this crack remained in the constant moment region of the girder, its existence would have little effect on the behavior of the member. If the crack extended out of the constant moment region, into the area of high shear, an unsymetrical shear section would exist, resulting in the member developing a torsional load propagating and changing the direction of the crack. This resulted in a section no longer capable of sustaining the high compressive stresses in the top flange. As illustrated in Figure 30, the top flange blew out during the test. It should be noted that in a typical application of bulb-tee girders a slab would be cast on top of the girder, hence this loading case would not occur. This failure does point out the need, however, to investigate the torsional and lateral buckling characteristics of high-strength bulb-tee sections.

8.7 STRAND TRANSFER LENGTH

As previously described, transfer length was experimentally evaluated for each bulb-tee specimen by measuring the change in concrete surface strains over a 5 ft distance from the ends of each bulb-tee specimen. A mathematical expression for calculating the required transfer length for prestressed strand is provided in both the ACI Building Code Requirements for Reinforced Concrete (ACI 318-89) [2] and in the AASHTO Standard Specifications for Highway Bridges[1]. According to the ACI 318-89 Commentary, the required development length is

equal to the sum of the transfer length plus an additional length over which the strand must be bonded to insure that bond failure does not occur at nominal strength of the member. An expression for the transfer length alone can be written as:

$$l_t = \left(f_{se}/3\right) d_b \qquad (25)$$

where l_t = transfer length, in.

f_{se} = effective stress in prestressing strand after losses, ksi

d_b = nominal diameter of prestressing strand, in.

Using the above expression and assuming prestress losses based on readings from the Carlson strain meters, a transfer length of approximately 31 in. (813 mm) would be expected. As shown in the Table 29, transfer lengths interpreted from the Whittemore readings were significantly less than the calculated values.

TABLE 29
MEASURED AND CALCULATED TRANSFER LENGTHS

Bulb-tee Specimen	Concrete Age	Average Transfer Length, in.	
		Measured	Calculated
BT1	At Release	21.0	31.4
	At 40 days	22.0	30.5
BT2	At Release	21.0	31.3
	At 40 days	23.0	30.1
BT3	At Release	21.0	32.0
	At 40 days	23.0	31.0

Metric Equivalent: 1 in. = 25.4 mm

8.8 CAMBER & DEFLECTION

As discussed in section 7.2.4 camber readings were taken on the bulb-tee specimens at release, at 30 days , and when the deck was cast on the beams. Previous research by Kelly, Bradberry, and Breen (5) found that camber and deflection of high-strength girders could be accurately predicted using moment area equations based on known concrete properties. To verify this, camber was calculated using the moment-area method for the bulb-tee specimens. In addition the maximum deflection of BT1 measured during the proof-of-design test was calculated and compared to the measured value. The calculated versus measured values for camber and deflection are listed in Table 30.

TABLE 30
CALCULATED VERSUS MEASURED CAMBER AND DEFLECTION*

Specimen	Event	Measured Values in.	Calculated Values in.
BT1	At Release	-0.688	-0.834
	At 30 days	-0.984	-0.789
	With Deck	-0.438	-0.434
	Proof of Design	-0.019	+0.011
BT2	At Release	-0.688	-0.834
	At 30 days	-0.984	-0.789
	With Deck	N.A.	N.A.
	Proof of Design	N.A.	N.A.
BT3	At Release	-0.672	-0.834
	At 30 days	-1.000	-0.789
	With Deck	-0.547	-0.434
	Proof of Design	N.A.	N.A.

*Negative values indicate an upward camber.

8.9 PRESTRESS LOSSES

As discussed in section 6.8, the AASHTO Standard contains provisions for calculating total prestress losses due to concrete shrinkage, elastic shortening, concrete creep, and steel relaxation. Based on these provisions, total prestress losses of approximately 23.2 percent are expected for BT1 and BT3, and 21.8 percent for BT2. However, only 35-45 percent of the total ultimate creep and shrinkage losses are expected to ccur with the first 28 days (27). Therefore, prestress losses of approximately 15.8 percent for BT1 and BT3, and 15.3 percent for BT2 are expected at an age of 28 days.

Concrete strains measured immediately after release were used to provide an indication of prestress losses due to elastic shortening. Based on these concrete strains, as reported in Chapter 7, losses due to elastic shotening averaged 6.4 percent between the three bulb-tee specimens. This value is in reasonable agreement with the average elastic shortening losses of 6.3 percent calculated using provisions from the AASHTO Standard and actual measured concrete and steel properties.

Concrete strains measured at a concrete age of 30 days indicated losses averaging approximately 9.6 percent. This value is significantly less than the average 15.55 percent calculated using the provisions of the AASHTO Standard and recommendations of the PCI Committee on Prestress Losses (27). Based on this information, it appears that the total actual prestress losses in the three bulb-tee specimens can be expected to be significantly less than the total losses predicted using the AASHTO Standard. However, as in the case of the pile specimens, calculated values for prestrress losses were based on the assumption that approximately 35 percent of the ultimate creep and 42 percent of the ultimate shrinkage will occur within the first 28 days. These percentages, although shown

to be reasonable for conventional concretes, may not be applicable for higher strength concretes. This may explain the noted difference between measured and calculated prestress losses at 28 days.

8.10 COMPARISON OF TEST RESULTS WITH CURRENT PROCEDURES

Based on the series of tests reported in Chapters 7 and 8, the bulb-tee specimens behaved in a manner that would be conservatively predicted using the provisions of the AASHTO Standard Specifications for Highway Bridges that relate to the following:

Flexural Strength

Cracking Moment

Inclined Cracking

Shear Strength

Strand Transfer Length

Estimation of Prestress Losses

Modulus of Elasticity

Modulus of Rupture

It is noted, however, that a limited number of specimens were tested and the conclusions drawn from those tests should be judged in light of the number of those tests.

9. BEHAVIOR AND ANALYSIS OF 130-ft (39.6-m) PILE

9.1 INTRODUCTORY REMARKS

The purpose of this chapter is to present the behavior of the 130-ft (39.6 m) pile specimen during transportation to the construction site, handling at the site, and driving. An analysis of the pile's behavior during driving based on the Pile Driving Analyzer (PDA) is also presented. A discussion of the concrete material properties, fabrication of the pile, and the full PDA report can be found in Appendix C.

9.2 TRANSPORTATION

The site selected for driving the pile was on Route La 415 at the new bridges located over the Missouri Pacific Railroad near Port Allen, Louisiana. The selection of this site resulted in a trucking distance of approximately 180 miles with most of this distance on interstate highways.

As described in Appendix C, three lifting loops were placed in the pile at the time of casting. When the pile was lifted from the casting bed, all three of these loops were used in a three point pick-up to limit the amount of bending stresses in the pile. Three point pick-up was also used at the fabrication yard when the pile was placed on the truck for transportation to the construction site. As shown in Figure C.3 the pile was supported in two locations during transportation. The pile arrived at the construction site with no visible signs of damage.

9.3 HANDLING AT THE CONSTRUCTION SITE

At the construction site, the contractor first tried to lift the pile from the truck using a two-point pick-up. This attempt was made using a lifting cable running between the two lifting points that was too short, resulting in a very "flat" angle and very high tensile forces in the lifting loops. Because of this high tensile force, one of the lifting loops failed in tension but did not pull out of the pile. To compensate for the lack of a lifting loop, a choker was placed around the pile at the location of the damaged lifting loop, and the two remaining loops were used in a three-point pick-up to get the pile off the truck. Other than the broken lifting loop, no damage was sustained by the pile during unloading operations.

To lift the pile into the pile leads, the same procedure that was used to get the pile off the truck was used. Again no visible signs of damage were noticed during this operation.

9.4 DRIVING THE PILE

As described in Appendix C, the pile was driven using a Vulcan 020 single acting external combustion hammer with a 3-ft (0.91-m) stroke. The maximum energy rating of the hammer was 60.0 kip-ft (81.5 kN-m) at a stroke of 3 ft (0.91 m). The pile cushion was a 6 in. (127 mm) thick compressed oak cushion. During driving the maximum measured energy transferred to the pile varied from 12.0 kip-ft (16.3 kN-m) in the first 22 ft (6.7 m) of penetration to 15.0 kip-ft (20.4 kN-m) for the remainder of the driving. This translates into an efficiency of 20 percent to 25 percent of maximum rated hammer energy.

The maximum allowable driving stresses for precast prestressed concrete piles recommended by the Federal Highway Administration are based on the following formulas:

$$\textbf{Maximum Compressive Driving Stress} = 0.85f_c' - \textbf{Effective Prestress}$$

$$\textbf{Maximum Tension Driving Stress} = 3\sqrt{f_c'} + \textbf{Effective Prestress}$$

Based on 14-day and 28-day strength tests, the strength of the concrete at the time of driving was 10,400 psi (71.7 MPa). The effective prestress was assumed to be 1,454 psi (10 MPa). Based on the above formulas, the concrete strength, and the assumed effective prestress, the maximum allowable compressive driving stress was 7.39 ksi (51 MPa) and the maximum allowable tension driving stress was 1.76 ksi (12.1 MPa). There were no visible signs of distress during driving.

9.5 PILE PERFORMANCE DURING DRIVING

The compressive driving stresses reached a maximum of 1.83 ksi (12.5 MPa) and then leveled off to an average of 1.70 ksi (11.7 MPa) throughout the remainder of the pile driving. The maximum tensile driving stresses increased from 0.86 ksi (5.9 MPa) at the beginning of driving to 1.31 ksi (9 MPa) at a pile tip penetration of 55 ft (16.8 m). The maximum tensile stress gradually reduced to 1.0 ksi (6.9 MPa) at a tip elevation of 86 ft (26.2 m) then dropped off sharply as driving resistance increased in the dense sand. The driving stresses were well below the maximum allowable compressive stress of 7.39 ksi (50.8 MPa) and the

maximum allowable tensile stresses of 1.76 ksi (12.1 MPa). A profile of the driving stresses is shown in the PDA Monitoring report included in Appendix C.

It should be noted that had the pile been fabricated using concrete with a strength of 5,000 psi (34.4 MPa) or 6,000 psi (41.3 MPa) damage to the pile would have likely resulted. The maximum allowable tensile driving stress for 5,000 psi (34.4 MPa) and 6,000 psi (41.3 MPa) concrete are 1.00 ksi (6.9 MPa) and 1.17 ksi (8 MPa), respectively.

According to the Pile Driving Analyzer, the pile had an integrity factor of 1.0 throughout the entire driving operation and was therefore not damaged during transportation, handling, or driving.

9.6 CONCLUSIONS

On the basis of this one test, it appears that high-strength concrete can be used effectively in long piles. The pile performed well during transportation, handling, and driving. The higher tensile strength and higher precompression is particularly valuable in soft driving conditions where tensile driving stresses are the highest.

10. SUMMARY

10.1 OUTLINE OF INVESTIGATION

The objective of this investigation was to evaluate the feasibility of using high-strength concrete in the design and construction of highway bridge structures. A literature search was conducted; a survey of five regional fabrication plants was performed; mix designs were studied in the laboratory and in the field; and a total of seven full-size specimens were fabricated and tested.

Results from 3 pile specimens tested in flexure are reported. Each pile specimen had a 24-in. (610-mm) square cross section with a 12-in. diameter void running its full length. All of the pile specimens were 24 ft (7.31m) in length. The specimens were prestressed with 24, seven-wire, 1/2-in. (12.7-mm) diameter, 270 ksi (1,862 MPa) low relaxation strands and were straight in all the pile specimens. The concrete, at the time of testing, had an average strength of 8,067 psi (55 MPa). The web reinforcement consisted of 1/4 (6.4 mm) wire spirals with an average tensile strength of 96,664 psi (666 MPa). All piles contained the same number of longitudinal strands and the same amount of web reinforcement. The pile specimens were tested in flexure with a span length of 22 ft (6.7 m) and with concentrated loads located 9 ft 6 in. (2.9 m) from the supports resulting in a constant moment region of 3 ft (.91 m).

Flexural tests of two full-size bulb-tee specimens are reported. The specimens were standard 54 in. (1,372 mm) deep bulb-tee sections with a 6 in. thick (152-mm) web. One of the test specimens, designated BT1, had a slab 9-1/2 in. (241 mm) thick and 10 ft (3,048 mm) wide cast on top of it. The slab had a

actual concrete strength of 7,000 psi (48 MPa). The second specimen, designated BT2, was tested without a slab. The specimens were 70 ft (21.3 m) in length, and when tested had a clear span of 69 ft (21 m). The bulb-tee specimens were prestressed using 30, 1/2-in. (12.7 mm), 270 ksi (1,862 MPa), low relaxation strands, six of which were draped. The concrete had an average 28-day compressive strength of 9,800 psi (68 MPa). The web reinforcement consisted of vertical No. 4 bars. All of the girder specimens contained the same number and configuration of longitudinal strands and the same amount of web reinforcement. The girders were loaded with concentrated loads located 28 ft 6 in. (8.69 m) from each end of the girder, resulting in a central constant moment region 12 ft (3.6 m) in length.

Three shear tests are also reported. These shear tests were performed using the ends of the two flexural test specimens. The shear test specimens were designated BT1-D, BT1-L and BT2-L. Since the shear specimens were taken from the flexural specimens, they had the same cross-sectional configuration and concrete strength. To maximize end shear and insure web shear failure, the shear specimens were loaded with four concentrated loads located 4 ft 6 in (1.37 m), 7 ft 6 in. (2.29 m), 10 ft 6 in. (3.2 m), and 13 ft 6 in. (4.11 m) from the support at the end of the member. The specimen was supported on a 27 ft (8.23 m) clear span.

A single field test of a pile specimen is reported. The pile specimen had the same cross-sectional configuration as the pile specimens tested in the laboratory The concrete had an average actual compressive strength of 10,453 psi (72 MPa). The length of the pile was 130 ft (39.6 m).

10.2 BEHAVIOR OF THE TEST SPECIMENS

All three laboratory pile specimens failed in flexural compression.

Of the two bulb-tee girders tested in flexure, BT1 experienced a tensile failure and BT2 experience a premature compressive failure of part of the top flange.

Of the three bulb-tee specimens tested in shear, BT1-D and BT1-L failed at the end of the member with the lower shear due to shear compression failure resulting from cracks formed during the flexure test of BT1. Web shear cracks did develop, however, at the end of the member with the highest shear. BT2-L developed web shear cracks as anticipated and failed due to shear compression failure over the bearing.

The field driven pile was transported, lifted and driven to its full length with no apparent damage.

10.3 CONCLUSIONS

Based on the test results and analyses described in this report, the following conclusions are made:

1. High-strength concrete with compressive strengths of 10,000 psi (69 MPa) can be produced using regionally available material.

2. Concrete with 10,000 psi (69 MPa) compressive strength requires more stringent quality control procedures than regional fabricators are presently accustomed to using. Successful production of high-strength concrete requires extreme care in all steps of the production process. Batching weights must match

the mix design as accurately as possible. Water content and admixtures must be closely monitored.

3. The laboratory pile specimens behaved in a manner that was conservatively predicted using the provisions of the AASHTO Standard Specifications for Highway Bridges. Test results included modulus of elasticity, tensile splitting strength, and modulus of rupture of concrete, transfer length, prestress losses at transfer and at 28 days, cracking moment, and flexural strength.

4. Results of concrete material property tests for the girder specimens indicate that calculated values for concrete modulus of elasticity using AASHTO provisions were in reasonable agreement with actual values when measured values for unit weight and concrete compressive strength are used in the equation. Based on results of the splitting tensile strength tests, it appears that the AASHTO provisions may slightly overestimate the tensile strength of higher-strength concrete.

5. Transfer lengths interpreted from strain readings were in reasonable agreement with values predicted by the AASHTO and ACI provisions.

6. Measured prestress losses in the bulb-tee specimens due to elastic shortening were in reasonable agreement with the values calculated using AASHTO provisions and actual measured concrete and steel material properties. Measured prestressed losses at 30 days were less (approximately 30 percent less) than values calculated using AASHTO provisions and recommendations of the PCI Committee on Prestress Losses (27). Based on these findings, AASHTO provisions and PCI Committee recommendations for predicting prestress losses may be too conservative for higher-strength concretes.

7. Measured initial stresses (immediately after release) in the girder extreme tension and compression fibers, extrapolated from strain gauge data, were within prescribed limits stipulated in the AASHTO provisions.

8. Girder camber/deflection measurements made subsequent to fabrication were consistent with values calculated using "conventional" methods. Measured girder deflections under full design dead load plus live load plus impact were also consistent with calculated values.

9. Measured cracking moment and ultimate flexural strength of Girder BT1 exceeded calculated values based on AASHTO provisions and actual measured material properties and prestress losses. Diagonal cracks that initiated from flexural cracks during the flexural test developed at shear loads that were greater than values of V_{ci} calculated using actual measured values of material properties and prestress losses.

10 Strain gauges placed across the top of the deck slab on Girder BT1 indicated full participation of the 120 in. wide slab as suggested by the AASHTO provisions.

11. Measured cracking moment of Girder BT2 exceeded calculated values based on AASHTO provisions and actual measured material properties and prestress losses. Measured ultimate strength of BT2 was slightly less than the calculated flexural strength because of the compression failure of the top flange of BT2 and apparent lateral buckling at ultimate load. Diagonal cracks that initiated from flexural cracks during the flexural test developed at shear loads that were greater than values of V_{ci} calculated using actual measured values of material properties and prestress losses.

12. Ultimate shear strength of the BT1 girder halves, BT1-D and BT1-L, could not be evaluated since the failure section occurred in an area which had already been damaged during the flexural test. However, since diagonal cracking did occur near the "formed" end of the girder halves during the shear test, the shear strength provided by the web concrete, V_{cw}, could be evaluated. The total applied shear coincident with the formation of diagonal web-shear cracks near the formed

girder end exceeded calculated values for V_{cw} based on AASHTO provisions and actual measured values for both halves of BT1 tested.

13. Ultimate shear strength of the live half of girder BT2, BT2-L, was evaluated even though the ultimate load was influenced by strand bond failure near the formed end of the girder. The total applied shear at the failure location exceeded the sum of calculated values for V_{cw} and V_s based on AASHTO provisions and actual measured values of material properties and prestress losses. In addition, the total applied shear coincident with the formation of diagonal web shear cracks near the formed end exceeded calculated values for V_{cw} based on AASHTO provisions.

14. Behavior of specimen P4, the 130-ft (39.6-m) pile, during transportation, handling, and driving was satisfactory. Driving stresses were well below levels that would cause damage to the pile.

15. As presented in Appendix C, it appears that steam curing of high-strength concrete may reduce strength development at late ages. Higher strengths were achieved using air curing of a small number of the specimens from the 130 ft (39.6 m) pile.

10.4 RECOMMENDATIONS

Based on the findings of this investigation thus far, the following recommendations are made:

1. The long term test presently underway on Girder BT3 should continue. The information gathered from this test will contribute to our understanding of the lower-than predicted prestress losses in the other specimens.

2. Fatigue tests on full-scale bulb-tee girders should be performed. Such tests would indicate the behavioral characteristics of high-strength girders under repeated live load.

3. An investigation into the lateral buckling characteristics of long slender high-strength concrete members should be performed.

4. An investigation into the effects of steam curing on the high-strength concrete should be performed.

5. A quality control training program should be developed to train local fabricators. The importance of the tighter quality controls required by high-strength concrete must be understood by the fabricator if successful production of high-strength concrete is to occur.

6. Concrete with strengths up to 10,000 psi (69 MPa)should be considered for use by the Louisiana Department of Transportation and Development.

7. High-strength concrete, up to 10,000 psi (69 MPa), should be implemented in a bridge. This bridge should be instrumented to determine long term behavior and consideration given to a modal analysis of the structure.

LIST OF REFERENCES

1. American Association of State Highway and Transportation Officials, Standard Specifications for Highway Bridges. Washington: American Association of State Highway and Transportation Officials, 1989.

2. American Concrete Institute Committee 318, Building Code Requirements for Reinforced Concrete (ACI 318-89) and Commentary-ACI 318R-89. Detroit: American Concrete Institute, 1989.

3. Law, S. M., and M. Rasoulian, Design and Evaluation of High Strength Concrete for Girders. FHWA Report No. FHWA-LA-80-138. McLean, Virginia: Federal Highway Administration, 1980.

4. Adelman, D. and T. E. Cousins, "Evaluations of the Use of High Strength Concrete Bridge Girders in Louisiana." Journal of the Prestressed Concrete Institute 35, no. 5 (Sep.-Oct 1990): 70-78.

5. Kelly, D. J., T. E. Bradberry, and J. E. Breen, Time Dependent Deflections of Pretensioned Beams. Research Report 381-1. Austin: Center for Transportation Research, 1987.

6. Hartman, D. L., J. E. Breen, and M. E. Kreger, Shear Capacity of High Strength Prestressed Concrete Girders. Research Report 381-2. Austin: Center for Transportation Research, 1988.

7. Castrodale, R. W., M. E. Kreger, and N. E. Burns, A Study of Pretensioned High Strength Concrete Girders in Composite Highway Bridges - Laboratory Tests. Research Report 381-3. Austin: Center for Transportation Research, 1988.

8. Canadian Standards Association, Design of Concrete Structures for Buildings (CAN3-A23.3-M84). Rexdale: 1984.

9. Castrodale, R. W., M. E. Kreger, and N. E. Burns, A study of Pretensioned High Strength Concrete Girders in Composite Highway Bridges - Design Considerations. Research Report 381-4. Austin: Center for Transportation Research, 1988.

10. Zia, P., J. J. Schemmel, and T. E. Tallman, Structural Applications of High Strength Concrete. Research Report 23241-87-3. Raleigh: Center for Transportation Studies, 1989.

11. Leming, M. L., "Comparison of Mechanical Properties of High Strength Concrete made with Different Raw Materials." presented at the 69th Annual Meeting of the Transportation Research Board, Washington, D. C., 1990.

12. Shin, S. W., M. Kamara, and S. K. Ghosh, "Flexural Ductility, Strength Predictions, and Hysteretic Behavior of Ultra-High-Strength Concrete Members." In High Strength Concrete - Second International Symposium, SP 121, 239-263. Detroit: American Concrete Institute, 1990.

13. Roller, J. J., and H. G. Russell, "Shear Strength of High Strength Concrete Beams with Web Reinforcement." Journal of the American Concrete Institute 87, no 2 (mar.-Apr. 1990): 191-198.

14. Peterman, M. B., and R. L. Carrasquillo. Production of High Strength Concrete. New Jersey: Noyes Publications, 1986.

15. Ahmad, S. H., and S. P. Shah, "Structural Properties of High Strength Concrete and its Implications for Precast Prestressed Concrete." Journal of the Prestressed Concrete Institute 30, no 6 (Nov.-Dec 1985): 93-119.

16. Carrasquillo, R. L., A. H. Nilson, and F. O. Slate, "Properties of High Strength Concrete Subject to Short Term Loads." Journal of the American Concrete Institute 78, no 3 (May-June 1981): 171-178.

17. Cook, J. E., "10,000 psi Concrete." Concrete International: Design & Construction 11, no 10 (Oct. 1989): 69-75.

18. Rabbat, B. G. and H. G. Russell, "Optimized Sections for Precast Prestressed Bridge Girders." Journal of the Prestressed Concrete Institute 30, no. 4 (Jul.-Aug 1982): 88-104.

19. Rabbat, B. G. and H. G. Russell, "Proposed Replacement of AASHTO Girders with New Optimized Sections." Transportation Research Record 950, vol. 2 (1982): 85-92.

20. MacGregor, J. G., M. A. Sozen, and C. P. Siess, "Strength and Behavior of Prestressed Concrete Beams with Web Reinforcement." Civil Engineering Studies, Structural Research Series 201. Urbana: University of Illinois, 1960.

21. American Society for Testing and Materials. Standard Test Method for Obtaining and Testing Drilled Cores and Sawed Beams of Concrete, ASTM C42-90. Philadelphia: 1986.

22. American Society for Testing and Materials. Standard Test Method for Compressive Strength of Cylindrical Concrete Specimens, ASTM C-39-86. Philadelphia: 1986.

23. American Society for Testing and Materials. Standard Test Method for Static Modulus of Elasticity and Poisson's Ratio of Concrete in Compression, ASTM C469-87. Philadelphia, 1987.

24. American Society for Testing and Materials. Standard Test Method for Splitting Tensile Strength of Cylindrical Concrete Specimens, ASTM C496-90. Philadelphia, 1990.

25. American Society for Testing and Materials. Standard Test Method for Flexural Strength of Concrete (Using Simple Beam with Third-Point Loading, ASTM C78-84. Philadelphia, 1984.

26. American Concrete Institute Committee 363. "State of the Art Report on High-Strength Concrete." Journal of the American Concrete Institute 81, no 4 (July-Aug., 1984): 364-411.

27. PCI Committee on Prestress Losses. "Recommendations for Estimating Prestress Losses." Journal of the Prestressed Concrete Institute 20, no. 4 (Jul-Aug., 1975): 44-75.

28. Nilson, A. H., Design of Prestressed Concrete. New York: John Wiley & Sons, 1987.

29. Collins, M. P., and D. Mitchell, Prestressed Concrete Structures. Englewood Cliffs: Prentice Hall, 1990.

30. Pucher, A., Influence Surfaces of Elastic Plates. New York: Springer-Verlag Wien, 1973.

31. Louisiana Department of Transportation and Development. Louisiana Standard Specifications for Roads and Bridges. Baton Rouge: Privately printed, 1982.

32. American Society for Testing and Materials. Standard Specification for Portland Cement, ASTM C150-89. Philadelphia, 1989.

33. American Society for Testing and Materials. Standard Specifications for Chemical Admixtures for Concrete, ASTM C494-90. Philadelphia, 1990.

34. American Society for Testing and Materials. Standard Specification for Air-Entraining Admixtures for Concrete, ASTM C260-86. Philadelphia, 1986.

35. American Society for Testing and Materials. Standard Specification for Fly Ash and Raw or Calcined Natural Pozzolan for Use as a Mineral Admixture in Portland Cement Concrete, ASTM C618-91. Philadelphia, 1986.

36. American Society for Testing and Materials. Standard Specifications for Steel Strand, Uncoated Seven-Wire Stress Relieved for Prestressed Concrete, ASTM C416-88. Philadelphia, 1988.

37. American Society for Testing and Materials. Standard Test Methods and Definitions for Mechanical Testing of Steel Products, ASTM A370-90a. Philadelphia, 1990.

38. American Society for Testing and Materials. Standard Test Method for Linear Thermal Expansion of Solid Materials by Thermomechanical Analysis, ASTM E831-86. Philadelphia, 1986.

39. U. S. Army Corps of Engineers. "Test Method for Coefficient of Linear Thermal Expansion of Concrete." Handbook for Concrete and Cement, Vol 1. Vicksburg: Waterways Experiment Station, 1981.

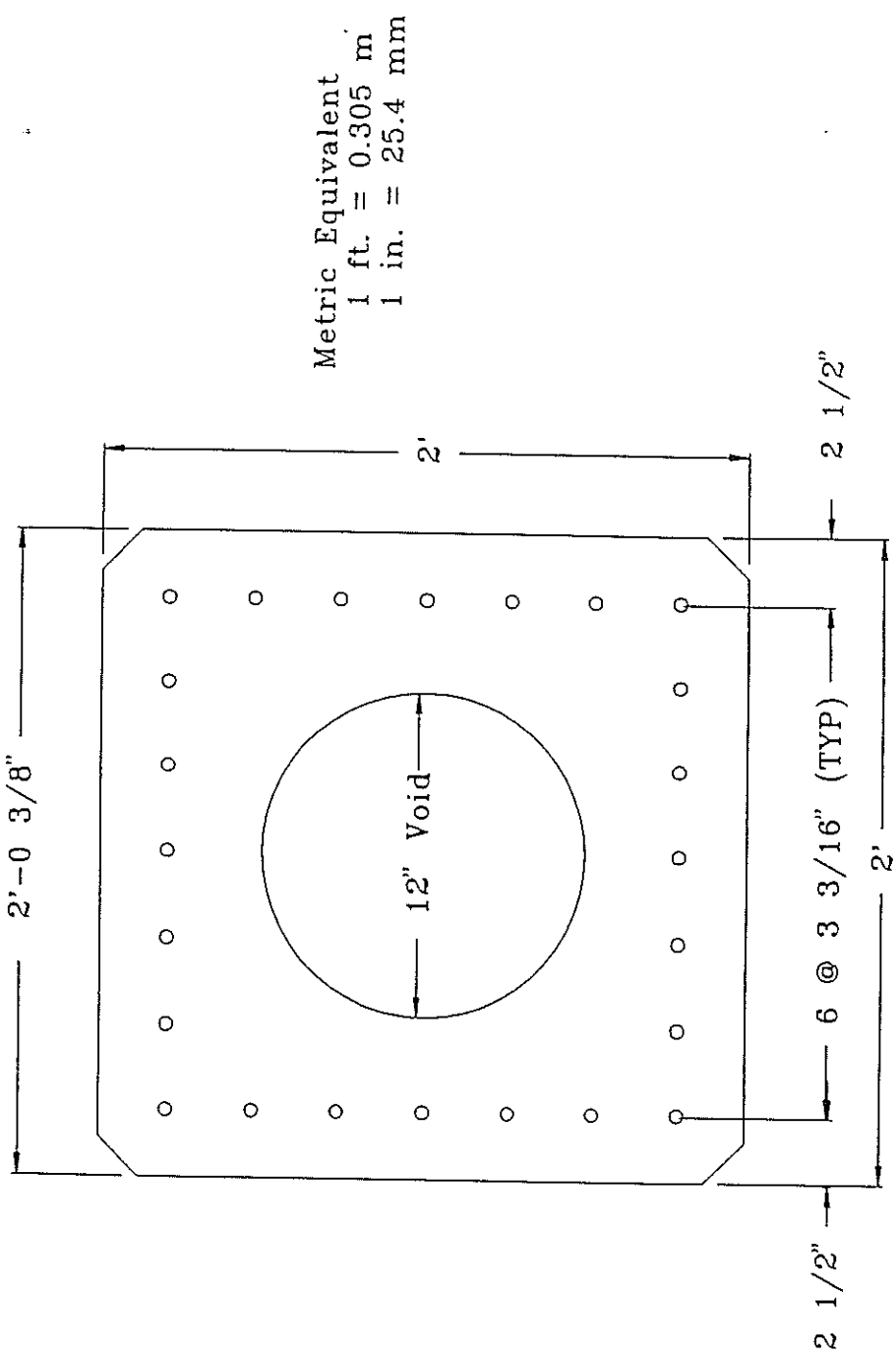

Figure 1. Cross section of pile specimens P1, P2, P3, and P4

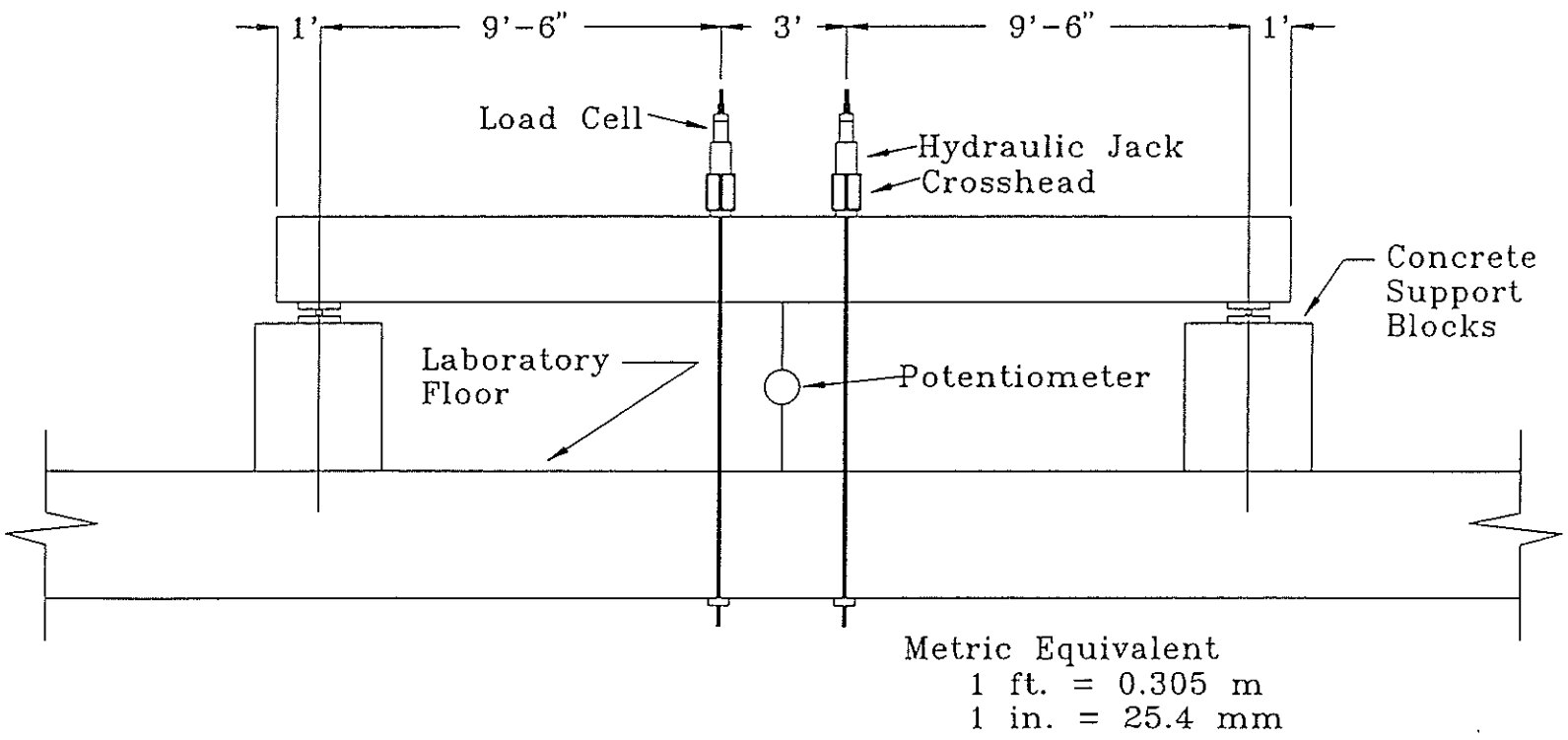

Figure 2. Testing configuration for pile specimens P1, P2, and P3

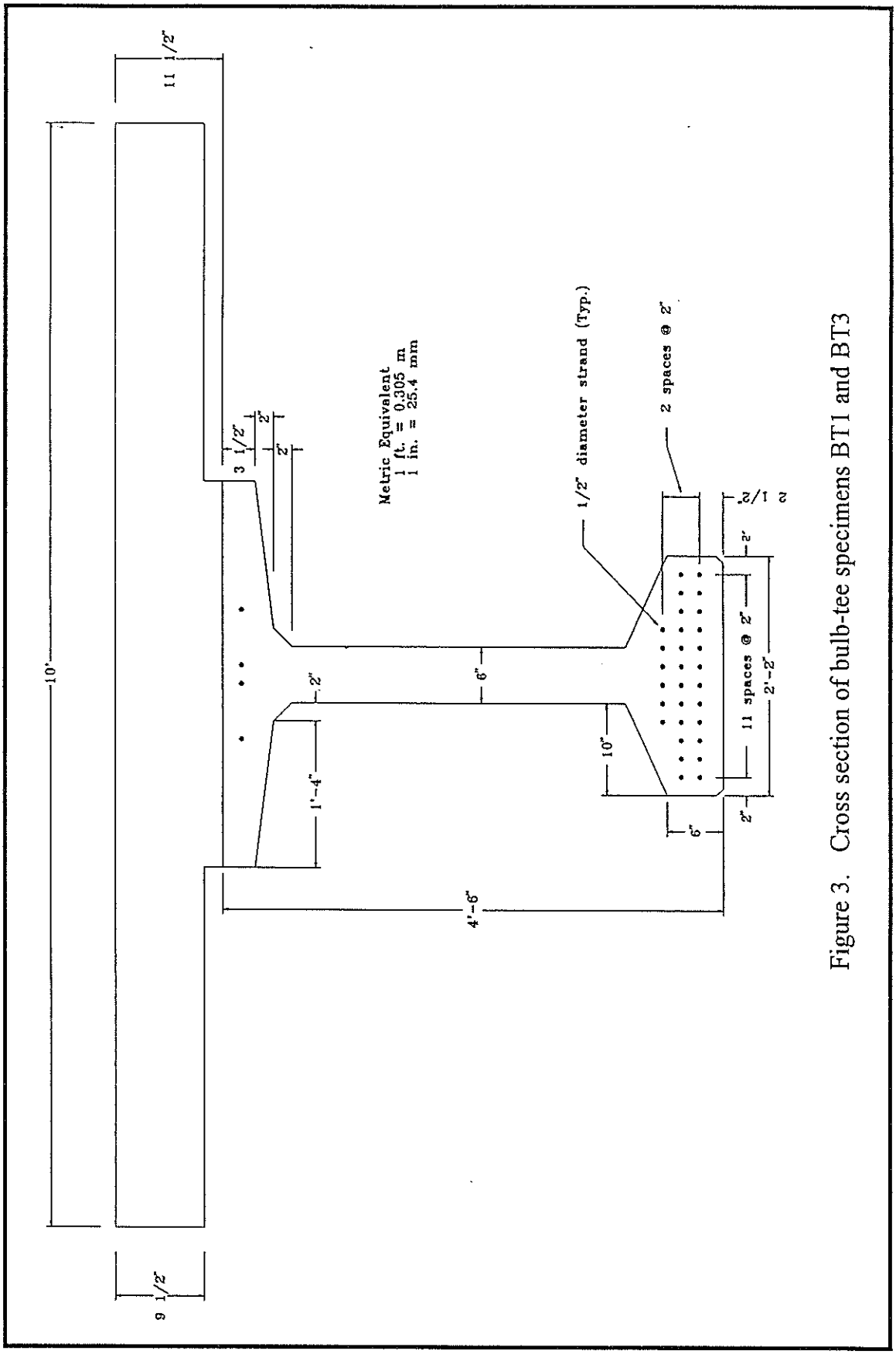

Figure 3. Cross section of bulb-tee specimens BT1 and BT3

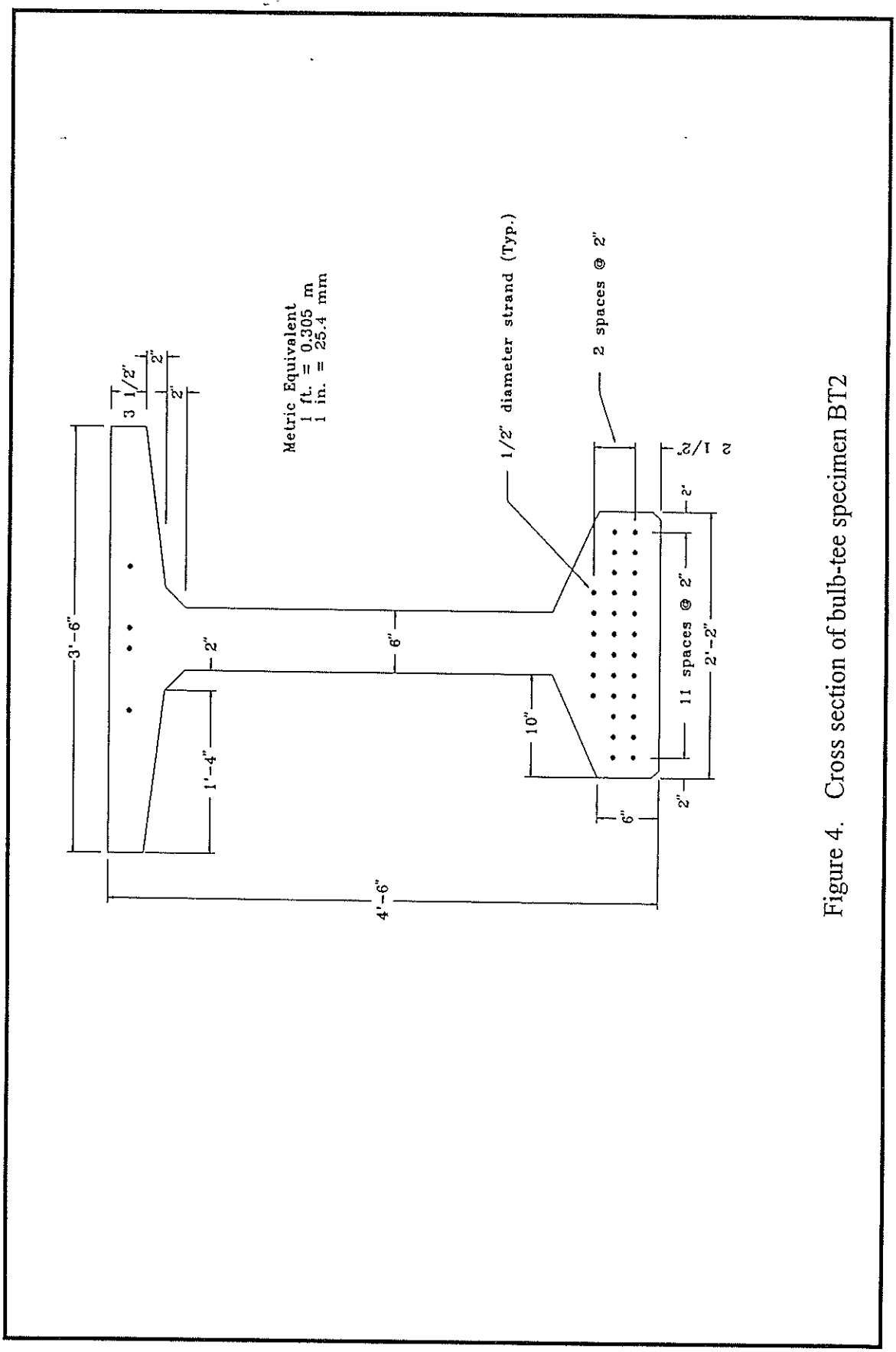

Figure 4. Cross section of bulb-tee specimen BT2

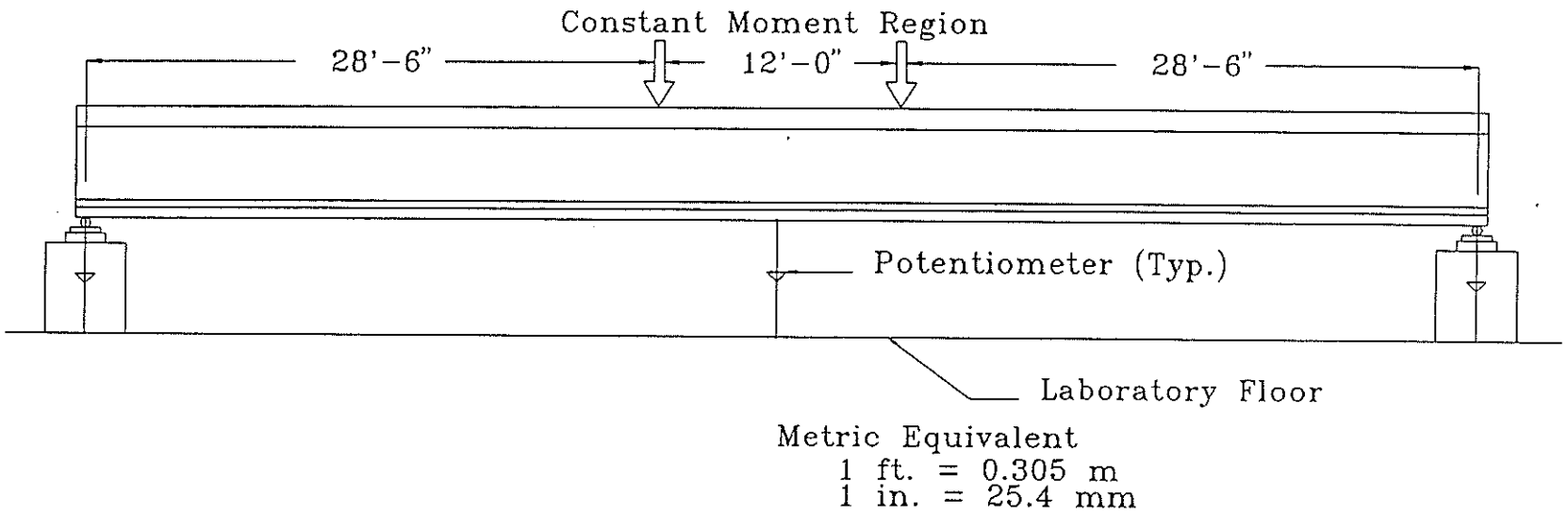

Figure 5. Testing configuration for bulb-tee specimens BT1 and BT2

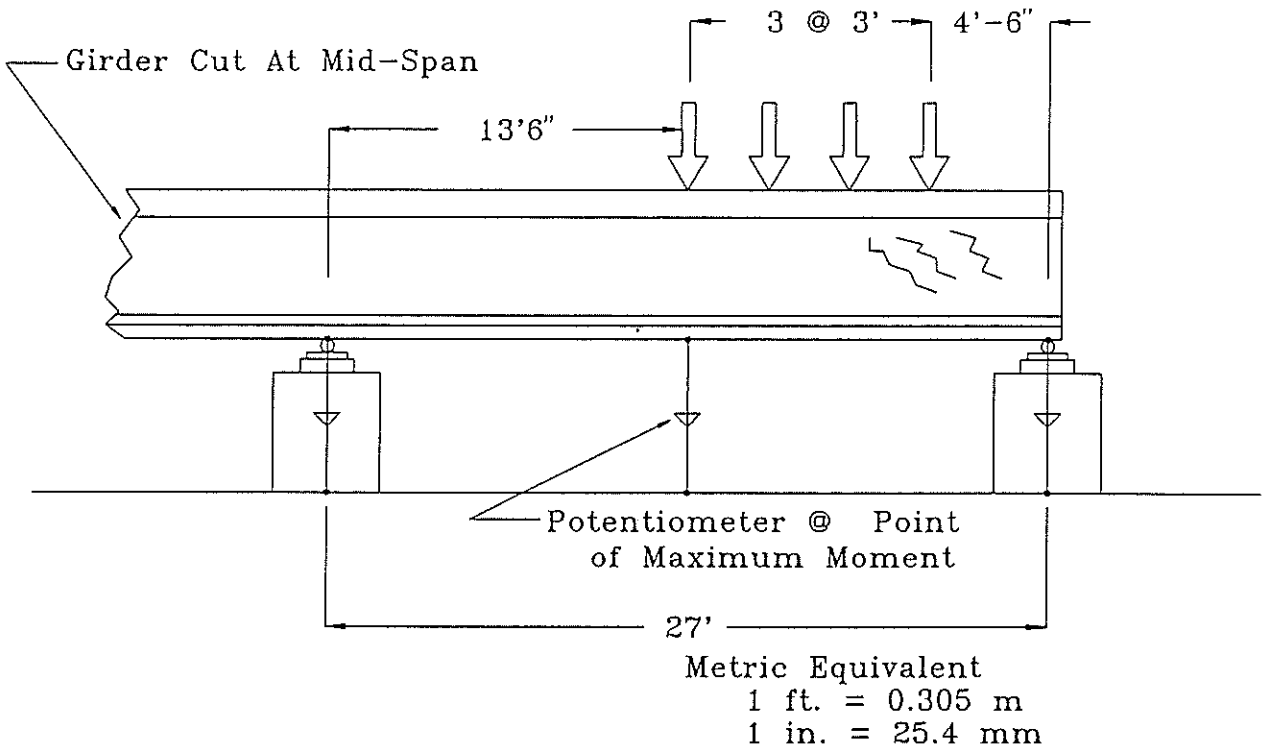

Figure 6. Testing configuration for bulb-tee shear specimens BT1-D, BT1-L and BT2-L

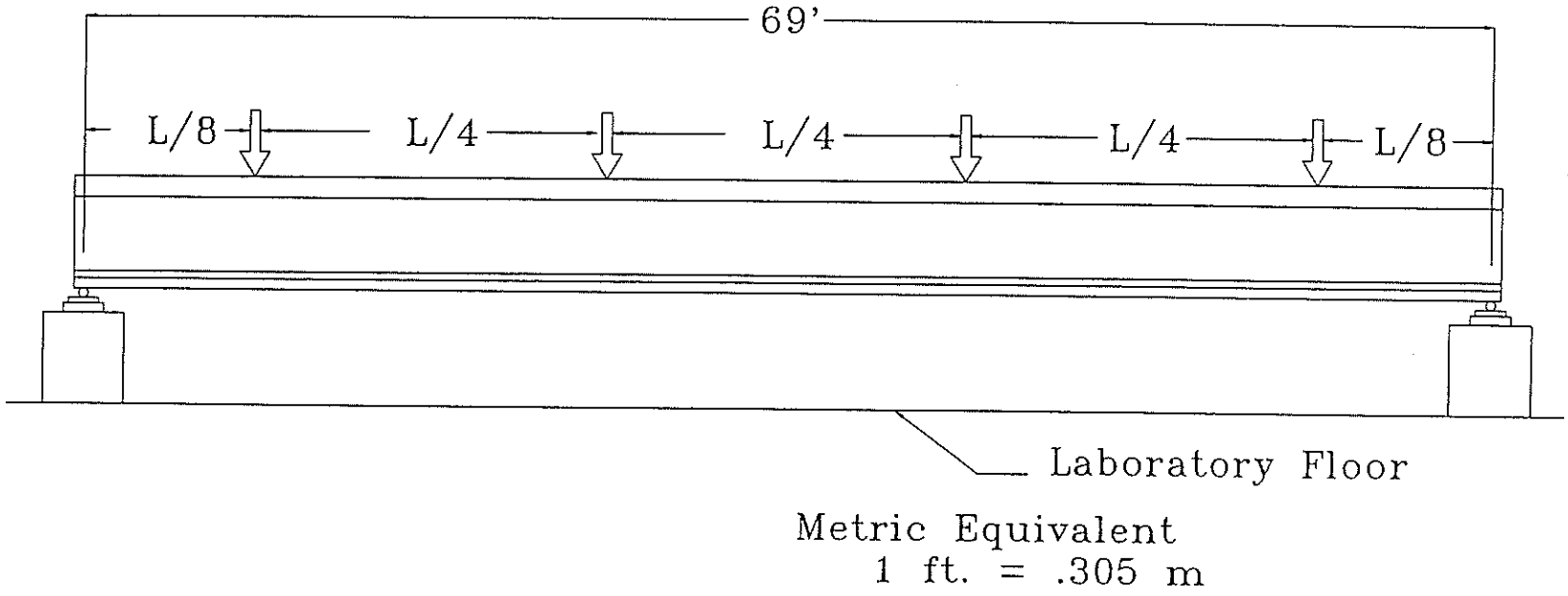

Figure 7. Long-term testing configuration for specimen BT3.

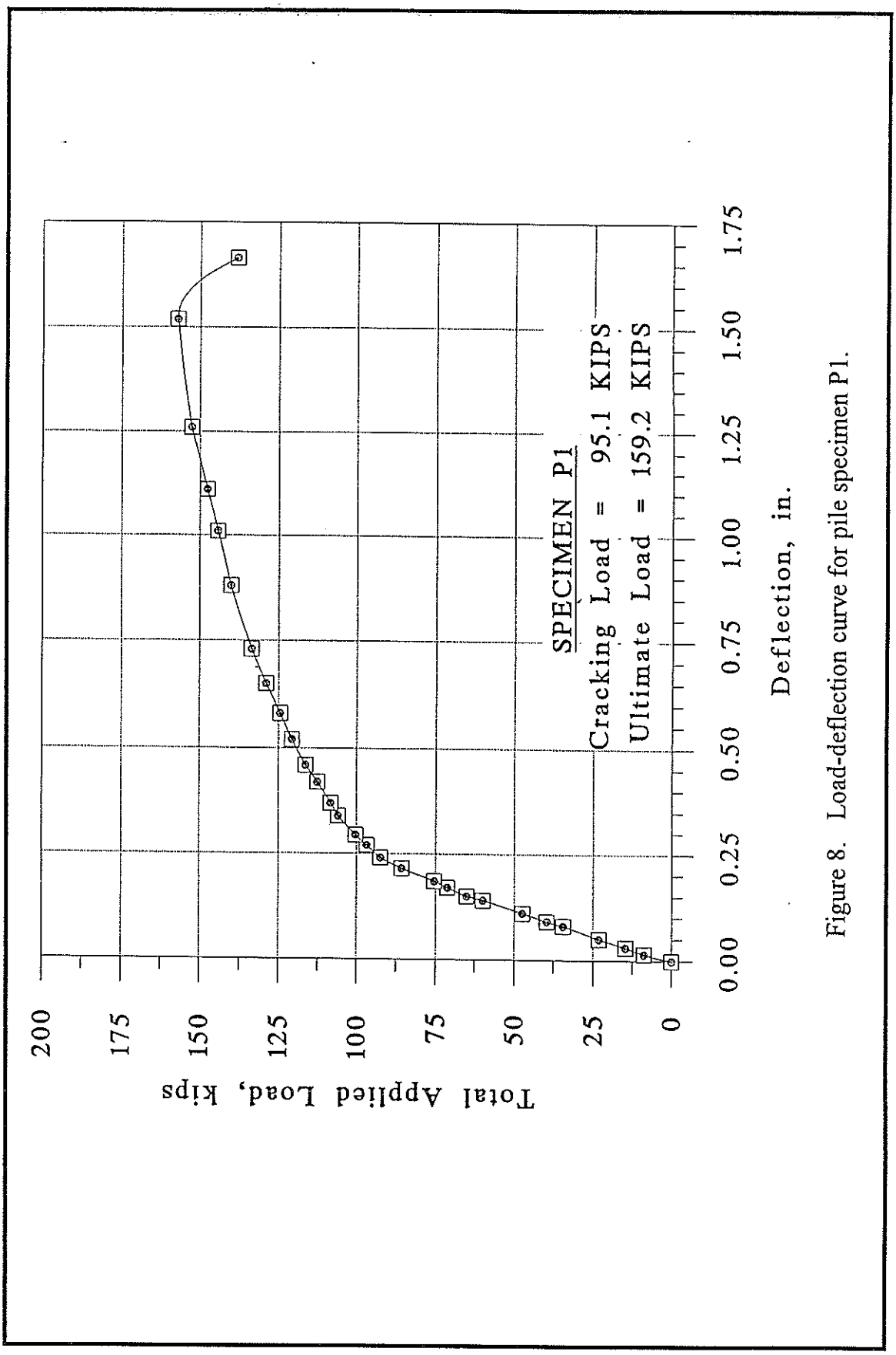

Figure 8. Load-deflection curve for pile specimen P1.

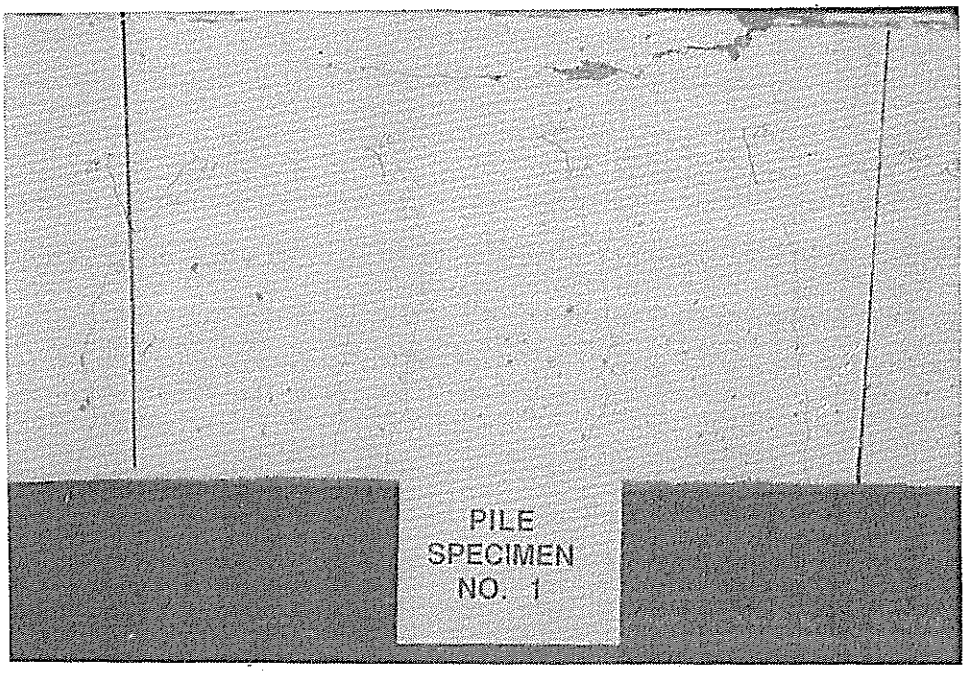

Figure 9. Flexure cracks in constant moment region of P1

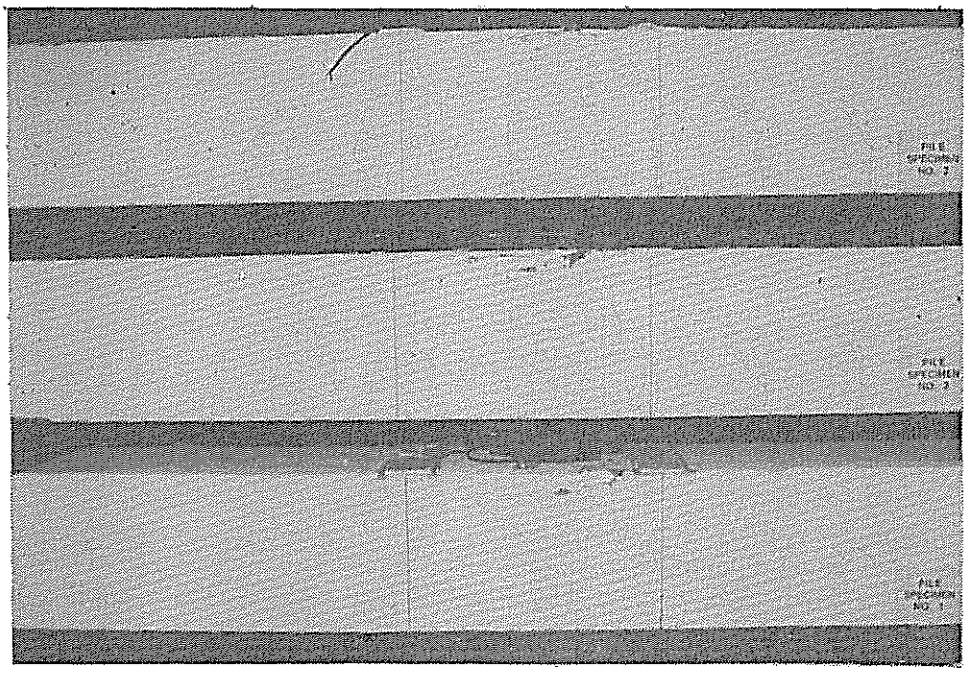

Figure 10. Flexure-shear cracks in P1, P2, and P3

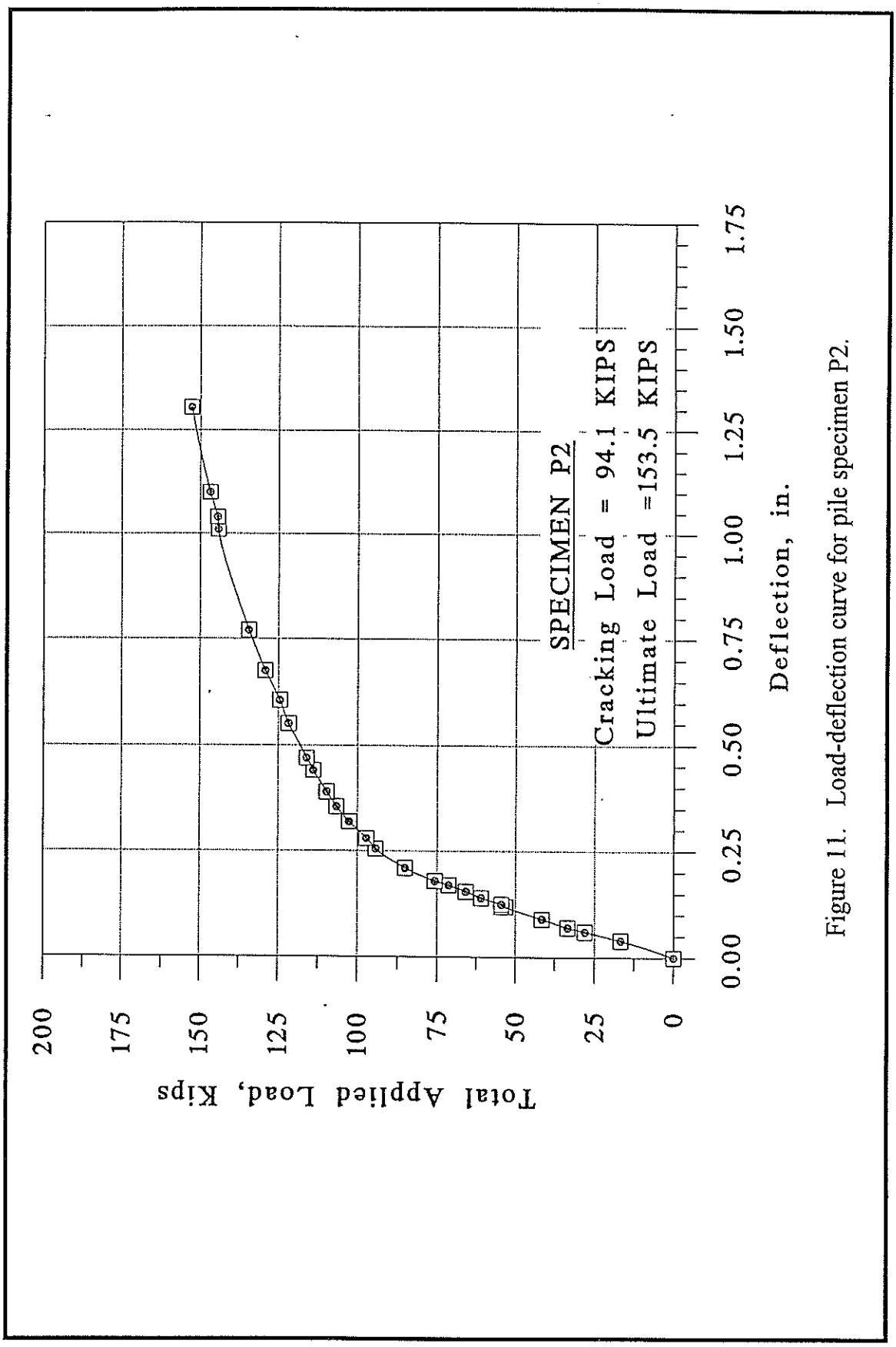

Figure 11. Load-deflection curve for pile specimen P2.

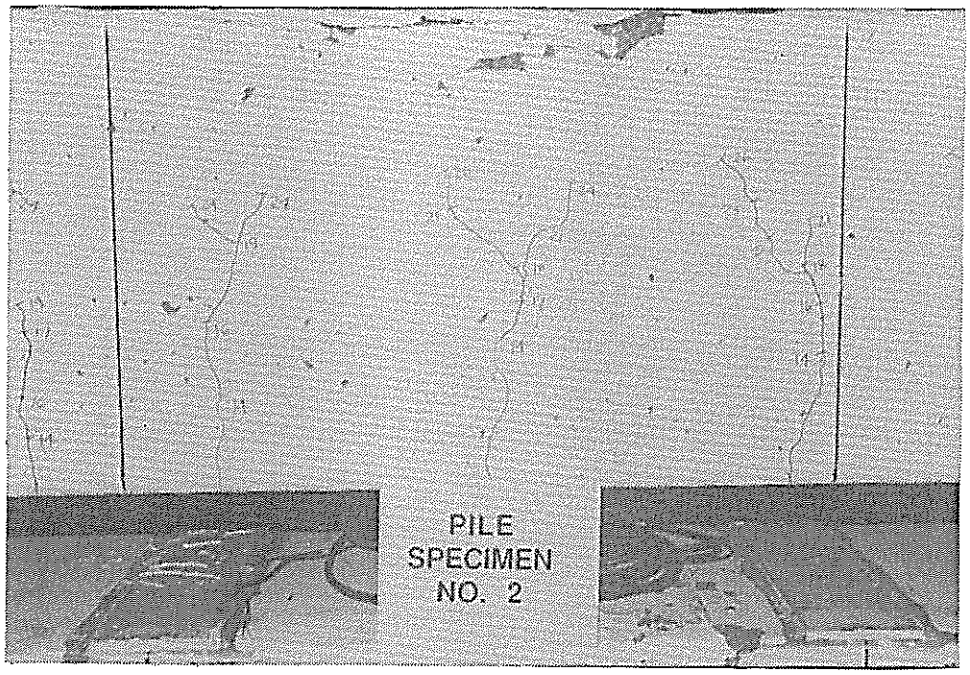

Figure 12. Flexural cracks in constant moment region of P2.

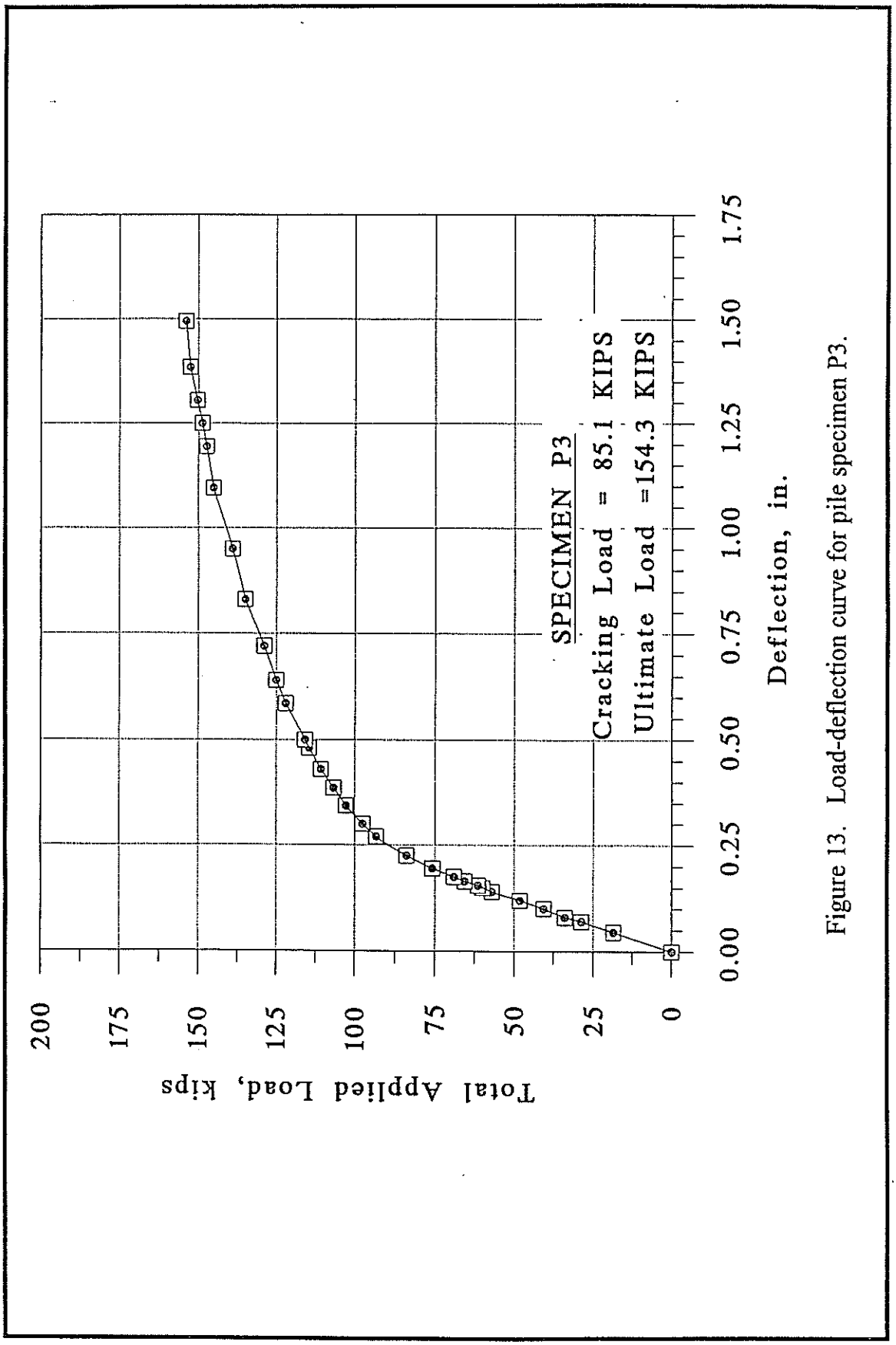

Figure 13. Load-deflection curve for pile specimen P3.

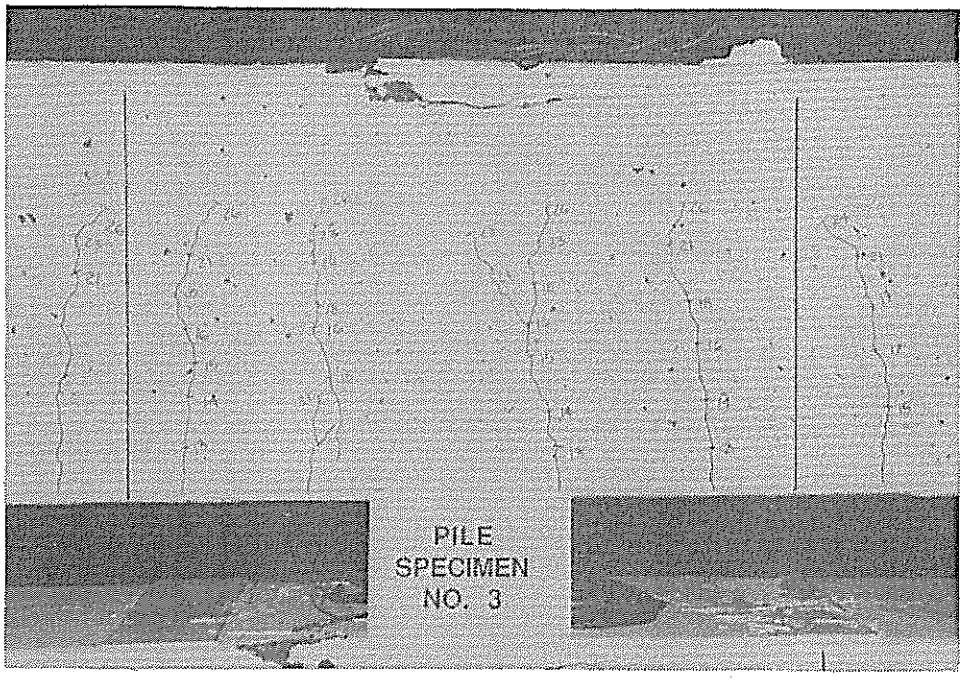

Figure 14. Flexural cracks in constant moment region of P3

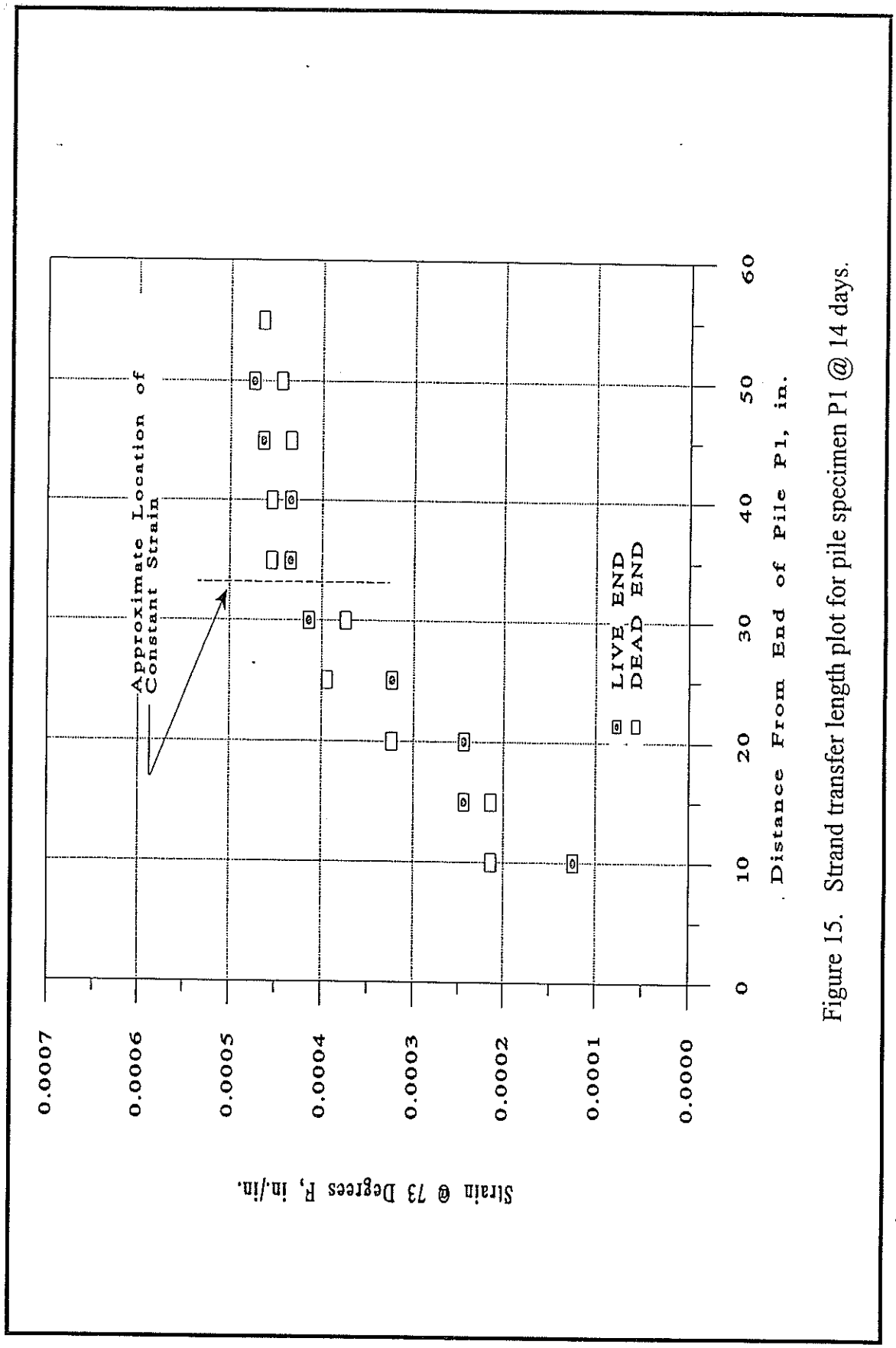

Figure 15. Strand transfer length plot for pile specimen P1 @ 14 days.

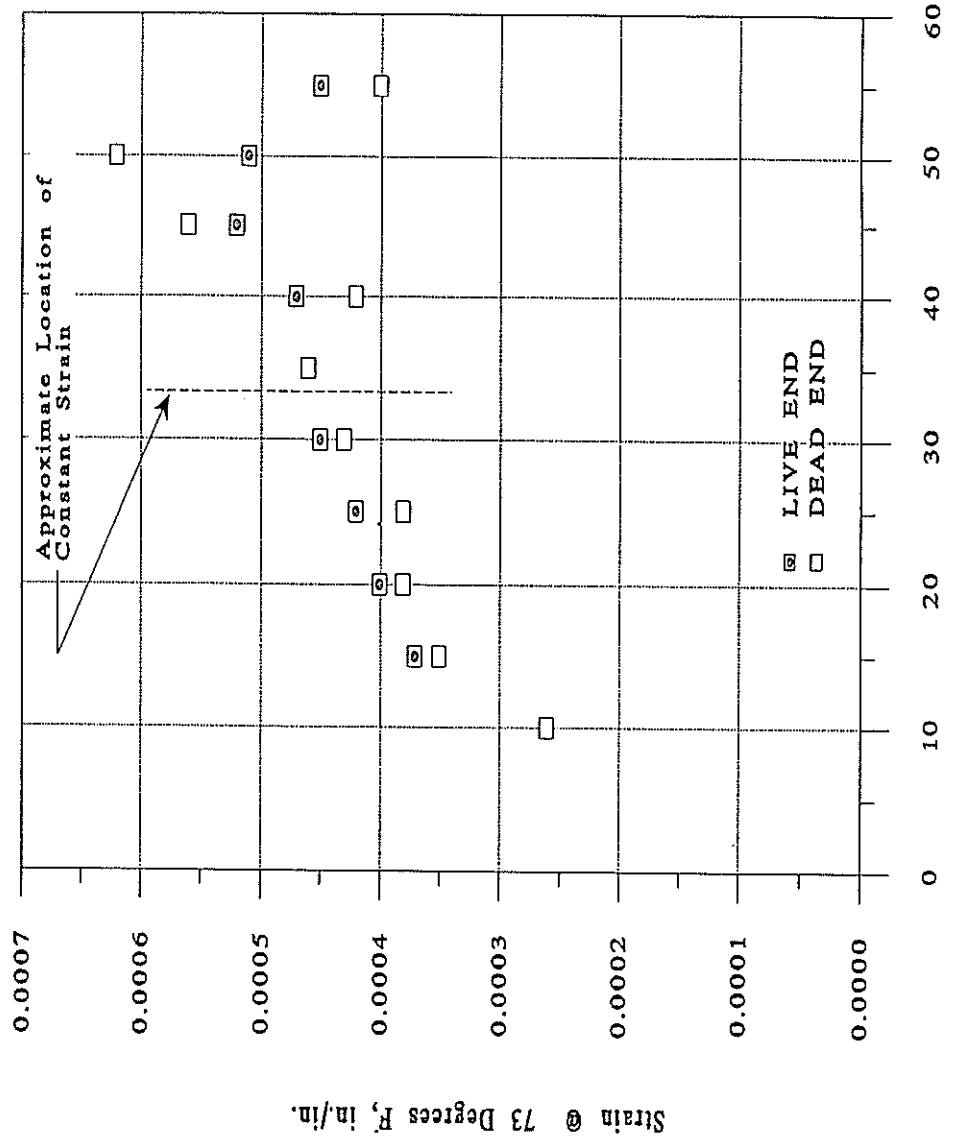

Figure 16. Strand transfer length plot for pile specimen P2 @ 14 days.

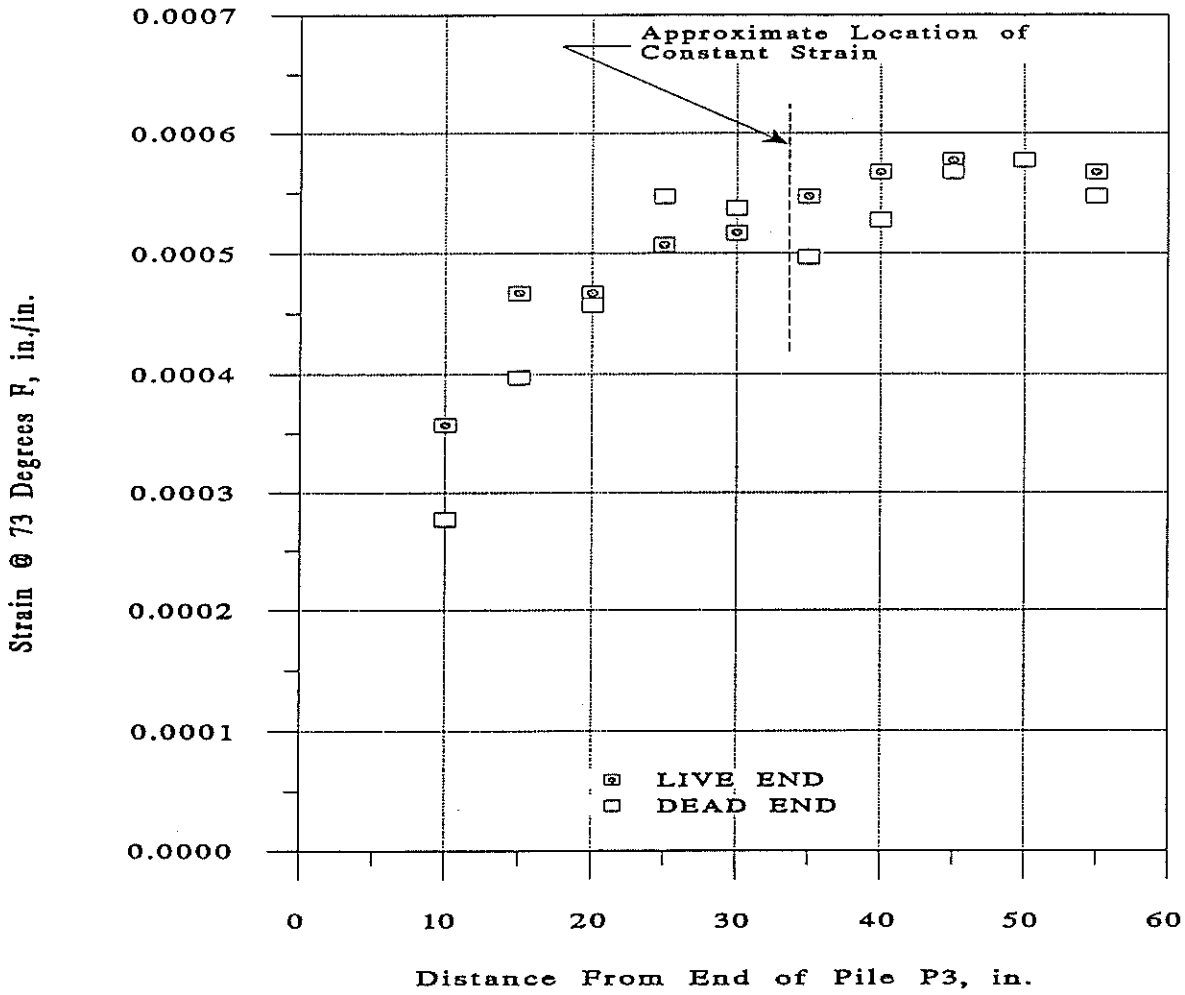

Figure 17. Strand transfer length plot for pile specimen P3 @ 14 days.

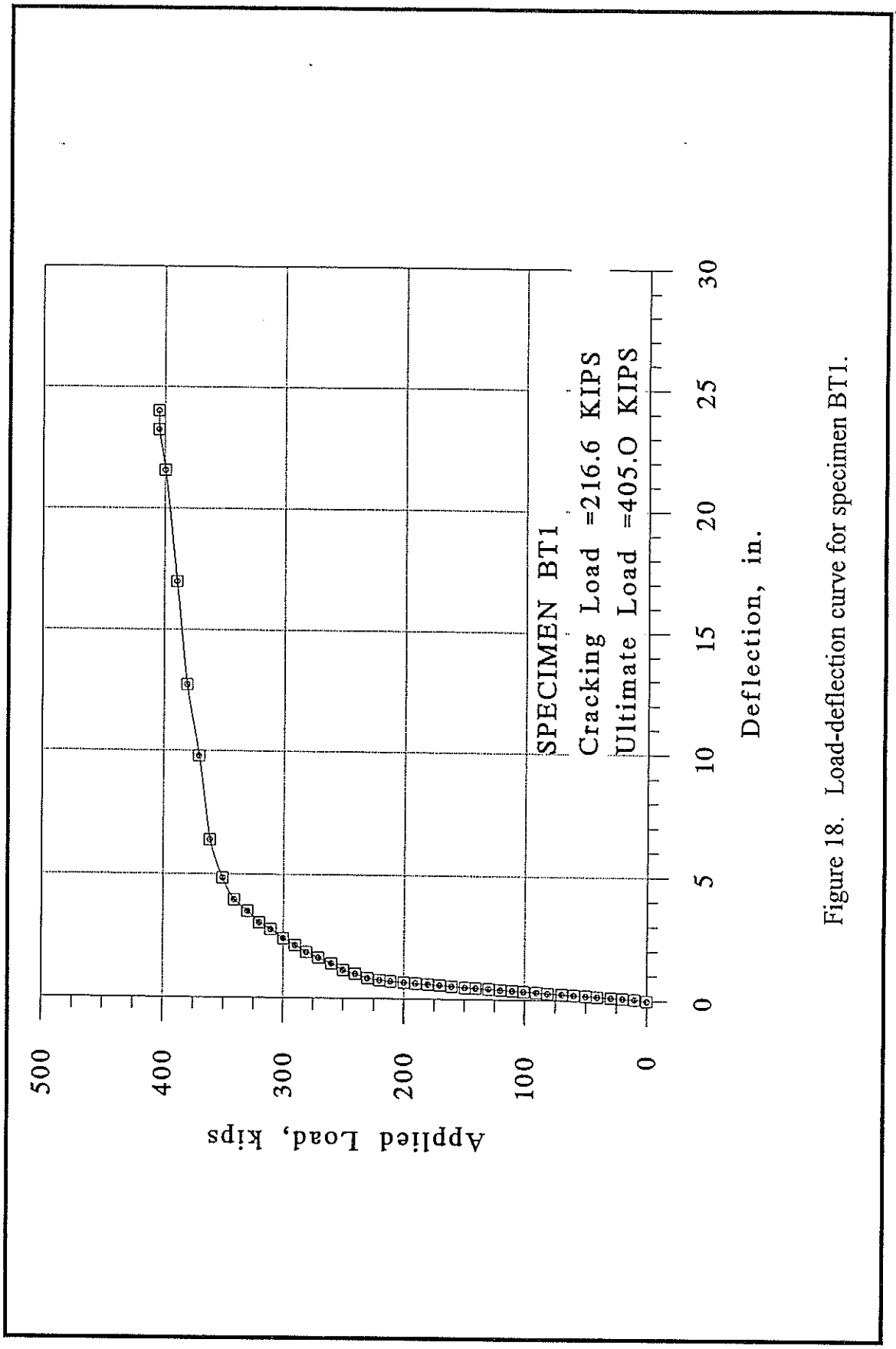

Figure 18. Load-deflection curve for specimen BT1.

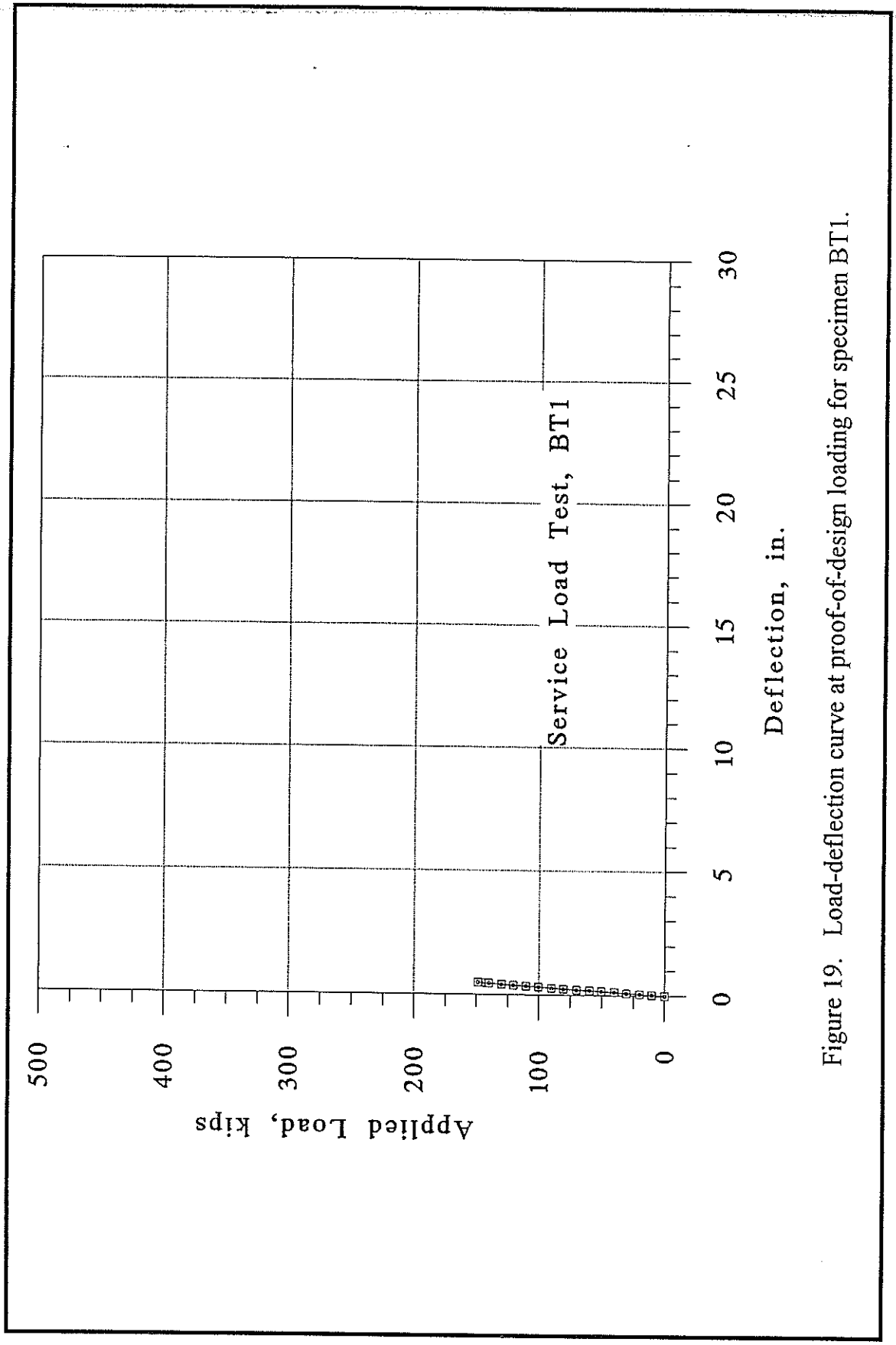

Figure 19. Load-deflection curve at proof-of-design loading for specimen BT1.

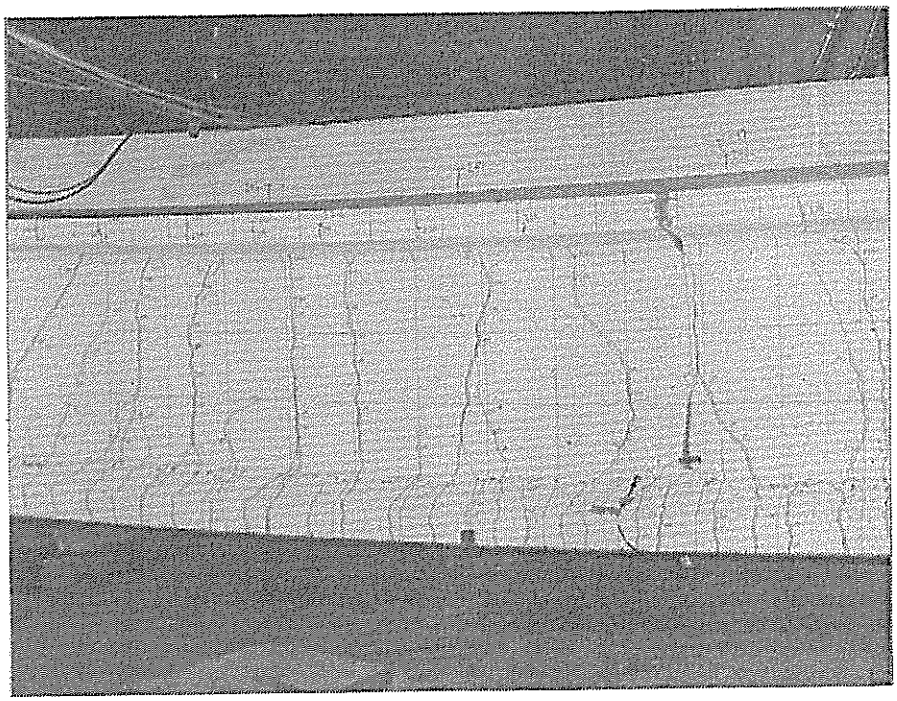

Figure 20. Flexural cracks in constant moment region of BT1 at 364 kips (1,619 kN) of total applied load.

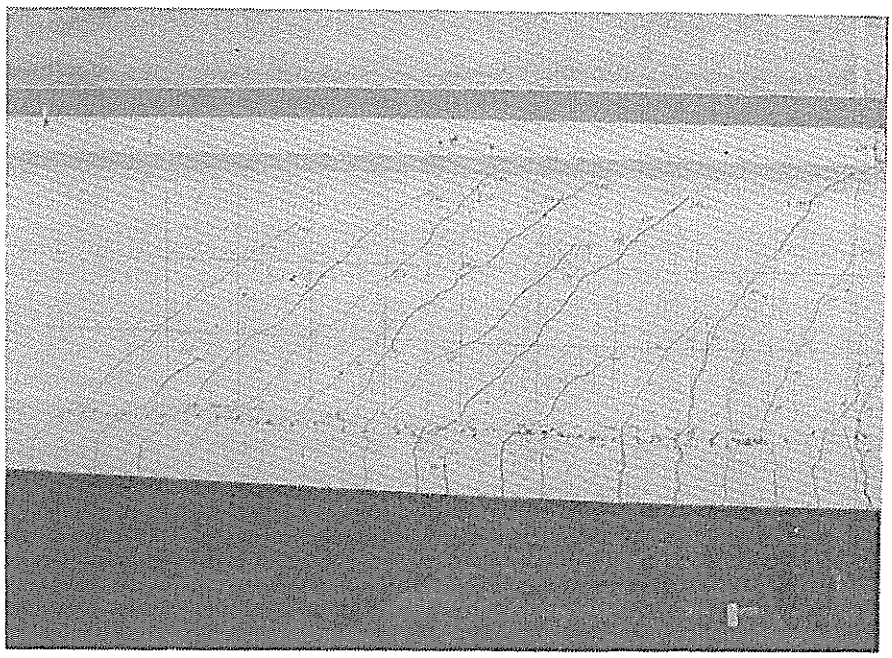

Figure 21. Flexure-shear cracks in BT1 @ applied load of 364 kips (1,619 kN).

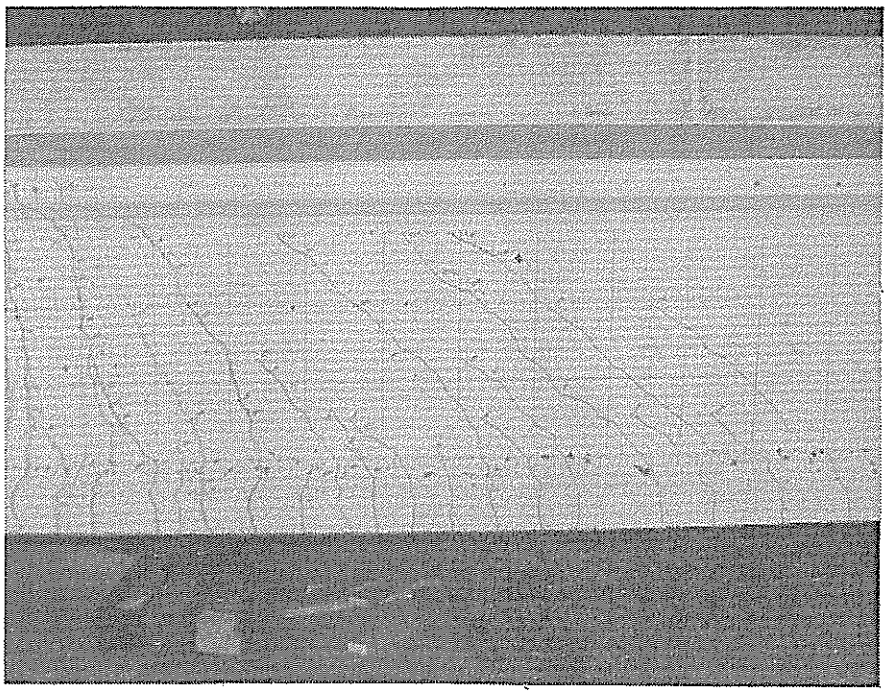

Figure 22. Flexure-shear cracks in BT1 @ applied load of 364 kips (1,619 kN).

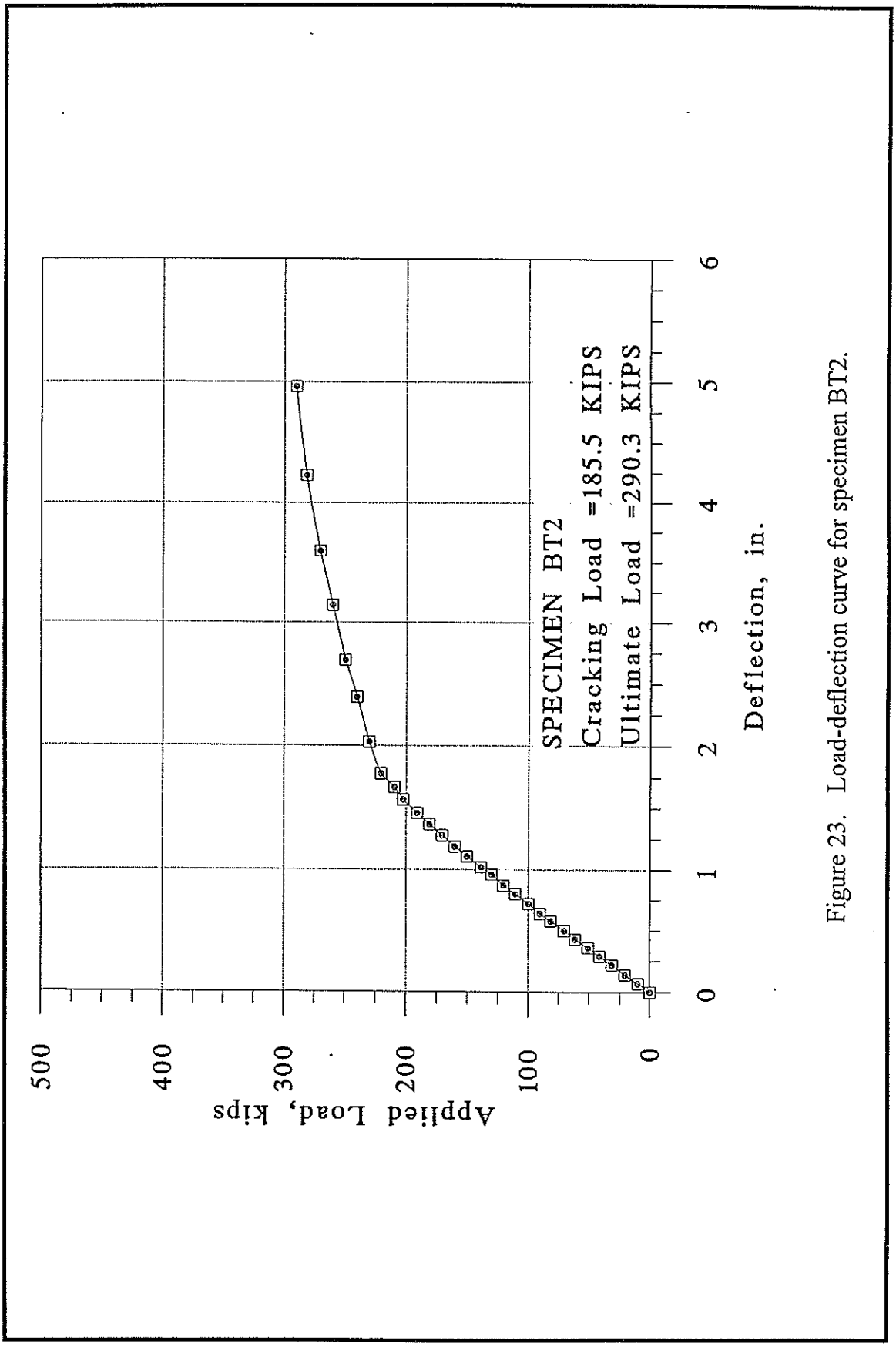

Figure 23. Load-deflection curve for specimen BT2.

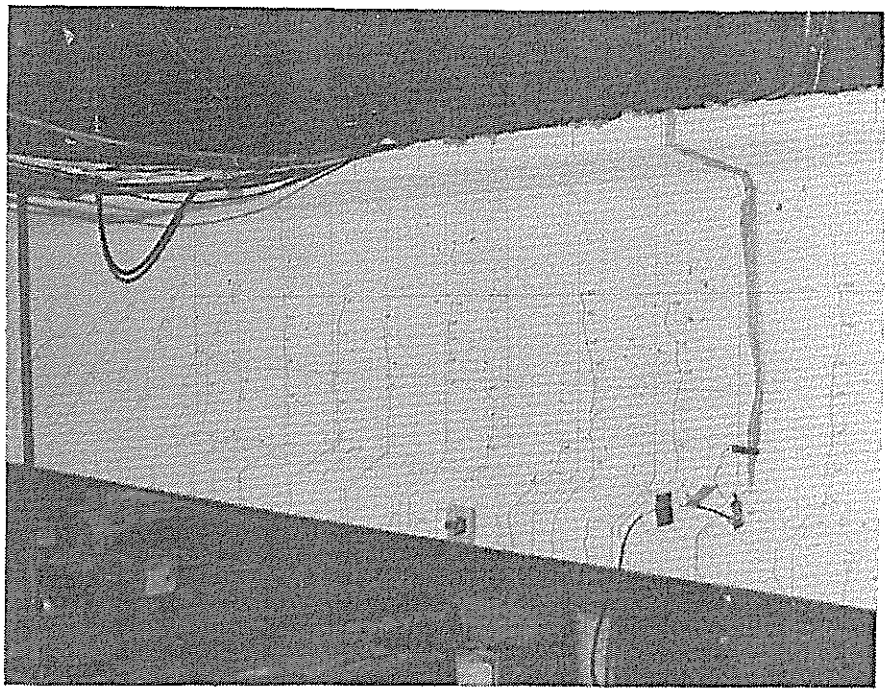

Figure 24. Flexural cracks in the constant moment region of BT2 @ load of 290 kips (1,290 kN).

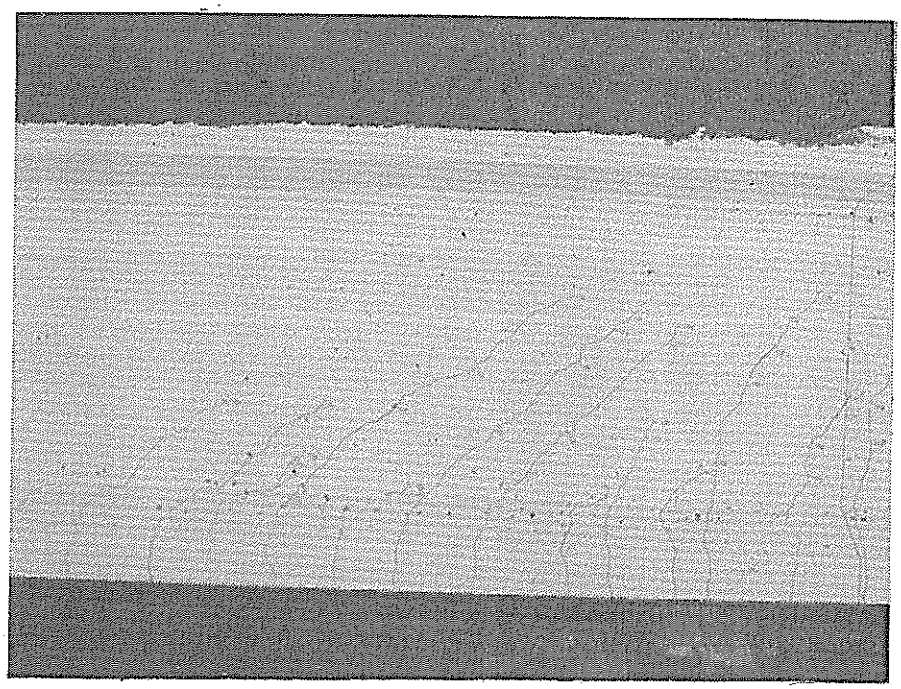

Figure 25. Flexure-shear cracks in BT2 @ applied load of 290 kips (1,290 kN).

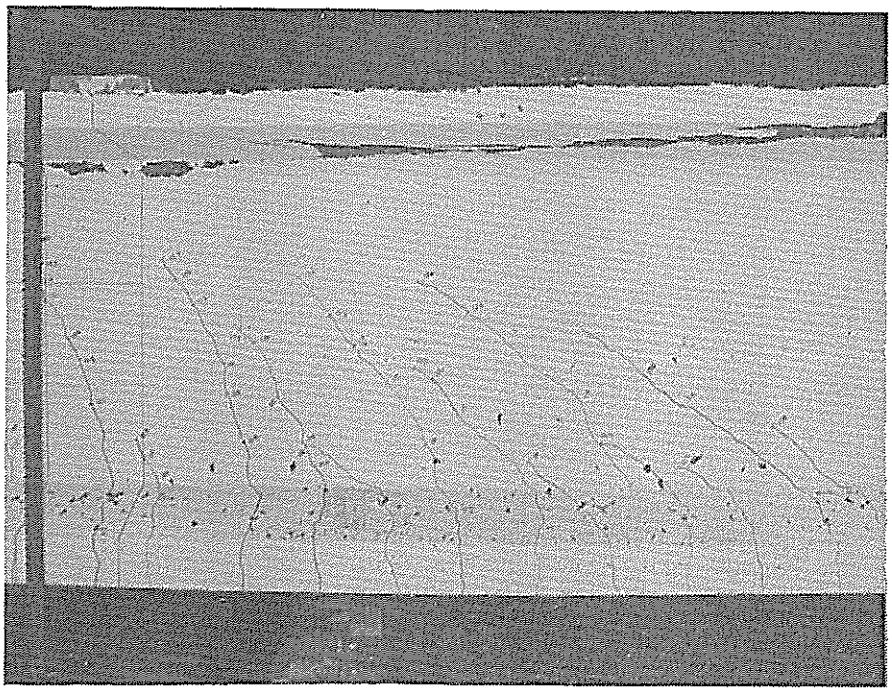

Figure 26. Flexure-shear cracks, BT2 @ applied load of 290 kips (1,290 kN).

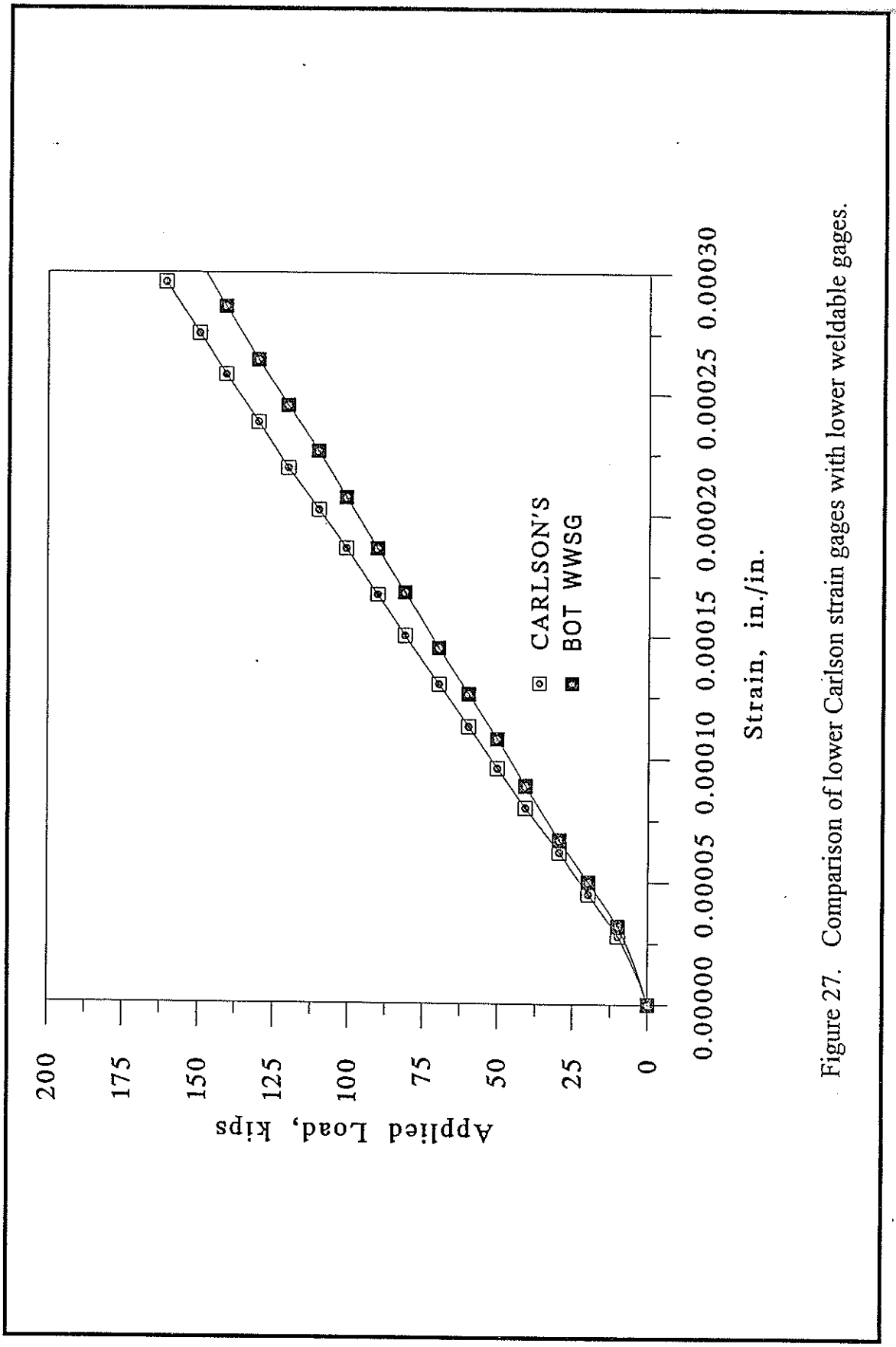

Figure 27. Comparison of lower Carlson strain gages with lower weldable gages.

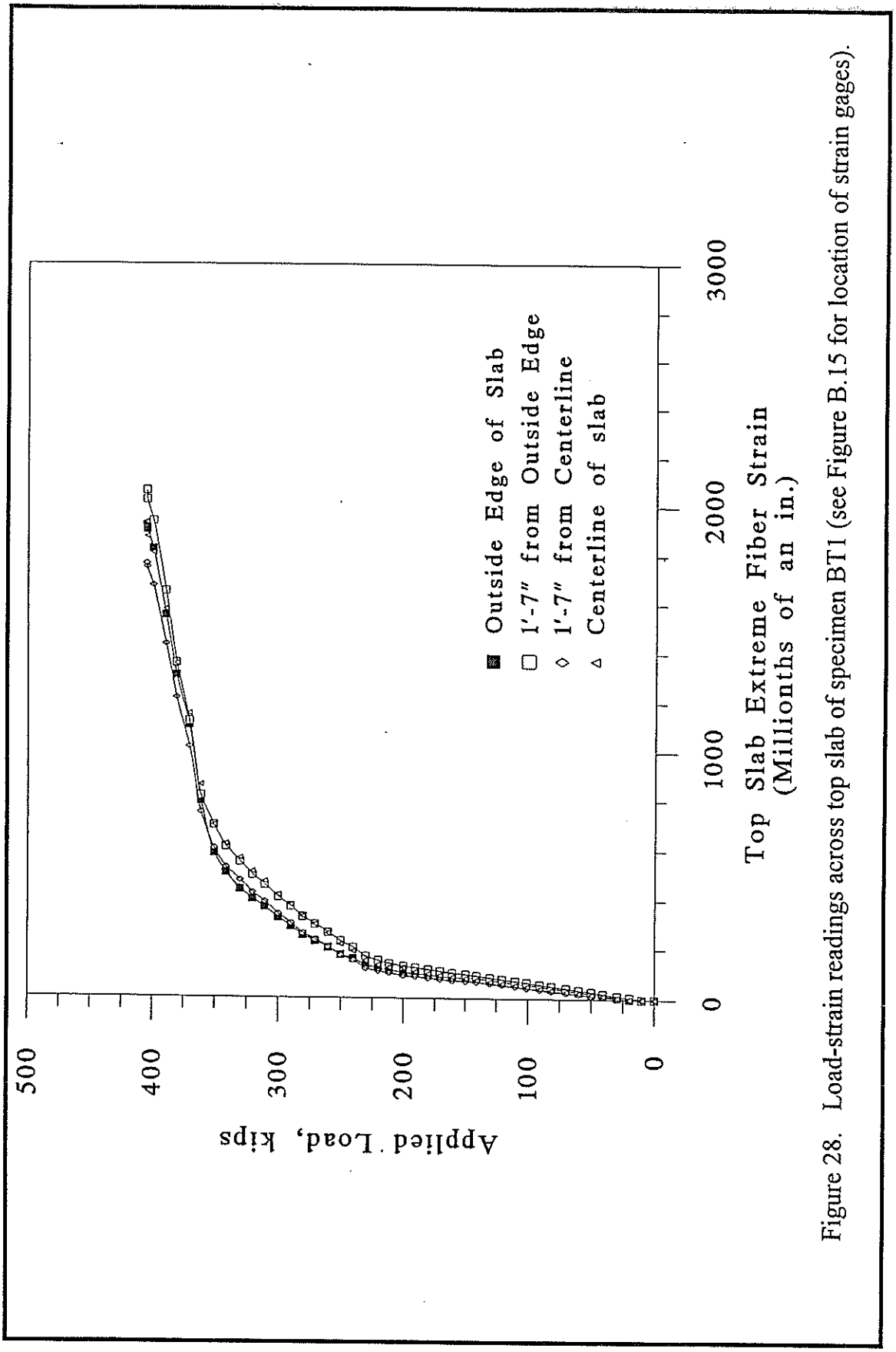

Figure 28. Load-strain readings across top slab of specimen BT1 (see Figure B.15 for location of strain gages).

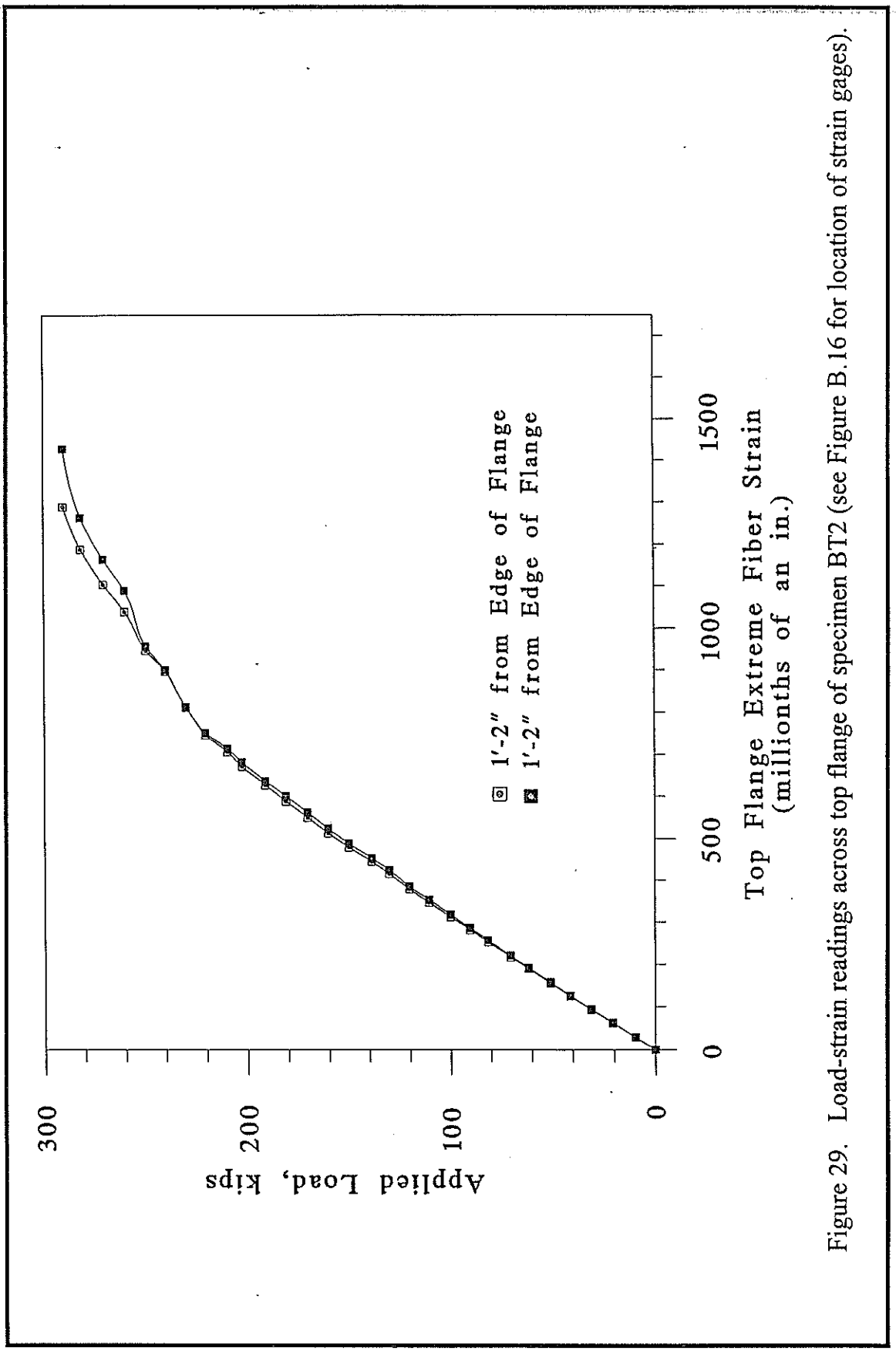

Figure 29. Load-strain readings across top flange of specimen BT2 (see Figure B.16 for location of strain gages).

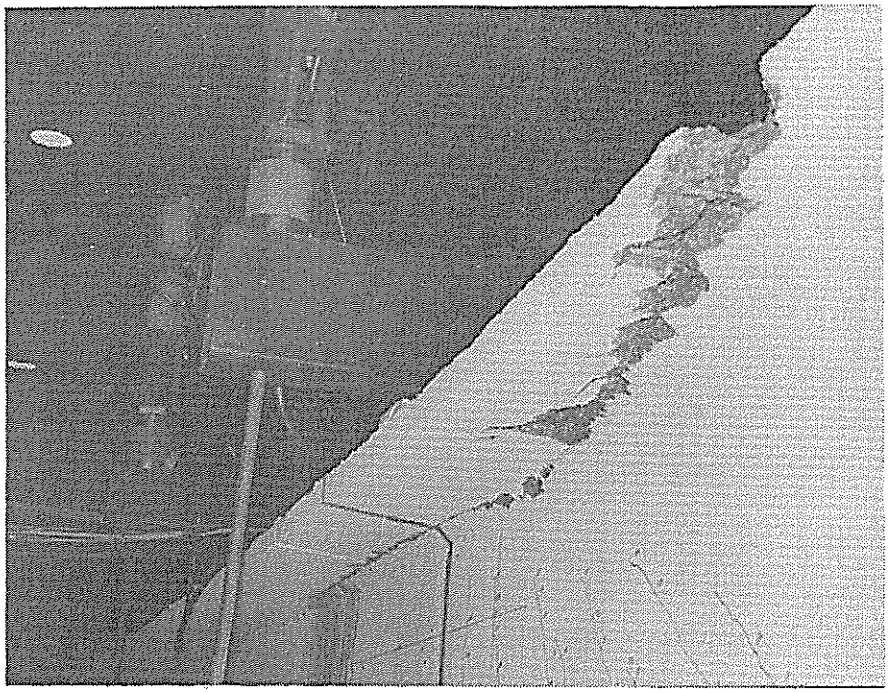

Figure 30. Failure region of BT2.

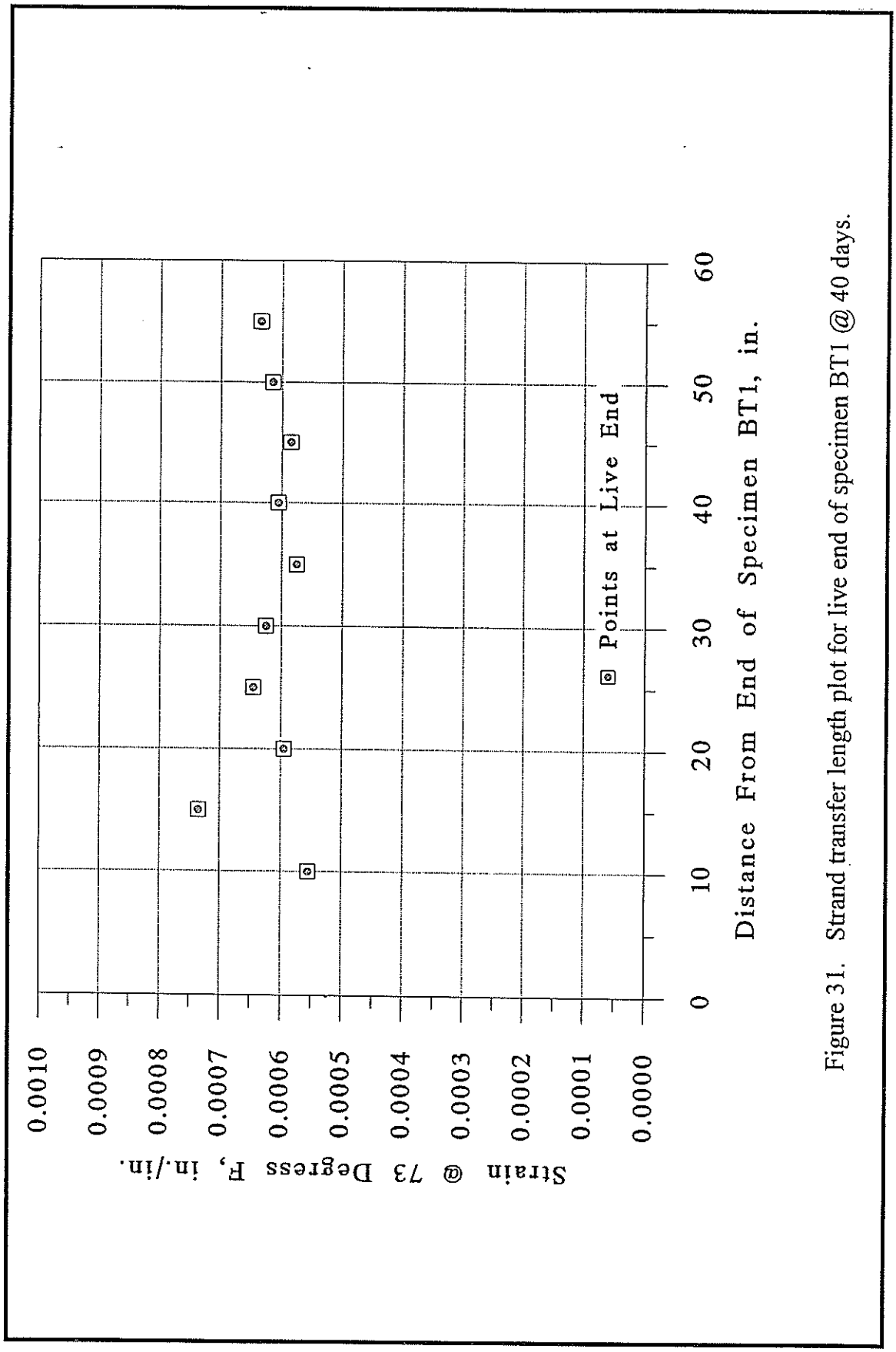

Figure 31. Strand transfer length plot for live end of specimen BT1 @ 40 days.

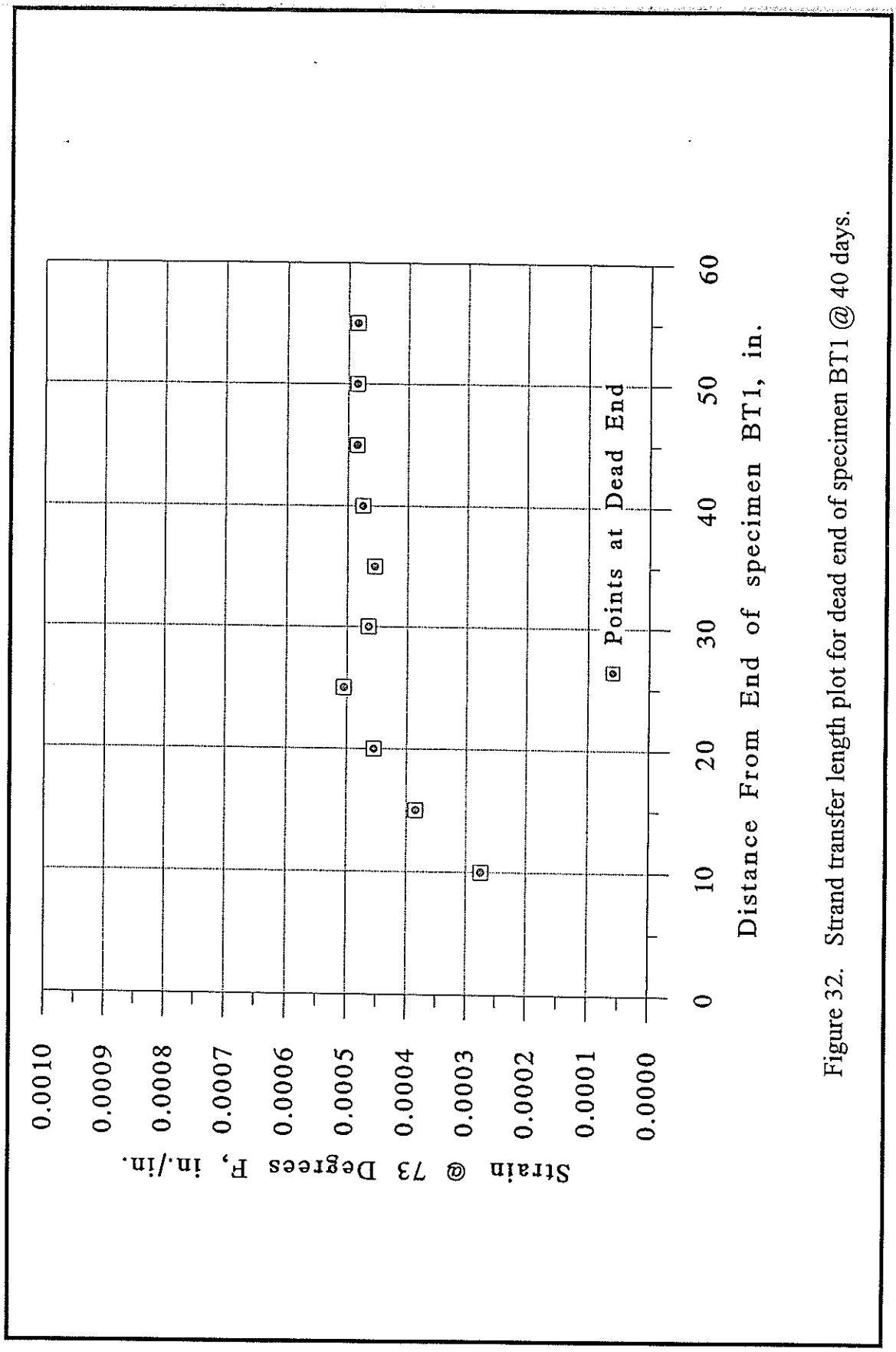

Figure 32. Strand transfer length plot for dead end of specimen BT1 @ 40 days.

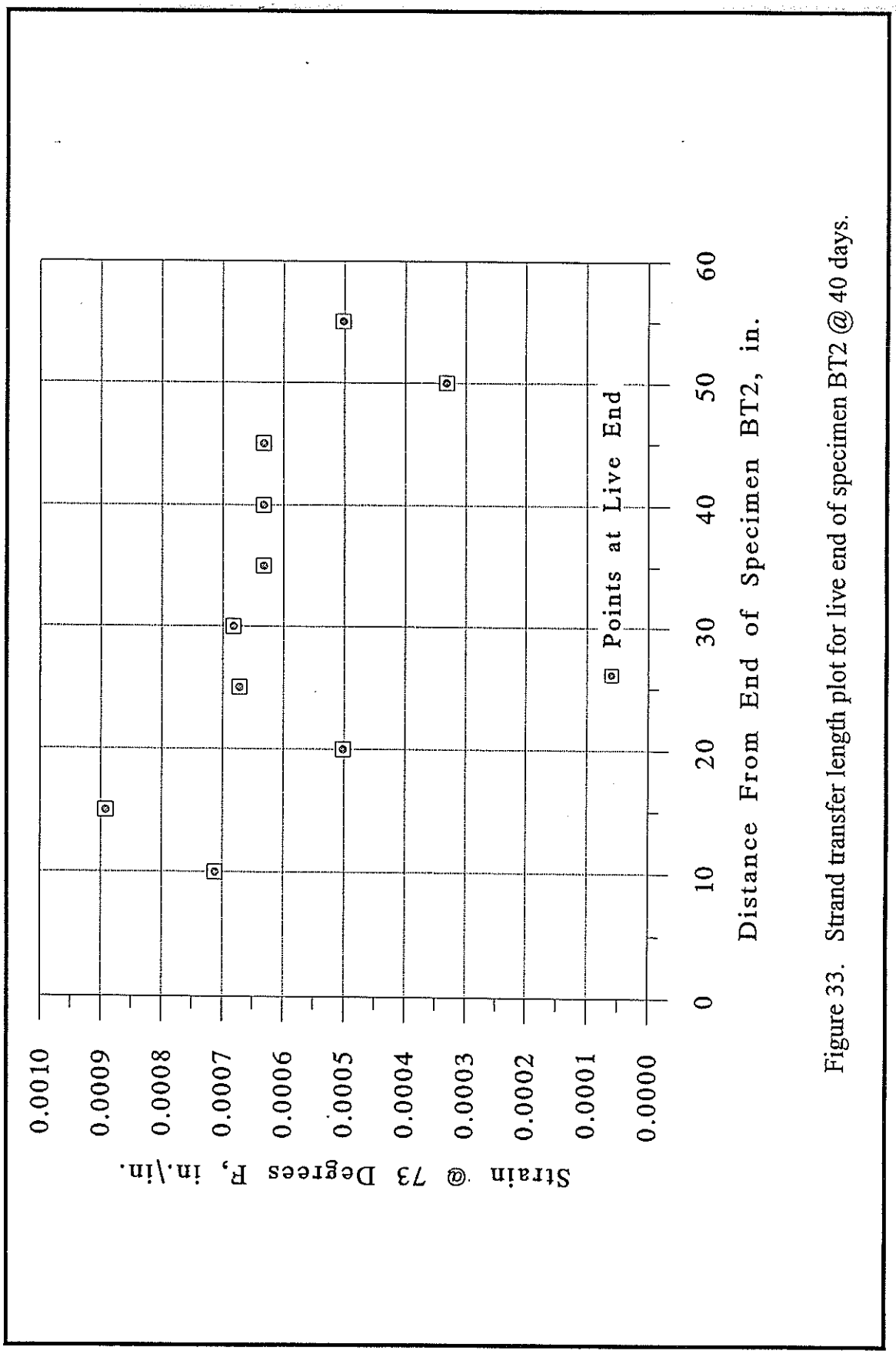

Figure 33. Strand transfer length plot for live end of specimen BT2 @ 40 days.

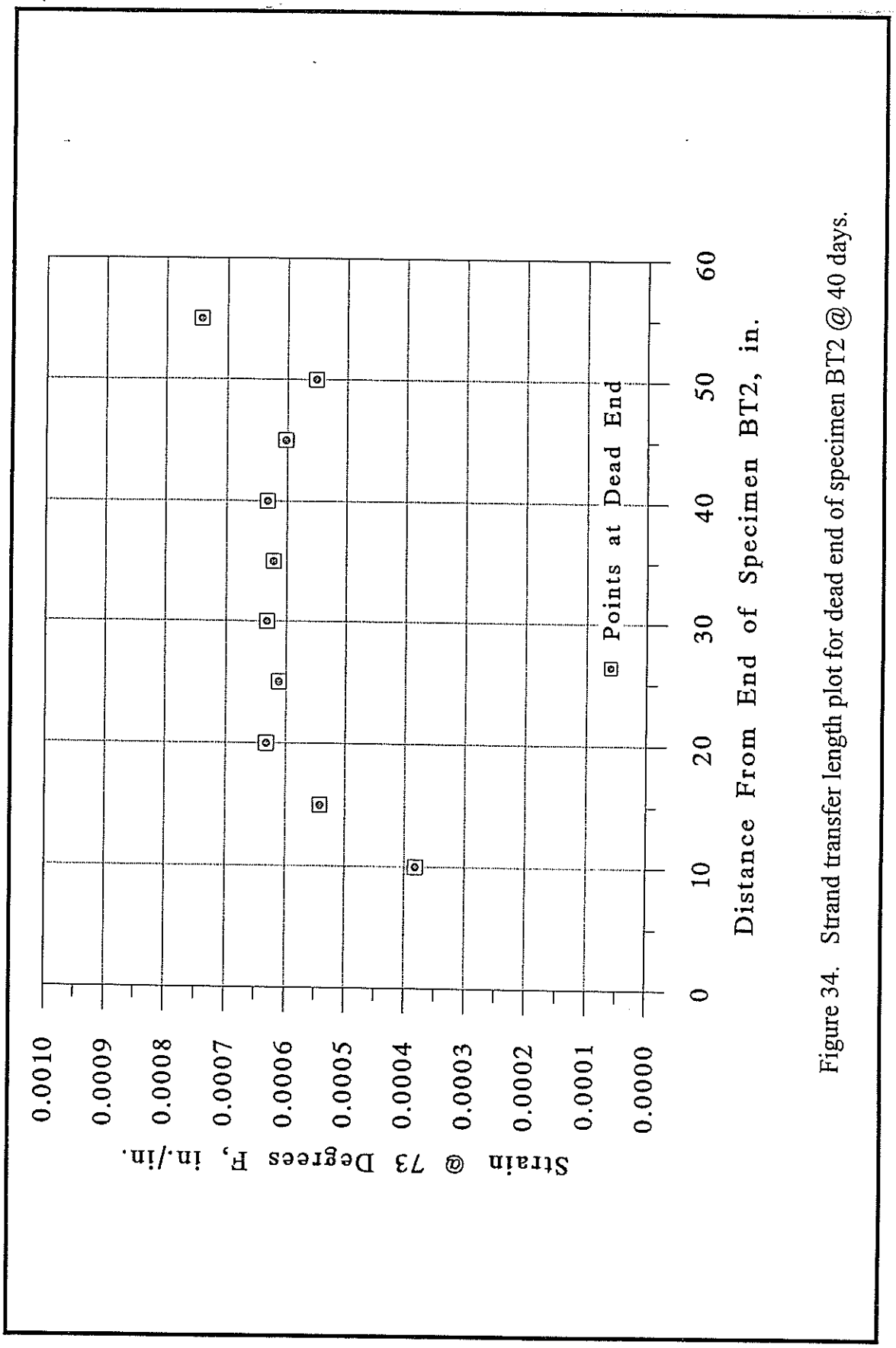

Figure 34. Strand transfer length plot for dead end of specimen BT2 @ 40 days.

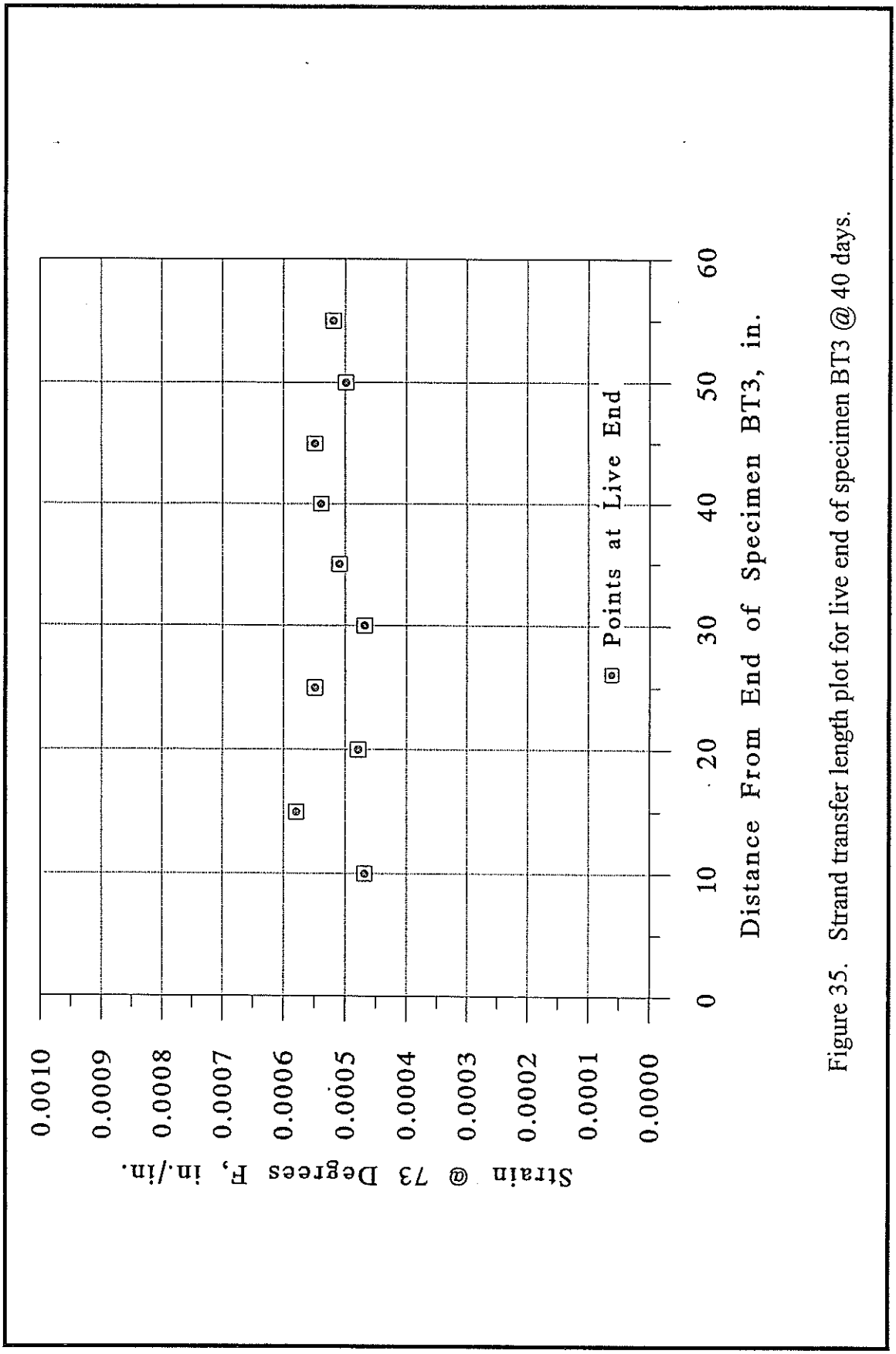

Figure 35. Strand transfer length plot for live end of specimen BT3 @ 40 days.

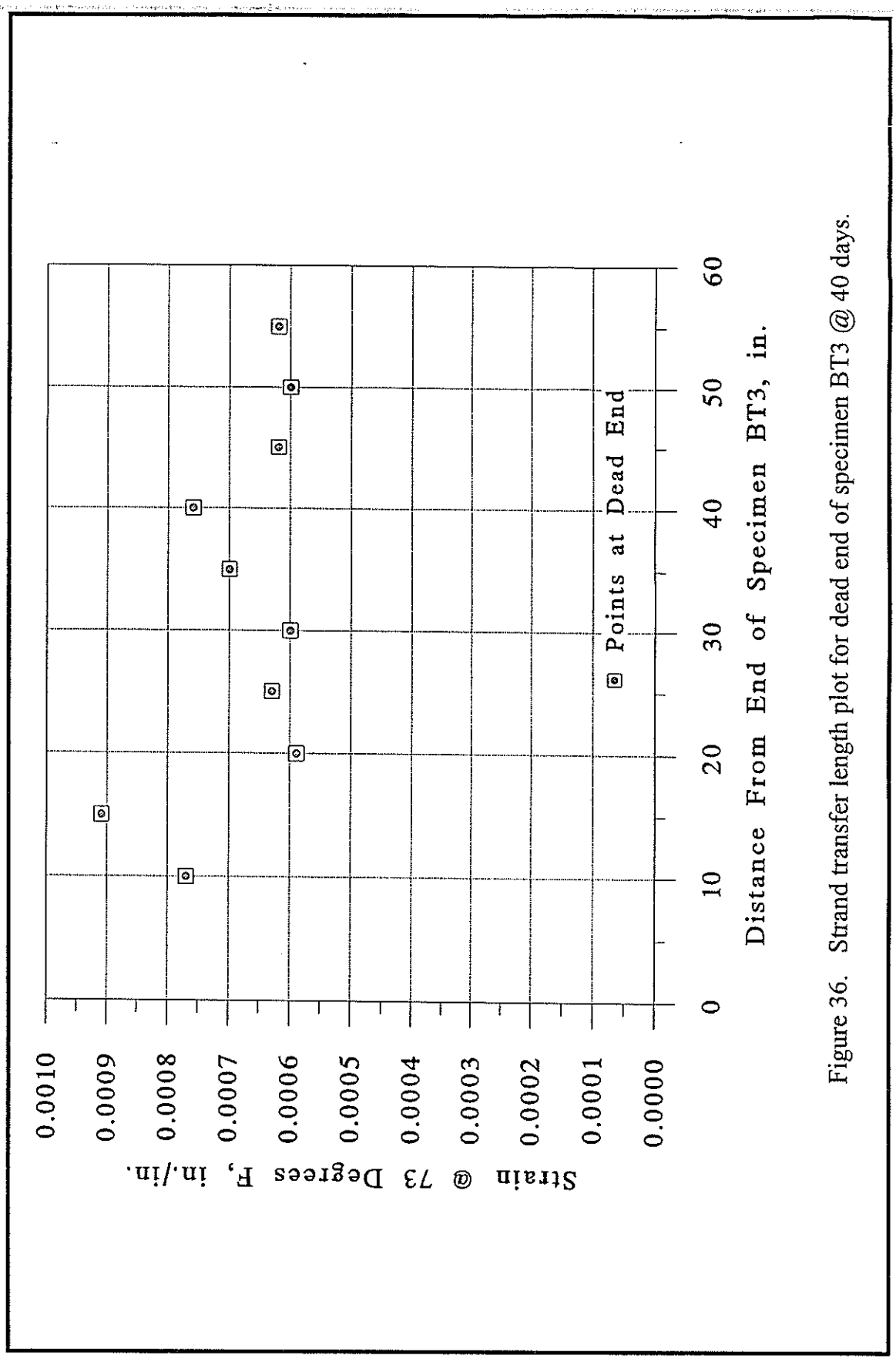

Figure 36. Strand transfer length plot for dead end of specimen BT3 @ 40 days.

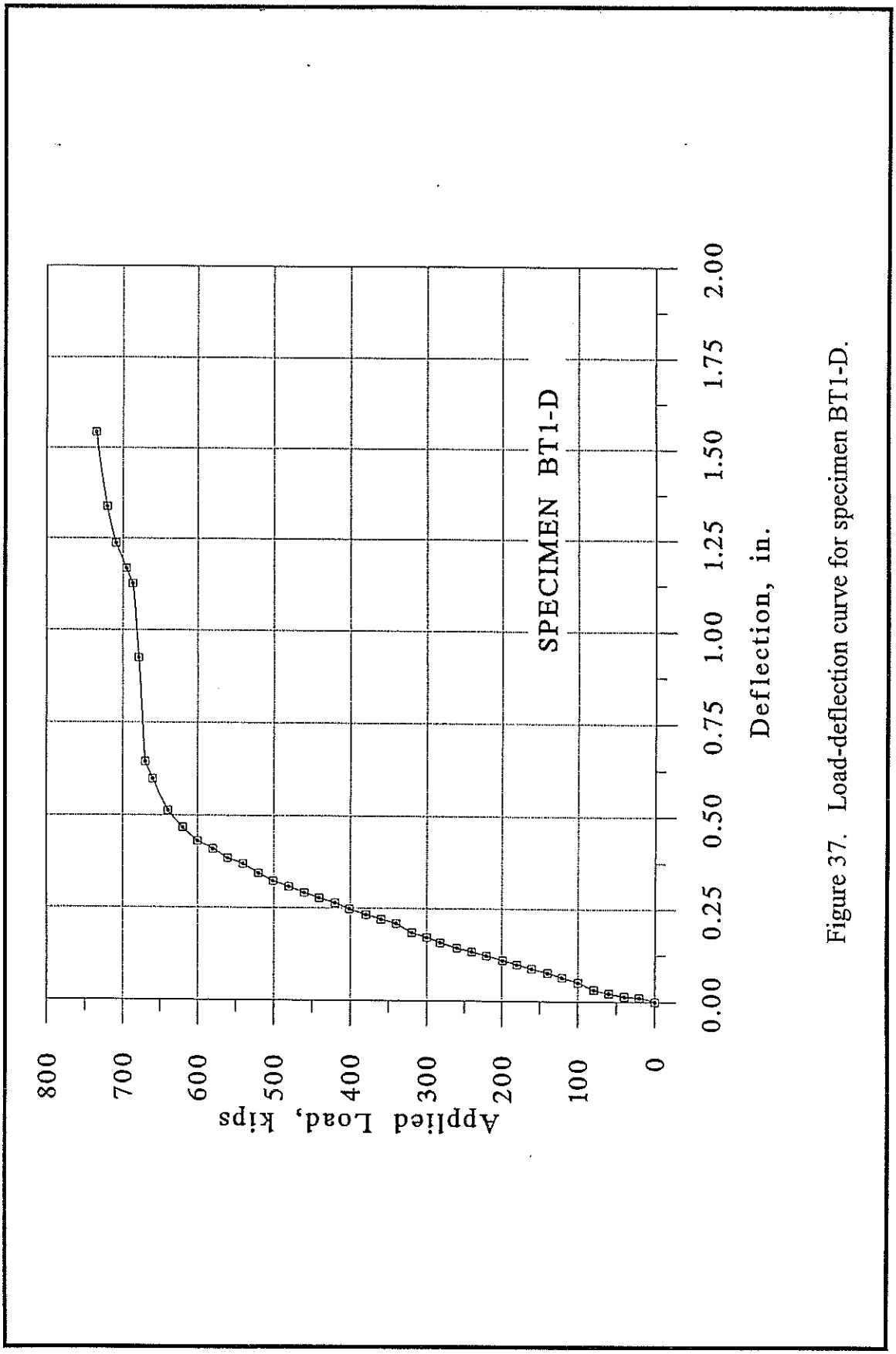

Figure 37. Load-deflection curve for specimen BT1-D.

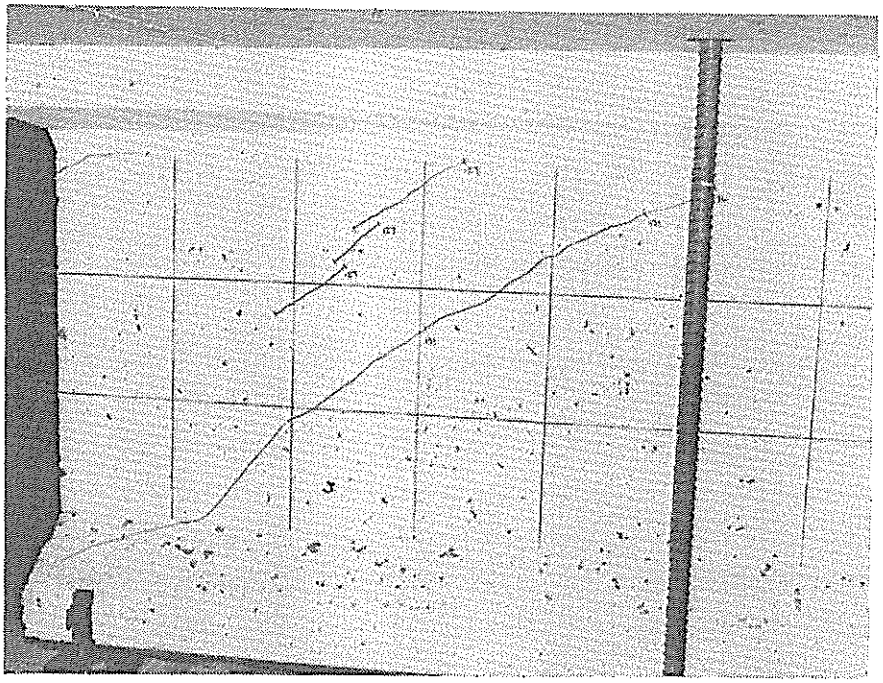

Figure 38. Web cracking of specimen BT1-D.

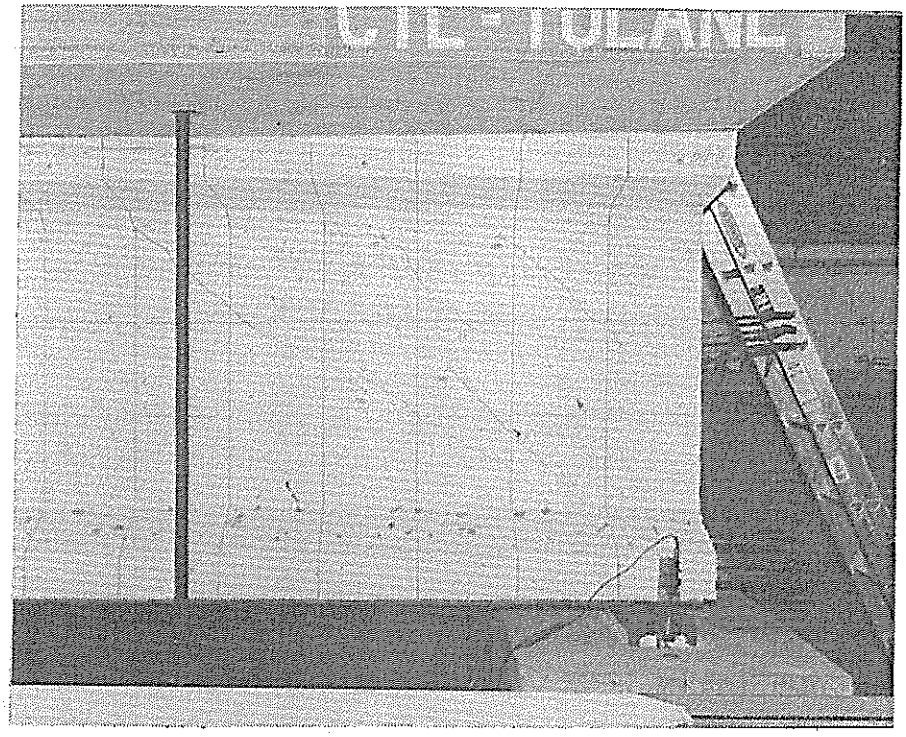

Figure 39. Web cracking of BT1-D.

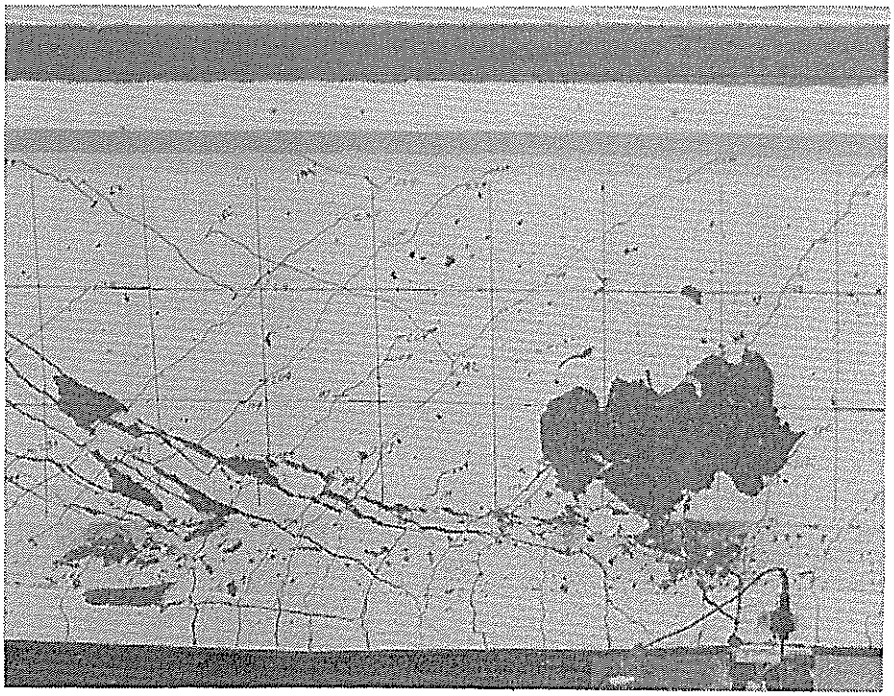

Figure 40. Failure region of specimen BT1-D.

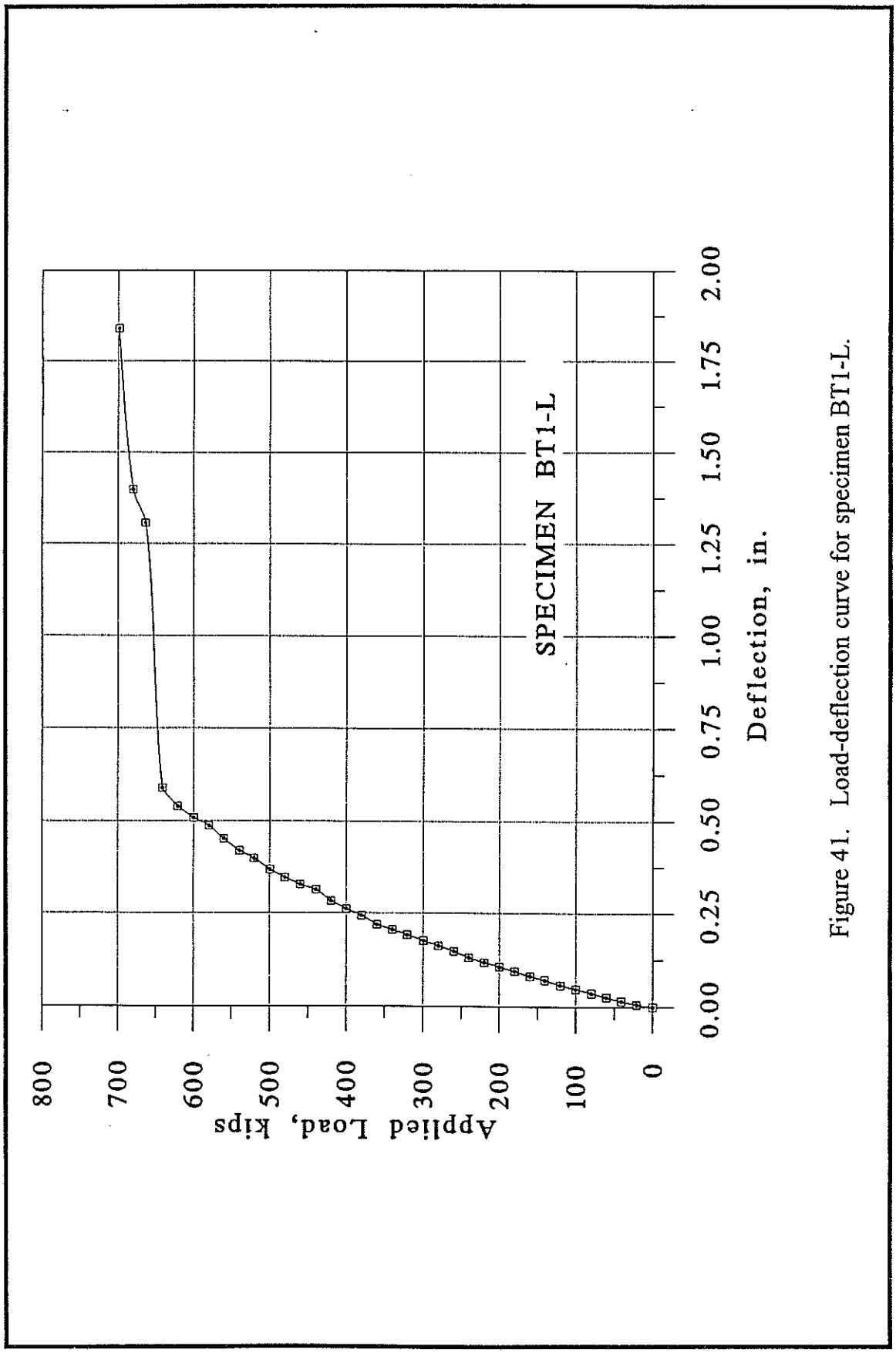

Figure 41. Load-deflection curve for specimen BT1-L.

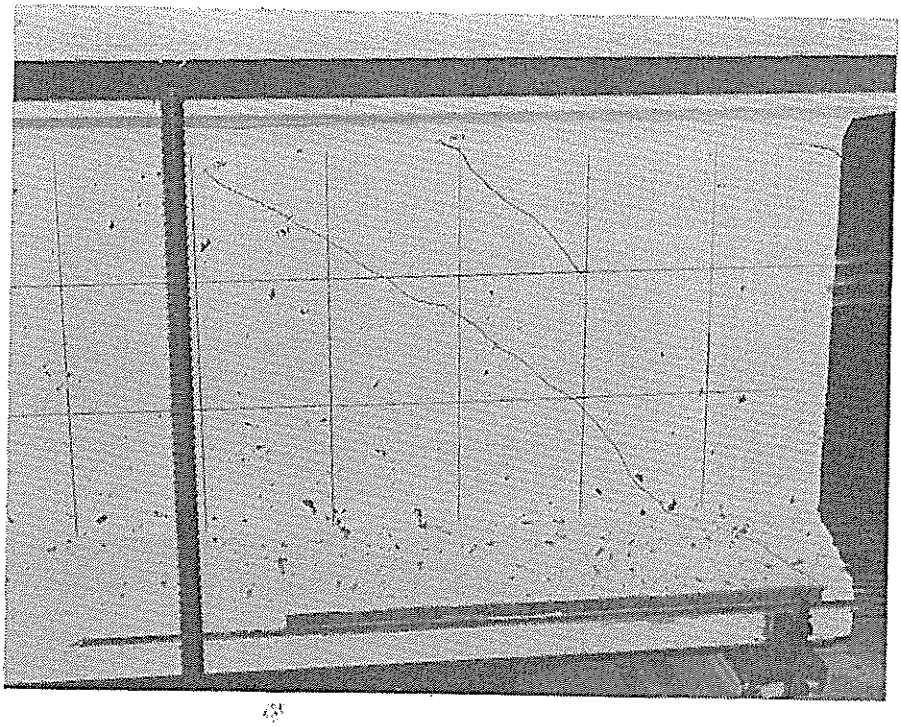

Figure 42. Web cracking of specimen BT1-L.

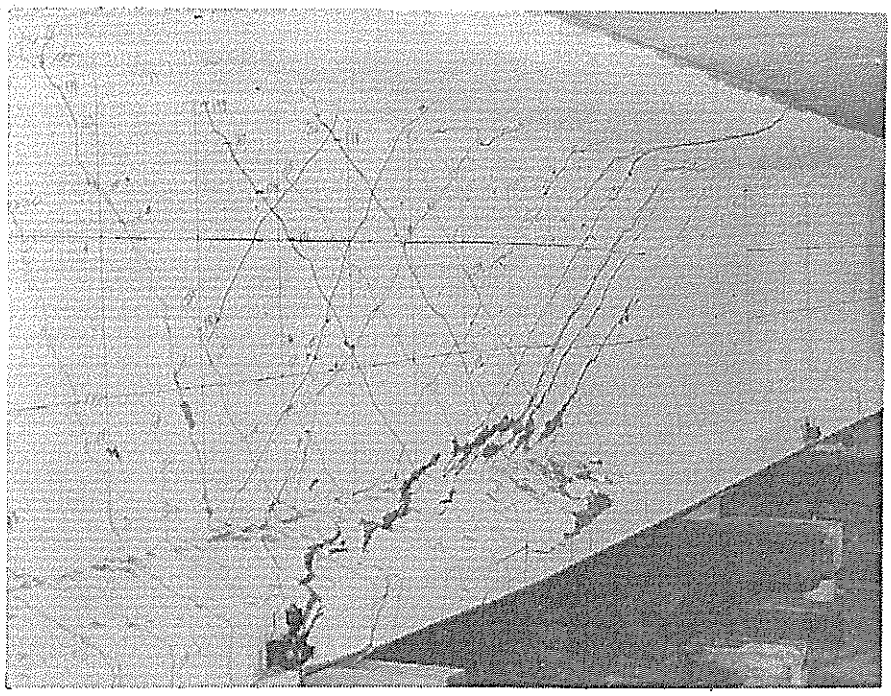

Figure 43. Web cracking of BT1-L.

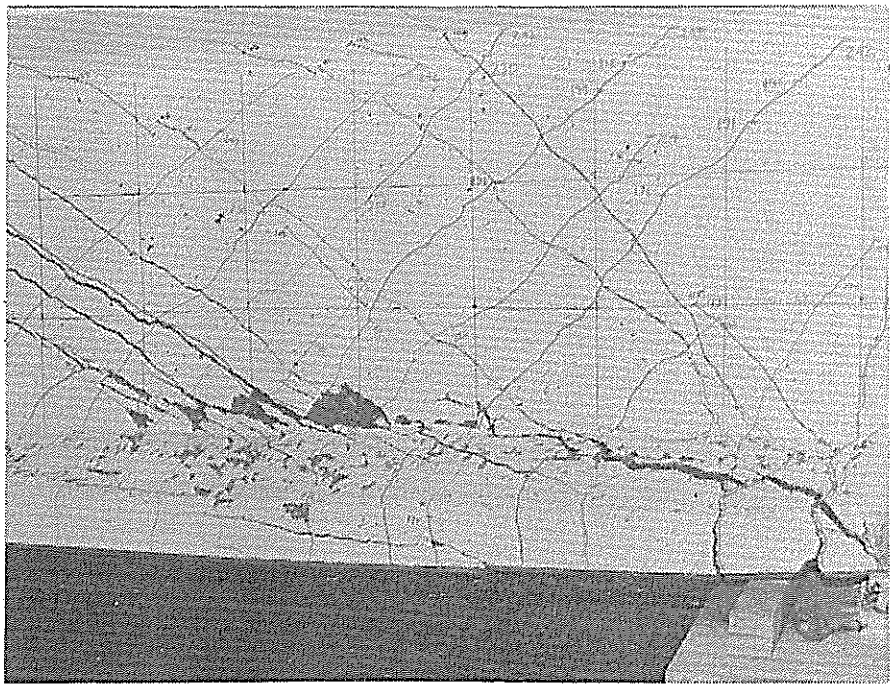

Figure 44. Failure region of specimen BT1-L.

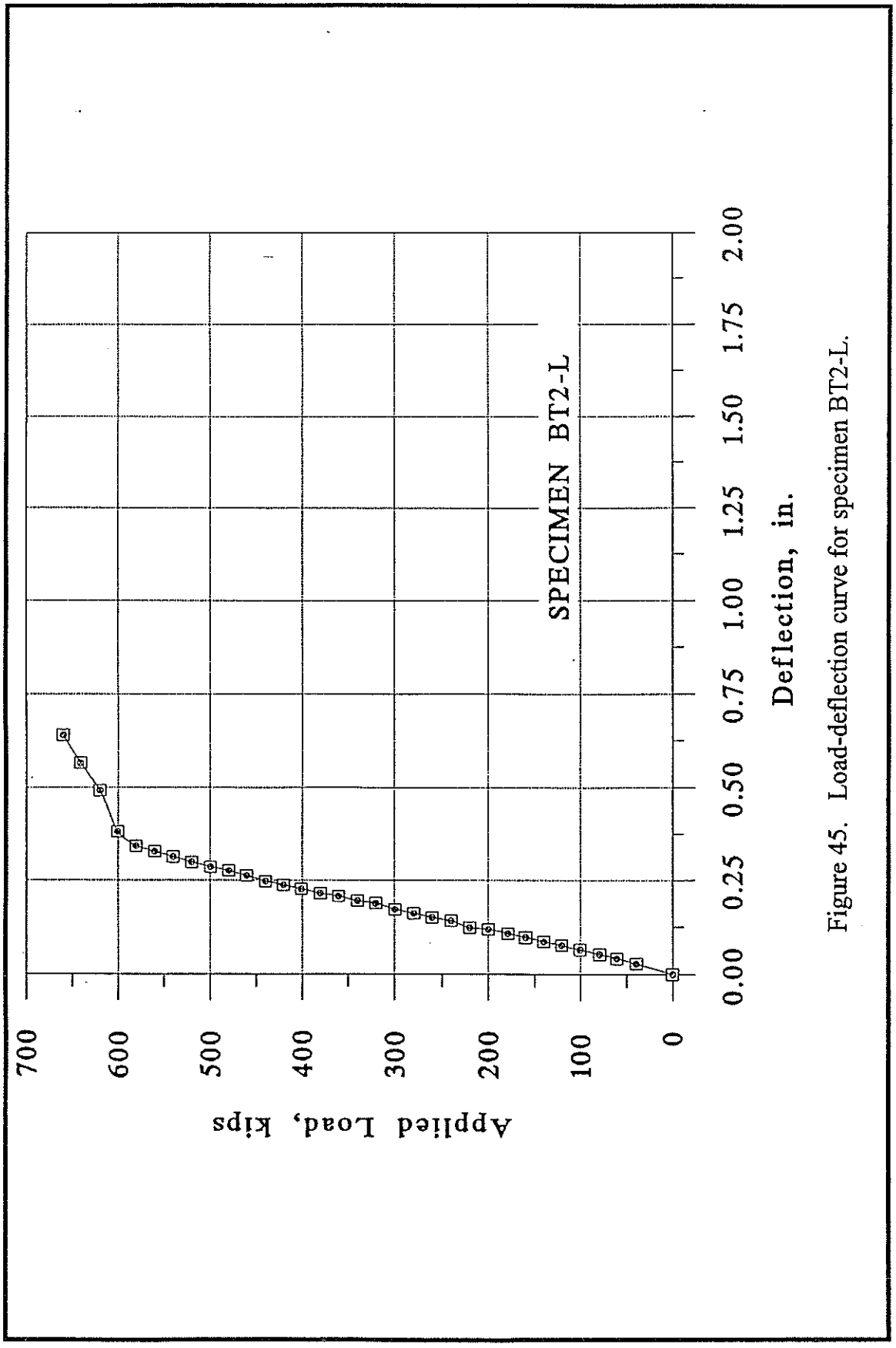

Figure 45. Load-deflection curve for specimen BT2-L.

f_{pe} = stress at the bottom of a specimen resulting from the effective prestressing force, psi

f_{ps} = calculated stress in the prestressing steel at beam failure, psi

f_{pu} = tensile strength of the prestressing strand, psi

f_r' = modulus of rupture of the concrete, psi

f_{se} = effective stress in prestressing strand after losses, ksi

f_t' = direct tensile strength of the concrete, psi

I = moment of inertia of the specimen, in^4

l_t = strand transfer length, in.

M_{cr} = bending moment at flexural cracking due to total applied load, P_{tot}, in.-lb

M_{DL} = dead load moment, in-lb

M_{cr}' = bending moment at flexural cracking due to total applied load P_{fsc}, in.-lb

M_u = ultimate strength of the specimen in bending, in-lb

P_{fc} = total applied load, not including member self-weight, at the time of flexural cracking, lb

P_{fsc} = total applied load, not including member self-weight, at the time of initial flexural-shear cracking, lb

P_{tot} = total observed applied load, not including member self-weight, lb

V_{ci} = total shear producing flexure-shear concrete crack, lb

V_{cw} = total shear producing web shear concrete crack, lb

V_d = dead load shear at the location under consideration, lb

V_p = vertical component of the force in the prestressing strands, lb

V_s = shear strength provided by shear reinforcement, lbs

y_b = distance from the centroid of the section to the bottom fiber of the specimen, in.

w_c = unit weight of concrete, lb/ft^3

β_1 = 0.65 for all concrete with compressive strength equal to or greater than 8000 psi

ϕ = capacity reduction factor. a value of 1 was used for experimental investigations

γ_p = factor for the type of prestressing strand

ρ = $\frac{A_{ps}}{bd}$

ρ_p = ratio of prestressed reinforcement

2. REVIEW OF PREVIOUS INVESTIGATIONS OF HIGH-STRENGTH CONCRETE

2.1 INTRODUCTORY REMARKS

This section contains a brief summary of selected recent experimental research regarding high-strength concrete and the use of high-strength concrete in prestressed elements of highway structures. A description and the results of each investigation are summarized. Only recent investigations providing the background necessary for this investigation are reported.

2.2 RESEARCH AT THE LOUISIANA TRANSPORTATION RESEARCH CENTER

To date there have been two research efforts performed by, or in cooperation with, the Louisiana Transportation Research Center. The first, performed by Law & Rasoulian, (3), concluded that concrete strengths of 6,500 psi (45 MPa) and higher could be fabricated using regionally available materials and such strengths could best be achieved through the use of crushed limestone as the coarse aggregate.

The second research effort was performed by Adelman and Cousins (4). The objective of this project was to investigate the cost effectiveness and material properties of high-strength concrete made with Louisiana available materials for use in prestressed, pretensioned bridge girders. A summary of the findings of this research is as follows:

1. A mix design was developed that consistently yielded 28-day concrete compressive strengths in excess of 10,000 psi (69 MPa). The mix consisted of crushed limestone with 3/4-in. (19-mm)

maximum size, Type I portland cement, Class C fly ash, and a superplasticizer. A mix yielding 10,000 psi (69 MPa) without a superplasticizer proved unworkable.

2. The concrete modulus of rupture compared well with results in the literature. The concrete modulus of elasticity, 6,800 ksi (46.9 MPa), represented the upper bound for other values reported in the literature.

3. An increase in concrete design compressive strength from 6,000 psi (41 MPa) to 10,000 psi (69 MPa) resulted in an approximate 10 percent increase in span length with an overall decrease in superstructure cost of five percent for a typical three-span LaDOTD bridge.

2.3 RESEARCH PERFORMED AT THE UNIVERSITY OF TEXAS AT AUSTIN

The University of Texas at Austin has performed a significant amount of research into the use of high-strength concrete in highway structures. Most of this research has been part of Research Project 3-5-84-381, "Optimum Design of Bridge Girders Made Using High Strength Concretes and Deflection of Long-Span Prestressed Concrete Beams". This research effort was performed for the Texas State Department of Highways and Public Transportation. From this research project four reports were written. Each of these are discussed below.

2.3.1 Kelly, Bradberry, and Breen- Report 381-1

In this investigation by Kelly, Bradberry, and Breen (5), field instrumentation of eight 127-ft (38.7 m) pretensioned AASHTO Type IV bridge

girders was reported. Four of the girders were in one bridge while the remaining four were in a second bridge. The girders were instrumented at the time they were cast and were monitored for three years. Two of the beams in each bridge were instrumented to measure concrete surface strains, prestressing strand strain, internal concrete temperature, and camber or deflection. The remaining two beams in each bridge were instrumented to measure only surface strains and camber.

The concrete mix used in the beams consisted of Type III portland cement, sand, crushed limestone aggregate, and a superplasticizer admixture. The mix had an average water/cement ratio of 0.4. The average 28-day strength of the concrete mix was 8,620 psi (59 MPa). The objectives of this research were to:

1. Measure the elastic and time-dependent deformations of the beams during field construction and early service life and determine the sensitivity of time-dependent behavior to variations in material properties and the construction time schedule.
2. Test material samples from the instrumented beams to determine the long- and short-term material properties.
3. Evaluate the accuracy of current analytical techniques for predicting time-dependent behavior and revise and improve those techniques where required.

Problems were encountered in this research project that complicated the achievement of the stated objectives. The concrete surface strain measuring system did not work properly due to a failure in the adhesive system used to attach the Demec points. The readings were considered totally unreliable within 100 days. The strand strain measuring system basically failed with most gauges no longer providing reasonable readings one month after installation. The system for

measuring internal temperature gradient and camber measurements, however, performed well.

The companion material tests on samples taken from the same batches of concrete from which the beams were made were successful. Tests were made to determine the concrete compressive strength and the modulus of elasticity as a function of time. In addition, measurements were made to determine the creep and shrinkage of the concrete used to cast the beams.

Some of the conclusions of this study were as follows:

1. The AASHTO formula for predicting the elastic modulus of concrete should not be used for predicting deflections with high-strength concrete ($f'c > 9{,}000$ psi (62 MPa)). It was recommended that the following formula be used in lieu of the one presently proposed by AASHTO:

$$E_c = 40{,}000\sqrt{f'_c} + 1.5 \times 10^6 \quad \text{psi} \qquad (1)$$

2. Elastic camber and deflection of high-strength concrete girders can be accurately predicted using moment area equations, if known concrete strengths are used.

3. The time-dependent camber or deflection of a beam is significantly affected by strength gain vs. age characteristics, the concrete creep coefficient, the relative humidity, the age of concrete at release and the construction schedule.

4. Additional research is needed to develop a reliable system for measuring long term strain of strand in pretensioned, prestressed concrete beams.

2.3.2 Hartman, Breen and Kreger - Report 381-2

In this research report, Hartman, Breen and Kreger (6) performed studies on the shear capacity of high-strength prestressed concrete girders. Ten pretensioned girder specimens made from concretes with compressive strengths ranging from 10,800 psi (74 MPa) to 13,160 psi (91 MPa) were tested. Six of the girders were cast specifically as shear strength test specimens and were 16 ft (4.9 m) long. The remaining four shear tests were performed on 17 ft 4 in. (5.3 m) long end sections of flexural specimens previously tested by Castrodale, Kreger, and Burns (7). All girders were one-third scale models of AASHTO Type IV girders.

The six shear specimens had a shear span to depth ratio, a/d, of 3.0 while the end sections of the flexural specimens had an a/d ratio of 3.2. The primary variable in these tests was the amount of shear reinforcement. Web reinforcement ratio values, Vs, ranged from 0.0 to $15\sqrt{f'c}\ b_w d$. The mix design used Type I portland cement, a coarse aggregate consisting of a very hard 3/8-in. (9.5-mm) maximum size crushed limestone, fine aggregate consisting of natural river sand, and a water-cement ratio of 0.25. A high range water reducer was also used in the mix design.

Internal strain gauges were placed on both the shear and longitudinal reinforcement. Surface strain gauges were placed at five locations at mid-span of three girders. In addition, strain rosette gauges were used on all specimens cast specifically for shear tests. In most cases the rosettes were placed 10 in. (254 mm) up from the bottom of the girder and 1d and 2d away from the support, where d equals the distance from the extreme compressive fiber to the centroid of the strand. Linear potentiometers were used to measure deflections of the specimens.

In addition to the laboratory tests, a comprehensive review of shear tests in high-strength concrete girders reported in American literature was carried out. All test results were evaluated in comparison with current AASHTO/ACI provisions

(1,2), the compression field theory recommended by the Canadian code (8), and the variable inclination truss models.

The results of the tests indicated that current maximum shear reinforcement limits could be substantially increased. It was also discovered that all three methods of shear evaluation presently in general use gave conservative results for both reinforced and prestressed high-strength concrete members. Any of the three design methods evaluated would be acceptable for concrete strengths up to 12,000 psi (83 MPa). It was also discovered that all three design procedures showed little variation in conservatism as a function of concrete strength.

2.3.3 Castrodale, Kreger and Burns - Report 381-3

In this research project, Castrodale, Burns, and Kreger (7) examined the stress transfer characteristics of 1/2-in. (13-mm) diameter low-relaxation strand in normal and high-strength concrete. In addition, two one-third scale Type IV girder specimens were fabricated with 12,000 psi (83 MPa) concrete, and tested in flexure to evaluate current design provisions and analysis techniques.

The findings of this investigation revealed the following:

1. The current AASHTO expression for estimating transfer length is conservative for high-strength concrete.
2. The maximum usable concrete strain to failure was lower for high-strength concrete than for normal strength concrete.
3. Placement of high-strength concrete in narrow, congested sections is possible through the use of high-range water reducers (superplasticizers).

2.3.4 Castrodale, Kreger, and Burns - Report 381-4f

In research report 381-4F, Castrodale, Kreger, and Burns (9) performed a review of the AASHTO and ACI Codes, current practices, previous tests, and recent literature to determine the safety and efficiency of using high-strength concrete in pretensioned bridge girders. Selected girder cross sections were reviewed to determine the sensitivity of different design parameters and to determine the effectiveness of those cross sections with the use of high-strength concrete. Some of the findings of this research were as follows:

1. The AASHTO and ACI simplified flexural design approach for strength appears to provide good, conservative estimates of the capacity.
2. Current expressions for determining strand stress at ultimate appear to be adequate.
3. Further study should be performed to determine the strain in the top fiber that leads to crushing in a member.
4. Further study should be conducted to determine the effects that concrete strength has on all aspects of design, including lateral stability, fatigue, cracking , and deflections.

2.4 RESEARCH PERFORMED AT NORTH CAROLINA STATE UNIVERSITY

Zia, Schemmel, and Tallman (10) performed parametric investigations to determine the feasibility of using high-strength concrete for bridge projects. Included in the investigation were prestressed concrete hollow core slabs, prestressed concrete girders, and reinforced concrete piers. The current AASHTO design procedures were used for the design of the flexural and compression

members; however, the modulus of rupture equation recommended by ACI Committee 363 was used in lieu of the one recommended by AASHTO.

The investigation recommended that 10,000 psi (69 MPa) concrete be used for bridge projects and that a demonstration bridge be built. Properties of high-strength concrete used in the studies were based on previous work performed by Leming (11) on high-strength concrete made using local North Carolina materials.

2.5 RECENT RESEARCH PERFORMED BY PORTLAND CEMENT ASSOCIATION AND CONSTRUCTION TECHNOLOGY LABORATORIES.

2.5.1 Shin, Kamara, and Ghosh

Shin, Kamara, and Ghosh (12) tested 36 specimens, each 6-in. x 12-in. x 10-ft (152-mm x 305-mm x 3-m). The specimens were manufactured using concrete strengths of 4,000 psi (28 MPa), 12,000 psi (83 MPa) and 15,000 psi (103 MPa). The specimens were reinforced as columns though they were tested in flexure. It was determined that the equivalent rectangular compression stress block of the ACI code was valid for the flexural strength computations of members with concrete strengths ranging up to 15,000 psi (103 MPa).

2.5.2 Roller and Russell

The purpose of this investigation by Roller and Russell (13) was to evaluate the shear strength performance of high-strength concrete beams with web reinforcement relative to the current ACI code. The investigation consisted of two test series with each series containing five beams. The beams of the first series ranged in depth from 25 in. (635 mm) to 29-1/4 in. (743 mm) and were fabricated using concrete with a compressive strength of 17,420 psi (120 MPa). All beams in the first series were 14 in. (356 mm) wide but had different quantities of shear

reinforcement ranging from the minimum amount required by ACI to the maximum amount that can be assumed when calculating shear capacity. In the second series, all beams were 34-1/4 in. (870 mm) deep with two of the specimens fabricated from concrete with a compressive strength of 10,500 psi (72 MPa) and the remaining three with a compressive strength of 18,170 psi (125 MPa). The second series of beams had a web width of 18 in. (457 mm) and had amounts of reinforcing varying from the minimum amount prescribed by ACI to three times the minimum.

The high-strength concrete in eight of the beams was made using Type I portland cement, Class C fly ash, silica fume, coarse aggregate with a top size of 1/2 in. (12.7 mm), sand, and a water-cement ratio of 0.26. A high-range water reducer and a water-reducing retarder were used to improve workability. The concrete in the remaining two beams contained all of the same constituents listed above except the silica fume and high-range water reducer. The water-cement ratio for these two beams was 0.31.

It was concluded from this study that the present ACI code provisions overestimate the nominal shear strength provided by the concrete when the compressive strength of the concrete exceeds 17,000 psi (117 MPa). A recommendation was also made that the minimum quantity of shear reinforcement specified in the ACI code be increased as the concrete compressive strength increases.

2.6 OTHER RECENT PERTINENT RESEARCH

2.6.1 Peterman and Carrasquillo

This report by Peterman and Carrasquillo (14) demonstrated that high-strength concrete could be produced using conventional batching procedures. Some of the other findings of this investigation were as follows:

1. The compressive strength of concrete increases as the amount of superplasticizer increases, up to the dosage which causes the concrete mix to become segregated and unworkable. Too much superplasticizer can result in the retardation of concrete hardening. There was a definite correlation between the brand of superplasticizer and the workability and compressive strength of the high-strength concrete.
2. High-strength concrete can be produced using natural gravel or crushed stone though crushed stone will yield higher strengths.,
3. More compressive strength can be gained through using a Class C fly ash than from using an equal amount of portland cement, if the ratio of the weight of fly ash to the combined weights of the fly ash and Portland cement is in the range from 20 to 30 percent.
4. The one-day strength of high-strength concrete is reduced slightly by the addition of fly ash; however, the addition of superplasticizer more than compensates for this reduction.
5. The 28-day compressive strength of high-strength concrete that has been cured under ideal conditions for seven days is not seriously affected by curing under hot, dry conditions from seven to 28 days after casting.

6. The modulus of rupture of high-strength concrete falls between $8\sqrt{f'c}$ and $12\sqrt{f'c}$.

7. The compressive strength of high-strength concrete specimens cast in steel molds is generally about 10 percent higher than that of specimens cast in cardboard molds.

2.6.2 Ahmad and Shah (1985)

In this report, Ahmad and Shah (15) investigated the structural properties of high-strength concrete and the implications that these properties may have for precast, prestressed concrete. Experimental data generated by the authors, as well as that generated by other investigators, was used to develop empirical expressions to substitute for those currently being used. Some of the most significant findings of this report are as follows:

1. The stress-strain curves of normal and high-strength concrete are significantly different. The high-strength concrete stress-strain curve is much more linear to a higher fraction of the compressive strength. It was also noted that the slope of the post maximum stress increases as the strength increases.

2. The present ACI code expression for modulus of rupture should be changed from $7.5\sqrt{f'c}$ to $2\,(f'c)^{2/3}$

3. The present ACI equation for estimating the secant modulus of elasticity predicts values as much as 20 percent too high for concrete with a compressive strength near 12,000 psi (83 MPa).

4. In general, high-strength concrete can reduce construction time. Since required release strength is attained earlier with high-strength concrete, stress transferring operations can be performed earlier.

2.6.3 Carrasquillo, Nilson, and Slate

Carrasquillo, Nilson, and Slate (16) studied concretes in three strength ranges in this investigation: high-strength with compressive strength of at least 9,000 psi (62 MPa), medium strength with compressive strength from 6,000 psi (41 MPa) to 9,000 psi (62 MPa), and normal strength with compressive strength from 3,000 psi (21 MPa) to 6,000 psi (41 MPa). All concrete mixes were made using Type I portland cement. The course aggregate used was either a crushed limestone or a crushed gravel. The purpose of the investigation was to determine the properties of high-strength concrete subject to short term loads. Compression tests were conducted on both 4-in. x 8-in. (102-mm x 203-mm) and 6-in. x 12-in. (152-mm x 305-mm) cylinders while plain concrete beams 4-in. x 4-in. x 14-in. (102-mm x 102-mm x 356-mm) were used for modulus of rupture tests. No other specimen types were used.

Some of the findings of interest from this study can be summarized as follows:

1. When moist cured for seven days and then allowed to dry at about 50 percent relative humidity until testing at 28 days, high-strength concrete showed a larger reduction in compressive strength than did normal strength concrete. High-strength concrete had an average reduction of 10 percent relative to continuous moist curing, while normal strength concrete showed only a four percent reduction. Significantly greater reductions in modulus of rupture occurred with high strength-concrete, showing a 26 percent reduction compared to an 8 percent reduction for normal strength concrete.

2. The following equations were recommended to replace those presently being used by ACI and AASHTO:

Modulus of elasticity

$$E = 40,000\sqrt{f'_c} + 1.0 \times 10^6 \text{ psi} \qquad (2)$$

Modulus of rupture

$$f'_r = 11.7\sqrt{f'_c} \text{ psi} \qquad (3)$$

3. Poisson's ratio is close to 0.20 regardless of the compressive strength or the testing age.

3. FEASIBILITY OF PRODUCING HIGH-STRENGTH CONCRETE

3.1 INTRODUCTORY REMARKS

One of the objectives of this research effort is to establish the feasibility of producing high-strength concrete using fabricators and materials indigenous to the southeastern region of the United States. To accomplish this objective, a survey of local fabricator capabilities was performed; a study of mix designs was made, both in the laboratory and the field; and actual specimens were fabricated using standard production techniques and procedures. The purpose of this chapter is to present the findings of the production feasibility portion of the study. Section 3.2 presents the results of the fabricator survey. Section 3.3 presents the mix design studies that were performed and the results of using those mix designs under actual production conditions. Section 3.4 presents the conclusions drawn from this portion of the study.

3.2 SURVEYS OF REGIONAL FABRICATORS

During the first phase of the research effort, a total of five fabrication companies in four different states were contacted to determine their interest in, and their capability of, producing concrete with a strength of 10,000 psi (69 MPa). Of the five firms contacted, three stated a reluctance to participate in the project citing concerns about consistently producing a 10,000 psi (69 MPa) mix using local materials under production conditions. The other two firms felt they could produce a 10,000 psi (69 MPa) mix.

3.3 MIX DESIGN AND PRODUCTION

Two approaches were used to establish the mix design for this research project. For the 24-ft (7.3-m) pile specimens, the fabricator submitted a mix design to the research team with an intended design strength of 10,000 psi (69 MPa) in 28 days. The proportions of that mix design by weight are shown in Appendix A. The fabricator had performed several trial mixes in the plant using Type III cement and had achieved the desired results in those tests. One change was made in the mix design prior to the fabrication of the pile specimens; the Type III cement used in the trial batches was changed to Type I at the request of LaDOTD. The change was made because Type I cement is more representative of the material normally supplied in Louisiana. No additional test batches were made after that change in cement type. Twenty-eight days after casting the pile specimens, the highest strength achieved by the control cylinders was 8,410 psi (58 MPa). At 56 days the highest control specimen strength was 8,290 psi (57 MPa). At 169 days, 4-in. x 8-in. (101-mm x 203-mm) concrete cores were taken from the pile specimens. The average strength of these cores was 9,780 psi (67 MPa). These cores indicated that the concrete mix design had the potential of eventually achieving 10,000 psi (69 MPa).

In the case of the mix design used for the bulb-tee specimens, a different approach was used. The Louisiana Transportation Research Center (LTRC) performed laboratory mix design tests to determine a mix design most likely to achieve the desired strength at 28 days. In order to achieve the desired 28-day strength a laboratory mix design was made to yield strengths in excess of the 10,000 psi (69MPa) desired. The mix design developed by LTRC is shown in Appendix B. All laboratory batches were prepared in a 3 ft^3 (0.09 m^3) mixer. In addition to batch proportions, batch sequencing and mixing times were developed.

The recommended LTRC laboratory mix resulted in an average 28-day strength of 12,395 psi (85.5 MPa). Following the development of a mix design in the laboratory, field tests were made by the fabricator using 3 yd^3 (2.3 m^3) batches. These trial batches resulted in an average 28-day strength of 10,854 psi (75 MPa). This correlated well with the findings of Cook (17) that an approximate 10 percent reduction in compressive strength will occur from the laboratory to the field tests. In both the laboratory and field tests, strengths in excess of 10,000 psi (69 MPa) were achieved.

With a mix design developed in the laboratory and tested in the field, production of the bulb-tee specimens was approved. A total of nine 4-1/4 yd^3 (3.25 m^3) batches were required to cast the three bulb-tee specimens. The mix proportions for the 4-1/4 yd^3 (3.25 m^3) batches, as well as the proposed mixing procedures, can be found in Appendix B. The first batch mixed using the proportions and procedures developed in the laboratory and field tests proved unworkable due to extremely low slump. This batch was discarded. For the second batch, the amount of water reducer was increased and the mixing times modified. This batch was discarded due to excessive slump. For the third batch, the same proportions and mixing times used in batch two were used again. The initial slump was acceptable and the mix was placed in the first bulb-tee specimen. However, toward the end of the pour, the batch began to get stiff and made placement difficult. This raised some concern and the water reducer was again increased. The same mix used in batch four was used for the remaining batches. The strengths of these batches are given in Appendix B. As can be seen in Appendix B, the average compressive strength of 9,750 psi (48 MPa) for the nine batches did not reach the desired 10,000 psi (49 MPa) at 28 days.

For the fabrication of the 130-ft (39.6-m) pile, the LTRC laboratory mix proportions were used without modification. Cylinders were cured under three

different environments. One environment was the same as that experienced by the pile specimen, 18 hours of steam followed by ambient air curing. The second curing environment was ambient air only and the third environment was a moist cure. This resulted in an a 28-day strength of 10,453 psi (72 MPa) for the steam / air cured specimens, 11,874 psi (82 MPa) for the air-cured specimens and 11,637 psi (80.4 MPa) for moist-cured specimens. A complete discussion of the fabrication of the 130-ft (39.6-m) pile specimen can be found in Appendix C.

3.4 CONCLUSIONS

As was stated above, laboratory tests and field tests produced the desired strengths while only the production batches used in the 130-ft (39.6-m) pile achieved the desired strength. To determine probable causes for the shortfall in production batch strength, petrographic analyses were performed on cores from the 24-ft (7.3-m) pile specimens and the bulb-tee specimens. These petrographic analyses revealed no explanation for the failure to achieve the desired strength. In addition to the petrographic analyses, samples of the coarse aggregate used in the bulb-tee specimen were tested by LTRC. These tests revealed that the coarse aggregate had the strength to reach the desired ultimate strength of the concrete, but with little reserve.

High-strength concrete, unlike lower strength concrete, requires a high degree of quality control. A mix design must be developed and then the standards used for measuring batch weights, measuring water content of aggregate, and maintaining quality of materials must be significantly "tighter" than those presently used in the industry in the southeastern United States. Any change in material source, material specifications, or batching procedures can have a dramatic effect on both the plastic consistency of the mix and the resultant concrete strength. To consistently produce high-strength concrete using regionally

available materials, fabricators will have to undergo a period of transition wherein the standard procedures used for producing "normal" strength concrete (5,000 to 8,000 psi (34 to 55 MPa) are replaced by the more exacting requirements of high-strength concrete. With this transition, consistent production of high-strength concrete (10,000 psi (69MPa) and higher) can be achieved.

4. DESIGN OF TEST SPECIMENS

4.1 INTRODUCTORY REMARKS

The specimens fabricated for use in this research program were intended to be representative of members presently in use by state departments of transportation. It was further intended to design these members to make efficient use of the properties of high-strength concrete. A discussion of the design considerations for the specimens used in each series of tests is presented below.

4.2 DESIGN OF THE PILE SPECIMENS

Concrete piles in Louisiana are often limited to lengths that can be picked up and placed in the leads without excessive bending stresses or driven without excessive tensile stresses. When the piles become too long, they fail in flexure when being picked up or, if driven in soft soils, fail due to tensile driving stresses. In an effort to alleviate this problem, the Louisiana Department of Transportation and Development, like many states, has long sought a dependable pile splice for long piles. Because LaDOTD has not yet found a satisfactory splice, the decision was made to investigate the possibility of taking advantage of the higher tensile strength and potentially higher level of precompression of high-strength concrete to increase the length of piles.

Hence, at the direction of LaDOTD, the 24-ft (7.3 m) and 130-ft (39.6 m) pile specimens were designed. Unlike the typical 24-in. (610-mm) square pile used by LaDOTD, these piles were to be fabricated using concrete with a compressive strength of 10,000 psi (69 MPa), instead of the usual 5,000 psi (34.5 MPa), and the piles were to have more prestressing strands. Twenty-four, 1/2-in.

(12.3-mm) diameter, low-relaxation strands instead of the normal 14 were to be used resulting in an initial precompressive stress of 1,606 psi (11 MPa) instead of 937 psi (6.5 MPa).

4.3 DESIGN OF THE BULB-TEE SPECIMENS

The design for the bulb-tee specimens was based on the requirements of the 1989 Standard Specifications of the American Association of State Highway Transportation Officials. The AASHTO Standard Specifications require that prestressed members be designed for both strength and serviceability.

Article 3.22 of the Standard Specifications requires that load factors be applied to the structure to insure its safety. Computed ultimate load capacity, as described by the AASHTO Standard Specifications, shall not be less than:

$$1.3\left[\mathbf{DL}+\frac{5}{3}(\mathbf{LL}+\mathbf{I})\right] \qquad (4)$$

where DL = dead load
LL = live load
I = impact

Article 9.15 of the Standard Specifications also outlines the allowable design stresses that were used in the design of the bulb-tee test specimens. The allowable stresses that were pertinent to this investigation, for prestressing steel are as follows:

The temporary stresses before losses due to creep and shrinkage shall be.....0.75 f's, psi

The stresses at service load after losses shall be.....$0.80\ f_y$, psi

where

$f's$ = ultimate strength of prestressing strand, psi

f_y = yield point stress of prestressing steel, psi

The allowable concrete stresses pertinent to this investigation are as follows:

The temporary compressive stresses before losses due to creep and shrinkage shall not exceed.....$0.60\ f'_{ci}$, psi

The compressive stresses after losses have occurred shall not exceed.....$0.40\ f'_c$, psi

The maximum tensile stresses before losses due to creep and shrinkage shall not exceed.....$7.5\sqrt{f'_{ci}}$, psi

The maximum tension in the precompressed tensile zone after losses shall not exceed.....$6.0\sqrt{f'_c}$, psi

where

f'_{ci} = compressive strength of concrete at the time of initial prestress, psi

The bulb-tee specimens were originally designed by a fabricator using a software package named Conspan, version 4.0, developed by Leap Software, Inc. of Tampa, Florida. This software is based upon the requirements of AASHTO listed above and is in use by a number of state departments of transportation. The

70-ft length of the girders, used in the preliminary design, was set by the project team to facilitate transportation to the laboratory.

Several assumptions were made by the fabricator concerning the properties of high-strength concrete. Since these assumptions were based on AASHTO relationships established for lower strength concrete, they were reviewed in light of the data obtained from the earlier pile tests.

A density of concrete of 150 pcf (2,435 kg/m^3) was assumed by the fabricator. The measurements from the piles indicated an average unit weight of 149.5 pcf (2,426 kg/m^3). Hence, the assumed unit weight appeared reasonable.

The fabricator, using the normal AASHTO equation relating modulus of elasticity to concrete compressive strength, assumed a modulus of elasticity of 6,062.2 ksi (41.8 MPa). Results of 28-day concrete tests for the earlier pile specimens indicated a modulus of elasticity approximately 11 percent higher than the value calculated by the conventional equation. Given the variations expected with the standard equation, the assumed value was deemed reasonable.

The maximum allowable tension assumed by the fabricator, as stated in AASHTO, was calculated as $7.5\sqrt{f'_c}$. Results of 28-day splitting tensile tests conducted on concrete used in the piles indicated a relationship of approximately $7.2\sqrt{f'_c}$. Results of modulus of rupture tests conducted at 28 days indicated a relationship of $8\sqrt{f'_c}$. Preliminary analysis of data from the pile tests indicated a tensile stress of about 1,000 psi (6.9 MPa) at cracking. Therefore, the design assumption for maximum tension seemed reasonably valid.

Prestress losses for the fabricators design was based on AASHTO procedures. Losses expected for high-strength concrete is expected to be less because AASHTO's procedure does not take into account that actual losses from

creep may be lower for high-strength concrete. Losses monitored in the piles support this theory.

The preliminary design, as prepared by the fabricator, assumed a girder spacing of 7 ft (2.1 m). This design resulted in 16 strands being required in each girder. The project team reviewed and recommended that the design be revised.

The revised design prepared by LaDOTD increased the spacing of the girders to 13 ft 4 in.(4.06 m). Previous studies (18,19) on optimization have indicated that maximum spacing is desirable and would result in more efficient use of high-strength concrete.

Using the standard deck-slab design tables of LaDOTD, a deck thickness of 9-1/2 in. (241 mm) was determined as necessary for the wider girder spacing. Next, the effective width of the compression flange had to be determined. Article 8.10.1 of the AASHTO Standard Specifications states that the effective compressive flange width of a tee-girder shall be the smaller of the following:

> The total width of slab effective as a tee-girder shall not exceed one-fourth of the span length of the girder - (in the instant case 207 in. (5.26 m))
>
> The effective flange width overhanging on each side of the web shall not exceed six times the thickness of the slab- (in the instant case 120 in. (3.05 m)
>
> The effective flange width overhanging on each side of the web shall not exceed one-half the clear distance to the next web- (in the instant case 160 in. (4.06 m)

As can be see from the above, the effective slab width, according to AASHTO Standard Specifications, would be 120 in. (3.05 m) This value was used for the effective slab width in the analysis for the 13 ft 4 in. (4.06 m) spacing.

Once the thickness and effective width of the slab was determined, LaDOTD, using a software package named Span, version 5.1, developed by Leap

Once the thickness and effective width of the slab was determined, LaDOTD, using a software package named Span, version 5.1, developed by Leap Software, Inc., analyzed the section and determined the number of strands required. This analysis was based on the deck slab being cast from LaDOTD's Class AA concrete mix. This mix has a minimum compressive strength of 4,200 psi (26 MPa). A review of this by the project team resulted in two suggestions being made. The first was to increase the design strength of the deck-slab concrete to a minimum of 6,000 psi (41 MPa), and the second was to delete the longitudinal distribution reinforcement required by Article 3.24.10 of the AASHTO Standard Specifications in the deck slab of the girder to be tested in flexure. Both of these suggestions were made in an attempt to increase the likelihood of a flexural failure in a tension mode during laboratory testing.

As stated previously, the software used to design the beams uses the allowable values and material properties prescribed by the AASHTO Standard Specifications. These allowable values are all functions of the concrete strength. As described earlier, the pile investigation preceded the bulb-tee girder fabrication. The information gathered from the pile tests verified the appropriateness of using the AASHTO Standard Specification for this phase of the program.

5. BEHAVIOR OF 24-ft (7.3-m) PILE SPECIMENS

5.1 INTRODUCTORY REMARKS

The purpose of this chapter is to present the observed behavior of the 24-ft (7.3-m) pile test specimens and to discuss their behavior. The pile test specimens were all 24 in. x 24 in. (610 mm x 610 mm) in cross-section with a central 12-in. (305-mm) diameter void extending the full length of the pile. All of the piles were concentrically prestressed using 24, 1/2-in. (12 mm) diameter, 270 ksi (1,862 MPa), low-relaxation strands. The intended design compressive strength of the concrete was 10,000 psi (69 MPa).

The investigation of the behavior of the 24-ft (7.3-m) pile specimens is discussed in Section 5.2. The concrete property tests, flexural tests, strand transfer length tests, and prestress loss tests on the 24-ft (7.3-m) pile specimens are discussed in Sections 5.2.1, 5.2.2, 5.2.3, and 5.2.4 respectively. Deatils of specimen materials, fabrication, and testing are given in Appendix A.

5.2 BEHAVIOR OF 24-ft (7.3-m) PILE SPECIMENS

The 24-ft (7.3-m) long pile specimens, designated P1, P2, and P3, were simply supported over a span length of 22 ft (6.71 m) and were loaded with concentrated loads of approximately equal magnitude located 1 ft 6 in. (457 mm) either side of mid span. Deflections were measured at mid span. The pile specimens were tested in flexure 56 days after fabrication. The pile specimens were all concentrically prestressed hence there was no intentional initial camber.

The response of the pile specimen to the applied flexural load is illustrated by means of a load-deflection curve that provides a graphical representation of the ductility. In members failing in flexure, the ductility is attributed to opening of cracks and strain in the concrete. For each pile specimen, load-deflection curves for the specimen midpoint were plotted.

A qualitative study of a typical load-deflection curve representative of the pile specimens reported herein is shown in Figure 8, the load-deflection curve for specimen P1. The measured deflection is linearly proportional to the applied load for a portion of the curve up to flexural cracking. Deflection up to flexural cracking may be calculated with reasonable accuracy using methods based on elastic analysis. However, after flexural cracking, measured deflections are no longer directly proportional to applied load as evidenced by the non-linearity of the load-deflection curve. The load-deflection curve is much flatter after flexural cracking, as shown in Figure 8.

In the following discussions, cracks are classified into three categories: flexural cracks, flexure-shear cracks, and web-shear cracks. This terminology, as applied to prestressed concrete members, is defined by MacGregor (20) as follows:

> Flexural cracks are cracks that form when the normal applied stress exceeds the compression due to prestress and the modulus of rupture of the concrete in the vicinity of the crack.
>
> Flexure-shear cracks are cracks that originate as flexure cracks in the shear spans of a member and become inclined toward the load point.
>
> Web-shear cracks are inclined cracks that originate in the web of I-shaped members. The cracks result from excessive principal tensile stresses in the web.

5.2.1 Concrete Property Tests

In order to establish material properties of the concrete in each pile specimen, six 6-in. x 12-in. (152-mm x 305-mm) concrete cylinders and two 6-in. x 6-in. x 20-in. (152-mm x 152-mm x 508-mm) concrete beams were made from each concrete batch. Concrete material property tests were conducted at release (approximately 21 hours after casting), and at concrete ages of 28 and 56 days. In addition to the tests on standard cylinder specimens, a 4-in. x 8-in. core was taken from each pile specimen. These cores were tested in accordance with ASTM C42-87 (21) at an age of 169 days. Concrete compressive strength tests of the cylinders were conducted in accordance with ASTM C39-86 (22). Modulus of elasticity tests of cylinders were conducted in accordance with ASTM C469-87 (23). Splitting tensile strength tests of cylinders were conducted in accordance with ASTM C496-90 (24). Modulus of rupture tests of beams were conducted in accordance with ASTM C78-84 (25). Results of these property tests are presented in Table 1 for the three pile specimens. With the exception of the compressive strength at release, which was the average of two test values, each value in Table 1 represents a single test result.

In addition to the above tests, concrete unit weight was determined from two core samples taken from each pile specimen. Average unit weights for pile specimens P1, P2, and P3 were 151.5 lbs/ft^3 (2,427 kg/m^3), 150.0 lbs/ft^3 (2,403 kg/m^3), and 147.1 lbs/ft^3 (2,356 k g/m^3), respectively.

TABLE 1
MEASURED MECHANICAL PROPERTIES OF CONCRETE
PILE SPECIMENS

Pile No.	Concrete Age	Compressive Strength psi	Modulus of Elasticity psi	SplittingTensile Strength psi	Modulus of Rupture psi
P1	Release	5,210	4,900	No Test	No Test
	28 days	7,400	5,550	575	720
	56 days*	7,660	5,350	494	733
	169 days**	9,790	No Test	No Test	No Test
P2	Release	5,480	5,950	No Test	No Test
	28 days	7,900	6,000	670	750
	56 days*	8,290	5,950	694	883
	169 days**	9,730	No Test	No Test	No Test
P3	Release	5,855	6,200	No Test	No Test
	28 days	8,410	5,750	690	665
	56 days*	8,250	5,530	592	817
	169 days**	9,810	No Test	No Test	No Test

* Properties at time of flexural tests
**4-in. (102-mm) x 8-in.(203-mm) cores taken from pile specimens

Metric Equivalents: 1 ksi = 1000 psi = 6.895 MPa

5.2.2 Flexural Tests

In the following discussions, the term "total applied load" is defined as the total external load applied to the specimen. Member dead load is not considered as part of the total applied load.

A. Load-deflection Relationship

The load-deflection relationship for the mid span of pile specimen P1 is shown in Figure 8. After several increments of load had been applied to specimen P1, flexural cracks appeared in the bottom region of the specimen near mid span. The observed total applied load corresponding to the formation of the initial flexural crack was 94.2 kips (419 kN). The initial flexural crack disturbed the

linear relationship between applied load and deflection as shown in Figure 8. Application of additional load caused more flexural cracks to appear in the bottom region of the specimen in the region of maximum moment between the load points, and caused the initial flexural cracks to propagate vertically. The flexural cracks in the constant moment region of pile specimen P1 are shown in Figure 9 and are relatively evenly spaced.

With additional increase in total applied load, flexural cracks appeared in the bottom regions of the pile specimen in the shear spans, the region between the load points and the reactions. These cracks propagated upward to the bottom of the void and then became inclined toward the load points. These cracks are termed flexure-shear cracks, since they originate as flexural cracks in the shear span. Figure 10 shows the development of flexure-shear cracks in the shear span of specimen P1. The total applied load at which the flexure-shear cracking occurs is not apparent from the load-deflection curve because the flexure-shear cracks originate as flexural cracks, forming after the development of other flexural cracks in the constant moment region. The total applied load measured corresponding to the formation of these initial flexure-shear cracks was 98.6 kips (439 kN) for specimen P1. With an increase in load, additional flexure shear cracks appeared in the pile specimen while the flexural cracks propagated vertically up toward the top of the specimen.

The load-deflection curve peaked at a total applied load of 159.2 kips (708 kN). Flexural compressive failure marked the limit of the load capacity of the pile specimen. The maximum deflection of specimen P1 just prior to failure was 1.53 in. (39 mm) with 157.8 kips (702 kN) of total applied load.

The load-deflection relationship for the mid span of pile specimen P2 is shown in Figure 11. The initial flexural cracks developed in the bottom region of the specimen near mid span at a total applied load of 94.1 kips (419 kN). These

initial flexural cracks disturbed the linear relationship between applied load and deflection as shown in Figure 11. Application of additional load caused more flexural cracks to appear in the bottom region of the specimen in the region of maximum moment between the load points, and caused the initial flexural cracks to propagate vertically. The flexural cracks in the constant moment region of pile specimen P2 are shown in Figure 12 and are relatively evenly spaced.

Flexure-shear cracks appeared at a total applied load of 102.7 kips (457 kN) for specimen P2, as shown in Figure 10. The load-deflection curve indicates member capacity at a total load of 153.5 kips (683 kN). Flexural compressive failure marked the limit of the load capacity of the pile specimen. The maximum deflection of specimen P2 just prior to failure was 1.30 in. (33 mm) with 152.9 kips (680 kN) total applied load.

The load-deflection relationship for the mid span of pile specimen P3 is shown in Figure 13. The initial flexural cracks developed in the bottom region of the specimen near mid span at a total applied load of 85.1 kips (379 kN). These initial flexural cracks disturbed the linear relationship between total applied load and deflection as shown in Figure 13. Application of additional load caused more flexural cracks to appear in the bottom region of the specimen between the load points, the region of maximum moment, and caused the initial flexural cracks to propagate vertically. The flexural cracks in the constant moment region of pile specimen P3 are shown in Figure 14 and are relatively evenly spaced.

Flexure-shear cracks appeared at a total applied load of 92.9 kips (413 kN) for specimen P3, as shown in Figure 10. The load deflection curve indicates member capacity at a total applied load of 154.3 kips (687 kN). Flexural compressive failure marked the limit of the load capacity of the pile specimen. The maximum deflection of specimen P3 just prior to failure was 1.5 in. (38 mm) with 153.9 kips (685 kN) of total applied load.

Due to the geometric configuration of the pile specimens, principle tensile stresses resulting from applied shear were very low and web-shear cracking was not a factor.

B. Concrete strains

As discussed in Appendix A, four Carlson strain meters were placed in each pile specimen at mid-length adjacent to each of the four sides of the piles. It was determined in the testing that the strain meters, though performing well in compression, did not perform well in tension. For this reason the strain readings of the strain meters were not used to measure tensile strains. The strain meter readings were used, however, to determine losses in the strands prior to testing.

C. Modes of Failure

Failure occurred in pile specimens P1, P2 and P3 when the applied loads caused flexural compression failure in the constant moment region.

5.2.3 Strand Transfer Length Tests

As discussed in Appendix A, transfer length was experimentally evaluated for each pile specimen by measuring the change in concrete surface strains over a 5-ft (1,524-mm) distance from the ends of each pile specimen. Concrete surface strains were measured using a 10-in. (254-mm) Whittemore gauge. Whittemore gauge readings were taken just prior to release (reference readings), just after release, after removing the piles from the forms, and 14 days after release. Transfer length plots for strain readings taken 14 days after release at each end of specimens P1, P2 and P3 are shown in Figures 15 through 17.

5.2.4 Prestress Losses Tests

As described in Appendix A, internal Carlson strain meters were installed in each pile specimen. The strain meters were monitored until an age of 28 days. Measured concrete strains were used to calculate prestress losses by multiplying the average measured strains by the average measured strand modulus of elasticity of 29,300 ksi (202,024 MPa).

Concrete strains measured immediately after release were used to provide an indication of prestress losses due to elastic shortening, while the subsequent changes in strain were considered time dependent losses. Table 2 shows the losses at release and at 28 days for each specimen.

TABLE 2
MEASURED PRESTRESS LOSSES AT RELEASE AND AT 28 DAYS
(Based on Strand Modulus of Elasticity of 29,300 ksi)

Pile No.	Specimen Age	Measured Strain in./in.	Loss in Prestress psi
P1	Release	306×10^{-6}	8,966
	28 days	462×10^{-6}	13,537
P2	Release	298×10^{-6}	8,731
	28 days	446×10^{-6}	13,068
P3	Release	342×10^{-6}	10,021
	28 days	473×10^{-6}	13,859

Metric Equivalents: 1 ksi = 1000 psi = 6.895 MPa

6. ANALYSIS OF TESTS OF 24-ft (7.3 m) PILE SPECIMENS

6.1 INTRODUCTORY REMARKS

The purpose of this chapter is to compare the observed behavior of the pile test specimens with their calculated behavior. Section 6.2 compares the laboratory measured material properties with those predicted using equations contained in the AASHTO specifications and ACI code. Section 6.3 contains a discussion of flexural cracking. Inclined cracking is discussed in section 6.4. Flexural strength is considered in section 6.5. Section 6.6 contains a discussion of transfer length, while prestress losses are discussed in section 6.7. Section 6.8 summarizes the comparisons of the test results with the current provisions of the AASHTO specifications and ACI code.

6.2 PROPERTIES OF CONCRETE

While the mechanical properties of high-strength concrete are not the major emphasis of this research effort, sufficient tests were performed to evaluate those mechanical properties necessary to predict behavior of structural members. In the present AASHTO and ACI documents, standard equations are provided to predict the modulus of elasticity and modulus of rupture based on the compressive strength of the concrete. These equations are based primarily on investigations performed for concrete with compressive strengths of less than 6000 psi (41 MPa). For this reason, ACI published Report no. ACI 363R-84, a State-of-the-Art Report

on High-Strength Concrete (26), listing alternate equations proposed by Carrasquillo (16). These equations are as shown in Table 3.

TABLE 3
COMPARISON OF MATERIAL PROPERTY EQUATIONS
ACI 318-89 / AASHTO VERSUS ACI 363-84

Property	ACI 318-89/ AASHTO	ACI 363
Modulus of Elasticity	$E_c = w_c^{1.5} 33\sqrt{f'_c}$ psi	$E_c = 40,000\sqrt{f'_c} + 1 \times 10^6$ psi
Modulus of Rupture	$f_r = 7.5\sqrt{f'_c}$ psi	$f_r = 11.7\sqrt{f'_c}$ psi

Using the above equations with the measured concrete compressive strength, the mechanical properties of the concrete used in each specimen were calculated. The mechanical properties developed using these equations and the mechanical properties measured in the laboratory at an age of 56 days are presented in Table 4. The measured results agree more closely with the ACI/AASHTO values than with the ACI 363 values.

TABLE 4
MEASURED VS. CALCULATED MECHANICAL PROPERTIES

Specimen	Compressive Strength	Property	Measured	ACI 318/ AASHTO	ACI 363
P1	7,660 psi	Mod. of Elasticity	5,350 ksi	5,306 ksi	4,500 ksi
		Mod. of Rupture	733 psi	656 psi	1,024 psi
P2	8,290 psi	Mod. of Elasticity	5,950 ksi	5520 ksi	4,642 ksi
		Mod. of Rupture	883 psi	682 psi	1,065 psi
P3	8,250 psi	Mod. of Elasticity	5,530 ksi	5,506 ksi	4,633 ksi
		Mod. of Rupture	827 psi	681 psi	1,063 psi

Metric Equivalents: 1ksi = 1,000 psi = 6.895 MPa

6.3 FLEXURAL CRACKING

In a prestressed concrete flexural member, flexural cracking occurs when the tensile stress resulting from the applied loads and dead load exceeds the compression due to the prestress and the modulus of rupture of the concrete at the location of the crack. The applied load at which flexural cracking occurs may be calculated if the following quantities are known: (1) the effective prestress force of the longitudinal reinforcement, (2) the cross-sectional properties and weight of the member, and (3) the modulus of rupture of the concrete. The effective prestress force can be determined from the initial jacking loads minus the losses as determined by the strain meter readings taken at the time of the test. The cross-sectional properties can be measured and the modulus of rupture of the concrete can be obtained from the standard tests.

The above quantities can be expressed in terms of a resisting moment by an equation of the following form:

$$M_{cr} = \frac{I}{y_b}\left(f_r + f_{pe} - f_o\right) \qquad (5)$$

where

M_{cr} = bending moment at flexural cracking due to total applied load, in.-lb

I = moment of inertia of entire uncracked section, $in.^4$

y_b = distance from the centroid of the section to the bottom fiber, in.

f_r = modulus of rupture of the concrete, psi

f_{pe} = stress at the bottom of the girder resulting from the effective prestressing force, psi

f_0 = flexural stress in the concrete at the bottom face of the beam due to self weight, psi

The total applied load corresponding to formation of the initial flexural crack can also be obtained from the load-deflection relationship of the specimens. As discussed previously in Chapter 5, the load causing the initial flexural crack disrupts the linear relationship between load and deflection. In this investigation, the observed cracking moment for a given specimen and the extrapolated values from the load-deflection curves were approximately the same.

For this investigation, the computed cracking moments, from Eq. (5), were calculated from the measured physical dimensions and properties and by using measured values of prestress losses. The prestress losses at 28 days were fairly consistent for the pile specimens tested with an average value of seven percent used for each specimen. The computed and observed total flexural cracking moments for the piles are shown in Table 5. The observed cracking moment was calculated using the following relationship:

$$M_{cr} = a\frac{P_{fc}}{2} \qquad (6)$$

where P_{fc} = Total applied load at the time of cracking, lb

a = Length of shear span, in.

TABLE 5
COMPUTED AND OBSERVED FLEXURAL CRACKING MOMENT
(Based on Measured Mechanical Properties)

Specimen No.	Computed Cracking Moment		Observed Cracking Moment		Observed/ Computed
	(kip-ft)	(kN-m)	(kip-ft)	(kN-m)	
P1	381.5	517.7	435.8	591.4	1.14
P2	410.0	556.4	454.8	617.2	1.11
P3	398.5	540.8	412.3	559.3	1.03

In order to determine the appropriateness of using the AASHTO equations, the cracking moments were calculated again based on the measured physical dimensions and prestress losses, and the AASHTO predicted values for material properties based on the compressive strength of the concrete. As shown in Table 6, for all three piles the observed to computed ratio exceeded unity. This indicates that design using AASHTO specifications for material properties will be conservative relative to first cracking.

TABLE 6
COMPUTED AND OBSERVED FLEXURAL CRACKING MOMENT
(Based on AASHTO predicted Mechanical Properties)

Specimen No.	Computed Cracking Moment		Observed Cracking Moment		Observed/ Computed
	(kip-ft)	(kN-m)	(kip-ft)	(kN-m)	
P1	343.1	465.6	435.8	591.4	1.27
P2	347.8	472.0	454.8	617.2	1.31
P3	346.2	469.8	412.3	559.5	1.19

6.4 INCLINED CRACKING

As discussed in Chapter 5, the second significant stage of cracking in the pile specimens was that of inclined cracking in the shear spans. The only type of inclined cracking experienced by the pile specimens was flexure-shear cracking. A flexure-shear crack originates as a vertical flexural crack in the shear spans and becomes inclined toward the load points. According to previous research (20), the flexure-shear crack which leads to failure of a specimen typically originates in the shear span at a distance from the load point corresponding approximately to the effective depth, d, of the member. The effective depth of the pile specimens, according to the requirements of the AASHTO specifications and the ACI code, is 80 percent of the total overall depth, or about 19.2 in. (488 mm).

The ACI code and the AASHTO specifications suggest that the applied shear to cause flexure-shear cracks in a prestressed concrete member consists of two basic components; the shear that results in the formation of a flexural crack, $\frac{V}{M}(M_{cr}')$, and the shear required to incline the crack, $0.6\sqrt{f_c'}\,b_w d$. Hence, the total shear, V_{ci}, resulting in flexure-shear cracks is expressed in the AASHTO specifications and the ACI code as follows:

$$V_{ci} = 0.6\sqrt{f_c'}\,b_w\,d + V_d + \frac{V}{M}(M_{cr}') \qquad (7)$$

where V_{ci} = total shear producing flexure-shear concrete cracking, lb

f_c' = strength of the concrete at time of test, psi

b_w = width of the web (12 in.)

d = effective shear depth, 0.8 times member depth, in.

V_d = dead load shear at the location under consideration, lb

M'_{cr} = moment required to cause flexural cracking at the section under consideration, in.-lb

$\frac{V}{M}$ = shear to moment ratio at location under consideration

In the laboratory, the total shear resulting in an inclined crack of approximately 45 degrees first reaching mid-depth of the section was considered as the concrete cracking shear, V_{ci}. To verify Equation 6, the crack identified as resulting from V_{ci} was traced to its origin on the tensile face of the member. As in the case of previous research, this origin occurred at an approximate distance equal to d from the point of applied load. M'_{cr} was then calculated at this location using Equation 5 for both the measured and AASHTO/ACI predicted values of the modulus of rupture. The calculated values of M'_{cr} compared to the measured values are shown in Tables 7 and 8.

TABLE 7

COMPUTED AND OBSERVED FLEXURE-SHEAR CRACKING MOMENT, M'_{cr}
(Based on Measured Mechanical Properties)

Specimen No.	Computed Flexure-Shear Cracking Moment		Observed Flexure-Shear Cracking Moment		Observed/ Computed
	(kip-ft)	(kN-m)	(kip-ft)	(kN-m)	
P1	383.0	519.8	389.3	528.3	1.02
P2	411.4	558.3	412.5	559.8	1.00
P3	398.0	540.1	392.4	532.5	0.99

TABLE 8

COMPUTED AND OBSERVED FLEXURE-SHEAR CRACKING MOMENT, M'_{cr}
(Based on AASHTO Predicted Mechanical Properties)

Specimen No.	Computed Flexure-Shear Cracking Moment		Observed Flexure-Shear Cracking Moment		Observed/ Computed
	(kip-ft)	(kN-m)	(kip-ft)	(kN-m)	
P1	344.6	467.6	389.3	528.3	1.13
P2	349.3	474.0	412.5	559.8	1.18
P3	347.7	471.8	392.4	532.5	1.13

Once the location of the flexure-shear crack was known, and M'_{cr} determined, the total shear, V_{ci}, producing diagonal concrete cracking was calculated using Equation 6. The computed and observed shear resulting in flexure-shear concrete cracking are shown in Tables 9 and 10.

TABLE 9

COMPUTED AND OBSERVED SHEAR RESULTING IN
FLEXURE-SHEAR CRACKING
(Based on Measured Mechanical Properties)

Specimen No.	Computed Cracking Shear		Observed Cracking Shear		Observed/ Computed
	(kips)	(kN)	(kips)	(kN)	
P1	62.0	275.8	73.0	324.7	1.18
P2	66.1	294.0	71.0	315.8	1.07
P3	64.4	286.5	71.0	315.8	1.10

TABLE 10
COMPUTED AND OBSERVED SHEAR RESULTING IN
FLEXURE-SHEAR CRACKING
(Based on AASHTO Predicted Mechanical Properties)

Specimen No.	Computed Cracking Shear		Observed Cracking Shear		Observed/ Computed
	(kips)	(kN)	(kips)	(kN)	
P1	57.2	254.4	73.0	324.7	1.28
P2	58.3	259.3	71.0	315.8	1.22
P3	58.0	258.0	71.0	315.8	1.22

6.5 FLEXURAL STRENGTH

The calculated ultimate moment for the pile specimens was computed using two methods. The first method utilizes the equivalent rectangular stress distribution presented in both the AASHTO Standard Specifications for Highway Bridges (1) and the ACI Building Code Requirement for Reinforced Concrete (ACI 318-89) (2). Since the properties of the concrete and strand were carefully determined, and the loading precisely applied, a reduction factor of unity is applied to the expression. The formula from which the ultimate moment capacity was calculated is

$$M_u = \phi A_{ps} f_{ps} d\left(1 - 0.6\frac{\rho f_{ps}}{f_c'}\right) \qquad (8)$$

where M_u = ultimate resisting moment, in.-lb

A_{ps} = area of prestressing in tension zone, $in.^2$

ϕ = capacity reduction factor

d = distance from extreme compression fiber to centroid, of prestressing steel, in.

ρ = $\frac{A_{ps}}{bd}$

b = width of compression face of member, in.

f_c' = specified compressive strength of concrete, psi

f_{ps} = calculated stress in prestressing steel at beam failure using the equation shown below:

$$f_{ps} = f_{pu}\left[1 - \frac{\gamma_p}{\beta_1}\left(\frac{\rho_p f_{pu}}{f_c'}\right)\right] \quad (9)$$

where f_{pu} = tensile strength of prestressing strand, psi

γ_p = factor for type of prestressing strand, 0.28 for f_{py}/f_{pu} not less than 0.90

β_1 = 0.65 for all concrete with f'c greater than 8000 psi

ρ_p = ratio of prestressed reinforcement

The observed ultimate moment is calculated by the following expression:

$$M_u = \left(\frac{P_{tot}}{2}\right)a + M_{DL} \quad (10)$$

where M_u = observed ultimate moment, in.-lb

P_{tot} = observed total applied load, lb

a = length of shear span, in.

M_{DL} = dead load moment at location of failure, in.-lb

The ultimate moment capacity computed using the method prescribed by AASHTO and ACI for flexural members and the observed total ultimate moment capacity for the specimens are shown in Table 11.

TABLE 11
COMPUTED AND OBSERVED ULTIMATE MOMENT
(Based on AASHTO/ACI Equations)

Specimen No.	Computed Ultimate Moment Capacity		Observed Ultimate Moment Capacity		Observed/ Computed
	(kip-ft)	(kN-m)	(kip-ft)	(kN-m)	
P1	606.8	823.5	793.0	1,076.3	1.31
P2	629.4	854.1	765.0	1,038.3	1.22
P3	628.0	852.2	769.0	1,043.7	1.22

As is evident from the above table, the equations normally used for flexural members in the AASHTO and ACI specifications significantly underestimate the ultimate capacity of the pile specimen. This underestimation is a result of the conservative nature of the code equations and the significant amount of prestressing strand in the compression region of the pile specimens. Both the AASHTO and ACI specifications recommend that a strain compatibility method be used when prestressing strand falls in the compression region of the member.

The second method used to compute the ultimate moment capacity of the pile specimens was strain compatibility. The properties of the concrete and strand, as measured in the laboratory, were used in the strain compatibility analysis. The ultimate moment capacity determined through an analysis based on strain compatibility, is compared to measured quantities in Table 12.

TABLE 12
COMPUTED AND OBSERVED ULTIMATE MOMENT CAPACITY
(Based on Strain Compatibility)

Specimen No.	Computed Ultimate Moment Capacity		Observed Ultimate Moment Capacity		Observed/ Computed
	(kip-ft)	(kN-m)	(kip-ft)	(kN-m)	
P1	771.0	1,046.5	793.0	1,076.3	1.03
P2	787.0	1,068.2	765.0	1,038.3	0.97
P3	786.0	1,066.8	769.0	1,043.7	0.98

The above table illustrates that the strain compatibility approach yields values significantly closer to the observed values for the pile specimens than the more general AASHTO and ACI equations.

6.6 STRAND TRANSFER LENGTH

As previously described, transfer length was experimentally evaluated for each pile specimen by measuring the change in concrete surface strains over a 5 ft (1.5 m) distance from the ends of each pile specimen. A mathematical expression for calculating the required transfer length for prestressed strand is provided in both the ACI Building Code Requirements for Reinforced Concrete (ACI 318-89) (1) and in the AASHTO Standard Specifications for Highway Bridges (2). According to the ACI 318-89 Commentary, the required development length is equal to the sum of the transfer length plus an additional length over which the strand must be bonded to insure that bond failure does not occur at nominal strength of the member. An expression for the transfer length alone can be written as:

$$l_t = \left(f_{se}/3\right) d_b \qquad (11)$$

where l_t = transfer length, in.

f_{se} = effective stress in prestressing strand after losses, ksi

d_b = nominal diameter of prestressing strand, in.

Using the above expression and assuming prestress losses based on readings from the Carlson strain meters, a transfer length of approximately 32 in. would be expected. As indicated in the following table, transfer lengths interpreted from the Whittemore readings were in reasonable agreement with the calculated values. These values are shown in Table 13.

TABLE 13
MEASURED AND CALCULATED TRANSFER LENGTHS

Pile Specimen	Concrete Age	Average Transfer Length, in.	
		Measured	Calculated
P1	At release	30.0	32.0
	After stripping	30.0	32.0
	At 14 days	31.0	32.0
P2	At release	17.5	32.0
	After stripping	22.5	32.0
	At 14 days	31.0	32.0
P3	At release	25.0	32.0
	After stripping	30.0	32.0
	At 14 days	31.0	32.0

Metric Equivalent: 1in. = 25.4 mm

6.7 PRESTRESS LOSSES

The AASHTO Standard Specifications for Highway Bridges contains provisions for calculating total prestress losses due to concrete shrinkage, elastic shortening, concrete creep, and steel relaxation. Based on these provisions, total prestress losses of approximately 19 percent are expected. However, only 35-45 percent of the total ultimate concrete creep and shrinkage losses are expected to occur within the first 28 days (27). Therefore, prestress losses of approximately 10 percent are expected at a concrete age of 28 days.

Concrete strains measured immediately after release were used to provide an indication of prestress losses due to elastic shortening. Based on these concrete strains, as reported in Chapter 5, losses due to elastic shortening averaged 4.6 percent between the three pile specimens. This value is in reasonable agreement with the average elastic shortening losses of 3.8 percent calculated using provisions from the AASHTO Standard and actual measured concrete and steel material properties.

Concrete strains measured at a concrete age of 28 days indicated prestress losses averaging approximately 6.7 percent among the three pile specimens. This value is significantly less than the 10.2 percent calculated using provisions from the AASHTO Standard and recommendations of the PCI Committee on Prestress Losses (27). Based on this information, it appears that the total actual prestress losses in the three pile specimens can be expected to be significantly less than the total losses predicted using the AASHTO Standard. However, calculated values for prestress losses were based on the assumption that approximately 35 percent of the ultimate creep and 42 percent of the ultimate shrinkage will occur within the first 28 days. These percentages, although shown to be reasonable for conventional concretes, may not be applicable for higher strength concretes. This

may explain the noted difference between measured and calculated prestress losses at 28 days.

6.8 COMPARISON OF RESULTS WITH CURRENT PROCEDURES

Based on the series of tests reported in Chapters 5 and 6, the pile specimens behaved in a manner that would be conservatively predicted using the provisions of the AASHTO Standard Specifications for Highway Bridges. It appears that the general equations given in the AASHTO specifications for modulus of elasticity and modulus of rupture as a function of compressive strength are acceptably conservative for the concrete strengths used in the pile specimens. The equations proposed in ACI 363-84 (26) are conservative for the modulus of elasticity and unconservative for the modulus of rupture. It is noted, however, that a limited number of concrete property specimens were tested and the conclusions drawn from those tests should be judged in light of the number of tests. The equations proposed in the AASHTO specifications and ACI code for moment capacity are conservative for members, such as the pile specimens, with prestressing strand in the compressive region. The use of a strain compatibility method provides a more precise method than the AASHTO and ACI equations for prediction of flexural capacity. The equations proposed in the AASHTO specifications and the ACI code for cracking moment and flexural shear cracking are also conservative. The present AASHTO and ACI equation for strand transfer length gives reasonably good results for concrete of the strength tested in the piles while it appears that the actual prestress losses in the piles can be expected to be siginificantly less than the total losses predicted using the AASHTO Standard.

7. BEHAVIOR OF BULB-TEE TEST SPECIMENS

7.1 INTRODUCTORY REMARKS

The purpose of this chapter is to present the observed behavior of the bulb-tee test specimens and to discuss that behavior in terms of load-deflection curves, crack patterns, strains, and modes of failure. Three, 54 in. (1372 mm) deep, bulb-tee specimens, designated BT1, BT2, and BT3, were cast for this phase of the research project. Each specimen was 70 ft (21.3 m) long and was fabricated from concrete having a mix design strength of 10,000 psi (69 MPa). Specimens BT1 and BT3 had a slab cast on their top flange that was 10 ft. (3 m) wide and 9-1/2 in. (241 mm) thick. The top slab was fabricated from concrete having a mix design of 7,000 psi (48.3 MPa). The second specimen, designated BT2, did not have a slab cast on top. Specimens BT1 and BT2 were tested first in flexure. Following the flexural test, the specimens were cut approximately in half. The two halves of BT1 and one half of BT2 were tested in shear. The shear specimens were given the designation BT1-D, BT1-L and BT2-L. The L in the designation denotes the jacking or live end of the member and the D designates the dead end of the member as determined in the fabricator's plant.

The investigation of the behavior of the 70-ft (21.3-m) BT specimens is discussed in section 7.2. The concrete property tests, flexural tests, strand transfer length tests, camber tests, and prestress losses tests on the 70-ft (21.3-m) BT specimens are discussed in sections 7.2.1, 7.2.2, 7.2.3, 7.2.4, and 7.2.5 respectively. The investigation of the inclined cracking behavior of specimens

BT1-D, BT1-L and BT2-L is discussed in section 7.3. Details of specimen materials, fabrication and testing are given in appendix B.

7.2 BEHAVIOR OF THE 70-FT (21.3-M) BULB-TEE SPECIMENS

Specmens BT1 and BT2 were 70 ft (21.3 m) long bulb-tee specimens tested in flexure approximately 40 days after fabrication. BT1 and BT2 were simply supported over a span length of 69 ft (21.0 m) and were loaded by means of hydraulic jacks manifolded together applying concentrated loads of equal magnitude at 6 ft (1.8 m) either side of center of the clear span. Deflections were measured across the width of the bottom flange of the specimen at mid span. For all specimens, the deflections were measured from an initial cambered position. Existing camber was measured just prior to testing. Dial gauges, as described in Appendix B, were used to detect any slippage of the prestressing strands in the specimens relative to the end of the specimens.

As was done with the pile specimens, the response of the specimens to the applied load is illustrated by means of load-deflection curves, which provide a graphical representation of the girder's ductility. The ductility of a member failing in flexure is attributed to the opening of cracks and strain in the concrete. For each specimen, load-deflection curves for the girder midpoint are plotted.

The load-deflection curve for BT-1, representative of the bulb-tee specimens reported herein, is shown in Figure 18. As was the case in the pile specimens, the measured deflection is proportional to the applied load for a portion of the curve, up to flexural cracking. Deflections up to flexural cracking may be calculated using methods based on elastic analysis with reasonable accuracy. However, after flexural cracking, there is no longer a direct relationship between applied loads and deflections as indicated by the non-linearity of the load-

deflection curve. In the case of members failing in flexure, the load-deflection curve is much flatter after flexural cracking as shown in Figure 18.

As was the case in the discussions of the pile specimen behavior, cracks in the following discussions will be classified into three categories: flexural cracks, flexure-shear cracks and web shear cracks. These terms are defined in Chapter 5 of this report.

Carlson strain meters were used as a means of evaluating the effective amount of prestress loss in the bulb-tee specimens. In addition to the Carlson meters, weldable strain gauges were placed near the top and bottom of the specimen. Polyester strain gauges were installed to measure strains at the top surface of the slab or girder flange.. The location of these strain gauges, along with a description of each type, can be found in Appendix B.

7.2.1 Concrete Property Tests

As a means of establishing material properties of the concrete in each bulb-tee specimen 135, 6-in. x 12-in. (152-mm x 305-mm) concrete cylinders were made at the time of casting. Approximately fifteen cylinders were cast from each batch. In addition, two 6-in. x 6-in. x 20-in. (152-mm x 152-mm x 508-mm) modulus of rupture beams were cast from the batches of concrete comprising the middle third of the beam specimens. Concrete material property tests were conducted at release (approximately 36 hours after casting) and at ages of seven, 28, and 40 days. As in the case of the pile specimens, concrete compressive strength tests, modulus of elasticity tests, splitting tensile strength tests and modulus of rupture tests were all conducted in accordance with appropriate ASTM requirements for those tests. In addition to the tests on the standard cylinder specimens, a 2.7-in. (69-mm) core was taken from the girders in the areas of each batch. These cores were tested in accordance with ASTM C42-87 (21) at an age

of 54 days. Results of these material property tests can be seen in Table 14. Each value in the table represents the average of three tests. A more detailed listing of properties, including poisson's ratio and the coefficient of expansion, can be seen in Tables B.3 and B.4 of Appendix B.

In addition to the above tests, concrete unit weight was determined from the core specimens taken from each bulb-tee specimen. Average unit weights for bulb-tee specimens BT1, and BT2 were 151.4 lbs/ft^3 (2,425 kg/m^3) and 146.3 lbs/ft^3 (2,343 kg/m^3) respectively. Since testing of specimen BT3 is still underway, coring has yet to be performed on that specimen.

TABLE 14
MEASURED MECHANICAL PROPERTIES OF CONCRETE
BULB-TEE SPECIMENS

Specimen No.	Concrete Age	Compressive Strength psi	Modulus of Elasticity ksi	Splitting Tensile Strength psi	Modulus of Rupture psi
BT1	Release	9,456	6,404	NO TEST	NO TEST
	7 days	9,625	6,150	703	NO TEST
	28 days	9,803	5,983	667	NO TEST
	40 days*	9,710	NO TEST	643	812
	56 days	9,940	5,933	657	NO TEST
	54 days**	9,427	NO TEST	NO TEST	NO TEST
BT2	Release	9,311	6,000	NO TEST	NO TEST
	7 days	9,147	5,950	680	NO TEST
	28 days	9,640	5,983	720	NO TEST
	40 days*	9,767	NO TEST	733	837
	56 days	9,660	5,950	723	NO TEST
	54 days**	9,940	NO TEST	NO TEST	NO TEST
BT3	Release	8,921	5,610	NO TEST	NO TEST
	7 days	9,537	6,133	650	NO TEST
	28 days	9,927	6,067	767	NO TEST
	40 days*	NO TEST	NO TEST	NO TEST	NO TEST
	56 days	9,973	6,067	703	NO TEST
	54 days**	NO TEST	NO TEST	NO TEST	NO TEST

*40 day results represent the material properties at time of flexural test.
**2.7 in. (68.6 mm) core taken from three locations in the girder.
Metric Equivalents: 1 ksi = 1000 psi = 6.895 MPa

7.2.2 Flexural Tests

As stated previously, three 54-in. (1,372-mm) bulb-tee specimens were cast for this project. These specimens were designated BT1, BT2, and BT3. The bulb-tees were all identical in structural details. The only difference in the specimens was that BT1 and BT3 had a slab 9-1/2 in. (241 mm) thick and 10 ft (3 m) wide cast on the top flange. The bulb-tee specimen design drawings shown in Appendix B indicate the strand arrangement as well as the stirrup spacing. The mechanical properties of the prestressing strand and stirrups are also given in Appendix B. Long term tests on specimen BT3 are underway and are not included in this report. The test set-up for specimens BT-1 and BT-2 is shown in Figure 5. The test set-up for specimen BT-3 is shown in Figure 7.

A. Load-deflection Relationship

Two flexural tests were performed on specimen BT1. Loads were applied in increments. Readings of all instruments were taken at each load increment followed by visual inspection for cracks. The first test applied the loads anticipated under full service load conditions (Dead Load + Live Load + Impact). The load-deflection curve for the first loading can be seen in Figure 19. No cracking was observed and the load-deflection relationship was linear. Once the applied load reached the service load level the load was slowly taken off the member. Maximum deflection of the specimen at service level load was 0.47 in. (12 mm). After unloading the specimen had a residual deflection of 0.03 inches. These deflections do not reflect the effect of the initial girder camber.

The second loading of specimen BT1 was intended to carry the member to failure or a predefined deflection limit of 24 in. (610 mm). The load-deflection relationship for the mid span of bulb-tee specimen BT1 is shown in Figure 18. During the test, cracking initiated in the constant moment region near mid-span.

The observed total applied load, P_{fc}, corresponding to the formation of the initial flexural crack was 220.4 kips (980 kN). The initial flexural crack disturbed the linear relationship between applied load and deflection as shown in Figure 18. Application of additional load caused more flexural cracks to appear in the bottom region of the specimen in the region of maximum moment between the load points and caused the initial flexural cracks to propagate vertically. The flexural cracks in the constant moment region of bulb-tee specimen BT1 are shown in Figure 20 and are relatively evenly spaced.

With additional increase in applied load, flexural cracks appeared in the bottom flanges of the bulb-tee specimen in the shear spans, the region between the load points and the reactions. These cracks propagated upward to the bottom of the web and then became inclined toward the load points. These cracks are termed flexure-shear cracks, since they originate as flexural cracks in the shear span. Figures 21 and 22 show the development of flexure-shear cracks in the shear span of specimen BT1. The load at which the flexure-shear cracking occurs is not apparent from the load-deflection curve because the flexure-shear cracks originate as flexural cracks, forming after the development of other flexural cracks in the moment span. The total applied load, P_{fsc}, measured corresponding to the formation of these initial flexure-shear cracks was 279.6 kips (1,244 kN) for specimen BT1. With an increase in load, additional flexure shear cracks appeared in the specimen while the flexural cracks propagated vertically up into the slab of the specimen.

The load-deflection curve peaked at a total applied load of 408.8 kips (1,818 kN). A deflection of 24 in. (610 mm) and audible indications of strand breakage at this applied load marked the limit of the load capacity of the bulb-tee specimen.

The load-deflection relationship for the mid-span of specimen BT2 is shown in Figure 23. An initial flexural crack developed in the bottom flange of the specimen near mid-span at a total applied load, P_{fc}, of 189.3 kips (826 kN). This crack opened at the location of a shrinkage crack, discovered at the time of fabrication prior to the release of the strands, and described in Appendix B. The applied load represents the load necessary to open a pre-existent crack and is not the true cracking load. This crack and additional flexural cracks disturbed the linear relationship between applied load and deflection as shown in Figure 23. Application of additional load caused more flexural cracks to appear in the bottom flange of the specimen in the region of maximum moment between the load points and caused the initial flexural cracks to propagate vertically. The flexural cracks in the constant moment region of specimen BT2 are shown in Figure 24 and are relatively evenly spaced.

Flexure-shear cracks appeared at a total applied load, P_{fsc}, of 259.1 kips (1,153 kN) for specimen BT2, as shown in Figures 25 and 26. The maximum vertical deflection of specimen BT2 just prior to failure was 4.97 in. (126 mm) with 294.1 kips (1,308 kN) total load. Measured deflections do not reflect initial camber.

B. Concrete strains

Three Carlson strain meters and two weldable strain gauges were placed in the lower flange and two weldable strain gauges were placed in the top flange of each bulb-tee specimen at mid-length during fabrication. As can be seen in Figure 27, these devices performed well during the test with good correlation between the lower Carlson meters and the lower weldable strain gauges. However, the weldable gauges were located closer to the bottom surface of the girder than the Carlson gauges and, therefore, would be expected to measure higher strains. All

strain measuring devices ceased to give meaningful readings once cracks had opened in the immediate vicinity of the gauges.

Concrete surface strain gauges were placed on the top slab of specimen BT1 and the top flange of specimen BT2 to measure extreme fiber compressive strain. The results of these measurements can be seen in Figure 28 for BT1 and Figure 29 for BT2. For BT1, the strain data indicates that the full width of the slab was participating in the flexural action with no shear lag.

C. Modes of Failure

Failure occurred in specimen BT1 after increased applied load caused a deflection of 24 in. and audible indications of strand breakage.

As is shown in Figure 30, BT2 failed when a portion of the top flange blew out in a compressive failure along one side of the girder. BT2 buckled laterally coincident with the ultimate load. The member did not reach flexural capacity due to failure at a load of approximately 93 percent of calculated ultimate. A more thorough discussion of this failure is presented in section 8.6, Flexural Strength.

7.2.3 Strand Transfer Length Tests

As described in Appendix B, transfer length was experimentally evaluated for each bulb-tee specimen by measuring the change in concrete surface strains over a 5-ft (1,524-mm) distance from the ends of each BT specimen. The surface strains were measured using a 10-in (254-mm) Whittemore gauge. Reference gauge readings were taken just prior to release, just after release, and several times prior to testing. Plots of the transfer length data for the 40 day-after-release case for each end of specimens BT1, BT2, and BT3 are shown in Figures 31 through 36.

7.2.4 Camber Tests

Immediately after casting, (while the concrete was still plastic) large stainless steel bolts were embedded in the top surface of each girder at mid-span and near both ends to provide a permanent fixed reference for camber measurements. The bolt embedded near each end was centered above the sole plate. Camber measurements were made using a level to site the relative elevations of each reference point. Mid-span camber measurements relative to the ends of each girder were measured prior to release, after release, at a concrete age of 30 days, and before and after deck casting (where applicable). In addition, the maximum deflection for the proof of design test (design dead plus live plus impact load), for BT1 was recorded. A listing of the camber and deflection readings is shown in in Table 15. Additional camber measurements in Girder BT3 are being made at regular intervals during the long term test.

TABLE 15

CAMBER MEASUREMENTS - TAKEN AT MID-SPAN*

Event	Specimen BT1	Specimen BT2	Specimen BT3
@ Release	-0.688 in.	-0.688 in.	-0.672 in.
@ 30 days	-0.984 in.	-1.016 in.	-1.000 in.
With deck	-0.438 in.	N. A.	-0.547 in.
Proof of Design	-0.019 in,	N.A.	N.A.

* Negative value indicates an upward camber.

Metric equivalents: 1 in. = 25.4 mm

7.2.5 Prestress Losses Tests

As described in Appendix B, internal Carlson strain meters were installed in each bulb-tee specimen at mid-span at the vertical centroid of the strand group. The strain meters were monitored for specimens BT1 and BT2 until an age of 30 days. Monitoring of strain meters in BT3 is continuing at the writing of this report and behavior beyond 30 days will be reported in the final report. Measured concrete strains were used to calculate prestress losses by multiplying the average measured strain by the average measured strand modulus of elasticity of 30,000 ksi (206,850 MPa).

Concrete strains measured immediately after release were used to calculate prestress losses due to elastic shortening, while subsequent changes in strain were considered time dependent losses. Table 16 shows the measured strain and calculated losses at release and at 30 days for each specimen.

TABLE 16
MEASURED PRESTRESS LOSSES AT RELEASE AND AT 30 DAYS
(Based on Strand Modulus of Elasticity of 30,000 ksi)

Specimen	Specimen Age	Measured Strain in./in.	Loss in Prestress psi
BT1	Release	473×10^{-6}	14,190
	30 days	666×10^{-6}	19,980
BT2	Release	484×10^{-6}	14,520
	30 days	733×10^{-6}	21,990
BT3	Release	346×10^{-6}	10,380
	30 days	548×10^{-6}	16,440

7.3 BEHAVIOR OF SHEAR SPECIMENS BT1-D, BT1-L, AND BT2-L

Following the completion of the flexural tests on specimens BT1 and BT2, the beams were cut in half and prepared for testing in shear. The specimens were placed on support blocks, as described in Appendix B and as shown in Figure 6, with a clear span of 27 ft (8.2 m). All the specimens were loaded by means of four pairs of hydraulic jacks, with concentrated loads of approximately equal magnitude, at four equally-spaced locations along the member. The loads were placed 4 ft 6 in. (1,372 mm), 7 ft 6 in. (2,286 mm), 10 ft 6 in. (3,200 mm), and 13 ft 6 in. (4,115 mm) from the centerline of the bearing. Deflections were measured at mid-span which was also the point of maximum moment. All deflections were measured from the initial cambered position of the member. Dial gauges, as described in Appendix B, were used to detect any slippage of the prestressing strands in the specimens relative to the formed end of the specimen. This was important since these specimens were previously subjected to a loading test.

As was done in the flexural tests, the response of the specimens to the total applied load is illustrated by means of load-deflection curves. This provides a graphical representation of the girder's behavior under load.

The load-deflection curve for specimen BT1-D is representative of the shear specimens, and is shown in Figure 37. As was the case in the flexural tests, the measured deflection is proportional to the load up to a point. In the case of the flexural specimens, this point represents flexural cracking. In the case of the shear specimens, this point represented the point of shear failure at the support adjacent to the "cut end" of the member. This shear failure resulted from pre-existing cracks that formed transverse to the flexure shear cracks that formed during the flexural testing of specimen BT1. These cracks were not initiated during the shear

test but propagated during the shear test thus providing a failure mechanism independent of the usual web shear cracking mechanism.

7.3.1 Shear Tests

As described earlier, three specimens were prepared using the ends of specimens BT1 and BT2. These specimens were designated BT1-D, BT1-L and BT2-L. Originally there were to be four shear specimens but damage during the failure of specimen BT2 prevented a specimen from being prepared from the dead end of the member. The only difference in the specimens was that specimens BT1-D and BT1-L had a slab, 9-1/2 in. (241 mm) thick and 10 ft (3 m) wide, cast on the top flange. BT2-L did not have a slab cast on the top flange. The bulb-tee specimen design drawings shown in Appendix B indicate the strand arrangement as well as the stirrup spacing. The mechanical properties of the prestressing strand and the stirrups are also given in Appendix B.

A. Load-Deflection Relationship

The load-deflection relationship for the mid-span of specimen BT1-D is shown in Figure 37. After the application of several increments of load on the specimen, preexisting cracks on the cut end of the specimen, as shown in Figure 38, began to open and extend towards the top and bottom flange. These cracks propagated toward the support bearing and continued to grow in length and width. When the cracks extended through the lower flange the linear relationship between the applied load and deflection was disturbed as shown in Figure 37. The first crack that could be considered as an applied-load induced web shear crack formed at the cast end of the member at a shear load of 416 kips (1,850 kN). Figure 39 shows that as additional load was applied to the member additional cracks formed at the formed end of the member and the cracks at the "cut" end of the member

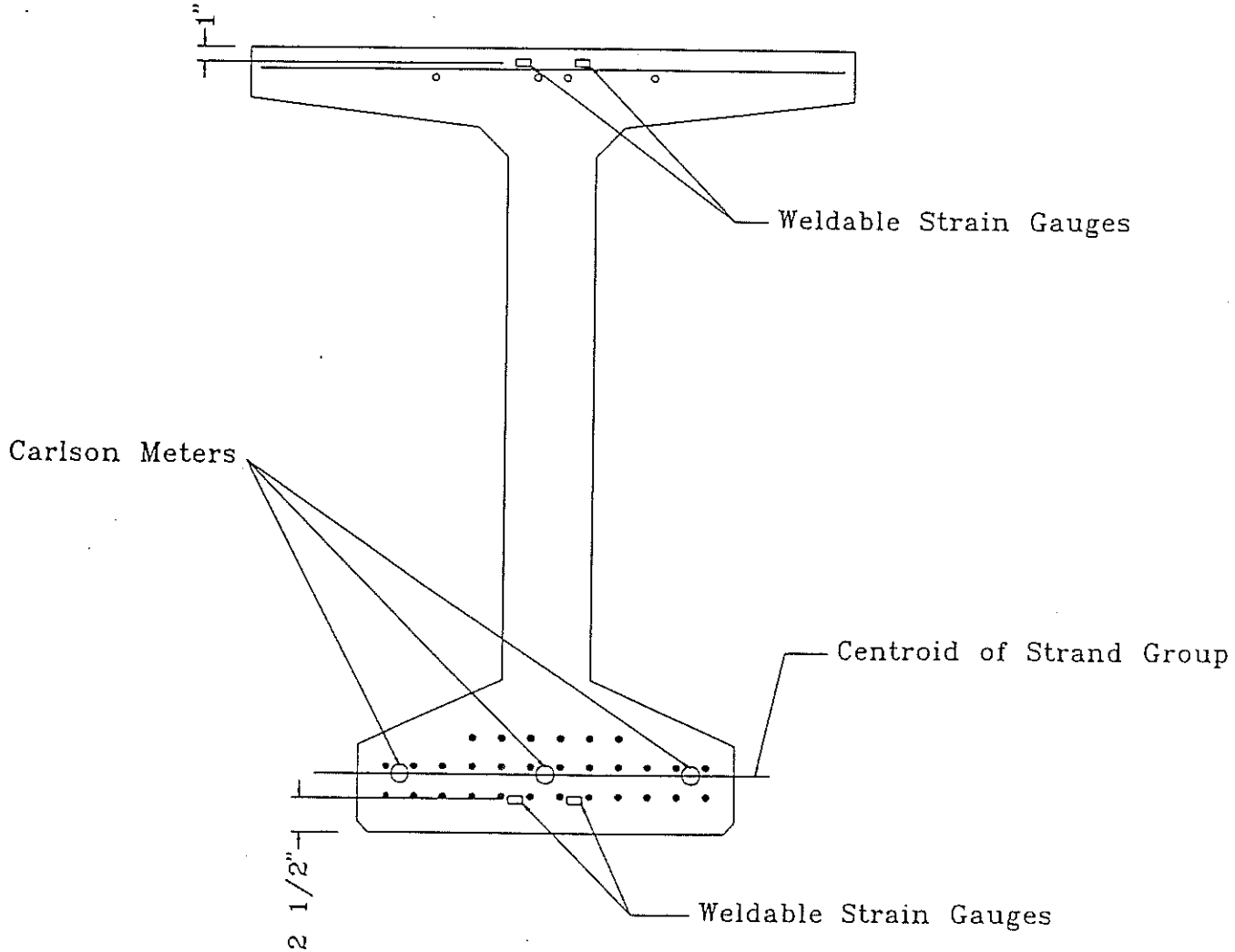

Figure B.6. Location of strain meters and strain gauges.

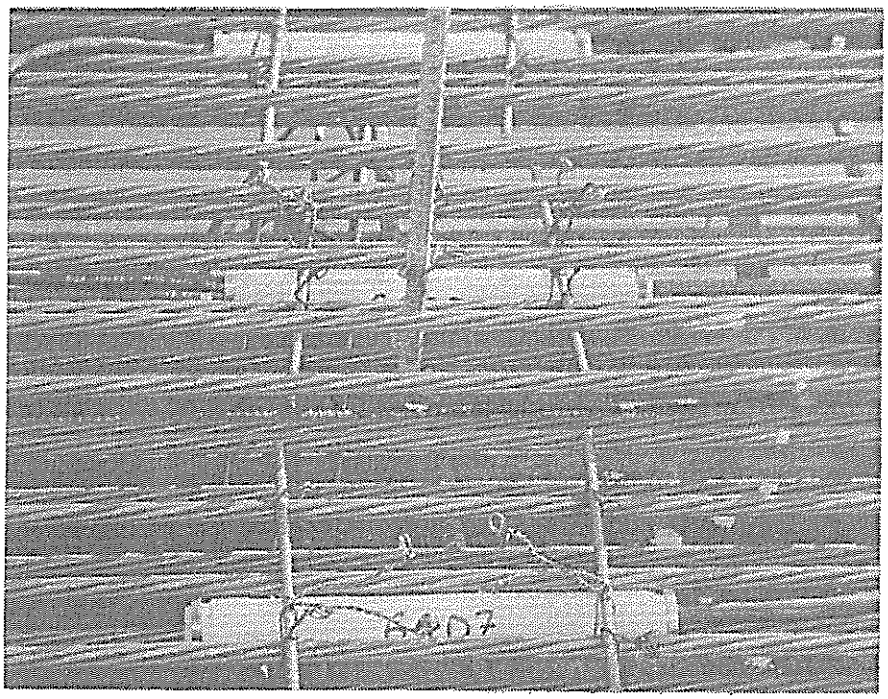

Figure B.7. Strain meters and weldable gauges in lower flange.

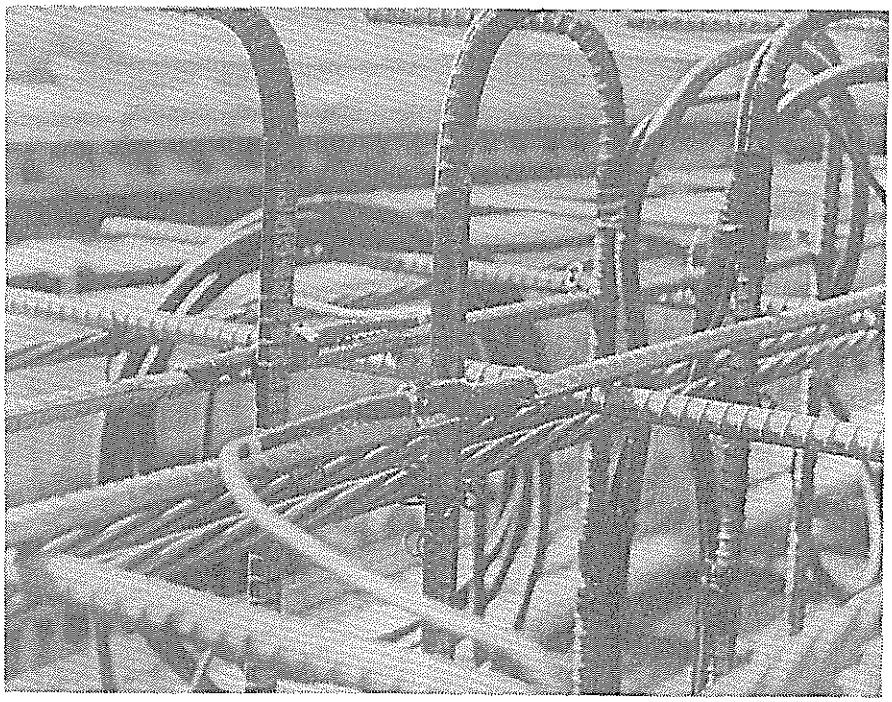

Figure B.8. Weldable strain gauges in top flange.

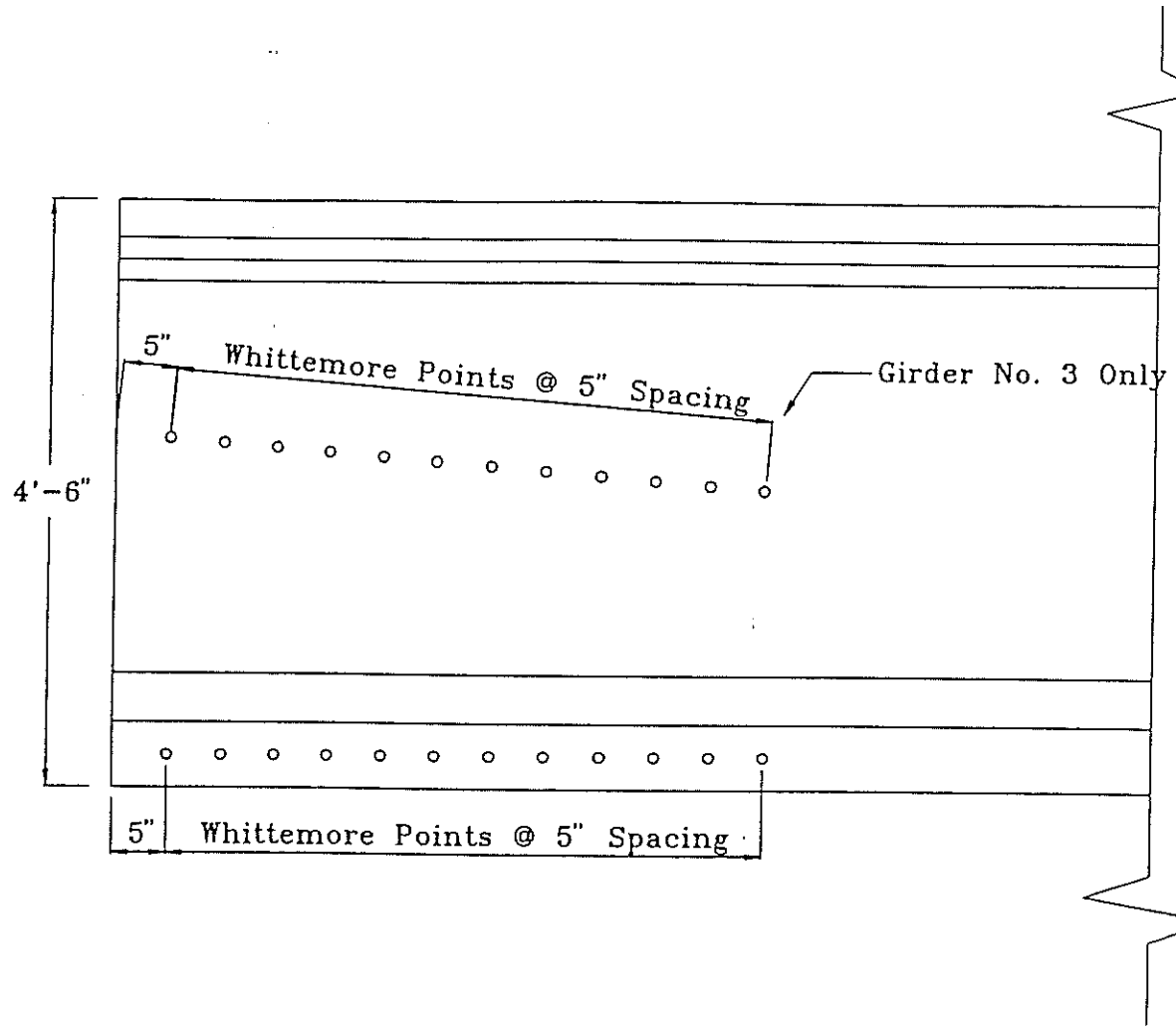

Figure B.9. Location of Whittemore points.

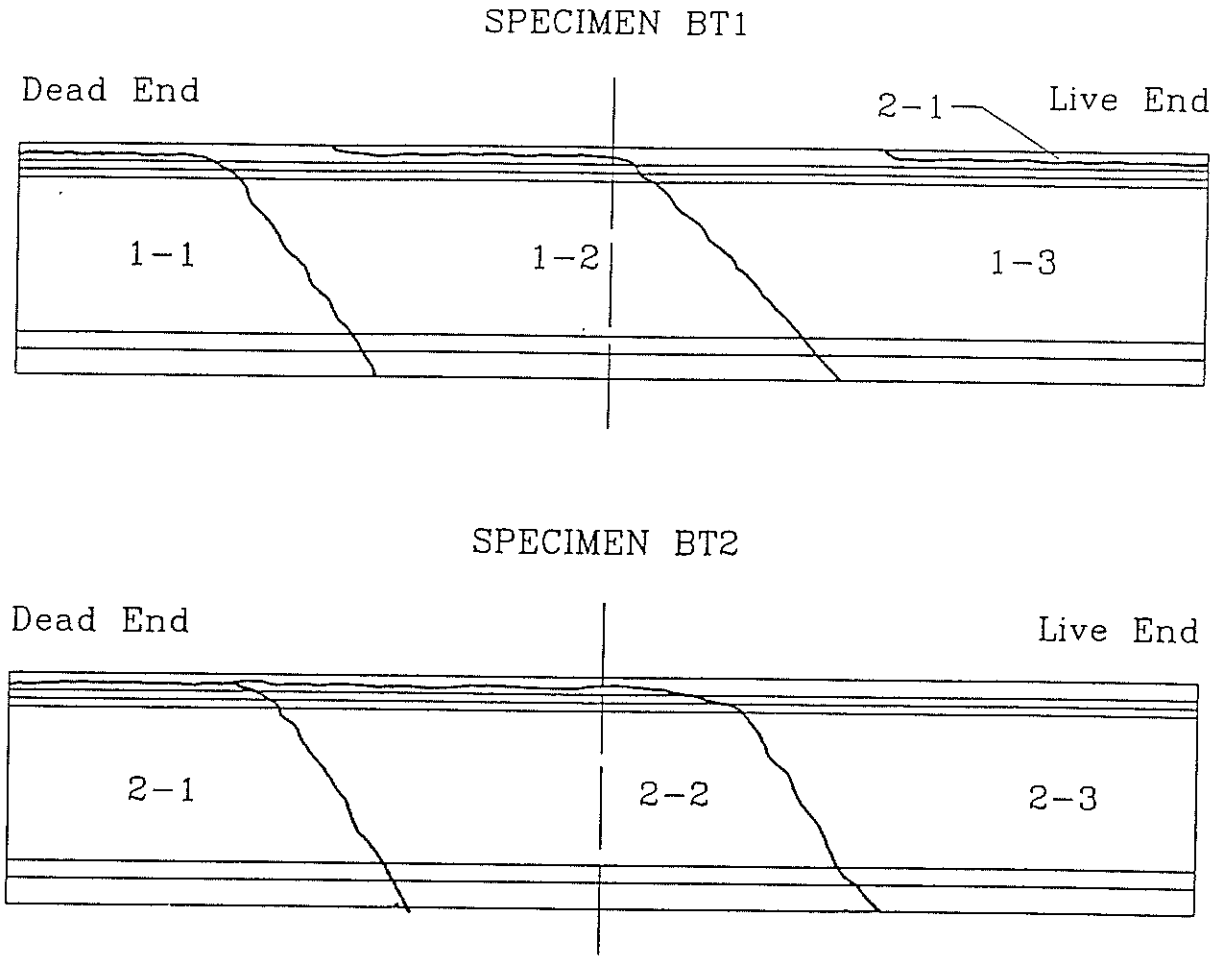

Figure B.10. Location of concrete batches in specimens BT1 and BT2.

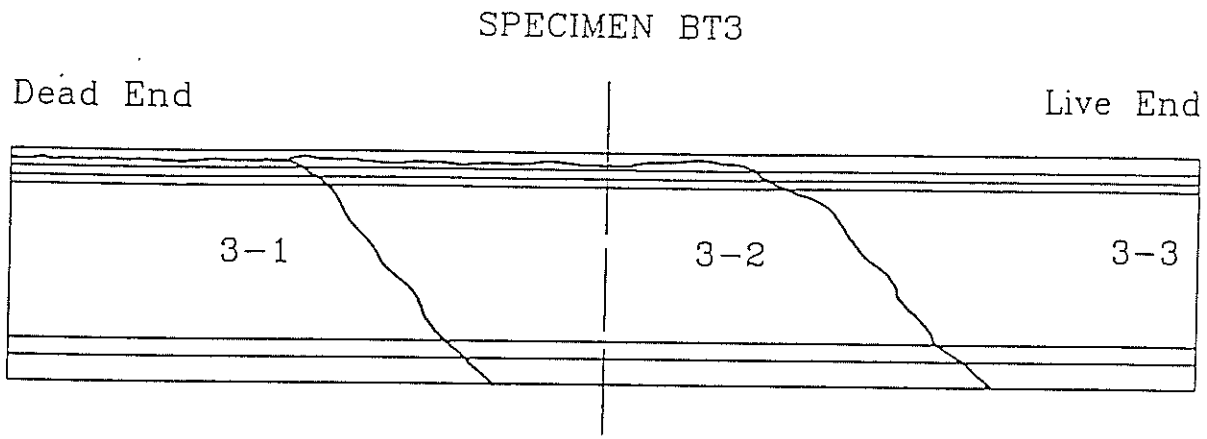

Figure B.11. Location of concrete batches in specimens BT3.

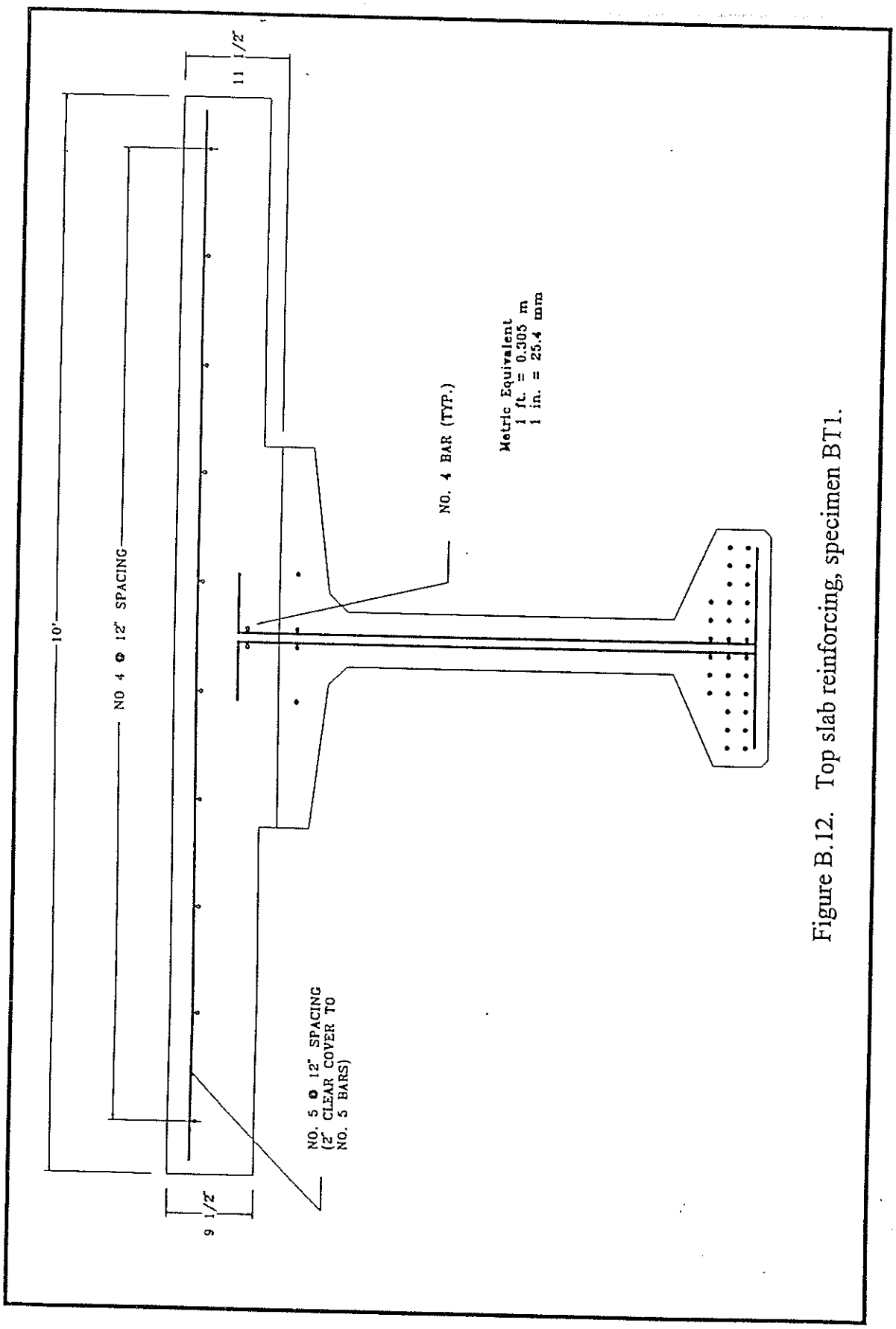

Figure B.12. Top slab reinforcing, specimen BT1.

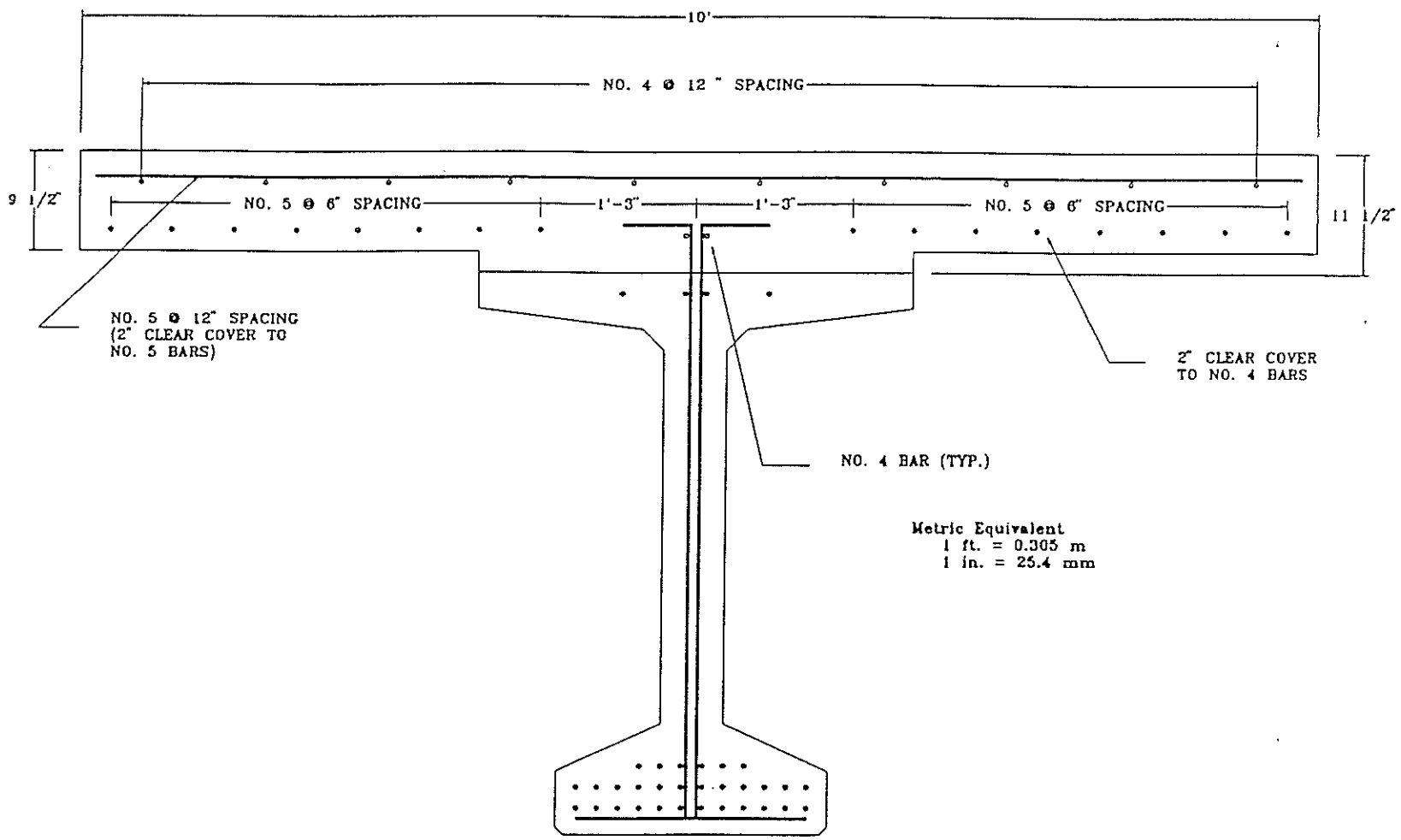

Figure B.13. Top slab reinforcing, specimen BT3.

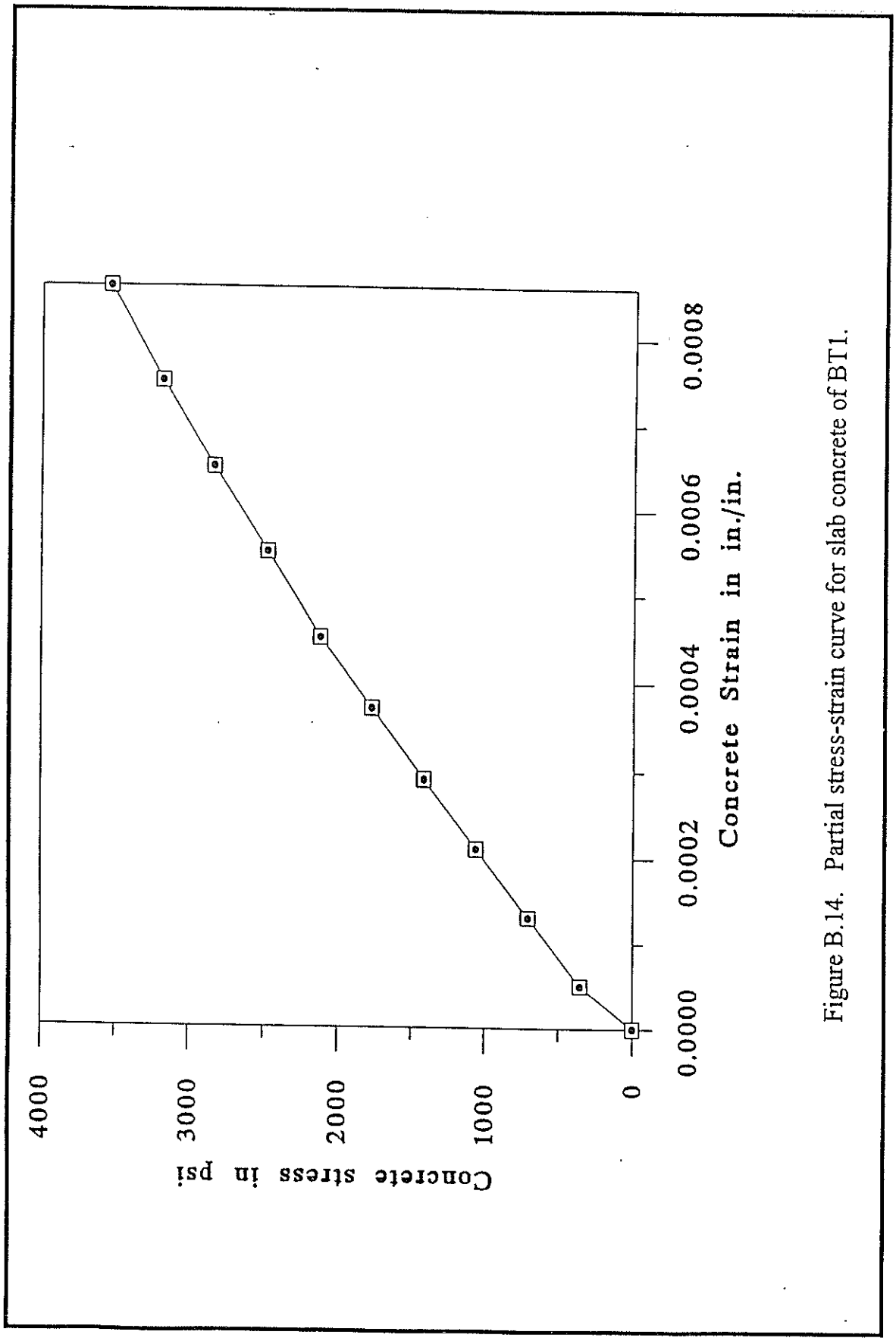

Figure B.14. Partial stress-strain curve for slab concrete of BT1.

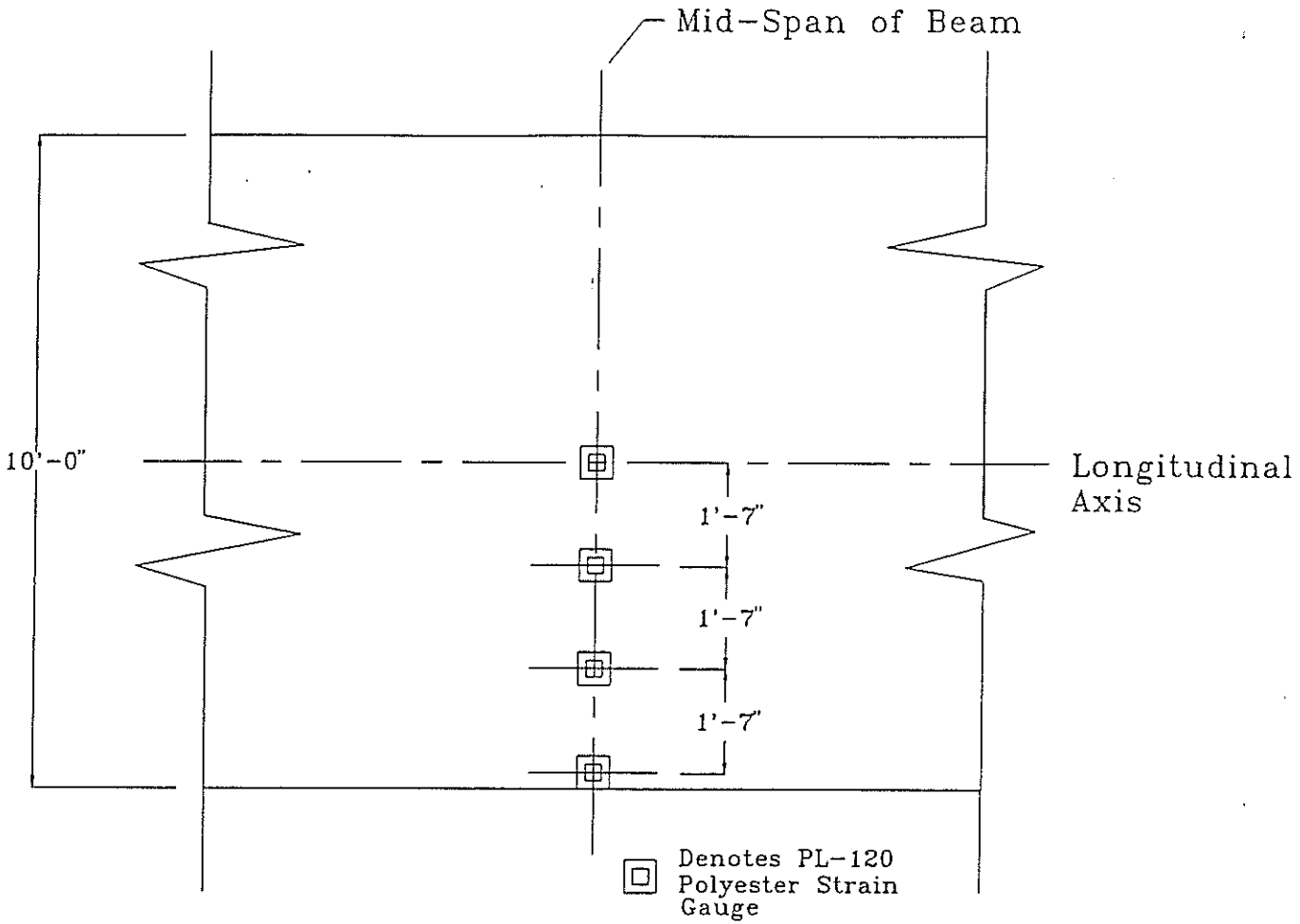

Figure B.15. Top slab surface strain gauge locations, specimen BT1.

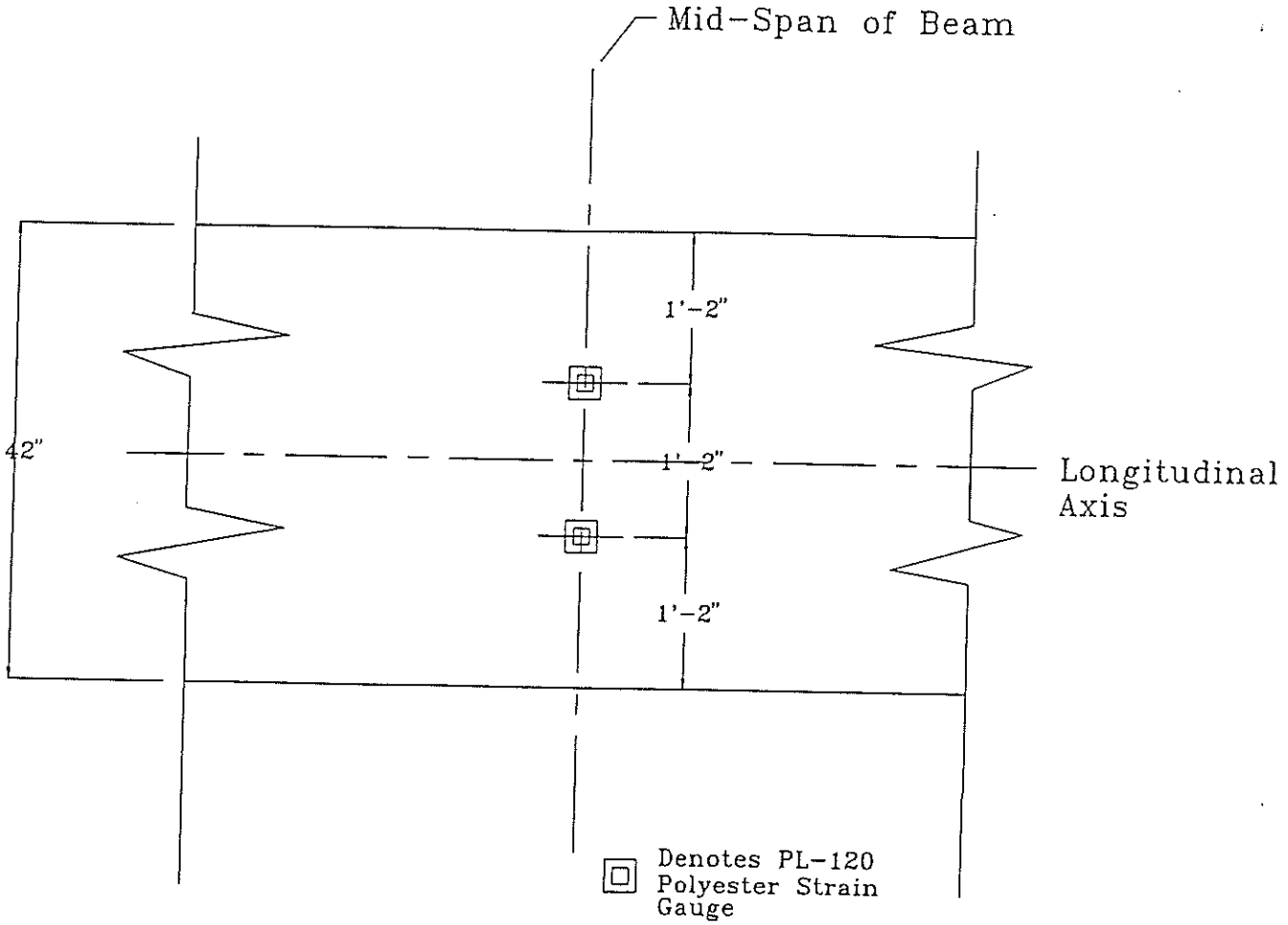

Figure B.16. Top flange surface strain gauge locations, specimen BT2.

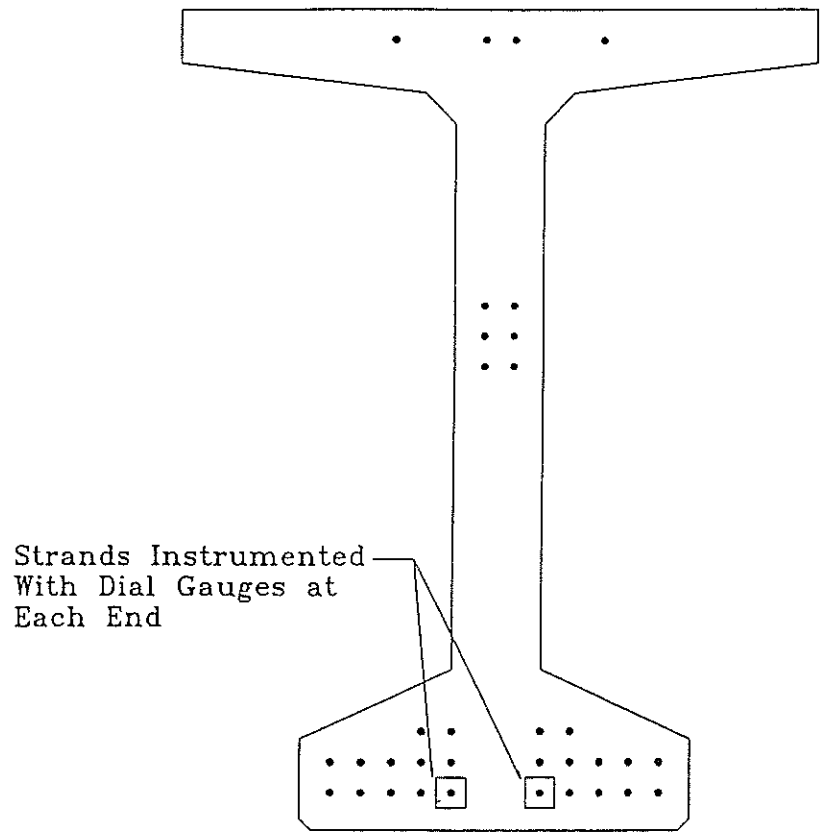

Figure B.17. Strand dial gauge locations.

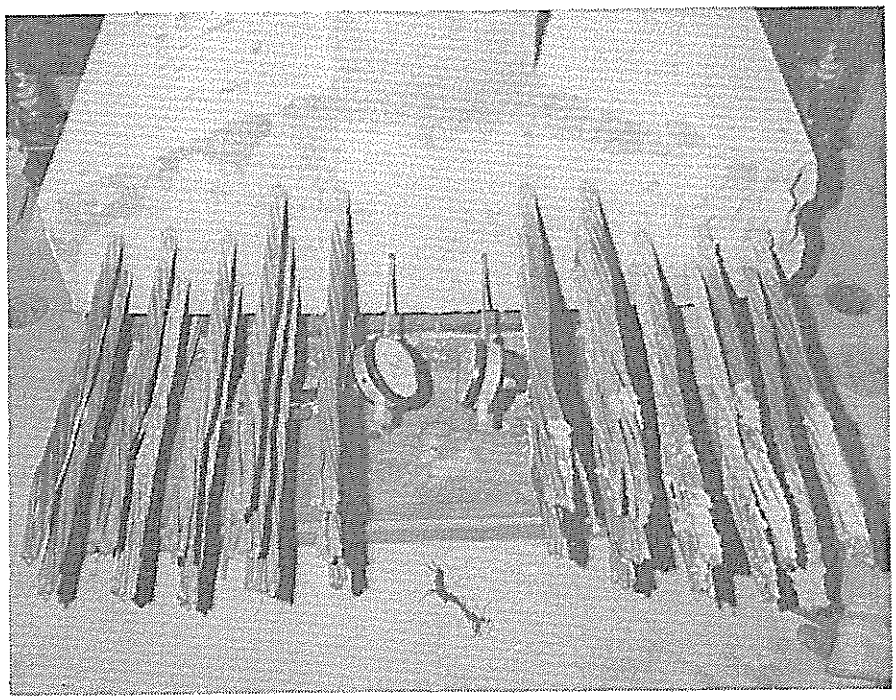

Figure B.18 View of dial gauges.

APPENDIX C

MATERIALS, FABRICATION, INSTRUMENTATION, AND DRIVING OF THE 130-ft (39.6 m), 24-in. (610 mm) SQUARE PILE SPECIMEN

C.1 MATERIALS

C.1.1 AGGREGATE

The sand for the concrete mix was obtained from a pit near Atmore, Alabama. The course aggregate was obtained from the Reed Quarry located near Gilbertsville, Kentucky. The course aggregate was a crushed limestone. Both aggregates were tested and found to be in conformance with the Louisiana Department of Transportation and Development (LaDOTD) Standard Specifications for aggregates (31). Sieve analysis of the aggregate used can be seen in Table C.1.

C.1.2 CEMENT

Type I-II FG portland cement was used for the pile test specimen. The cement was manufactured by the Holnam Corporation and was certified to conform to ASTM Standard C150-89 , Specifications for Portland Cement (32).

C.1.3 WATER

The water used in the concrete was obtained from the Sherman Prestress, Inc. underground well. The water conformed to LaDOTD Standard Specifications for water used in portland cement concrete.

C.1.4 ADMIXTURES

Four admixtures were used in the concrete mix. None of the admixtures used in the mix are on the present LaDOTD Qualified Products List. The admixtures were as follows:

1. FRITZ FR-2 high range water reducer conforming to ASTM C494-90, Type A, B & D (33).
2. FRITZ SUPER 6 high range water reducer conforming to ASTM C-494-90, Type F (33).
3. FRITZ AIR PLUS air entraining admixture conforming to ASTM C260-86 (34).
4. FRITZ PAK silica fume - 100 percent solids.

C.1.5 CONCRETE MIX

The mix was designed by LTRC to yield a minimum nominal 28-day compressive strength of 10,000 psi (69 MPa). The proportions of the four yard batches, by weight, are given in Table C.2.

Concrete control specimens were made from each batch. The pile specimen required five batches of concrete. The control specimens were identified with the batch number; for example control specimen two denotes the specimen taken from the second batch used to make the pile specimen.

Selected mechanical properties of the concrete and the age of the specimen at the time of testing are given in Table C.3.

C.1.6 PRESTRESSING STRAND

The prestressing strand used in the pile specimens was domestically fabricated using domestically manufactured steel and was obtained from Wiremill, Inc. of Jacksonville, Florida. The nominal diameter of the strand was 1/2 inch.

The strand conformed to ASTM A-416-88, Specifications for Steel Strand, Uncoated Seven Wire Stress Relieved for Prestressed Concrete(36).

A complete stress-strain curve for the production lot from which the project strand was drawn was provided by the manufacturer. This stress-strain curve is reproduced in Figure C.1.

C.1.7 WEB REINFORCEMENT

The spiral reinforcement used in the pile specimens was domestically manufactured by Florida Wire and Cable Company of Jacksonville, Florida. The W4.5 wire had a diameter of 0.211 in. (5.35 mm). The average tensile strength of samples tested by the manufacturer was 3,447 lb (`15.3 kN), or 98,588 psi (680 MPa).

C.2 FABRICATION

The pile specimen was fabricated by Sherman Structural Marine Inc. at their plant in Mobile, Alabama in accordance with the shop drawings shown in Figure C.2. The pile specimen was fabricated in a 240 ft 8 in. (73.3 m) casting bed. All work was performed by the fabricator. All phases of the pile specimen fabrication and preparation of the control specimens were observed and supervised by the research personnel to insure all quantities and measurements were known accurately.

Casting of the pile specimen began at 10:45 a.m. on May 29, 1992 and was completed at 12:30 p.m. of the same day. The daytime temperature on the day of the pour ranged from 78 degrees to 80 degrees F. The pile specimen, along with all but two of the control specimens, were steam cured for 18 hours after initial set under a tarpaulin consisting of 1/4-in. (6.4-mm) foam insulation sandwiched between two layers of waterproof canvas. With the exception of three air cured

cylinders, the control specimens were also placed under the tarpaulin to undergo the same curing process as the ples. The members were steam cured for 18 hours at an average temperature of 140 degrees. In all, two days were expended for fabrication of the pile specimen from prestressing of the strand to removal from the form..

C.2.1 PLACING OF THE LONGITUDINAL STRAND

The seven wire prestressing strands were drawn from a single reel located in an outdoor storage area adjacent to the casting bed. Each strand was taken from the reel and threaded through a template at each end of the casting bed. The strands were tensioned using a single strand jack manufactured by G.T. Bynum. The jack had been calibrated within the past three months to have an average gauge reading error of less than 0.86 percent.

C.2.2 PRESTRESSING OF THE STRAND

In accordance with the present AASHTO code each of the strands was initially stressed to a value of 0.75 fpu or 30,980 lb (138 kN). In order to accomplish this the strands were initially tensioned to a proof load of 3000 lb (13.4 kN) based on gauge readings. After being subjected to the proof load the strands were marked and stressed to an average elongation of 18.6 in. (472 mm). The load corresponding to this elongation can be obtained from the following expression:

$$\mathbf{e} = \frac{\mathbf{P\,L}}{\mathbf{A\,E}} \qquad (30)$$

where

e	=	elongation of strand in inches
P	=	load per strand in pounds
L	=	nominal length between stressing ends, 120 ft 10 in. (36.8 m)
E	=	modulus of elasticity of the strand 28,600,000 psi (197,000 MPa)

Using the above expression the load in the strand beyond the proof load is calculated to be 27,970 lb (129 kN). If the proof load is added to this value, a force of 30,970 lb (138 kN) per strand resulted in each strand. This was confirmed using the gauge readings of the jack. The jack gauges were found have an average gauge reading error of less than one percent for the load range used in recent calibration tests.

C.2.3 PLACING OF SPIRAL REINFORCING AND FORM ERECTION

The spiral reinforcing was placed after the full prestress force had been applied to the longitudinal strand. The 12-in. (305-mm) void in the center of the pile was formed using a cardboard tube. The cardboard tube was hung from short lengths of steel angles that were bolted to the top of the forms. These steel angles also served to hold the cardboard tube down during the concrete pour. The exterior sides of the pile were formed by a steel pan with an open top. The form could not be broken apart, hence the pile was removed by lifting it up out of the forms.

C.2.4 CASTING AND CURING

The concrete was mixed in the fabricator's batch plant located adjacent to the pile casting bed. The batch plant had a single four cubic yard (4 m^3) drum type central mixer. The mixer was initially charged with the stone, sand, silica fume, and 80 percent of the water. Next, the air entraining agent was added, followed 30 seconds later by the water reducer, followed 30 seconds later by the super plasticizer. Following this charging of the mixer, the batch was mixed for 200 seconds. Water was added as required to obtain a slump of 5 in. (127 mm) with mixing continuing for at least 90 seconds after the last water addition. Aggregate was initially weighed to the required amount after adjustments were made for the free moisture content on the scales located above the central mixer. The free moisture in the sand was measured at 7.5 percent while the free moisture of the stone was 0.9 percent. The cement was weighed in another set of scales also located above the central mixer. Water was added and controlled by an automatic dispenser/meter. Admixtures were added by hand in weighed bags.

The concrete was mixed in four cubic yard batches and then placed into a screw type transporter, taken to the casting bed and placed in the forms. The pile specimen required slightly less than 18 cubic yards of concrete, hence four, four cubic yard batches and one three cubic yard batch were mixed for the member.

Control specimens were made during the casting operation. Seven standard 6-in. x 12-in. (152-mm x 305-mm) cylinders were made from each batch.

After casting, internal vibration of the concrete using hand held vibrators was performed carefully to insure proper concrete placement. Short segments of strand were embedded in the pile segment to provide lifting eyes. The members were steam cured for 18 hours at an average temperature of 140 degrees.

C.2.5 RELEASE OF PRESTRESS

Approximately 20 hours after completion of casting, a control cylinder was removed from the casting bed to the plant testing laboratory, and tested to determine its compressive strength. A minimum of 6,000 psi (41.4 MPa) was required before release of the prestress. The average compressive strength of the three cylinders was 9,071 psi (62.4 MPa), thus satisfactory for release of the prestress.

The prestress was released by cutting the strands with an acetylene torch simultaneously at each end of the pile.

C.2.6 TRANSPORTING AND HANDLING OF THE PILE

Immediately following release of the strands, the pile was lifted out of the form and transported to another location in the casting yard. The control specimens remained with the pile segments until the time of shipment. Thirteen days after release, the pile was loaded onto a truck as shown in Figure C.3 and transported to a bridge under construction on Route La 415 over the Missouri Pacific Railroad in West Baton Rouge Parish. The control specimens were picked up by LTRC and transported to their laboratory in Baton Rouge, Louisiana.

C.3 INSTRUMENTATION

C.3.1 INSTRUMENTATION OF PILE

The only instrumentation for the pile was two strain gauges and two accelerometers installed on the surface of the pile about four feet from the driving end as shown in the PDA report.

C.4 PILE DRIVING EQUIPMENT

The pile driving equipment consisted of a Vulcan 020 hammer with a 20,000 lb ram operating at a maximum stroke of three feet and a rated energy of 60,000 ft-lbs. The hammer cushion consisted of an 18 in. thick pad of alternating one inch layers of Micarta and aluminum. Between the hammer cushion and pile cushion was a 2,600 lb helmet. The pile cushion consisted of an oak pad six inches thick. A complete description of the efficiency of the hammer can be found in the PDA report.

C.5 PILE DYNAMIC ANALYZER REPORT

The following is a copy of the pile Dynamic Analyzer report prepared by the Pavement and Geotechnical Design Section of the Louisiana Department of Transportation and Development. The conclusions of this report indicate that the pile survived driving without damage and that a pile fabricated of the typical strength used for prestressed concrete piles in Louisiana would have probably sustained damage during driving.

STATE OF LOUISIANA
DEPARTMENT OF TRANSPORTATION AND DEVELOPMENT

PDA MONITORING

HIGH STRENGTH PRECAST PRESTRESSED CONCRETE PILE

S.P. 736-15-0079/LTRC NO. 90-4C
FEASIBILITY EVALUATION OF HIGH STRENGTH CONCRETE

S.P. 13-01-0024
BRIDGES OVER MISSOURI PACIFIC RAILROAD
ROUTE LA 415
WEST BATON ROUGE PARISH

PAVEMENT AND GEOTECHNICAL DESIGN SECTION

July 16, 1992

STATE OF LOUISIANA
DEPARTMENT OF TRANSPORTATION AND DEVELOPMENT
P. O. Box 94245
Baton Rouge, Louisiana 70804-9245

EDWIN W. EDWARDS
GOVERNOR

JUDE W. P. PATIN
SECRETARY

July 16, 1992

Department of Civil Engineering
206 Civil Engineering Building
Tulane University
New Orleans, Louisiana 708118-5698

Re: PDA Monitoring
S.P. 736-15-0079/LTRC No. 90-4C
Feasibility Evaluation of High Strength Concrete
S.P. 13-01-0024
Bridges over Missouri Pacific Railroad
Route LA 415
West Baton Rouge Parish

Attention: Dr. Robert N. Bruce, Jr.
Principal Investigator

This report summarizes our findings from dynamic monitoring of a research pile driven on the above referenced project.

BACKGROUND

The LA DOTD Bridge Design section requested that we monitor a 24" high strength precast prestressed concrete pile during pile driving with the Pile Dynamic Analyzer™ (PDA). This pile is part of a research study, *Feasibility Evaluation of High Strength Concrete*, being performed by Tulane University. The pile was driven at the LA 415 bridge construction project (S.P. 13-01-0024). Our general requirements to perform the PDA testing were transmitted to the Project Engineer in our letter dated April 2, 1992. We received the completed *Pile Driving And Equipment Data Form* on June 6, 1992. Related correspondence is enclosed in the appendix.

On June 16, 1992, a field trip was made to prepare the research pile for dynamic monitoring with the PDA. Several dynamic wave speed measurements were taken for PDA input during dynamic monitoring. In order to expedite PDA monitoring, several concrete anchors were set into the pile surface for future attachment of strain gauges and accelerometer transducers.

The high strength concrete research pile was monitored during driving with the Pile Driving Analyzer™ on June 22, 1992. The pile was driven on the northbound bridge Bent 10 (pile no. 3) at station 217+74.43. The PDA is a computerized data acquisition system which uses two strain gauges and two accelerometer transducers to record the strain and acceleration at the gauge location (4' below pile top). The PDA converts the strain and acceleration signals for each hammer blow to force and velocity data versus time. The recorded measurements are used to estimate the pile capacity, monitor hammer performance and energy transfer, measure pile driving stresses, and evaluate pile damage. Pile capacity computations are based on the Case Method of analysis.

A review of our records indicates that soil core borings, electronic cone penetration test (ECPT) probings, and test pile reports are available in the vicinity of the test site for this research project. A soil boring was taken at station 218+65, 20' Lt. C.L. The ECPT probing was taken at Bent 10 of the southbound roadway. Test Pile 3 and four piles in Bent 14 (Sta. 218+85, 50'Rt. C.L.) were monitored with the PDA by the FHWA in March of 1990 as part of the FHWA Demonstration Project 66. Test pile 3 was driven to tip elevation -63 feet, which is above the dense sand. The four piles tested in Bent 14 had an ABB splice and were driven into the dense sand to a pile tip elevation of -69 feet. PDA test results of the FHWA Demonstration Project 66 are included in the appendix.

TEST DETAILS

High Strength Precast Prestressed Concrete Pile

The tested pile is a 130 ft long 24" prestressed precast high strength concrete pile. The high strength concrete has been prepared for a minimum 28 day concrete strength of 8500 psi and a release strength of 5000 psi. The pile was driven 24 days after casting it on May 29, 1992. The LTRC concrete strength test results for different curing times are as follows:

AGE	AVERAGE COMPRESSIVE STRENGTH - f'c
7-days	9,596 psi
14-days	10,264 psi
28-days	10,453 psi

The following effective prestresses were computed by LA DOTD Bridge Design section.

AGE	EFFECTIVE PRESTRESS
Initial	1606 psi
18-hours	1512 psi
10-days	1463 psi
90-days	1410 psi

Based on the above concrete information, we estimate that at the time the pile was driven, the concrete strength was 10,400 psi and the effective prestress was 1454 psi. The unit weight was assumed to be 150 pcf. The average measured material stress wave speed is 14,700 ft/sec which corresponds to a dynamic elastic modulus of 6990 ksi.

The maximum allowable driving stresses for precast prestressed concrete piles that are recommended by the FHWA are based on the following formulas:

$$\textit{Maximum Compressive Driving Stress} = 0.85f'c - \textit{Effective Prestress}$$

$$\textit{Maximum Tension Driving Stress} = 3\sqrt{f'c} + \textit{Effective Prestress}$$

Based on these formulas, the maximum allowable compressive driving stress is 7.39 ksi and the maximum allowable tensile driving stress is 1.76 ksi.

Pile Driving Hammer

Pile driving was done with a Vulcan 020 single acting external combustion hammer, SECH, with a 3 foot stroke. This hammer has a manufacturer's maximum energy rating of 60.0 kip-ft at 3.0 ft length of stroke. The pile cushion used was a 5 inch thick compressed oak cushion. The oak cushion was originally 6 inches thick. The *Pile And Driving Equipment Form* is in the appendix.

Soils

The ground surface is at approximately elevation 26 feet, M.S.L. Prior to stabbing the pile, the pile location was pre-drilled to 20 feet below natural ground. The pile was driven to tip elevation -68.57 feet. The soil profile consists of soft to medium clays and silty clays down to elevation -64 feet underlain by a layer of medium to very dense sand. The soil boring log is shown in Figure 2 and the ECPT probing is shown in Figure 3.

CONCLUSIONS

Dynamic pile monitoring and subsequent data analysis support the following conclusions:

Hammer and Driving System Performance

The maximum transferred energy averaged 12.0 kip-ft in the first 22 feet of pile penetration, which translates into an efficiency of 20% of the maximum rated hammer energy. The maximum transferred energy averaged 15.0 kip-ft for the remainder of the driving, which is 25% efficiency of the maximum rated hammer energy. The total measured energy transfer efficiency for the same hammer in the Federal Demonstration Project was 27% to 28%. A relative evaluation of this energy transfer is possible by statistical comparison with a database of results under similar end of drive conditions. See Figure 4 for statistical energy transfer comparison.

Pile Performance

The compressive driving stresses measured at the gauge location reached a maximum of 1.83 ksi and then leveled off to an average of 1.70 ksi for the remainder of the pile driving. The maximum pile driving tension stresses increased from 0.86 ksi at the beginning of driving to 1.31 ksi at a pile tip penetration of 55 feet. The maximum tensile stress gradually reduced to 1.0 ksi at a pile tip penetration of 86 feet then sharply dropped off as the driving resistance increased in the dense sand. These driving stresses are well below the maximum allowable compressive driving stress of 7.39 ksi and maximum allowable tensile driving stress of 1.76 ksi. A profile of the driving stresses is shown in Figure 1.

The maximum measured tension driving stress of 1.31 ksi would have been considered damaging if 5,000 psi or 6,000 psi concrete strengths would have been used. The maximum allowable tensile driving stress for 5,000 psi and 6,000 psi concrete are 1.00 ksi to 1.17 ksi, respectively.

No structural damage was detected by the pile top dynamic data. Figure 5 is a PDA screen printout that shows a graph of the Force (solid line) and Velocity (dashed line) measurements versus time for one blow. This record shows the maximum tensile stress of 1.31 ksi recorded during pile driving. The Force and Velocity traces are proportional and do not indicate any change in impedance. The PDA computes a pile integrity factor, BTA, which is a ratio of the reduced pile cross-section to original pile cross-section. Pile damage guidelines based on BTA factor are shown in Table 1.

Table 1 - PILE DAMAGE GUIDELINES (Rauche & Goble, 1979)

BTA	SEVERITY OF DAMAGE
1.0	Undamaged
0.8 - 1.0	Slightly Damaged
0.6 - 0.8	Damaged
Below 0.6	Broken

The PDA recorded a pile integrity factor, BTA, of 1.0 for the entire pile driving operation. Based on the pile damage guidelines shown above, the pile is undamaged.

SUMMARY

A 24" high strength precast prestressed concrete pile was monitored with the Pile Dynamic Analyzer™. The PDA computed both compressive and tensile driving stresses which were within FHWA maximum allowable driving stresses. The dynamic data, Force and Velocity wave traces, showed no pile damage.

If we can be of further assistance, please advise.

J. B. Esnard
Pavement and Geotechnical
Design Engineer

Ed Tavera

Ed Tavera, P.E.
Geotechnical Design Engineer

Attachments:

Figure 1, PDA Test Data Plot
Figure 2, Soil Boring Log - Sta. 218+65, 20' LT. C.L.
Figure 3, ECPT Probing - Southbound Bent No. 10
Figure 4, GRL Hammer Performance - SECH Concrete/Timber Piles
Figure 5, PDA Screen Printout
Appendix:

Bridge Design Section Letter - March 24, 1992
Pavement & Geotechnical Design Sec. Letter - April 2, 1992
Pile And Driving Equipment Form - June 6, 1992
High Strength Precast Prestressed Concrete Pile Plan Sheet
LTRC Concrete Strength Letter - July 15, 1992
FHWA Demonstration Project 66 - PDA Test Results

Figure 1

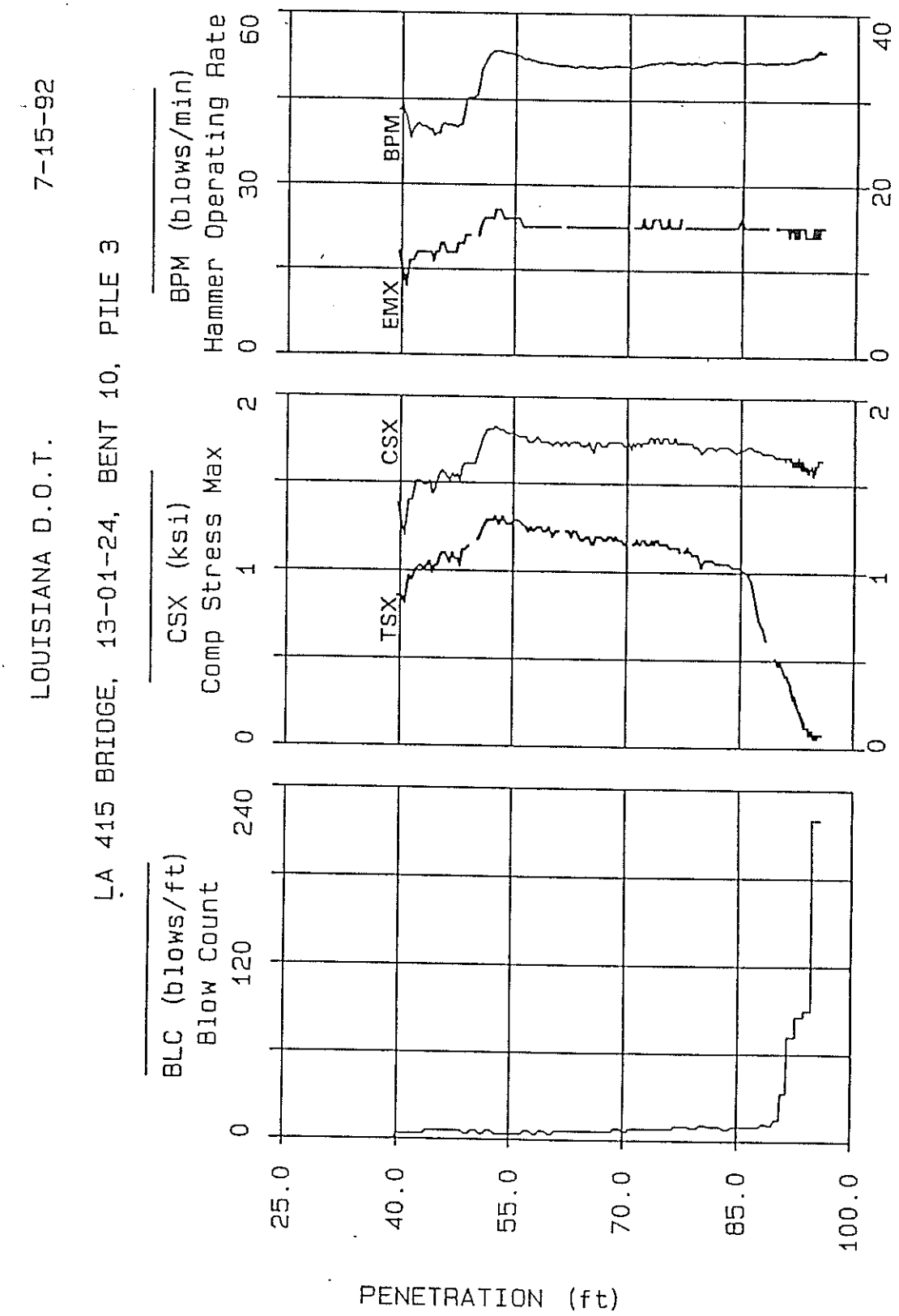

Note: Pile penetration is referenced to ground surface. Assume ground surface at elevation 26 feet.

TABLE C.1
GRADATION ANALYSIS OF FINE AND COARSE AGGREGATE

Fine Aggregate - Atmore Sand

Sieve #	Weight Retained	Percent Retained	Percent Passing
3/8"	0	0	100
#4	22	4	96
#8	59	10	90
#16	96	16	84
#30	284	49	51
#50	433	74	26
#100	566	97	3
Pan	584		

Coarse Aggregate - #57 Stone from Reed Quarry

Sieve #	Weight Retained	Percent Retained	Percent Passing
1-1/2"	0.0	0	100.0
1"	0.74	3	97.0
3/4"	0.0	0	0.0
1/2"	11.02	42	58.0
3/8"	0.0	0	0.0
#4	24.20	93	7.0
#8	25.75	99	1.0
Pan	26.12		

TABLE C.2
CONCRETE MIX PROPORTIONS
(Per Cubic Yard)

	Mix Designations				
Components, lbs	#2	#3	#4	#5	#6
Cement	752 lb	753 lb	755 lb	753 lb	757 lb
Silica Fume	96 lb	95 lb	97 lb	95 lb	95 lb
Water	136 lb	127 lb	125 lb	125 lb	142 lb
Sand	1,105 lb	1,105 lb	1,110 lb	1,105 lb	1,107 lb
Stone	1,890 lb	1,890 lb	1,890 lb	1,890 lb	1,893 lb
Water Reducer	10 oz	10 oz	10 oz	10 oz	10 oz
Air Entrainment	3 oz	3 oz	3 oz	3 oz	3 oz
High Range Water Reducer	78 oz	78 oz	78 oz	78 oz	78 oz

*Fabricator recorded a "free" moisture on the sand of 7.5% and 0.9% on the stone.
Metic Equivalents:

1 lb = 0.454 kg

1 oz = 29.574 cc

TABLE C.3
CONCRETE MATERIAL PROPERTIES

Concrete Age	Compressive Strength, psi		
	Curing Conditions		
	Steam/Air	Air/Air	Moist
18 hours	8,449		
24 hours	9,071		
7 days	9,596		
14 dyas	10,264		
28 days	10,453	11,874	11,637

Metric Equivalents: 1 ksi = 1000 psi = 6.895 MPa

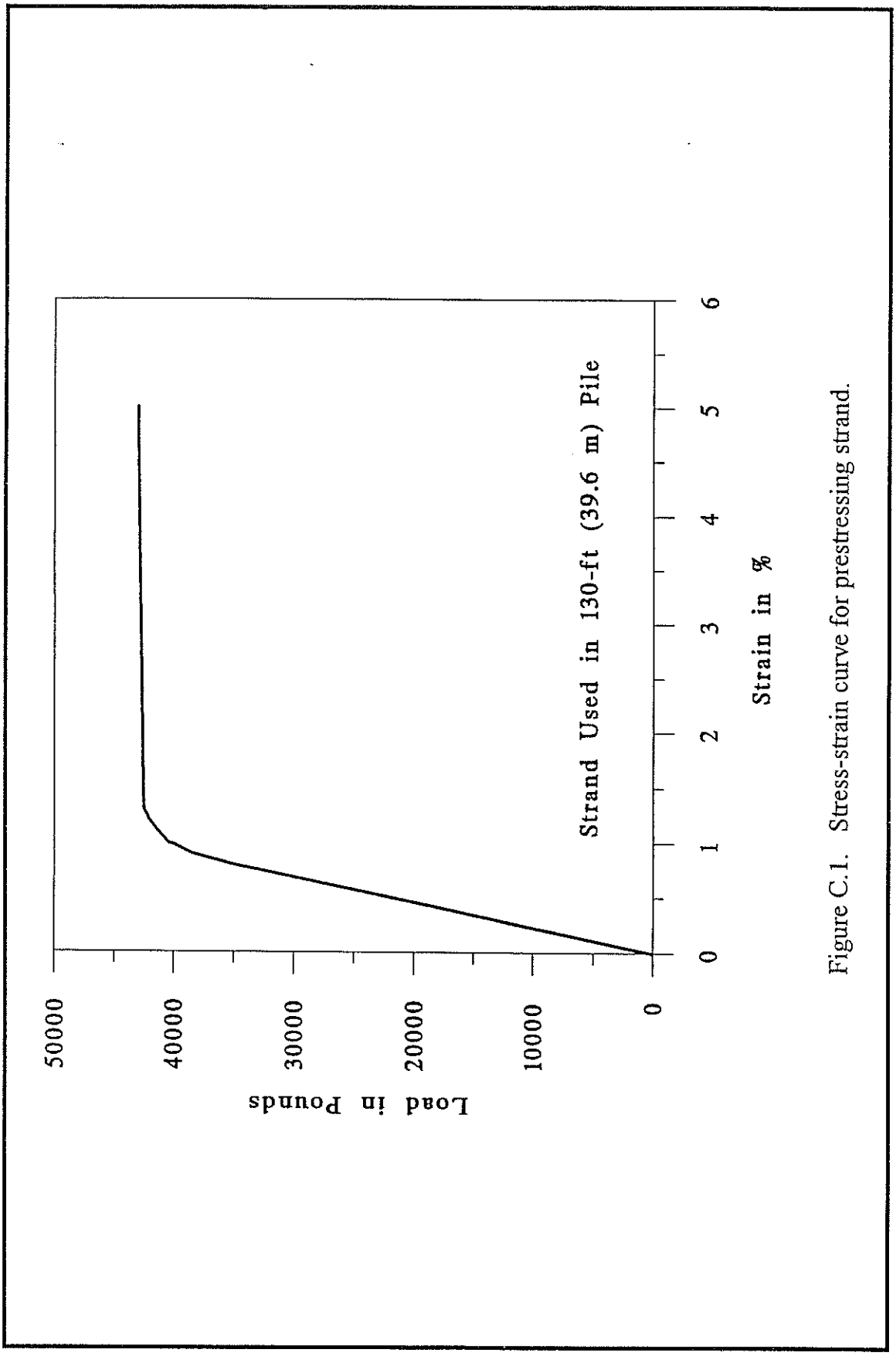

Figure C.1. Stress-strain curve for prestressing strand.

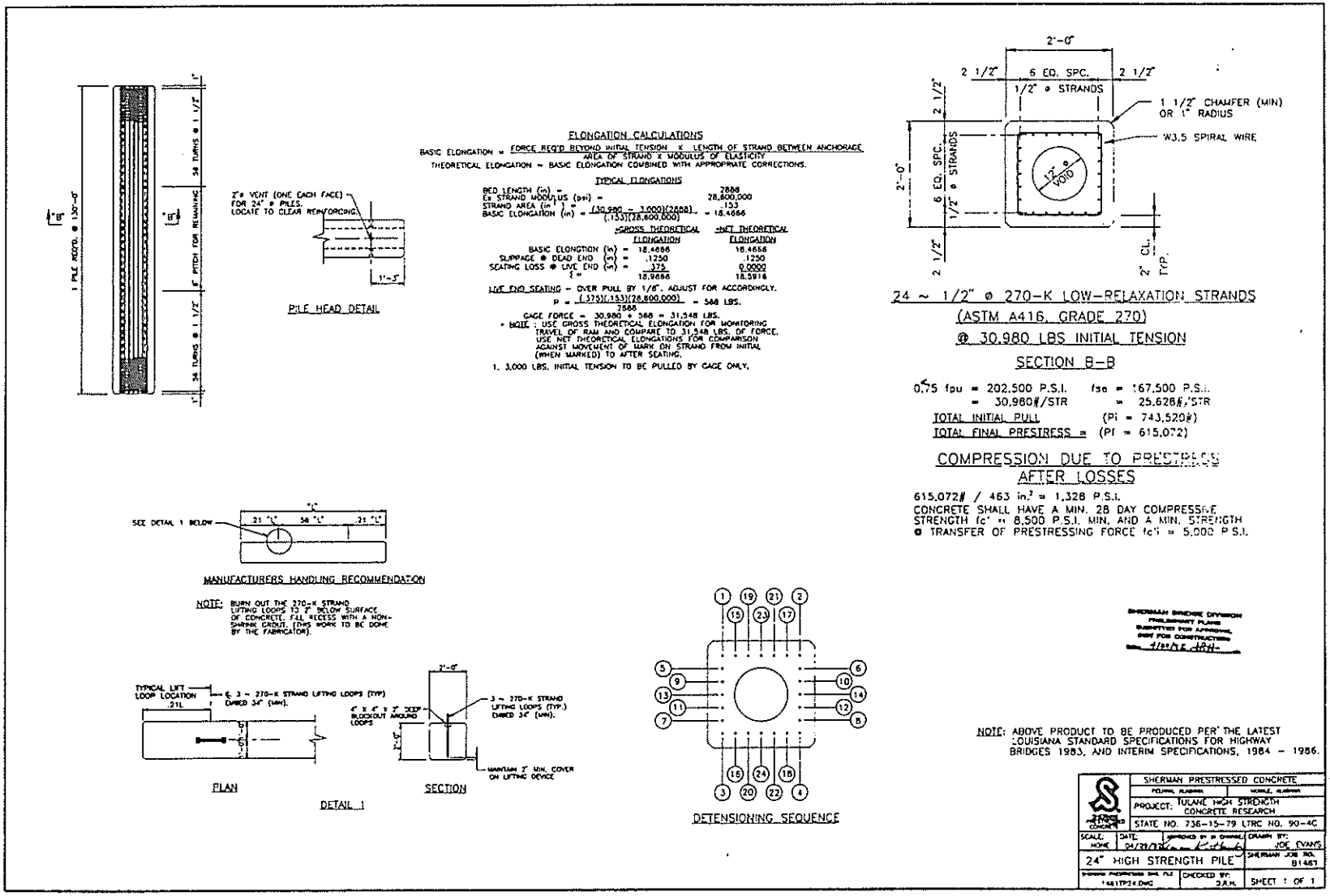

Figure C.2 Shop drawing for 130 ft. (39.6 m) pile.

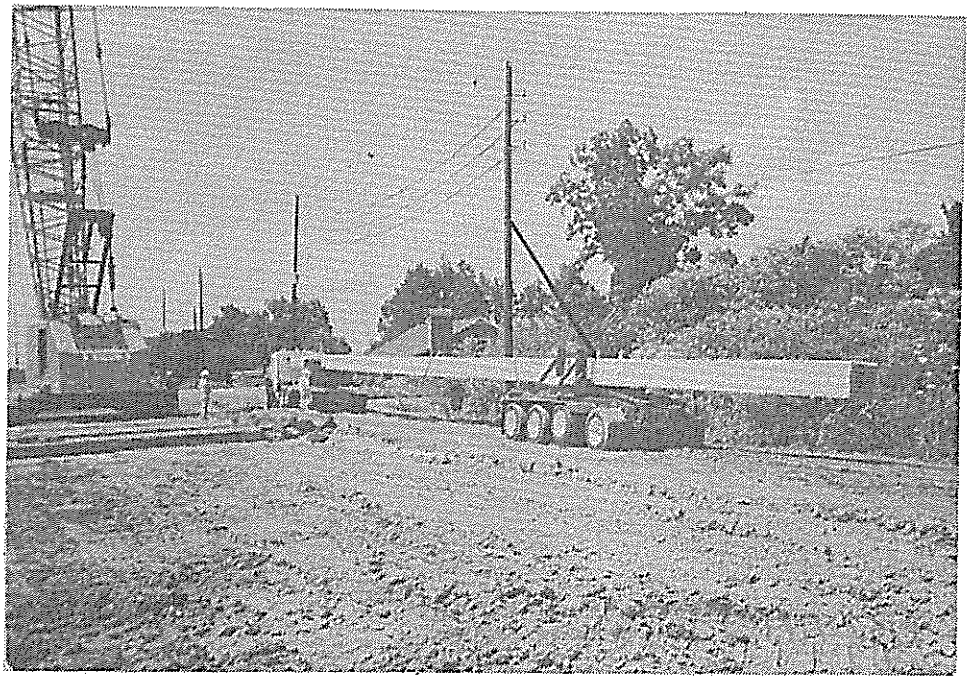

Figure C.3 View of pile on truck and dolly.